

# FOUNTAIN DARTER MODELING SYSTEM FOR THE COMAL AND SAN MARCOS RIVERS

---

Edwards Aquifer Habitat Conservation Plan  
Contract No. 13-637-HCP

## FINAL REPORT

---

### **Prepared for**

Edwards Aquifer Authority

### **Prepared by**

Dr. William Grant (Texas A&M University)

Dr. Todd Swannack (US Army Engineer Research and Development Center)

Dr. Hsiao-Hsuan (Rose) Wang (Texas A&M University)

Dr. Thom Hardy (Watershed Systems Group)

Dr. George Ward (University of Texas Austin)

Dr. Robert Doyle (Baylor University)

Dr. Timothy Bonner (Texas State University)

BIO-WEST, Inc.

**May 19, 2017**

---

## EXECUTIVE SUMMARY

This document reports on the project to develop and apply a computer-based model of the fountain darter in the San Marcos and Comal rivers. The fountain darter is an endangered species dependent upon the springflow-dominated ecosystems of these two river systems. The objective of the Fountain Darter Modeling System (FDMS) is to simulate the population dynamics of fountain darters in response to changes in habitat conditions that might result directly or indirectly from changes in water flow within the two rivers. The FDMS is comprised of four major submodels, which address river hydraulics, water quality, submerged aquatic vegetation (SAV) and the fountain darter population. The basic structure of the FDMS is diagrammed in Figure ES-1, which is also the present conceptual model of the river ecosystem as it affects the fountain darter. The FDMS is fundamentally deterministic (mechanistic) with the arrows in the diagram of Fig. ES-1 indicating cause → effect. However, all watercourse models are hybrids, employing both deterministic and empirical (statistical) relations, and the FDMS is no exception, relying upon the results of the extensive biomonitoring program of the Edwards Aquifer Habitat Conservation Plan (HCP). The hydraulic and water quality submodels have been developed through previous projects sponsored by the Edwards Aquifer Recovery Implementation Program (EARIP), and were adopted for use in the FDMS.

Like all watercourse models, the FDMS submodels include “free parameters”, numerical constants in the model equations that quantify some process, but whose values are unknown. These parameters are determined by multiple runs of the model with different parameter values and the results compared to observations, the parameters then being assigned the value(s) that result in a best fit to the observations. This process is referred to as “model calibration.” A direct comparison of model output with measured data without any internal adjustments to the model is carried out to evaluate the accuracy of the model. This process is referred to as “model validation” (or “verification”). In addition, the model may be subjected to standardized changes in input and parameter values to determine the model responses, including sensitivity, stability and thresholds. These testing and diagnosis protocols together constitute performance evaluation of the model.

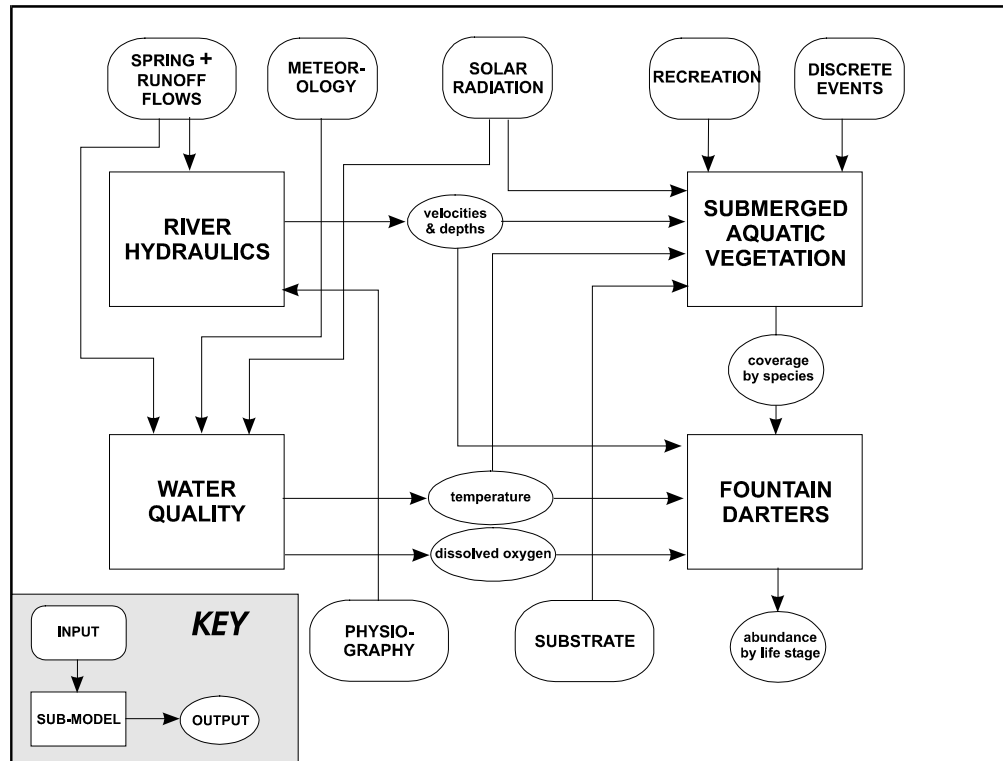


Figure ES-1. Structure of Comal or San Marcos river ecosystem as it affects the fountain darter

The two-dimensional hydraulic model addresses detail in the longitudinal and transverse currents across the river channel. The basic equations are solved numerically based on a curvilinear, boundary-following coordinate system with nominal 0.25 m spatial increment. The present model is implemented on a U.S. Geological Survey platform, the Multidimensional Surface Water Modeling System (MDSWMS). The computational grid of the hydraulic model is based on detailed bathymetric surveys of the two river channels and serves as the basic spatial framework for the SAV and fountain darter population submodels.

Water quality was modeled using the Environmental Protection Agency QUAL2E model. Water quality parameters are not considered to vary with the same spatial detail as water velocities, thus a cross-section average computation using a link-node network of segments was employed. The model has been enhanced with radiation and algal photosynthesis terms to model the diurnal variations in water temperature and dissolved oxygen (DO).

Given the importance of SAV in the fountain darter life cycle, understanding the factors that affect SAV persistence is paramount for successful aquatic ecosystem management in the Comal and San Marcos rivers. The SAV submodel simulates vegetation growth, density, and colonization of several important SAV species in the rivers. This submodel is process-based with stochasticity. The formulations for the SAV submodel are based on earlier models but have been modified for clear water, spring-fed, limited-temperature-range conditions of the two rivers.

In aquatic systems, the availability of light is the driving factor controlling photosynthesis. Irradiance follows daily and seasonal cycles, resulting in heterogeneous spatio-temporal patterns of light availability and growth patterns. Maintenance respiration is needed for plants to continue to live. The model estimates maintenance respiration based on modeled daily temperature and the biomass of the above- and belowground sections of the plants. The difference between gross photosynthesis and maintenance respiration is the amount of assimilate available for growth. This growth is expressed as biomass and converted to areal coverage.

A major effort in the SAV modeling addressed the spatial dispersal of vegetation. In nature, dispersal of aquatic vegetation can take place through seed deposits, clonal growth, and/or fragments settling and rooting downstream. Generally, this is not accounted for in SAV models. We have developed an approach that simulates changes in vegetative cover over time based on a combination of ecological dispersal theory and on empirical estimates from vegetation mapping data, expressed as a transition matrix.

Fountain darter population is simulated in an agent-based model (ABM) using the NetLogo environment. This submodel determines fountain darter population responses to spatial-temporal changes in the distribution and species composition of SAV, water temperature, DO concentration, water depth, and velocity, as the darters pass through egg, larval, juvenile, and adult life stages. For computational efficiency, the SAV submodel and the fountain darter submodel have been combined as part of the same computer program in NetLogo. The fountain darter and SAV models use the same grid as the hydraulic model, subsampled to 1-m resolution. The grid elements (also referred to as “cells” and “habitat patches”), whose properties include location, vegetation type, water temperature, DO concentration, depth, and velocity (all of which

vary in time except location), are populated with thousands of fountain darter “individuals” with attributes including location (i.e., by habitat patch), sex, age, life stage, and (for females) reproductive state. The simulated darters are subjected to aging, development, mortality and reproduction, which are advanced daily, coupled with hourly movements. Egg production proceeds probabilistically based upon data on monthly proportions of reproductively active females and fecundity. Movement rules are generally directed from higher population cells to lower, and toward better habitat, and are governed by random choices constrained by maximum density for each SAV type. For each computational day, these results are aggregated to determine the total number of juvenile and adult fish in the modeled reach and the total number within each vegetation type.

Figure ES-2 diagrams the operation of the FDMS. The two rectangles diagram computer operations. Various input and operational selections are made through the graphical user interface (GUI) on the left, which initiates, populates and activates the NetLogo program containing SAV and fountain darter submodels, on the right. The intervening oblong boxes indicate flow of information, either as input data, or computed data exchanged automatically between models.

The FDMS operates in two modes, dictating the role of the SAV submodel. The first is coupled mode, in which both the SAV and the fountain darter submodels are advanced together in time, with the SAV coverage and the fountain darter population being determined by all of the above processes operating simultaneously. The second is the decoupled mode, in which the SAV coverage is read in as inputs, either from field surveys or from user-specified distributions. The decoupled mode was used to isolate model error arising from the SAV submodel from that of the darter submodel, to carry out separate performance evaluations. The decoupled mode has also proved useful for routine model runs of the FDMS. Although the SAV submodel has significantly advanced the science, the details of its formulation and its linkage within the coupled model remain provisional at this time. The coupled modeling framework is provided as a “beta” version. It is expected that this version of the model will require a number of user-specified scenarios to be run and evaluated rigorously in order to update and refine the modeling system as part of any normal software development cycle.

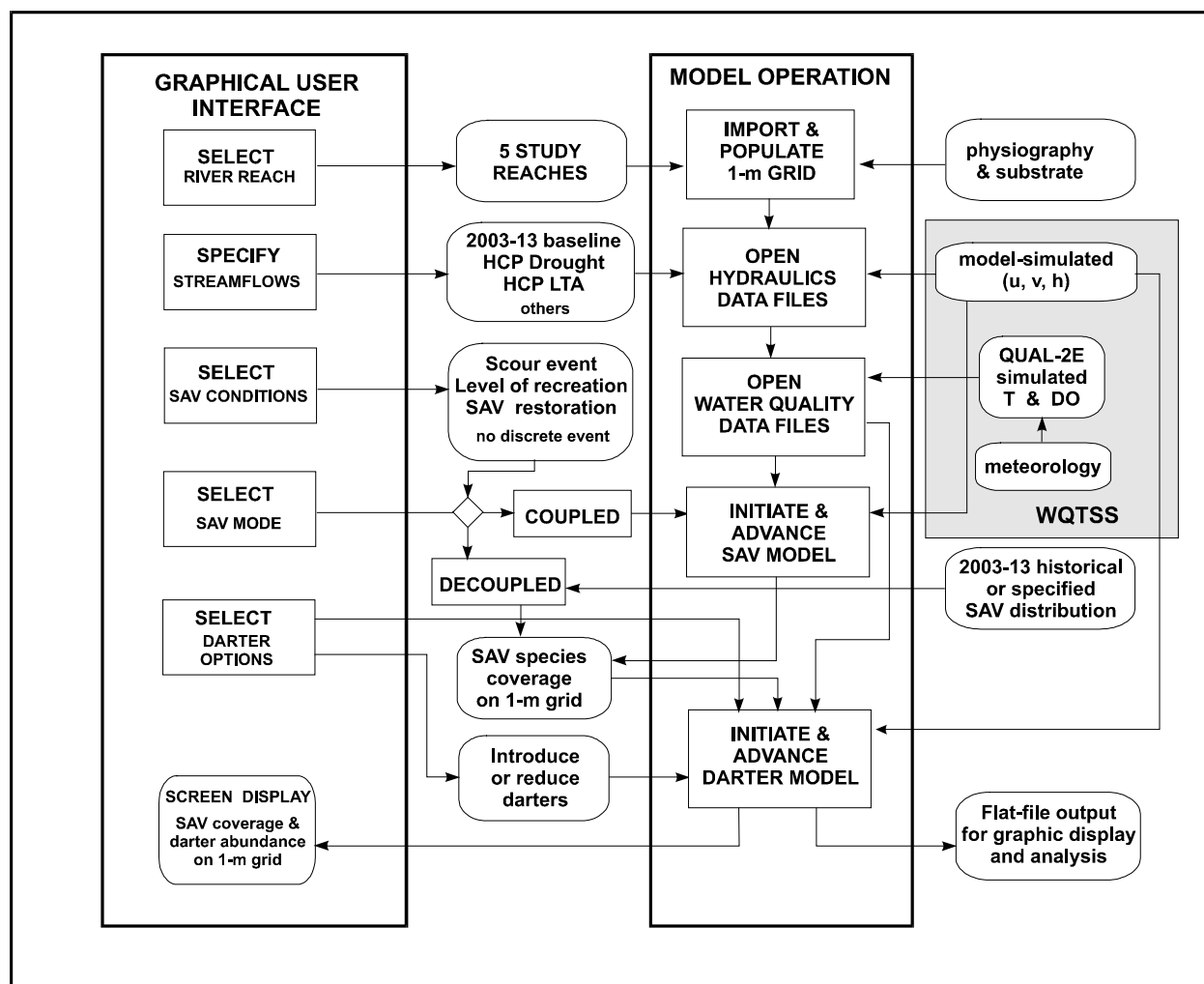


Figure ES-2. Schematic flow chart of operation of Fountain Darter Modeling System

Pending further development, use of the coupled modeling system for arbitrary scenario evaluations or isolated interpretations will require that the user has a complete understanding of the various modeling components and the existing limitations of the coupled modeling system. For this reason, we recommend use of the decoupled model for management purposes.

For clarity, both the conceptual model of Fig. ES-1 and the model operation diagram of Fig. ES-2 suppress the time-space nature of the submodels and connecting variables. In fact, simulations are driven by daily time series of river water discharge and meteorology. Computed velocity and water levels across the river channel produced by the hydraulic model, along with water temperatures and DO concentrations distributed across the same network from operation of the water quality model, are input daily into the SAV and fountain darter submodels under coupled

operation. In the decoupled operation, observed SAV distributions are used to update the inputs at time points in the year corresponding to the field surveys. During each model simulation, the system is initialized by assigning each habitat cell a vegetation type, as well as a water temperature, DO concentration, depth, and velocity, and by assigning each individual fountain darter a sex, age, life stage, and location. For simulation purposes, the number of fountain darters in a grid cell is taken to be the sum of juveniles and adults (as these are the sizes most likely to be observed in the field). The initial number of juvenile plus adult darters is calculated based on the estimated maximum darter density that can be supported by the aquatic vegetation within the reach. The maximum darter density associated with each type of aquatic vegetation is based on analyses of drop-net data collected from 2003 to 2010 in the particular reach of the Comal River or the San Marcos River being simulated.

The analyses and mathematical formulations undergirding the model relied heavily upon historical data collections in the rivers, mainly those undertaken through the auspices of the Edwards Aquifer Authority (EAA) prior to and subsequently as part of the HCP over the past 15 years. The project focused on five study reaches, which exhibit a range of habitats and vegetation, namely (proceeding downstream) City Park, IH 35 on the San Marcos River, Upper Spring Run, Landa Lake and Old Channel on the Comal River. Model development and calibration of the SAV and fountain darter submodels were carried out on the Old Channel study reach, using data from the period 2003-2010. (The hydraulic and water quality model were validated in previous projects, so they were applied directly to the study reaches.) Once calibrated, the parameters characterizing growth, senescence and dispersal of SAV's and growth, development, and movement of the fountain darters were transferred to the other four study reaches. Data from 2011-2013 were then used to evaluate model performance on all five study reaches.

Calibration and validation results show the SAV submodel simulates realistic seasonal variation in vegetation growth and respiration. Plant attributes were cyclical in that the patterns showed increased growth during the spring and summer and decreased growth in the winter.

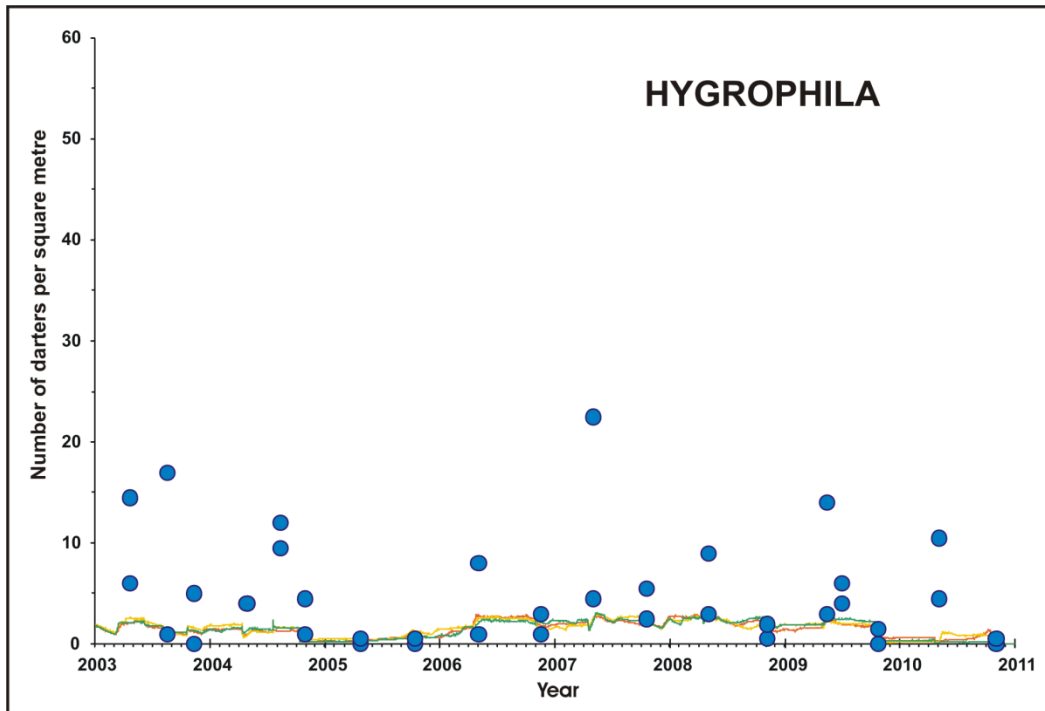


Figure ES-3. Fountain darter model (continuous traces) and drop-net data (filled circles) for *Hygrophila* in Upper Spring Run study reach of Comal River, 2003-2010

Simulated patterns in amount of vegetative cover matched observed patterns of cover in City Park, and Landa Lake relatively well, but underestimated vegetative cover in Old Channel, I35, and Upper Spring Run. In the latter three reaches, the underestimation indicates that there are likely processes other than photosynthesis, respiration, and state conversion that drive vegetative cover.

For the fountain darter submodel, the single calibration parameter was the number of consecutive moves that a darter can survive without finding acceptable habitat. When this limit on the number of consecutive moves was removed, darter population increased exponentially, and when the movement rules were replaced with random movement the population could not sustain. The number of moves that achieved the best fit to 2003-2010 observations was determined to be 12, using the Old Channel study reach as the calibration case. Other model parameters were determined through literature or applied research. Example comparisons of model to data for the other reaches for the time period 2003-2010 are shown in Figures ES-3 and ES-4. One example of model performance for the validation years of 2011-2013 is shown in Figure ES-5 for *Vallisneria* in Landa Lake.

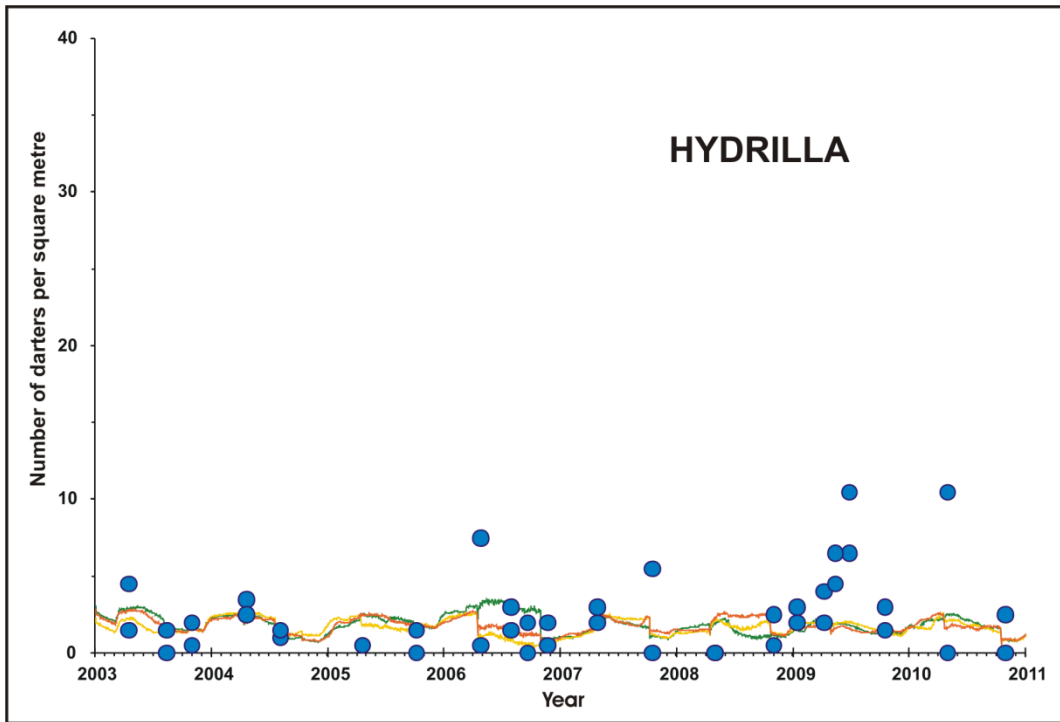


Figure ES-4 - As Fig. ES-3 for *Hydrilla* in IH 35 study reach of San Marcos River, 2003-2010

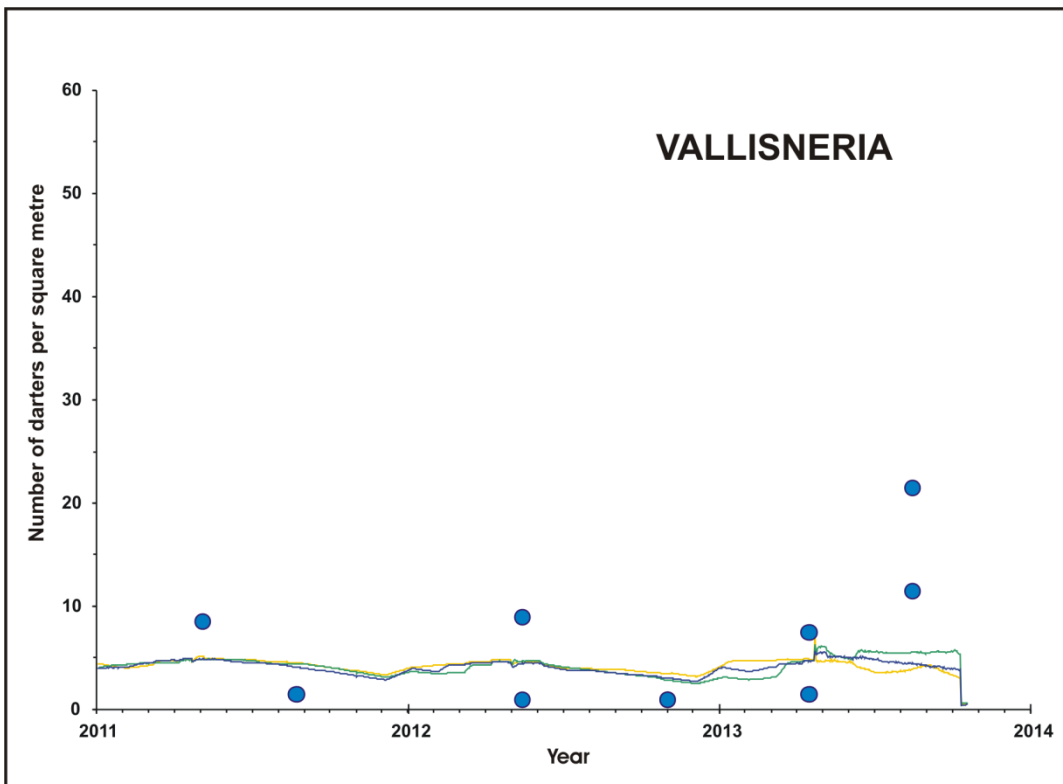
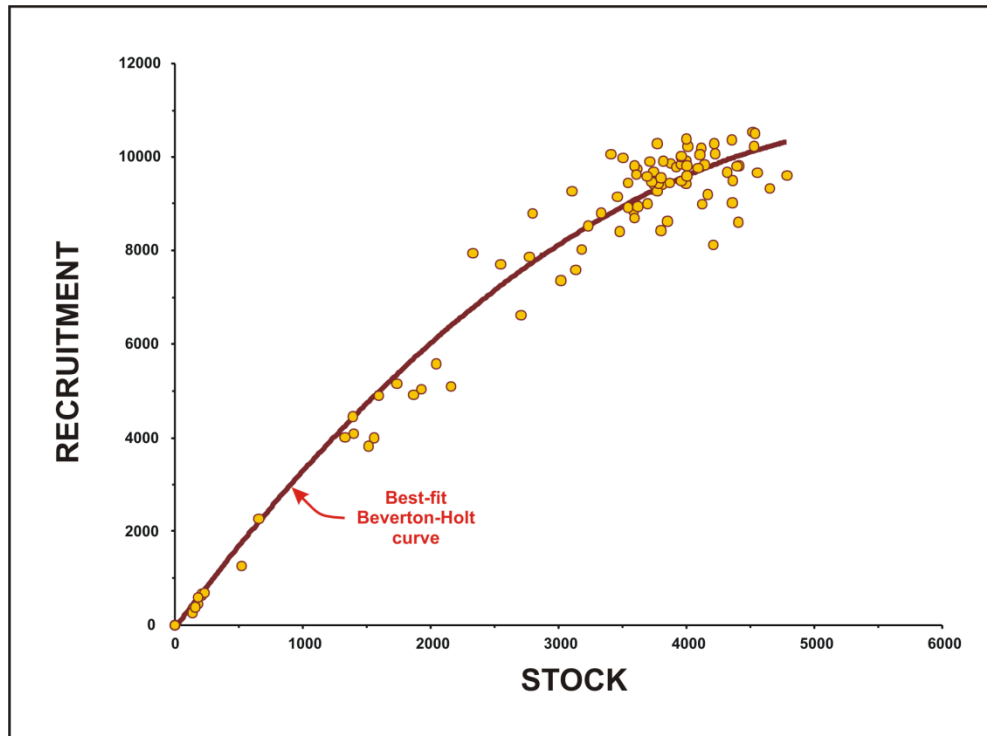


Figure ES-5. As Figure ES-3 for *Vallisneria* in Landa Lake study reach of Comal River, 2011-2013

These examples are neither the best nor the worst in model performance, but are representative. Biological field data in general, and the drop-net data from the San Marcos and Comal rivers in particular, are noisy, that is, they exhibit large fluctuations not obviously the result of external variables. Given this noise, and the uncertainty it represents, the model performance is judged satisfactory for the historical conditions. Generally, when the model is in error compared to observations, it tends to under-predict fountain darter abundance, and therefore, from a management standpoint, is conservative.

Additional support for the functioning of the fountain darter submodel is the agreement between the simulated and the expected stock-recruitment relationships for fountain darters. The curve in Figure ES-6 is a Beverton-Holt type spawner-recruit relationship, with a weak response characterized by a steepness coefficient of 0.5 to 0.7, which would be expected for the fountain darter given its life history. The data points are from a simulation of the Old Channel study reach for 2003-2010 with steady-state environmental conditions and SAV distributions from fall 2012. Stock size was calculated as the mean number of adults alive during a calendar year. Annual recruitment was calculated as the number of eggs laid during a calendar year that reached the adult stage within the same year. The best-fit relations ( $r^2 = 0.96$ ) has a steepness coefficient of 0.40.

The FDMS is scenario-driven. Several example scenarios are shown in the report, and the user can specify many more. Model calibration and validation were carried out for the baseline scenario of historical flows and meteorology for the period 2003-2013. The most important scenario, however, is the HCP-specified Phase-1 flow regime, since this informs the question of whether this flow regime is protective of the fountain darter. A series of simulations were carried out for the HCP drought scenario, based on drought-of-record streamflows, a 10-year scenario with long-term average equal to that specified by the HCP, and, for comparison, the baseline scenario. (A second set of the same three scenarios was run with a hypothetical density-dependent negative feedback on population.) All three scenarios show maintenance of the fountain darter population.



**Figure ES-6. Stock recruitment diagram for fountain darter model with best-fit Beverton-Holt relation, no density-dependent feedback**

It is evident throughout this report and from these model runs that aquatic vegetation is the primary driver of the numerical size of the fountain darter population during most conditions with the possible exception at the extremes when water temperature can have an overriding effect. It should be re-emphasized that the primary purpose of this modeling tool is to provide guidance on HCP management issues, both at present and into the future. As such, the interpretation of any model results (like those provided herein) need to be extensively vetted amongst the various EARIP tiers before conclusions can be drawn to serve that purpose. It is not within the purview of this project to answer the HCP Phase 1 question regarding survival and recovery of the fountain darter in the wild. Rather, it was our charge to create the tool and provide guidance on interpretation of its results, which includes discussions on model assumptions, model performance, strengths and shortcomings, and lessons learned from the prosecution of the project.

Several assumptions were made in the development of this management tool, delineated in this summary and in the text of the report, whose ecological implications need to be considered as

part of any interpretation of model results. Some of these, such as sufficiency of fountain darter food supply, or diminishment of the threat of gill parasites are based on specific HCP applied research results and/or long-term monitoring of the rivers. Another assumption made because of the complexities and resources necessary to study ecological interactions is that behavior, competition, predation, etc. are implicit within the drop-net density data results. Other potential impactors such as disease and pollution were not addressed because of lack of data or because they would require major efforts in dynamic modeling of hydraulics and water quality far beyond the scope of this project.

As anticipated in the HCP, Tier A and tier B applied research along with continued biological monitoring has provided a wealth of information useful in model development. In fact, presented with the direct observations during the extended drought from 2013 through 2014 in the Comal system, one could contend that the primary question laid out for the ecomodel, *viz.* “Is the HCP Phase 1 flow regime sufficient to support the survival and recovery of the fountain darter?” might have been answered using the Upper Spring Run as a surrogate for the system without reliance on any modeling. (Of course, the worst drought for the Comal system in nearly a quarter of a century was not something forecast in the HCP. Nor do these observations necessarily extend to the San Marcos.) Finally, Section 6.3.4.2 of the HCP states, “Tier C will investigate the implications of the timing, frequency, and duration of multiple events in varying sequences and include specific research efforts designed to assess ecological model predictions (e.g., model validation).” Tier C concepts highlighted in the HCP include assessing “simple or complex parameters and single or multiple low-flow events” through controlled experimentation in applied research channels. The completion of the technical aspects of the Phase 1 ecological model for the fountain darter provides an excellent opportunity for testing and validation as proposed in the HCP.

There are also weaknesses in the present model that could be repaired by directed research efforts. Several recommendations are proffered. Validation of DO concentrations from the Water Quality submodel (in the previous developmental work on QUAL2E) were hampered by too limited a range of data, especially for low DO concentrations during low-flow, high-temperature conditions in vegetated reaches. We recommend institution of specifically targeted

dissolved oxygen monitoring in the two rivers using rigorously maintained automated monitors. This data can be analyzed directly for community production and respiration, and related to SAV growth in the vicinity of the monitors. The DO submodel part of the calculation should be expanded to include SAV coverage. This could be most expeditiously accomplished by merging the DO calculation into the NetLogo program. The dispersal component of the SAV submodel was given little application in the scenarios evaluated here. This is new science and needs additional work to better simulate areal encroachment, regrowth and competition as exhibited by SAV species in the field. Finally, the FDMS can be enhanced to examine other scenarios, such as nonpoint pollution, warmer water temperatures, and longer duration drought events. Extensions to address other threatened or important species could be accommodated in the same modeling framework.

It is our judgment that the model offers the necessary capabilities to serve its intended function as a resource for assistance in managing the San Marcos and Comal river systems for maintenance of fountain darters. The platform is scenario-driven with sufficient options to enable EAA staff or EARIP participants to apply the model to many management questions concerning the fountain darter within these watercourses. The model was envisioned to be organic, that is, to develop over time to meet expanded requirements of management of the aquifer and the rivers, to incorporate new results from research and monitoring programs, and to address emerging scientific issues of the river ecosystems. The model is capable of being enhanced to address additional ecological processes, other organisms of concern, pollutant impacts, and additional water-quality parameters, as the needs of the EARIP evolve.

## Table of Contents

1	Introduction.....	9
1.1	The Study Reaches of the Comal and San Marcos Rivers.....	9
1.2	Strategy and conceptual basis of the model.....	15
1.3	Key Decision Points.....	17
2	Model Components, Structure and Function.....	18
2.1	Main Components.....	18
2.1.1	Hydrology and hydraulics.....	18
2.1.2	Water quality.....	22
2.1.3	Submerged aquatic vegetation submodel.....	23
2.1.4	Fountain darter submodel.....	42
2.2	Model Structure.....	44
2.2.1	Model space-time structure, operation and inputs.....	45
2.2.2	SAV submodel.....	46
2.2.3	Fountain darter submodel.....	51
2.3	Model performance.....	56
2.3.1	SAV submodel testing and evaluation.....	56
2.3.2	Fountain darter submodel testing and evaluation.....	61
3	Model Applications.....	85
3.1	Scenarios.....	85
3.1.1	Baseline: 2003-2013 historical flows.....	86
3.1.2	HCP Flow Regime – Drought: minimum 10-year period flow.....	89
3.1.3	HCP – LTA: 10-year average flow approximating the HCP LTA.....	89
3.1.4	Stressed habitat scenarios.....	92
3.2	Model set-up and operation.....	92
3.3	Results.....	95
3.3.1	Baseline and HCP scenarios.....	95
3.3.2	Stressed habitat scenarios.....	101
3.4	Model conclusions and interpretation.....	108
3.4.1	Assumptions.....	108
3.4.2	Existing Model Shortcomings.....	109
3.4.3	Cumulative reach or full system consideration.....	110
4	Validation and Lessons Learned.....	111

4.1 Validation..... 111

4.2 Lessons Learned..... 112

4.3 Lessons Learned: 2013-14 drought impacts compared to FDMS results ..... 118

5 Next Steps and Future Considerations..... 121

5.1 Dissolved oxygen kinetics and modeling ..... 121

5.1.1 DO monitoring ..... 122

5.1.2 DO modeling including SAV influence..... 122

5.2 Advanced SAV modeling ..... 123

5.3 Future Considerations ..... 124

6 References..... 125

## List of Figures

Figure 1-1. Comal River Study Reaches (Old Channel, Landa Lake, and Upper Spring Run) ...	10
Figure 1-2. San Marcos River Study Reaches (City Park and I35) .....	11
Figure 1-3. Location map of Upper Spring Run study reach on Comal River .....	12
Figure 1-4. Location map of Landa Lake study reach on Comal River .....	12
Figure 1-5. Location map of Old Channel study reach on Comal River .....	14
Figure 1-6. Location map of City Park study reach on San Marcos River .....	14
Figure 1-7. Location map of IH 35 study reach on San Marcos River .....	15
Figure 1-8. Conceptual model of Comal or San Marcos river ecosystem as it affects the fountain darter .....	17
Figure 2-1. Example of field-measured topography points, depth contours, computational mesh overlay mapped onto topography, 3-dimensional numerical grid geometry used in MDSWMS hydraulic model, for the Sewell Park section of the San Marcos River from Hardy et al. (2010).....	20
Figure 2-2. Submerged Aquatic Vegetation (SAV) conceptual submodel.....	24
Figure 2-3. Example of routine vegetation survey in Comal River, Old Channel study reach, Fall 2008, from BIO-WEST (2009a) .....	27
Figure 2-4. Maps of total vegetation coverage in fall surveys, Upper Spring Run study reach in Comal River.....	27
Figure 2-5. Maps of total vegetation coverage in fall surveys, Landa Lake study reach in Comal River .....	30
Figure 2-6. Maps of total vegetation coverage in fall surveys, Old Channel study reach in Comal River .....	32
Figure 2-7. Maps of total vegetation coverage in fall surveys, City Park study reach in San Marcos River.....	36
Figure 2-8. Maps of total vegetation coverage in fall surveys, IH 35 study reach in San Marcos River.....	37
Figure 2-9. Depiction of frequency of occupancy of a given cell over time. Old Channel (A), City Park (B) Red and orange indicate oscillation between vegetated and unvegetated during 2000-2013; green indicates mostly vegetated. ....	41
Figure 2-10. Conceptual diagram of the spatially-explicit, individual-based, simulation model representing fountain darter population dynamics in response to changes in aquatic vegetation and hydrological conditions.....	44
Figure 2-11. Alternative model structure in decoupled configuration, cf. Fig. 1-8.....	47
Figure 2-12. Example of logistic function used to calculate probability of dispersal based on percent cover of vegetation for each cell, following Railsback and Grimm (2014).....	50

Figure 2-13. Chord diagrams for City Park reach, showing seasonal transitions between SAV types .....	50
Figure 2-14. Overview of the sequence of events and processes involved in the execution of the fountain darter submodel .....	52
Figure 2-15. Summary of fountain darter movement rules.....	54
Figure 2-16. Net Biomass Accumulation over time for each of the five study reaches. ....	58
Figure 2-17. Results from Sensitivity Analyses for total vegetation in City Park study reach ....	60
Figure 2-18. Fountain darter model (continuous traces) and drop net data (filled circles) – Old Channel study reach of Comal River, 2003-2010 (a–Hygrophila; b-Ludwigia; c-filamentous algae) .....	63
Figure 2-19. Fountain darter model (continuous traces) and drop net data (filled circles) – Upper Spring Run study reach of Comal River, 2003-2010 (a–Hygrophila; b-Sagittaria; c-bryophytes).....	64
Figure 2-20. Fountain darter model (continuous traces) and drop net data (filled circles) – Landa Lake study reach of Comal River, 2003-2010 (a–Hygrophila; b-Ludwigia; c-Vallisneria; d-Cabomba; e-bryophytes) .....	66
Figure 2-21. Fountain darter model (continuous traces) and drop net data (filled circles) – City Park study reach of San Marcos River, 2003-2010 (a–Hygrophila; b-Hydrilla; c-bare substrate).....	68
Figure 2-22. Fountain darter model (continuous traces) and drop net data (filled circles) – IH 35 study reach of San Marcos River, 2003-2010 (a–Hygrophila; b-Hydrilla; c-Cabomba) .....	70
Figure 2-23. Fountain darter model (continuous traces) and drop net data (filled circles) – Old Channel study reach of Comal River, 2011-2013 (a–Hygrophila; b-Ludwigia; c-bryophytes).....	72
Figure 2-24. Fountain darter model (continuous traces) and drop net data (filled circles) – Upper Spring Run study reach of the Comal River, 2011-2013 (a–Hygrophila; b-Sagittaria; c-filamentous algae; d-bryophytes) .....	73
Figure 2-25. Fountain darter model (continuous traces) and drop net data (filled circles) – Landa Lake study reach of the Comal River, 2011-2013 (a–Hygrophila; b-Ludwigia; c-Vallisneria; d-Cabomba; e-bryophytes) .....	75
Figure 2-26. Fountain darter model (continuous traces) and drop net data (filled circles) – City Park study reach of the San Marcos River, 2011-2013 (a–Hygrophila; b-Hydrilla; c-Sagittaria; d-Potamogeton).....	78
Figure 2-27. Fountain darter model (continuous traces) and drop net data (filled circles) – IH 35 study reach of the San Marcos River, 2011-2013 (a–Hygrophila; b-Hydrilla; c-Sagittaria; d-Cabomba).....	80
Figure 2-28. Stock recruitment diagram for fountain darter model with best-fit Beverton-Holt relation, no density-dependent feedback .....	84

Figure 2-29. Stock recruitment diagram for fountain darter model with best-fit Beverton-Holt relation, six density-dependent feedback mechanisms .....	84
Figure 3-1. Estimated discharges in the Old Channel reach of the Comal River for 2003-2013 (red) and flows as percent of total Comal River discharges (blue).....	88
Figure 3-2. Daily flows and Weekly Average Flows in the San Marcos River.....	88
Figure 3-3. Comal River historical total system discharge (blue) and modeled total system discharge (red [No Action] and green [HCP Phase 1 bottom up package]) presented in the HCP for time period of 1947 to 1960 .....	90
Figure 3-4. As in Fig. 3-3, for the San Marcos River. ....	90
Figure 3-5. Comal River historical total system discharge (blue) and modeled total system discharge (red [No Action] and green [HCP Phase I bottom up package]) presented in the HCP. Period 1966 to 1979 exhibits mean total system discharge of 225 cfs for HCP Phase I scenario over 13-years. ....	91
Figure 3-6. As Fig. 3-5 for San Marcos River. Period 1961 to 1974 exhibits mean total system discharge of 140 cfs for HCP Phase I scenario over 13-years.....	91
Figure 3-7. Schematic flow chart of operation of Fountain Darter Modeling System .....	93
Figure 3-8. Model predictions of number of juvenile + adult fountain darters within the Old Channel Study Reach of the Comal River under baseline, HCP long-term average, and HCP drought scenarios .....	96
Figure 3-9. Model predictions of number of juvenile + adult fountain darters within the Upper Spring Run Study Reach of the Comal River under baseline, HCP long-term average, and HCP drought scenarios .....	97
Figure 3-10. Model predictions of number of juvenile + adult fountain darters within the Landa Lake Study Reach of the Comal River under baseline, HCP long-term average, and HCP drought scenarios .....	98
Figure 3-11. Model predictions of number of juvenile + adult fountain darters within the City Park Study Reach of the San Marcos River under baseline, HCP long-term average, and HCP drought scenarios .....	99
Figure 3-12. Model predictions of number of juvenile + adult fountain darters within the IH 35 Study Reach of the San Marcos River under baseline, HCP long-term average, and HCP drought scenarios .....	100
Figure 3-13. Model predictions of number of fountain darters within the Old Channel Study Reach of the Comal River under high temperature, bad vegetation, and combined adverse scenarios.....	102
Figure 3-14. Model predictions of number of fountain darters within the Upper Spring Run Study Reach of the Comal River under high temperature, bad vegetation, and combined adverse scenarios.....	103
Figure 3-15. Model predictions of number of fountain darters within the Landa Lake Study Reach of the Comal River under high temperature, bad vegetation, and combined adverse scenarios.....	104

Figure 3-16. Model predictions of number of fountain darters within the City Park Study Reach of the San Marcos River under high temperature, bad vegetation, and combined adverse scenarios.....105

Figure 3-17. Model predictions of number of fountain darters within the IH 35 Study Reach of the San Marcos River under high temperature, bad vegetation, and combined adverse scenarios.....106

Figure 4-1. Upper Spring Run reach.....116

Figure 4-2. Landa Lake Floating Vegetation Mats .....117

Figure 4-3. Old Channel Environmental Restoration and Protection Area .....118

**List of Tables**

Table 2-1. Hydraulic model simulation flows (cfs) for the Comal and San Marcos study reaches ..... 21

Table 2-2. List of species being modeled in the Comal and San Marcos systems. .... 24

## List of Appendices

APPENDIX A: Key Decision Points.....	132
APPENDIX B: Submerged Aquatic Vegetation Modeling – Technical Supplement .....	138
APPENDIX C: Fountain Darter Submodel – Technical Supplement .....	181

# 1 Introduction

The goal of the Edwards Aquifer Habitat Conservation Plan (HCP) Ecosystem Modeling project is to develop a mathematical model of key elements of the Comal and San Marcos riverine ecosystems, which can then be employed to estimate the effects of prescribed spring flow regimes for these rivers. Put another way, the model needs to be capable of depicting *responses* of key components of the river ecosystem to various external factors (including scenarios of Covered Activities, see Edwards Aquifer Recovery Implementation Program, EARIP, 2012), which can be used to *assist* the management of the Edwards Aquifer. In particular, this model will address the efficacy of the HCP Phase 1 flow regimes in meeting the biological goals for the Covered Species (EARIP, 2012).

The model was envisioned to be organic, that is, to develop over time to meet expanded requirements of management of the aquifer and the rivers, to incorporate new results from research and monitoring programs, and to address emerging scientific issues of the river ecosystems. The first stage of model formulation and development, reported here, focuses on the endangered fountain darter (*Etheostoma fonticola*) as the principal species whose response must be determined, for which the set of controls governing the response is the characteristics of stream habitat.

## 1.1 The Study Reaches of the Comal and San Marcos Rivers

Three study reaches of the Comal River and two study reaches of the San Marcos River were selected for model development and application. The study reaches on the Comal are indicated on aerial photography in Figure 1-1, and those on the San Marcos in Figure 1-2. These reaches provided a diversity of habitat conditions as well as various anthropogenic influences. Each reach selected has had intensive biological data collected since 2000. Detailed descriptions of each study reach and data collected over time are presented in BIO-WEST (2001a,b – 2017 a,b). Brief summaries of key features and functions per reach are presented below.



**Figure 1-1. Comal River Study Reaches (Old Channel, Landa Lake, and Upper Spring Run)**

The Upper Spring Run reach of the Comal River, see the location map of Figure 1-3, is the first reach in either system to experience impacts from low flow conditions. In 2014, for example, nearly five consecutive months occurred of less than 2 cubic feet per second (cfs) total discharge, resulting in impacts to aquatic vegetation and reduced densities of fountain darters (BIO-WEST, 2015a). Since then, vegetation and fountain darters have responded favorably to the return of above average discharge conditions (BIO-WEST, 2017a).

The Landa Lake reach, Figure 1-4, has supported very static high quality fountain darter habitat conditions over the past 15 years (BIO-WEST, 2017a). This reach also maintains some of the deepest areas of the system which are anticipated to support wetted area at very low discharges. Only limited recreational activity is present in this reach. Finally, this reach supports an immense amount of aquatic vegetation biomass, which has raised some water quality concerns should a die-off occur during low-flow conditions.

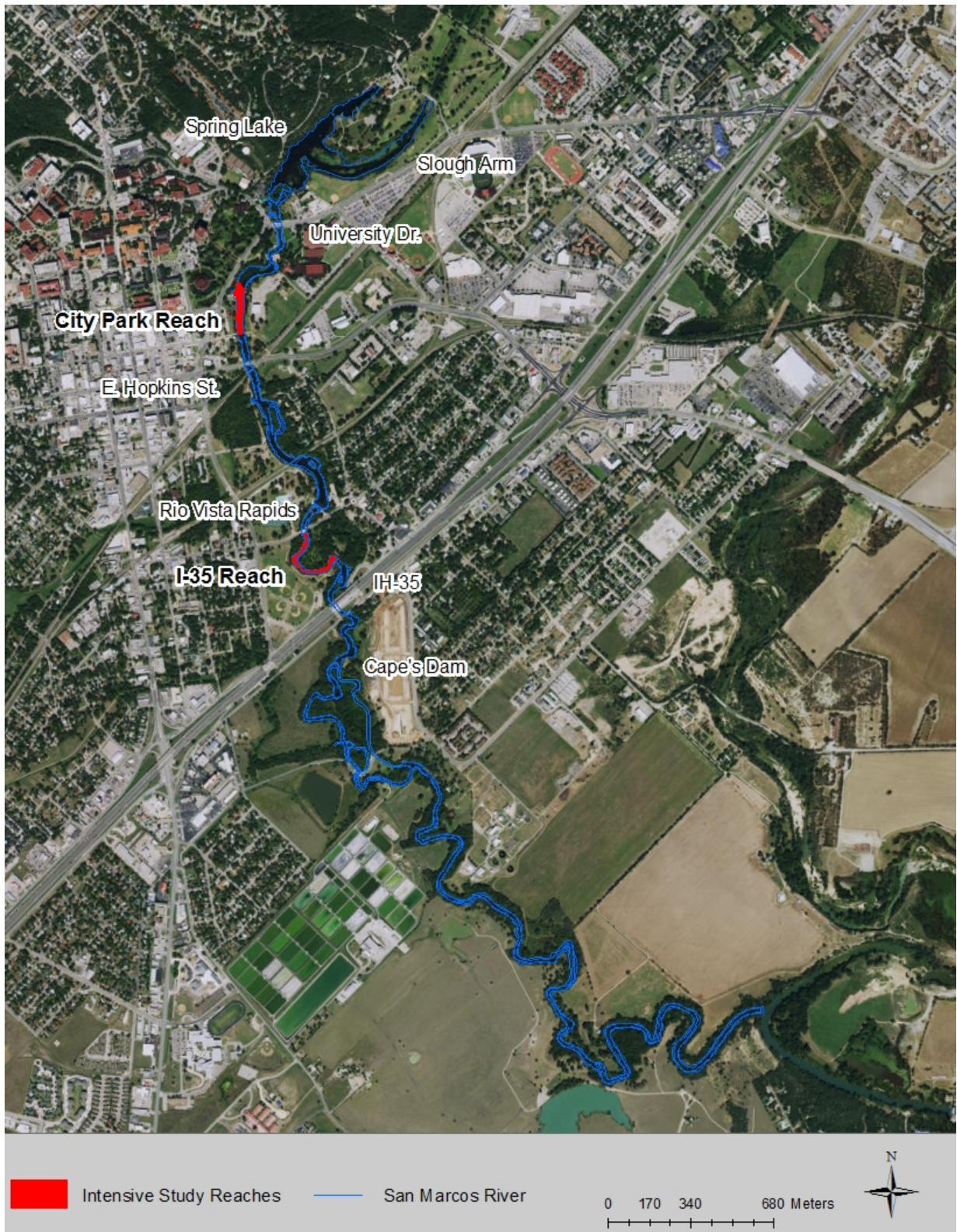


**Figure 1-2. San Marcos River Study Reaches (City Park and I35)**

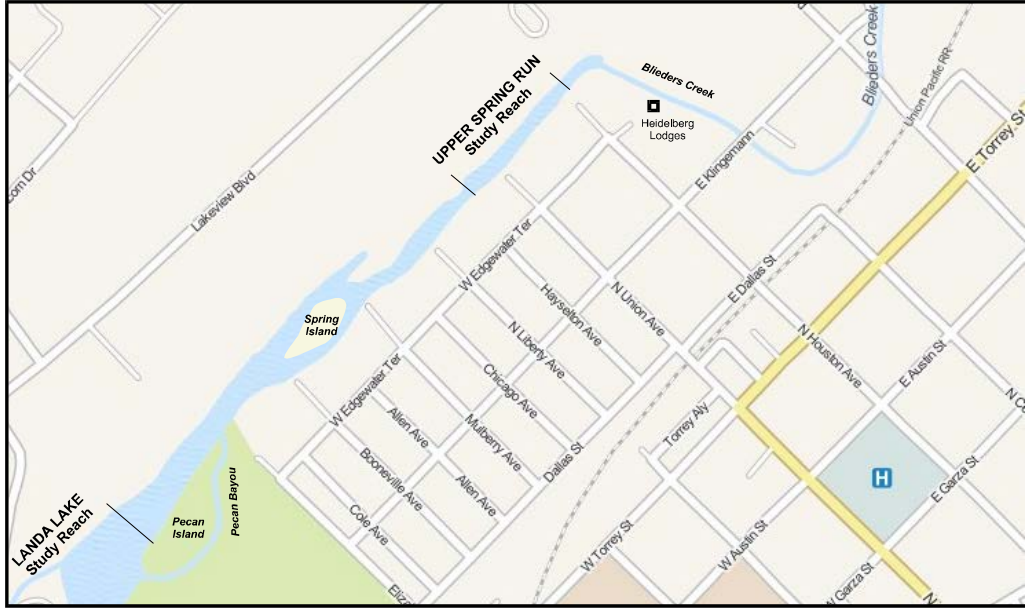


**Figure 1-3. Location map of Upper Spring Run study reach on Comal River**



**Figure 1-4. Location map of Landa Lake study reach on Comal River**

The Old Channel study reach is located on the natural channel of the Comal River, see Figure 1-5. A fairly constant flow is maintained in the Old Channel reach due to various diversion structures. Similar to Landa Lake, only limited recreational activity is present in this reach. Historically, high quality fountain darter habitat has been found here, but a new culvert structure resulted in altered flow conditions during the wet period of 2003 - 04. This caused drastic changes to aquatic vegetation, and upon return to more typical flow conditions the vegetation changed from native to non-native, resulting in decline of fountain darter habitat (BIO-WEST, 2007c). The Old Channel study reach comprises the downstreammost extent of the Environmental Restoration and Protection Area (ERPA) highlighted in the HCP. Extensive HCP habitat restoration is presently being conducted in the entire ERPA which is confined to the old channel of the Comal River.

The City Park reach of the San Marcos River, Figure 1-6, is heavily recreated, and thus experiences considerable changes in aquatic vegetation from spring to fall and then back to spring each year (BIO-WEST, 2017b). This study reach has exhibited relatively low quality fountain darter habitat over time, in part a result of higher flows along with large quantities of non-native vegetation.

The I-35 reach of the San Marcos River, Figure 1-7, historically supported higher quality habitat than City Park, with less overall recreation (BIO-WEST, 2017b). This reach also has a more natural channel with riparian coverage and channel meanders, as opposed to the straight channel with concrete bulkheads and limited tree coverage of the City Park reach. This reach historically supported a more diverse community of aquatic vegetation. The I-35 reach has experienced significant flow-related changes to fountain darter habitat since the reconstruction of Rio Vista Dam in 2006 (BIO-WEST, 2013b).

Basic model development was carried out on the Old Channel (Comal) and City Park (San Marcos) reaches. Models of the remaining three reaches were then created based upon the experience from the first two reaches.



**Figure 1-5. Location map of Old Channel study reach on Comal River**

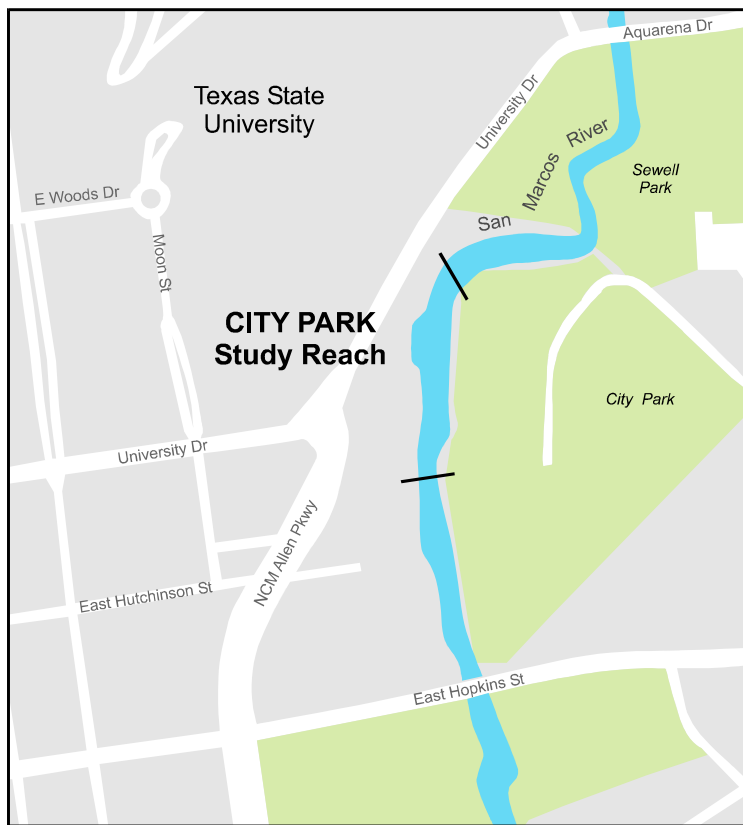


**Figure 1-6. Location map of City Park study reach on San Marcos River**

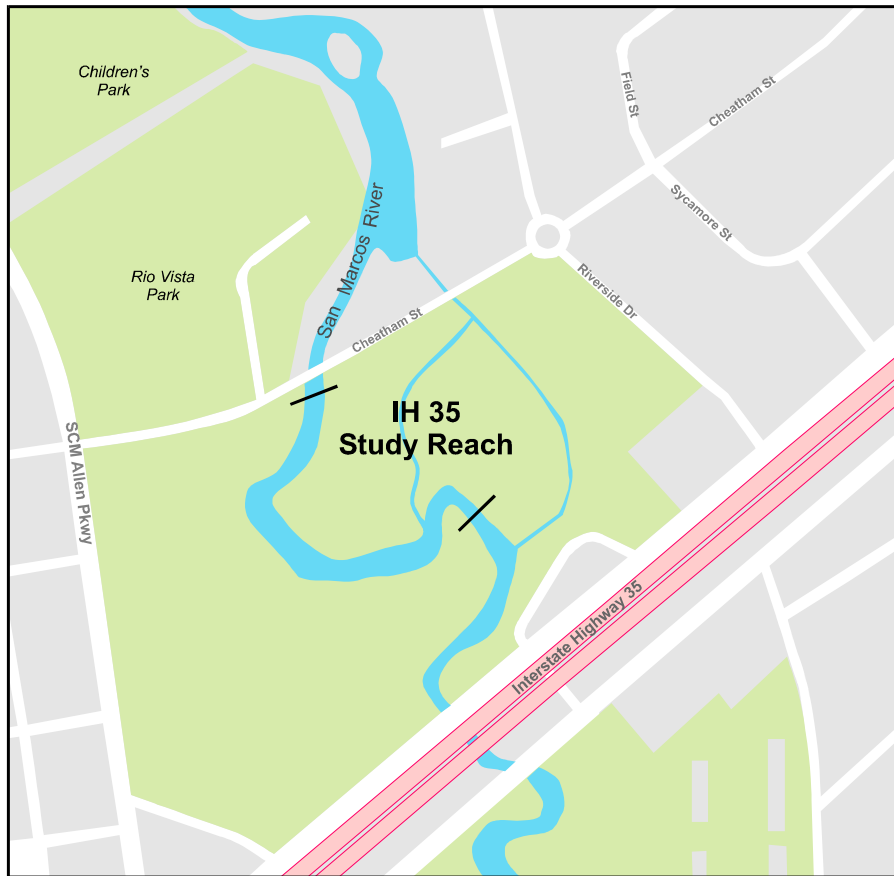


**Figure 1-7. Location map of IH 35 study reach on San Marcos River**

## **1.2 Strategy and conceptual basis of the model**

At the outset, several attributes were considered fundamental to the model's meeting its goal as a utilitarian management tool. First, the model formulation is founded on the principle of determinism, that is, the model is intrinsically mechanistic. This means that the key causal relations are explicitly depicted in the model.

Second, the model development exploits the substantial empirical resources on these river systems, especially the field data collections and laboratory studies carried out under the auspices of the HCP. Despite the mechanistic philosophy of model formulation, statistical inferences are important in establishing the basic relationships represented in the model. Field and laboratory data are used to assess the dependencies of physical and biological variables, whose relations are parameterized in various statistical submodels. Field data are also used to test the predictive capability of the model, and to quantify its residual uncertainty.

Third, due to the mathematical complexity of the model, as well as to facilitate its application in the management enterprise, the model is implemented as a set of numerical solutions on a personal computer (with enhanced processor and memory, as necessary), using special-purpose software. Generally, these model solutions exhibit variation in both space and time, in order to depict the ecosystem response to *scenarios* of springflow and surface-water hydrology time histories, as a function of the various physiographic configurations in these river systems.

Fourth, model operation, that is, the specification of various categories of model inputs, and the compilation and display of model outputs, is accomplished by a graphical user interface (GUI) with standardized user-tolerant protocols. The philosophy of model development and application generally follows Grant and Swannack (2008).

Development began with the formulation of a conceptual model of the river ecosystem as it affects the fountain darter. This conceptual model (as well as its submodels, to be addressed later) has been repeatedly revised during the course of the project, the present version of which is shown in Figure 1-8. Oblong boxes indicate external controls (“inputs”), which may originate from data (perhaps involving a separate model) or by direct specification. The boxes identify the key submodels, whose development proceeded separately at the outset of the project. (Two of these, the hydraulic and water quality submodels, were developed by previous USFWS and HCP projects, and adapted for use in the present work.) Ovals indicate variables predicted by the submodels (“output”). The arrows show the direction of causality, and can also be regarded as the flow of information.

The fundamental causal schema is FLOW → HYDRAULICS → WATER QUALITY → VEGETATION → FOUNTAIN DARTERS. (There are several alternate causal pathways that differ in detail, involving the numerous variables in each submodel, but this fundamental schema applies to all.) The ecosystem submodels have full dependency upon both space and time, but these dimensions of the model are suppressed in the causal-connection (information-flow) diagram for clarity, e.g. Fig. 1-8. Each of the main submodels will be addressed separately in this report.

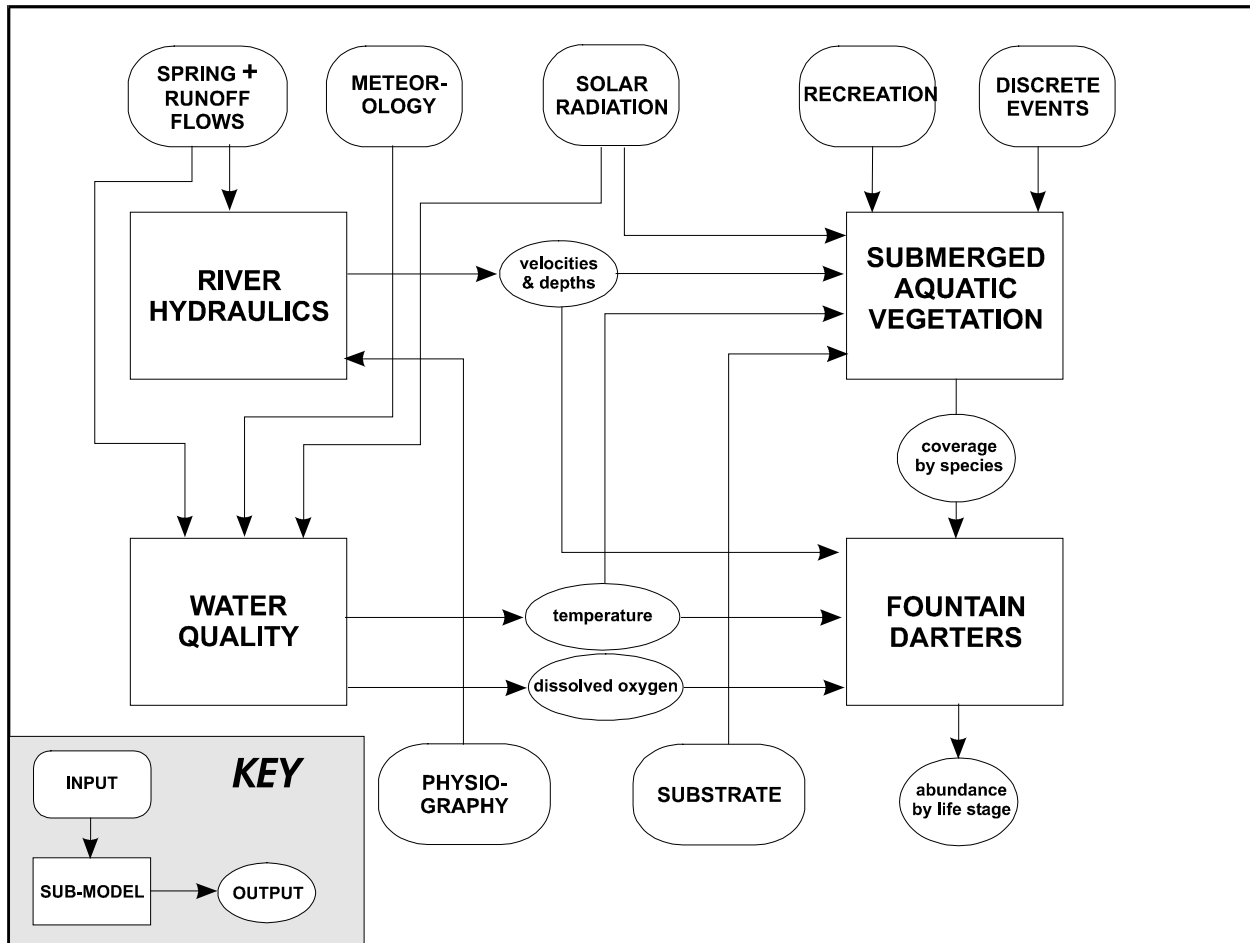


Figure 1-8. Conceptual model of Comal or San Marcos river ecosystem as it affects the fountain darter

### 1.3 Key Decision Points

Throughout the process of model development, a series of decisions on model formulation and implementation were confronted. Some of these decisions were matters of technical detail and were resolved or informed by a series of specifically targeted HCP applied research projects. These specific projects were summarized in the Interim Report (BIO-WEST, 2015c) with full reports provided as appendices. In other cases, upon further evaluation and sensitivity analysis it was revealed that certain decisions did not have a crucial impact on model development. However, some remain key decisions that represent forks in the road of model development. The major decisions are summarized in Appendix A.

## 2 Model Components, Structure and Function

### 2.1 Main Components

This section provides an overview of the general formulation of the fountain darter modeling system (FDMS), with brief summaries of the four main submodels, internal operations, and information exchange. Detail is provided in Section 2.2, following. General background on modeling and its application are addressed by Grant and Swannack (2008).

#### 2.1.1 Hydrology and hydraulics

There are two levels of characterization of the movement of water through the river systems, which differ in their scale of coverage and in their time-space resolution. First is the hydrology, that is, the large-scale water inflows, outflows and internal transfers in the river system, including both surface flows developed from runoff, and spring flows from groundwater (see, e.g., Dingman, 2002). Hydrology is determined basically from field data and water-budget analyses of the two rivers and their subreaches. From the standpoint of model development and operation, hydrology is one of the principal inputs to the models. The basic modeling scenarios are defined to a large extent by hydrology. (Hydrology is detailed in the Interim Report, BIO-WEST et al., 2015c, and citations therein.)

One hydrological scenario of considerable importance in the development and evaluation of the FDMS is the historical observed flows in each river, particularly since 2000, encompassing the period of intensive data-collection in the two rivers. Specifically, we identify the 11-year period 2003-2013 as the historical or baseline scenario. This is used for model calibration and evaluation, and is also a useful diagnostic scenario with a high range of hydrometeorological conditions, including flood events and intense drought periods. Additional scenarios for various modeling exercises are detailed in Section 3.1.

The second level of characterization of water movement is hydraulics, that is, the detailed water velocities and water levels along and across the river channel, delineating its transverse movements. The necessary time-space resolution cannot be obtained from field measurements, at least practically, so numerical simulations approximate these velocities and water levels. The

USGS Multi-Dimensional Surface-Water Modeling System (MDSWMS) Flow and Sediment Transport and Morphological Evolution of Channels (FaSTMECH) computational model was used to simulate water-surface elevation, depth water depth and depth-averaged water velocity (McDonald et al. 2005, 2006). This software solves the two-dimensional steady-state, depth-averaged Navier-Stokes equations, which are the governing equations of fluid motions expressing the principle of conservation of momentum in fluid flow (Batchelor, 1967). These equations are solved at each node of a user-defined computational curvilinear mesh. Models were calibrated by adjusting each site's variable roughness height via a multiplier until the predicted water surface elevations matched observed water surface elevations (+/- 0.05 m). Lateral eddy viscosity and water surface drag coefficient input parameters were also adjusted to improve model fit. Model predictions were iteratively compared to water surface elevations during the calibration process. Calibrated models were run for 6,000 iterations and converged with less than one percent mean error in the computed versus simulated discharge at each calibration flow.

The need for a sophisticated, laterally detailed hydraulic model for the Comal and San Marcos rivers had been anticipated from the increasing reliance on such models over the past quarter century in the determination of stream flows needed to maintain (or attain) healthy fluvial ecosystems, i.e., "environmental flows" (Annear et al., 2004; Committee of Review etc., 2005). This was an outgrowth of the PHABSIM method, in which such a model was central to quantifying habitat suitability, founded on hydrologic triggers of life-stage development in aquatic organisms, particularly fish (Milhous et al., 1984; Jowett, 1997). In Texas, this method has figured prominently in the scientific basis for flow standards as part of the Senate Bill 3 (SB3) studies on major river basins (e.g., GSA BBEST, 2011; CL BBEST, 2011).

As noted earlier, the five study reaches are implemented in the USGS MDSWMS hydraulic modeling platform (see Hardy, 2010, Hardy et al., 2010, and BIO-WEST et al., 2015c). The model operates on a detailed curvilinear grid, locally rectilinear, with nominal resolution of 0.25 m, Figure 2-1 (Hardy et al., 2010). It was desirable that this same curvilinear grid be used for the SAV and darter submodels, but at a coarser resolution. (See *Fountain darter model grid* in Appendix A.)

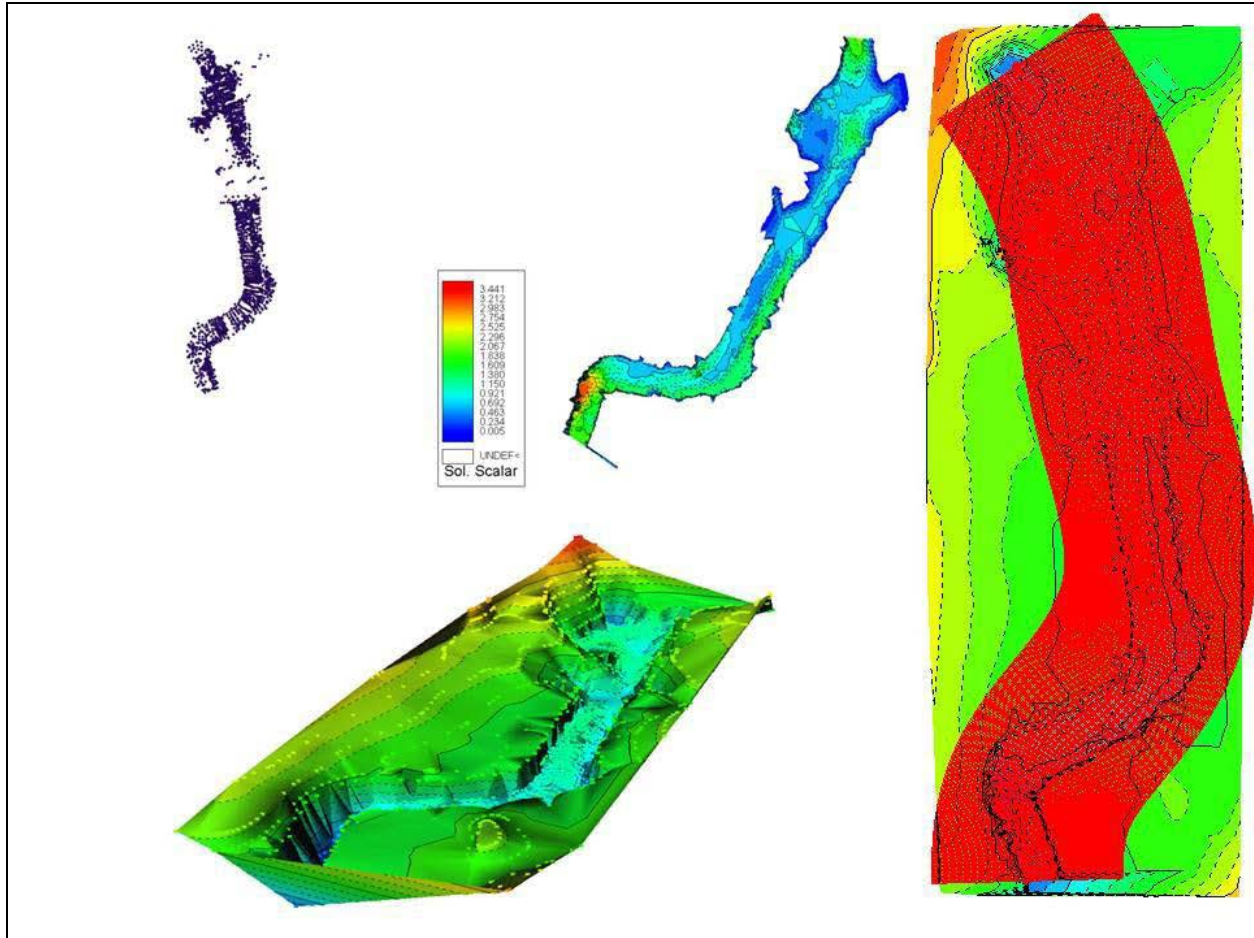


**Figure 2-1. Example of field-measured topography points (above left), depth contours (above center), computational mesh overlay mapped onto topography (right), 3-dimensional numerical grid geometry used in MDSWMS hydraulic model (lower left) for the Sewell Park section of the San Marcos River, from Hardy et al. (2010)**

The consensus of the modeling team was that representing the environmental data at 1-m spacing would be a satisfactory compromise between approximate depiction of darter abundance and computational overhead of the darter model. Therefore, the original 0.25-m computational grid points for the hydrodynamic model (including substrate properties) were subsampled to derive 1-m resolution grids for output files to the fountain darter model. This was accomplished by extracting the corresponding grid points at 1 m increments from the orthonormal rectilinear grid structure (see BIO-WEST et al., 2015c).

**Table 2-1. Hydraulic model simulation flows (cfs) for the Comal and San Marcos study reaches**

	<i>Comal</i>			<i>San Marcos</i>	
	<i>Upper Spring Run</i>	<i>Landa Lake</i>	<i>Old Channel*</i>	<i>City Park</i>	<i>I35</i>
	1.7	25.4	10	30	30
	3.4	49.99	20	45	45
	5.7	74.15	30	50	50
	42.9	99.97	35	55	55
	86.7	224.1	40	60	60
			45	70	70
			50	80	80
			55	90	90
			60	100	100
			70	120	120
			80	140	140
				160	160
				180	180
				200	200
				220	220
				240	240
				260	260

\* For the Old Channel, hydraulic runs are available at 1 cfs increments. These were mainly employed in model development, but are available to the user.

Running the hydraulic models in dynamic mode required an unacceptable cost in computational time for direct linkage with the fountain darter submodel. As an alternative, the hydraulic model for each study reach was run at a number of steady state solutions for target discharges for each river system, and these pre-computed solutions were formatted for use within the fountain darter model. These “standard” discharges are tabulated in Table 2-1.

The original hydraulic models were calibrated to existing vegetation type and distribution (Hardy et al., 2010). The hydraulics do not change in response to SAV distribution/type during simulations. That is to say the hydraulics are fixed based on the conditions at the time the models were originally calibrated. Attempting to recalibrate or simulate the hydraulics on the fly during simulations is computationally infeasible.

### **2.1.2 Water quality**

For the purposes of determining the sufficiency of the HCP (Phase 1) flow levels for maintaining the population of fountain darters, two water quality parameters were considered to be crucial, *viz.* temperature and dissolved oxygen (DO). Each of these is potentially impacted by low spring flows and the associated reduced water depths under drought conditions. Under these conditions, we do not anticipate effects arising from, for example, altered nutrient concentrations or various toxics. (We note that both rivers lie in urban areas and may eventually be exposed to excessive loads, but this is currently beyond the scope of this HCP Phase 1 modeling effort.)

As with the hydraulic model, it was judged more efficient to separate the actual operation of the water quality model from that of the vegetation and darter models by first computing temperature and DO values over the entire simulation period based upon hydrology and meteorology. The QUAL2E models for each of the Comal and San Marcos rivers (see Hardy et al., 2010, and BIO-WEST et al., 2015c) were adopted for use in the present project. The original models were calibrated to hourly data for a typical summer low flow condition and then used to simulate the 2009 calendar year for use in the evaluation of HCP flow regimes for both systems. As noted in Hardy et al. (2010) predicted versus observed sub-daily temperature data were generally within 0.5 – 1.0 °C within each of the five study reaches. Calibration involved iterative changes to the dust attenuation coefficient, reaeration rates, and dispersion coefficient. Channel geometric parameters were obtained from the measured field data on width, depth and velocity profiles collected during field measurements of hydraulic model calibration data and averaged over the longitudinal extent of each computational reach in QUAL2E. In the present project, the models were extended to cover the entire January 1, 2003 through December 31, 2013 historical simulation period. The validation work on these models is summarized in BIO-WEST et al. (2015c) and citations therein, where it is remarked that the data base for DO was inadequate for a thorough validation of the model.

The computational depiction of a watercourse in QUAL2E is a link-node configuration, in which the river is divided into a network of reaches of uniform hydraulic, thermodynamic, and kinetic properties, each reach being depicted by a longitudinal series of computational

elements of uniform length. The model depicts the water-quality variables as cross section means, averaged in turn over each computational element of the network. The implicit assumption is that the spatial variation in water quality varies on such a large spatial scale that each reach may be considered uniform. The study reaches are represented in the model segmentation as: for the Comal, Upper Spring Run, QUAL2E Reach 3; Landa Lake, QUAL2E Reaches 5 and 7, combined; and Old Channel, QUAL2E Reach 20; for the San Marcos, City Park, QUAL2E Reach 7; and IH 35, QUAL2E Reach 9. The complete segmentation is presented in BIO-WEST et al. (2015c).

QUAL2E is a quasi-steady-state model, in which river flow, kinetics, waste loads and dispersion are assumed constant in time, but a diurnal variation in insolation is used which drives a diurnal variation in water temperature and in a turn a diurnal variation in oxygen solubility (Chapra, 1997). The output from QUAL2E is simplified for the FDMS, as flat files (ASCII-encoded text files) containing minimum, average and maximum daily water temperature and minimum daily DO at each study reach. These associated daily values are then provided as flat-file inputs to the SAV and/or fountain darter submodels.

### ***2.1.3 Submerged aquatic vegetation submodel***

Submerged aquatic vegetation is considered one of the major drivers of fountain darter population dynamics by serving as shelter and by providing habitat for aquatic invertebrate prey. Given the importance of SAV in the fountain darter life cycle, understanding the factors that affect SAV persistence is paramount for successful aquatic ecosystem management in the Comal and San Marcos rivers. The role of SAV in the overall conceptual model of fountain darters is shown in Figure 1-8. A detailed conceptual model of the SAV component alone is displayed in Figure 2-2. Its elements are summarized here, basic structural information presented in Section 2.2.1, and detail given in Appendix B.

The SAV submodel simulates vegetation growth, density, and colonization of several important SAV species found in the spring-fed Comal and San Marcos rivers, see Table 2-2. The model is process-based with stochasticity. It is spatially-explicit, i.e., geo-referenced and grid-based with a cell size of 1 m<sup>2</sup>, using the same grid system as the fountain darter model (see Section 2.1.4), in turn subsampled from the hydraulic model grid.

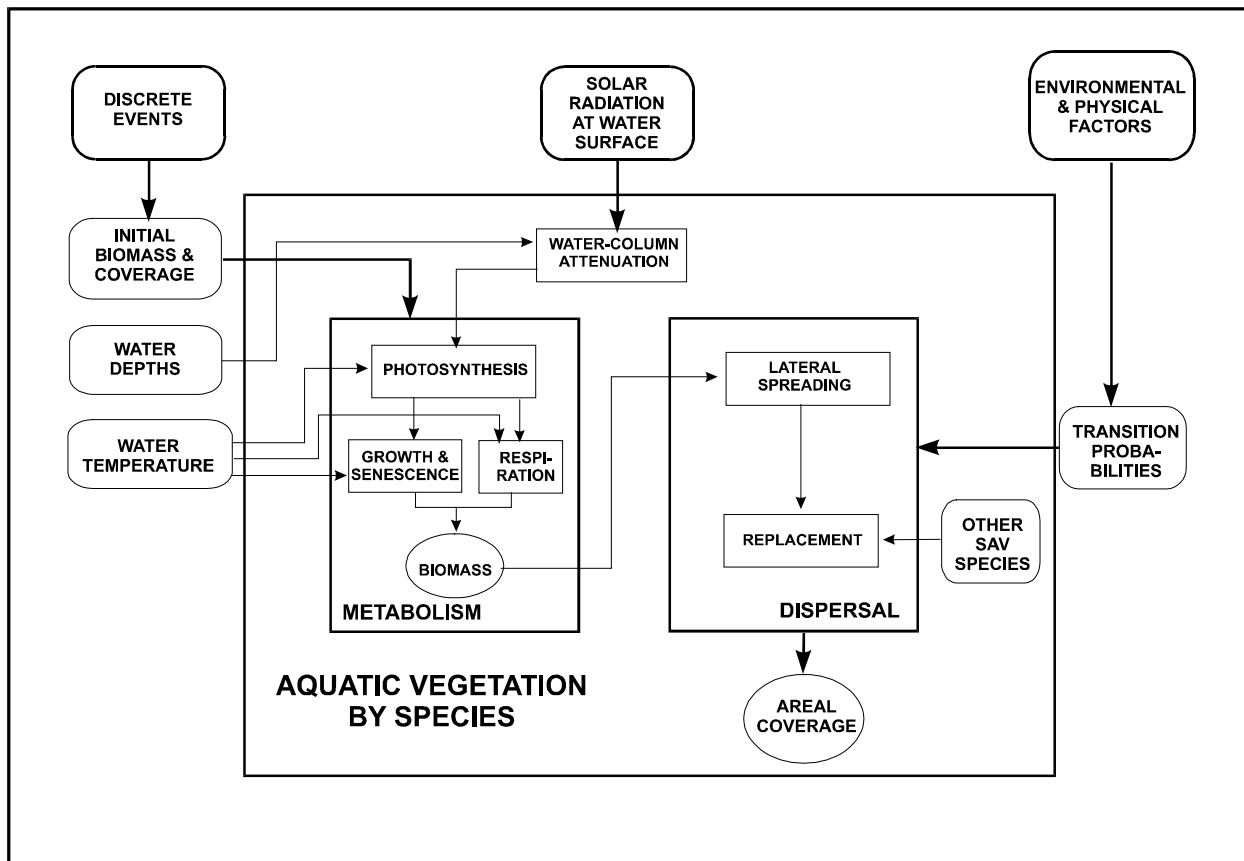


Figure 2-2. Submerged Aquatic Vegetation (SAV) conceptual submodel

Table 2-2. List of species being modeled in the Comal and San Marcos systems.

Cabomba	Potamogeton
Hydrilla	Sagittaria
Hygrophila	Vallisneria
Ludwigia	Zizania (Texas wild rice)

The formulations for the SAV model are based on earlier models (Best and Boyd, 1996; 1999; 2001; 2003; 2007; 2008; Scheffer et al., 1993; van Nes et al., 2003), but have been modified for clear water, spring-fed, limited-temperature-range conditions of the two study rivers. A key decision not to include nutrients in the SAV submodel was based on the general assumption that the aquatic macrophytes in the Comal and San Marcos systems are not nutrient limited. This is

based on the considerations that aquatic macrophytes get most nutrients from sediments (via roots and stems), not the water column (Barko and Smart, 1980), and that the sediments in these systems, which remain mostly undisturbed, provide the nutrients for the aquatic macrophyte communities. This assumption is supported by the abundant and vibrant aquatic macrophyte communities present in both systems. The equation used for photosynthesis is adaptable, and can add a nutrient component if sediment nutrient data becomes available contrary to our present understanding. (Note that the nutrient supply for phytoplankton is nutrients dissolved in the water column, which is a different matter.)

In aquatic systems, the availability of light is the driving factor controlling photosynthesis for both floating and rooted plants (Carr *et al.* 1997). The SAV model simulates daily accumulation of biomass through photosynthesis, which is controlled largely by photosynthetically-active solar radiation and water depth. Light attenuates with passage through water, so diminishes with depth in the water column. Irradiance follows daily and seasonal cycles, resulting in spatio-temporal patterns of light availability and growth patterns. These are internally calculated in the program code.

Maintenance respiration is needed for plants to continue to live. The model estimates maintenance respiration based on daily temperature and the biomass of the above- and below-ground sections of the plants. The difference between gross photosynthesis and maintenance respiration is the amount of assimilate available for growth.

Senescence is based on overall growth patterns and temperature. It is lowest in the summer, and highest in the winter. Death rates and their corresponding temperatures were based on existing models (Best and Boyd, 1996, 1999, 2001, 2003, 2007, 2008; Scheffer *et al.*, 1993; Teh, 2006; van Nes *et al.*, 2003;). The City Park study reach also includes a recreation mortality based on observed human recreation patterns within the reach. The model assumes disturbance associated with a recreation event causes direct mortality to plants through excess flow or human-mediated disturbance. Therefore, any plants within cells that are impacted by these events die.

Plant growth, in terms of biomass gained or lost is calculated daily as net of photosynthetic gain over losses due to respiration and mortality. Self-shading is included in the model, and is based

on species-specific light attenuation coefficients. This provides a negative feedback for growth (i.e., the more biomass that accumulates the less light reaches the lower layers of the plants).

An essential resource for this modeling work is the mapping of SAV's in the two river systems carried out under the auspices of EAA initially, and subsequently transitioned to the HCP (BIO-WEST 2001a,b – 2017a,b). Vegetation coverage by species for each reach has been mapped at least twice a year from 2000 through the present, including the eleven-year study period 2003-2013. An example of the SAV survey is shown in Figure 2-3. (Additional surveys are presented in BIO-WEST 2001a,b – 2017a,b). This data was employed to address dispersal of aquatic vegetation in the two rivers. Spatial analysis of this data indicated that both vegetation coverage and species composition were highly variable. This is apparent from the maps of total vegetation coverage (i.e., without differentiation of individual species) used for model development shown in Figures 2-4 through 2-8. There is so much variation in total SAV, i.e. without discrimination of different species, that, despite the large variation in fountain darter density among SAV types, the total SAV coverage dominates the total fountain darter numbers in the study reach.

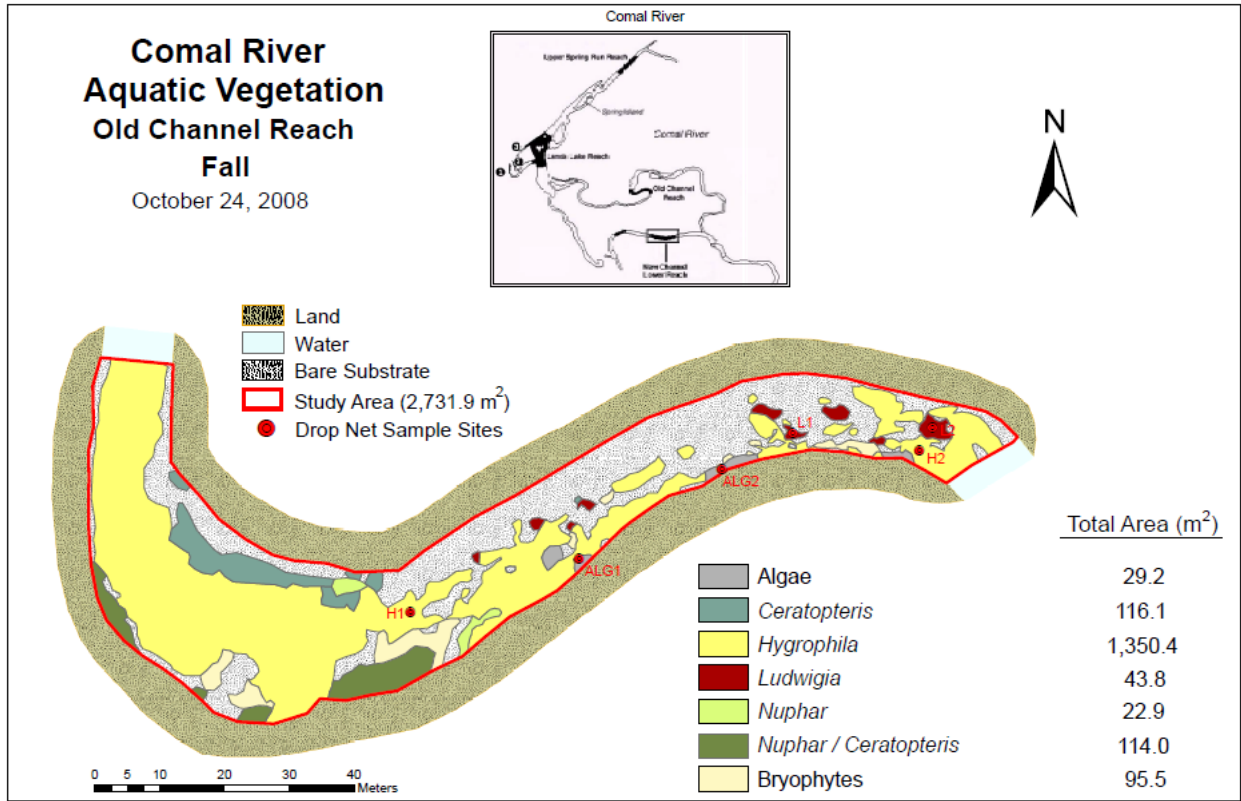


**Figure 2-3. Example of routine vegetation survey in Comal River, Old Channel study reach, Fall 2008, from BIO-WEST (2009a).**

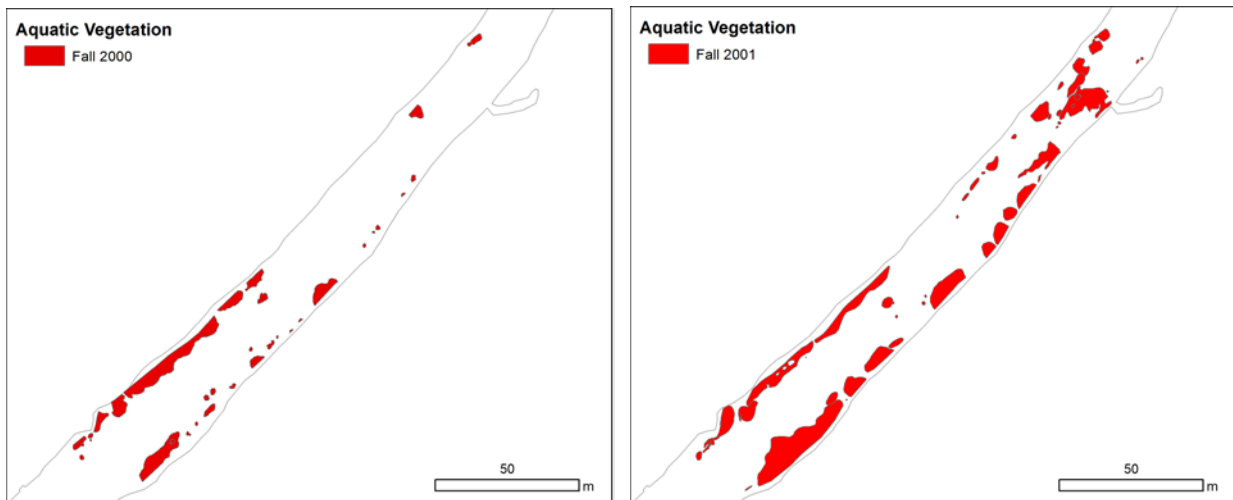


**Figure 2-4. Maps of total vegetation coverage in fall surveys, Upper Spring Run study reach in Comal River**

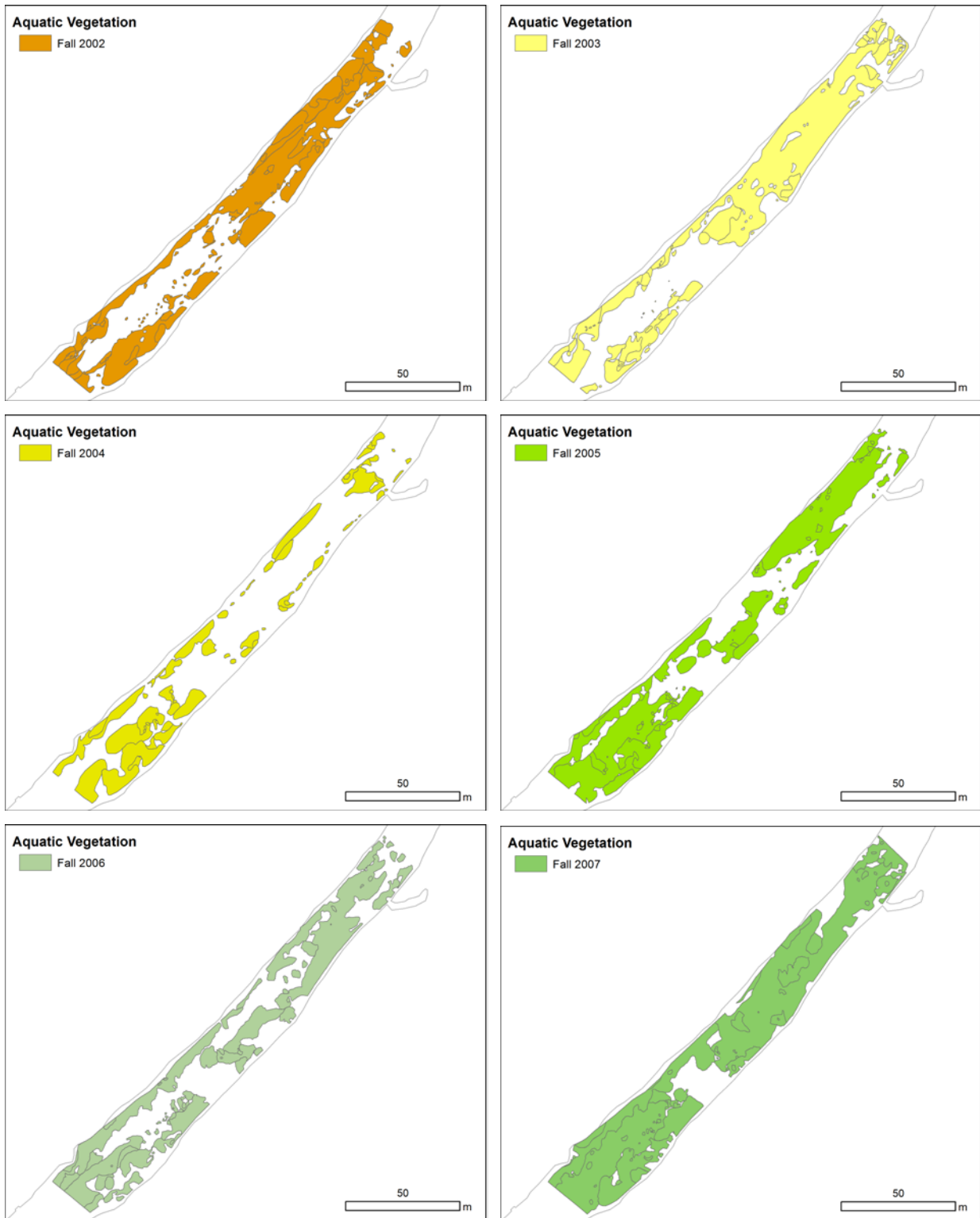


**Figure 2-4 (continued). Upper Spring Run**

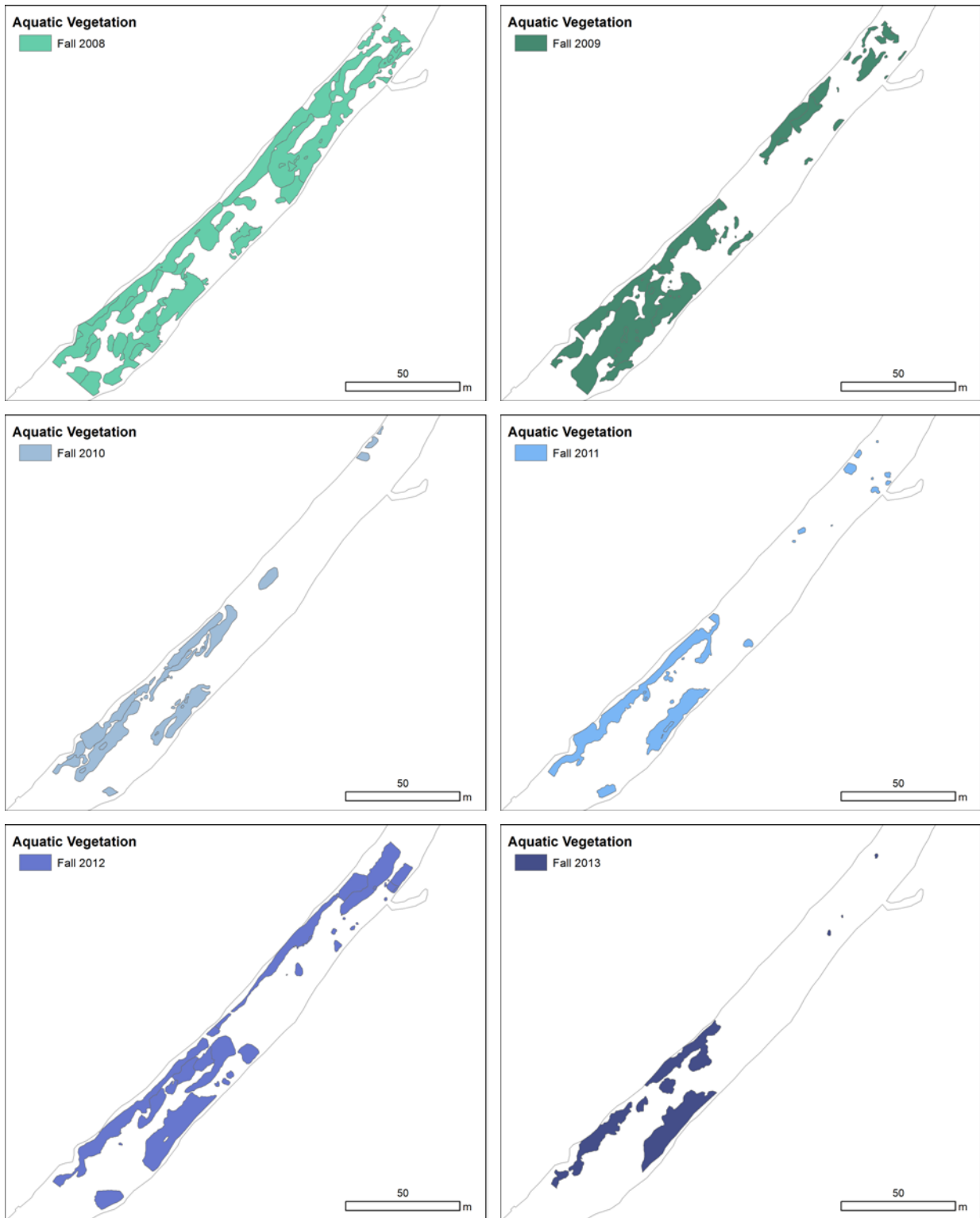


**Figure 2-4 (concluded). Upper Spring Run**

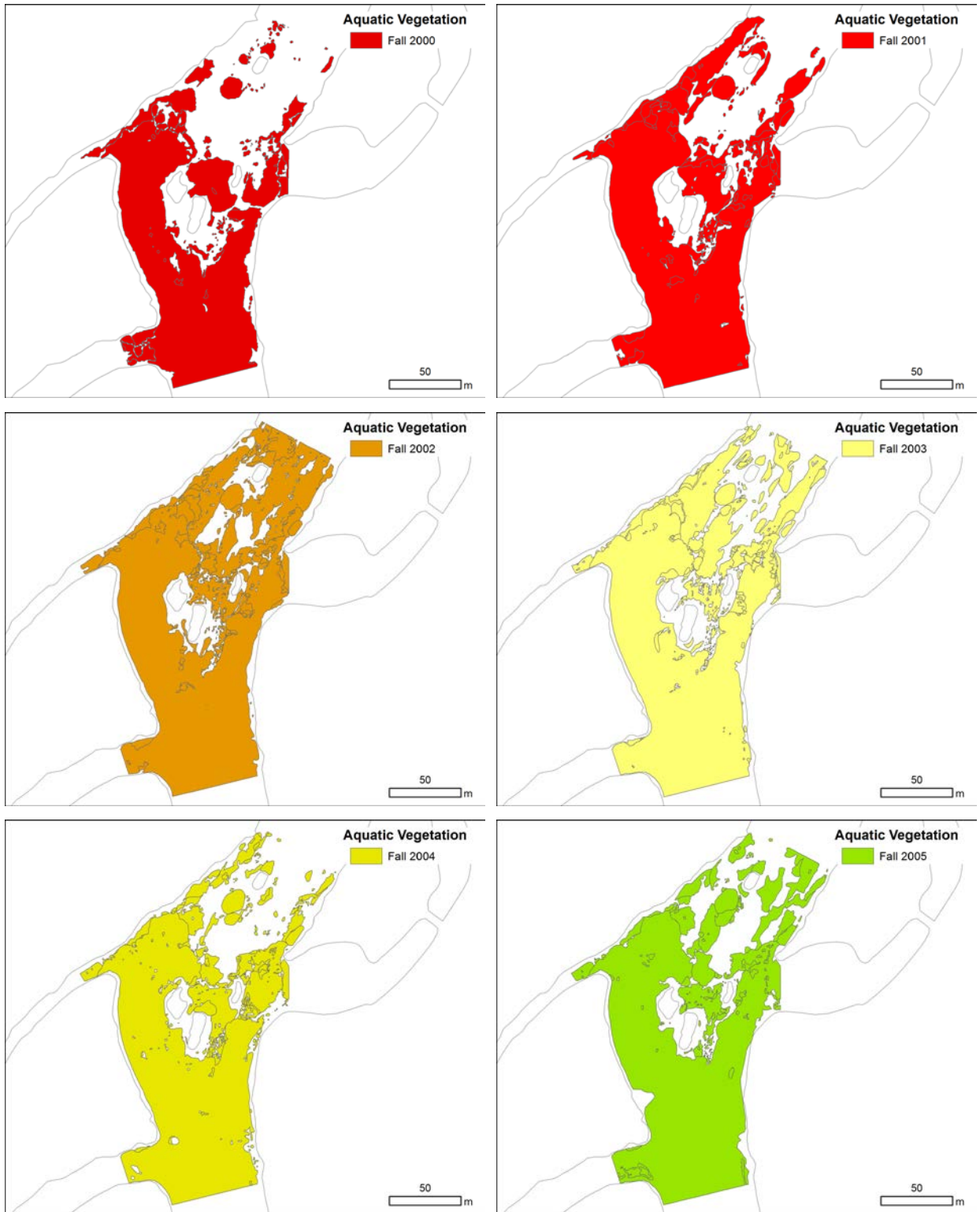


Figure 2-5. Maps of total vegetation coverage in fall surveys, Landa Lake study reach in Comal River

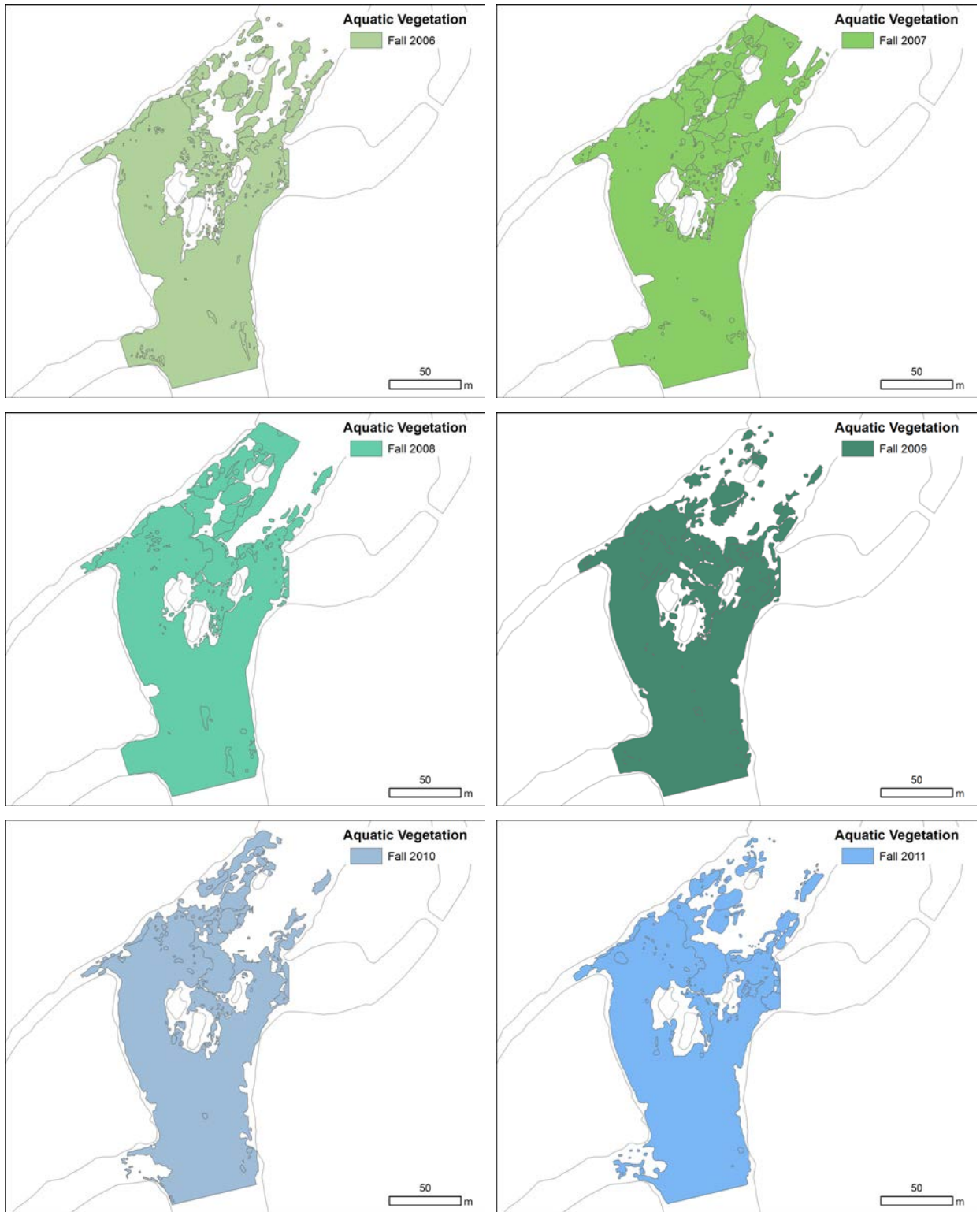


Figure 2-5 (continued). Landa Lake

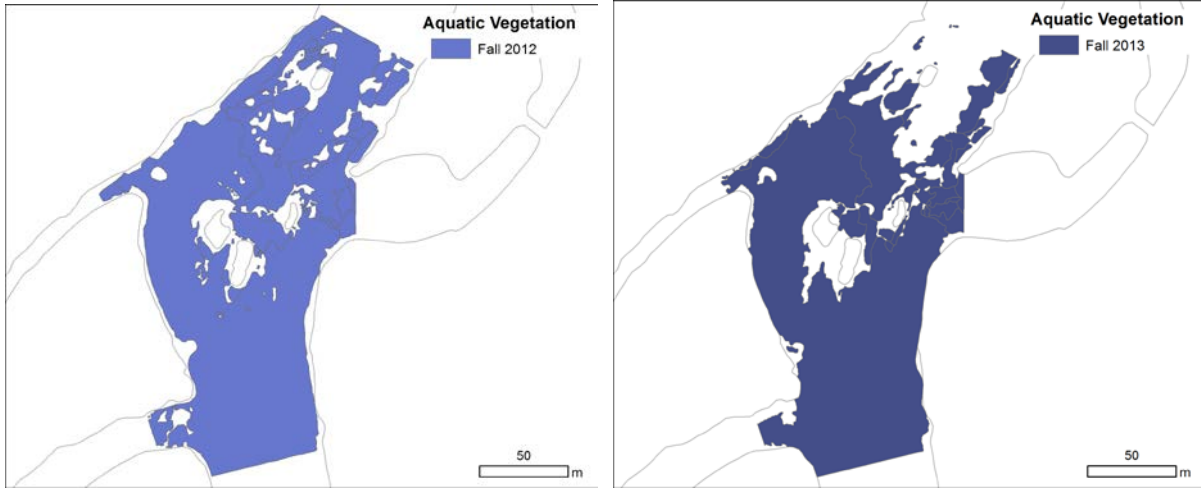


Figure 2-5 (concluded). Landa Lake

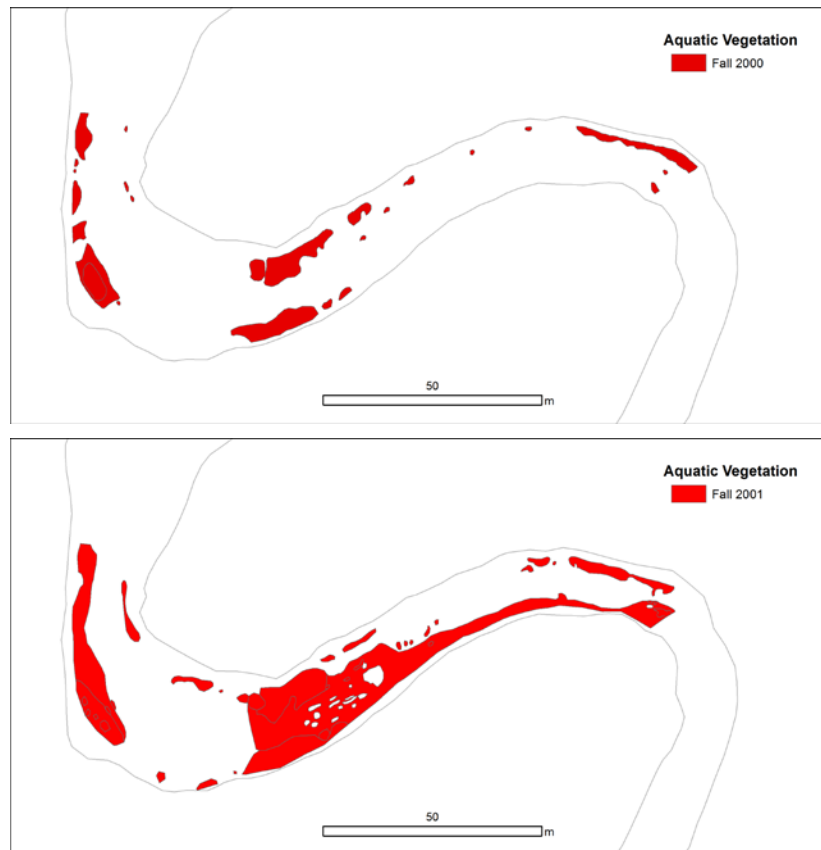
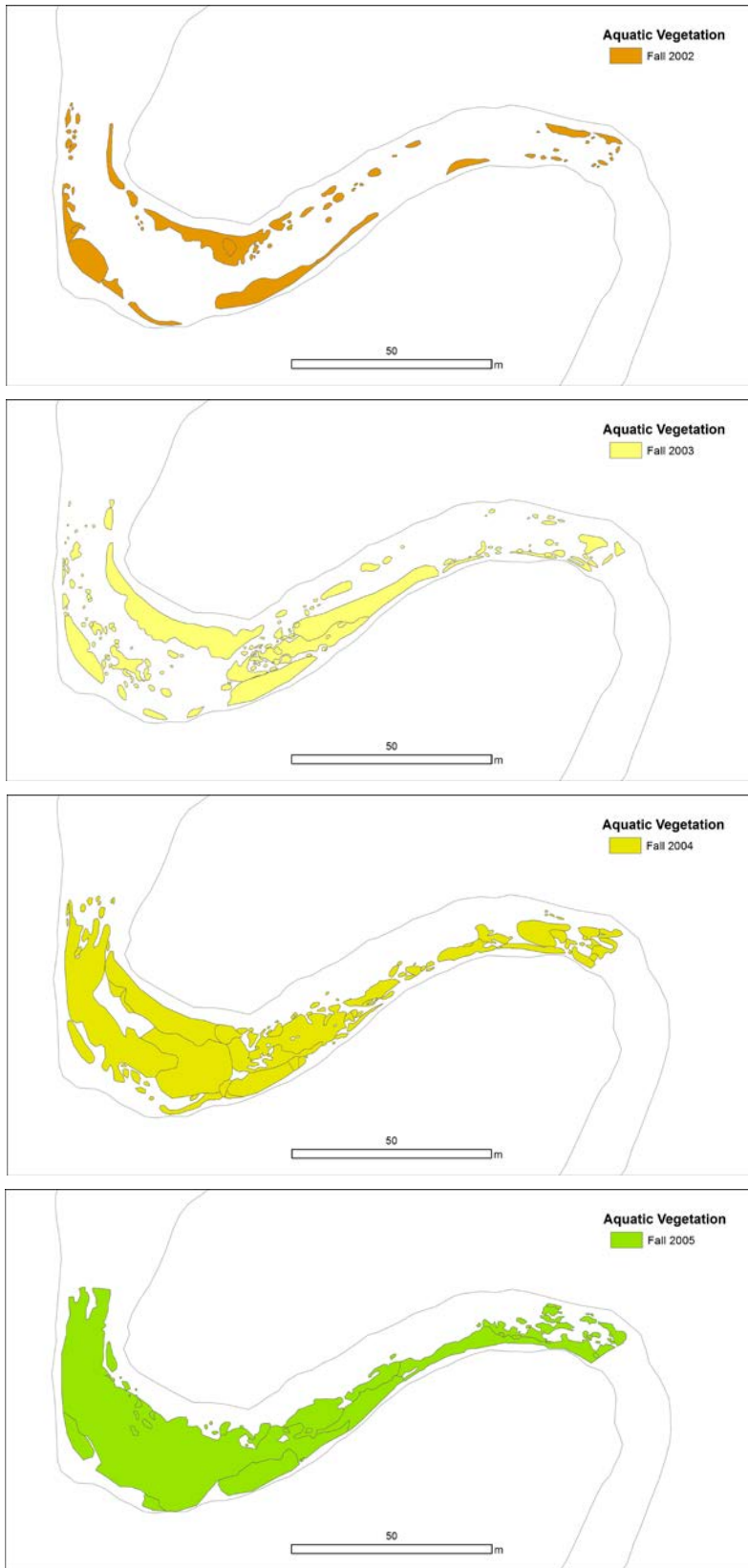


Figure 2-6. Maps of total vegetation coverage in fall surveys, Old Channel study reach in Comal River



**Figure 2-6 (continued). Old Channel**



**Figure 2-6 (continued). Old Channel**

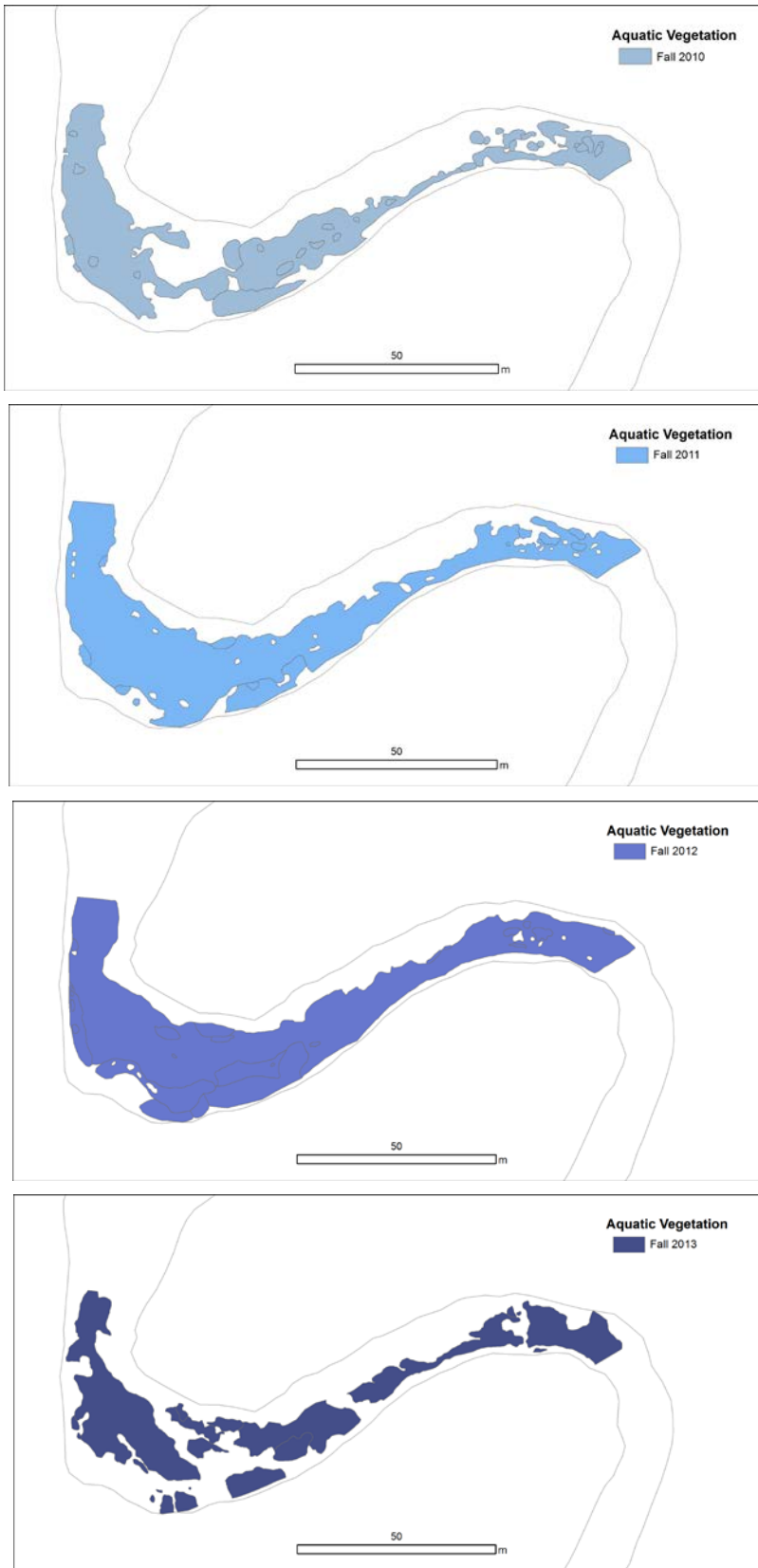


**Figure 2-6 (concluded). Old Channel**

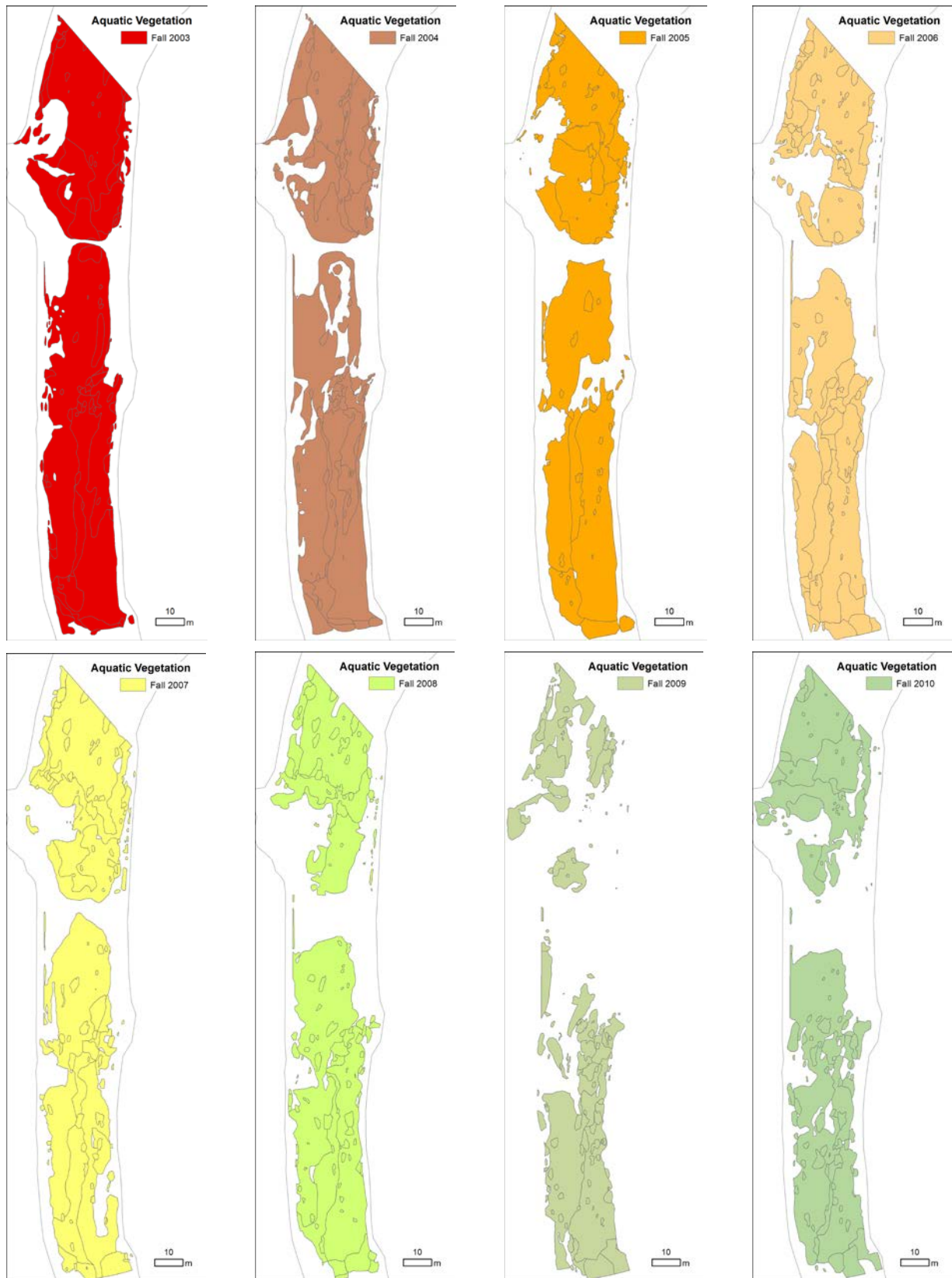


**Figure 2-7. Maps of total vegetation coverage in fall surveys, City Park study reach in San Marcos River**

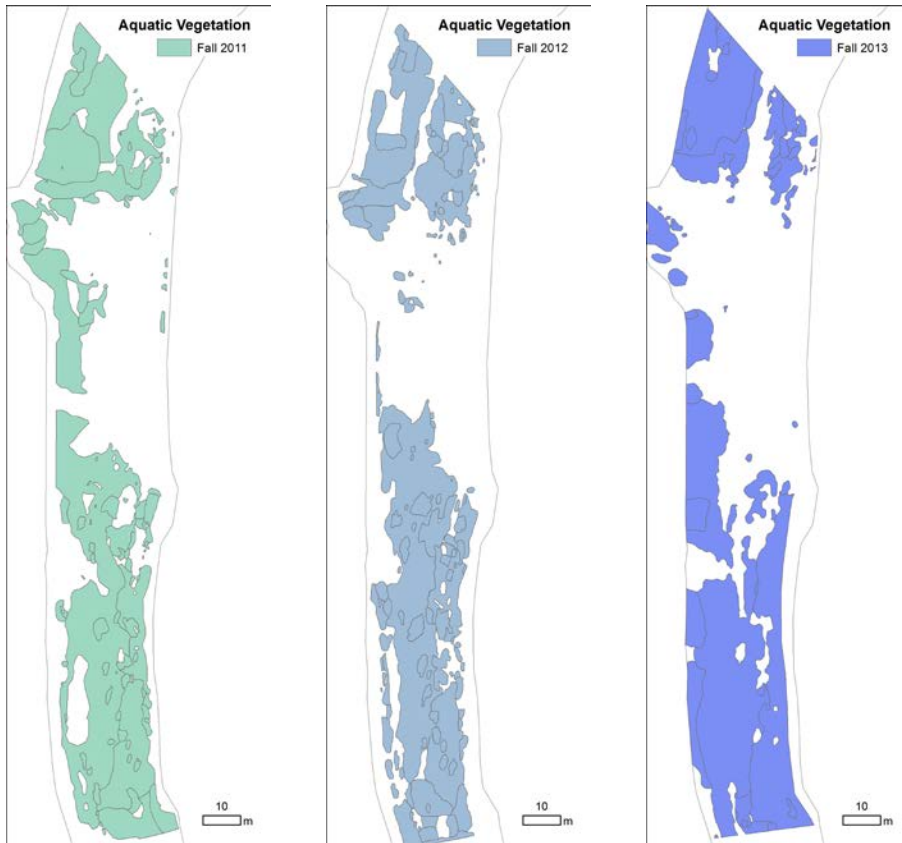


**Figure 2-7 (concluded). City Park**

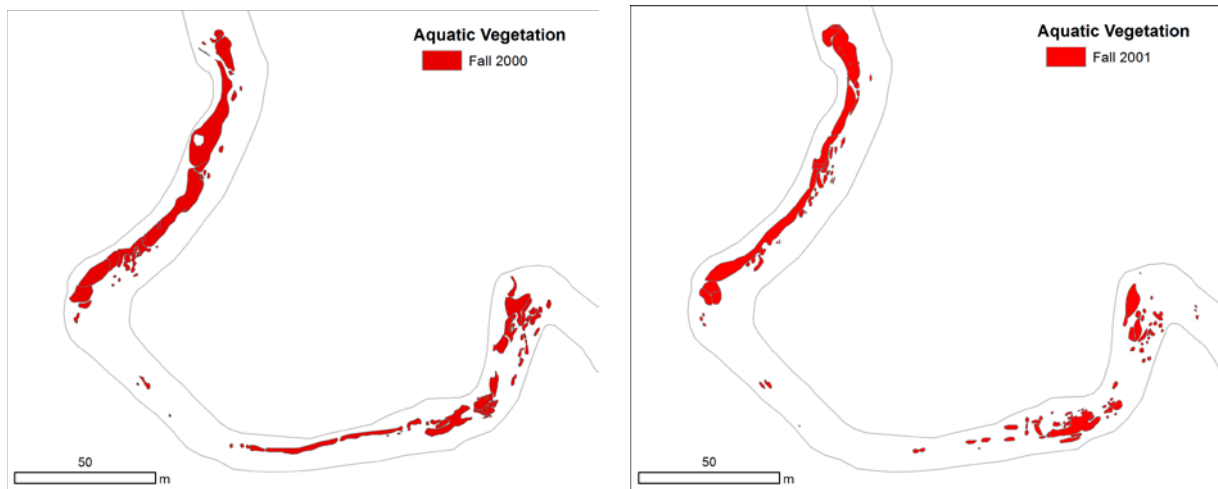


**Figure 2-8. Maps of total vegetation coverage in fall surveys, IH 35 study reach in San Marcos River**

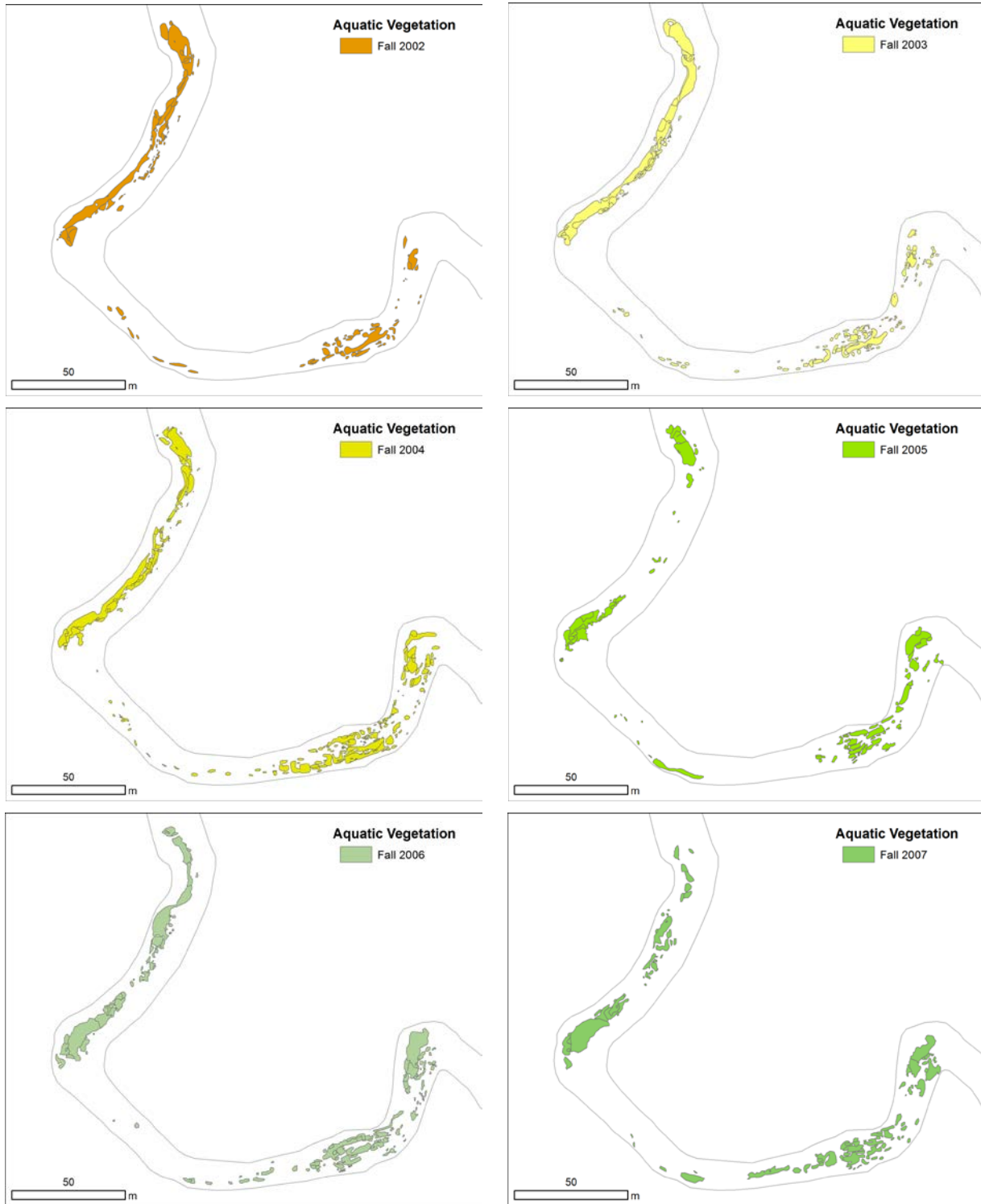
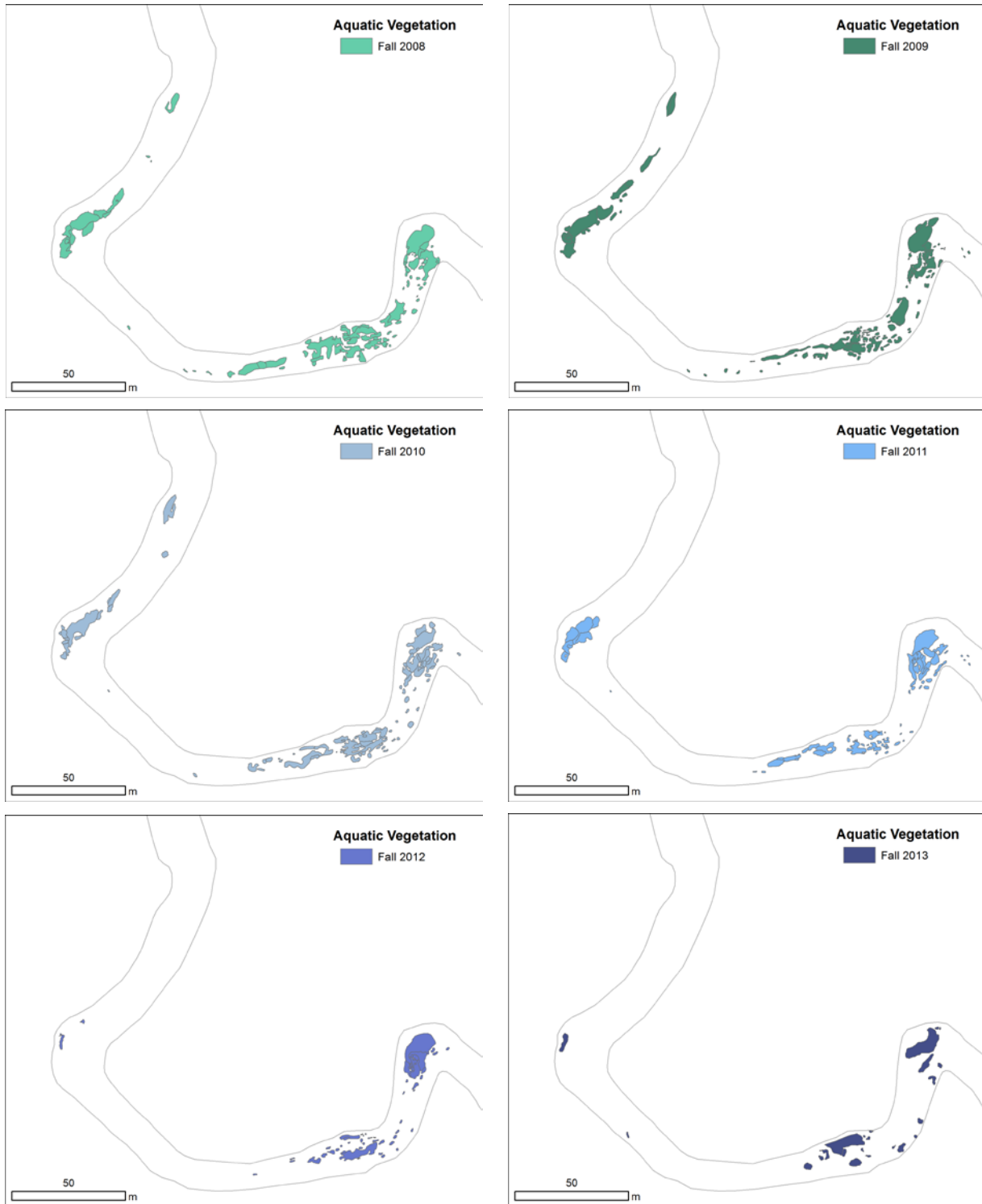


Figure 2-8 (continued). IH 35

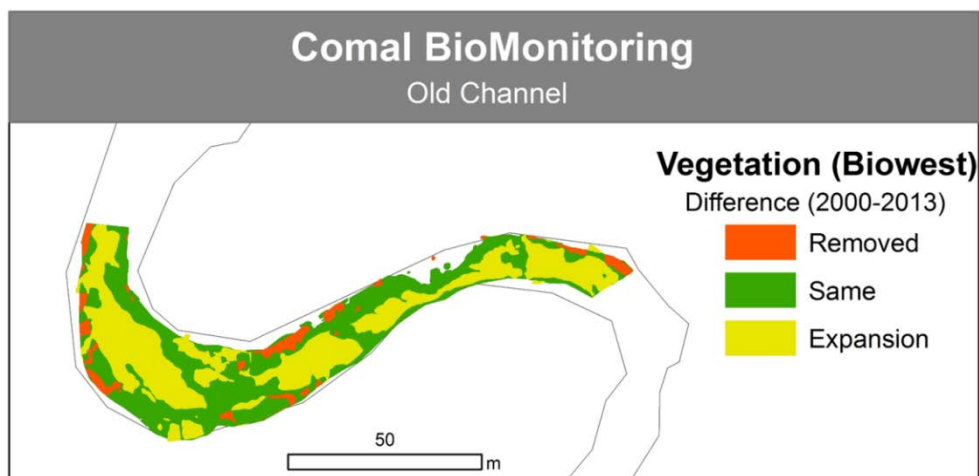


**Figure 2-8 (concluded). IH 35**

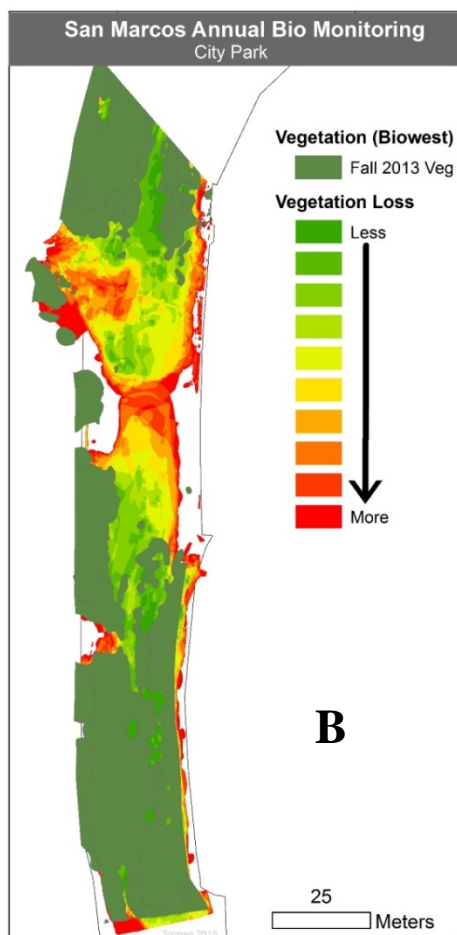
It emerged from analysis of this data that, while fountain darter populations varied according to the species of SAV present in a given habitat, by far the more significant differences in darter numbers was between bare substrate and any sort of vegetation. Within each reach, there were specific areas that were never vegetated, others that remained vegetated with perhaps different species, and others that oscillated between vegetated and unvegetated, as exemplified by Figure 2-9. Vegetation community composition within the study reaches was dynamic, and would often change within a given year or across years.

In nature, dispersal of aquatic vegetation can take place through seed deposits, clonal growth, and/or fragments settling and rooting downstream. Currently, there are few models that explicitly quantify the relationship between environmental conditions, and the ability of a plant to colonize new areas or be replaced by another species. We have developed an approach that simulates changes in vegetative cover over time based on a combination of ecological dispersal theory and on empirical estimates based on the vegetation mapping data.

Vegetation change was modeled by quantifying the likelihood (i.e., probability) that a vegetated point within each mapped site remains occupied with the same species, changes to another species or becomes bare. We calculated mean relative transition probabilities for each species using data from all available years and the spring and fall seasons. Transition probabilities were calculated for each reach independently. The probability of transition was determined for two seasonal passages, spring-fall and fall-spring, changed in early May and early November, respectively.



**A**



**B**

**Figure 2-9. Depiction of frequency of occupancy of a given cell over time. Old Channel (A), City Park (B) Red and orange indicate oscillation between vegetated and unvegetated during 2000-2013; green indicates mostly vegetated.**

#### **2.1.4 Fountain darter submodel**

The fountain darter submodel is the final component of the conceptual model of how darters respond to external conditions, see the conceptual model diagram of Figure 1-8. While the overall ecosystem model is deterministic, it has empirical components which exploit the considerable resource of field data available from the five study reaches. Each submodel is therefore a hybrid of mechanism and statistics. As noted earlier, the general causal structure of the model is HYDRAULICS → WATER QUALITY → VEGETATION → FOUNTAIN DARTERS. This is also a map of increasing reliance on empiricism (which is true of ecosystem models in general).

Unlike the more physical components of the overall model, *viz.* the hydraulics and water quality models, we do not have sound deterministic physical principles for fountain darter populations upon which a numerical model may be based. For hydraulics and water quality, we have the equations of momentum (derived from Newton's laws of motion) and continuity, coupled with physically or chemically-based process equations, such as frictional loss at the streambed, evaporation from the water surface, reaeration at the surface, and kinetics within the water column. In contrast, for fountain darters, we have only the principles of accounting and criteria differentiating life stages. External forcing must be specified based upon empirical relations inferred from observation. Following a detailed literature search and evaluation of existing data, our goal was to develop a spatially-explicit, time-dependent individual-based model representing fountain darter population dynamics using HCP biological monitoring data collected since 2000 as the foundation.

The objective of the submodel is to simulate the population dynamics of fountain darters in response to changes in habitat conditions that might result directly or indirectly from changes in water flow within the Comal River and the San Marcos River. The ability to simulate fountain darter population responses to spatial-temporal changes in the distribution and species composition of aquatic vegetation, as well as water temperature, DO concentration, depth, and velocity, as the darters pass through egg, larval, juvenile, and adult life stages, is of particular interest. Here we present an overview of the submodel. Model structure and execution are described in Section 2.2.3, and its validation in Section 2.3.2. Details on submodel formulation,

implementation and performance are given in Appendix C, following the protocol suggested by Grimm et al. (2006, 2010) for describing individual-based models.

Figure 2-10 displays a conceptual diagram for the fountain darter submodel, explicitly showing the space-time computation processes intrinsic to the individual-based model. Input data for each reach included time series of water depth, velocity, temperature, and DO concentration, as well as the spatial distribution of aquatic vegetation types, from 2003 through 2013 for the particular reach of the river being simulated (the Old Channel, Upper Spring Run, or Landa Lake reach of the Comal River, or the City Park or I35 reach of the San Marcos River). The model simulates fountain darter reproduction, development through egg, larval, juvenile, and adult life stages, mortality, and movement among the various types of aquatic vegetation.

The fountain darter submodel uses the same grid as the SAV submodel, derived by subsampling the hydraulic model grid (which is boundary-following curvilinear, but is mapped to a rectilinear depiction, so in both the SAV and the fountain darter, the model grid is referenced as though it is Cartesian). The grid elements are also referred to as “cells” and “habitat patches,” whose properties include location (geo-referenced coordinates), vegetation type, water temperature, DO concentration, depth, and velocity, all of which except location may vary in time. The model domain is populated with thousands of fountain darter “individuals” with attributes including location (i.e., by habitat patch), sex, age, life stage, and (for females) reproductive state, all of which may vary in time. Though the SAV and fountain darter submodels are addressed separately in this report, both are combined in the same program code in NetLogo.

The simulated darters are subjected to aging, development, mortality and reproduction, which are advanced daily, coupled with 24 movements per day. Each day, the number of habitat patches of each SAV type, number of darters in each SAV type, and numbers of eggs larvae, juveniles, young adults, old adults, males and females are aggregated and output. The submodel is initiated with observed SAV distributions, temperature, DO, and fountain darter numbers from spring 2003, and current velocities and water depths based upon observed total flow, including spring flow, in the study reaches. The submodel is then advanced in time with daily inputs of total flow (including spring flow), radiation, and meteorology.

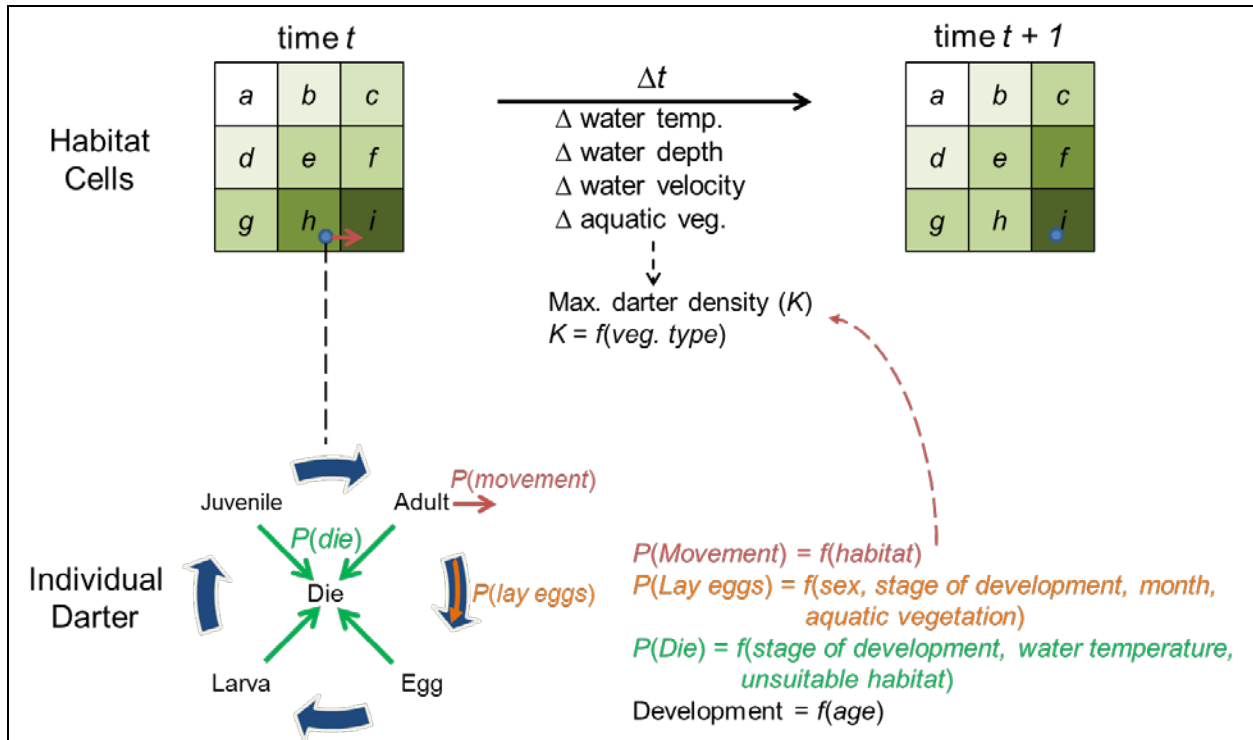


**Figure 2-10. Conceptual diagram of the spatially-explicit, individual-based, simulation model representing fountain darter population dynamics in response to changes in aquatic vegetation and hydrological conditions**

Movement rules, which are hypothetical, but which result in movement patterns generally consistent with those based on field data collected from marked individuals (BIO-WEST, 2014c), are generally directed from higher populations cells to lower, and toward better habitat, governed by random choices and constrained by maximum density for each SAV type. These rules also include limits to movements within unsuitable habitats, by specifying that the individuals die after a specified number of movements. The movement rules are given in more detail in Section 2.2.3 and in Appendix C. For each computational day, these results are aggregated to determine the total number of juvenile and adult fish in the modeled reach and the total number within each vegetation type, along with several ancillary calculations.

## 2.2 Model Structure

The general philosophy and properties of the four submodels were summarized in Section 2.1, above. The present section provides detail about the actual model operation and internal calculations, particularly those of the SAV and fountain darter submodels. (The hydraulic and

water-quality submodels, which were developed in previous projects for the USFWS, EARIP and EAA, are summarized in BIO-WEST et al., 2015c, and citations therein.) The presentation is generally qualitative, though with technical details not included in the preceding overview section, the mathematical formulations being reserved for the appendices.

### ***2.2.1 Model space-time structure, operation and inputs***

The complete FDMS as it affects the fountain darter, depicted in Figure 1-8, is implemented in the computer as a time-advancing calculation over a spatial domain discretized by a curvilinear, boundary-following coordinate system mapped to a rectilinear grid. The hydraulic model grid is the basis for the spatial network of both the SAV and fountain darter submodels, which is subsampled to create the (nominal) 1-meter spatial grid of computational nodes (cells, patches, elements) for these submodels. The results from the one-dimensional, section-mean water quality model are distributed over this same grid to provide values of water temperature and DO throughout the model computational domain. As previously described, while the SAV and fountain darter submodels are depicted in Figure 1-8 as separate, they are coded as a combined calculation, programmed in NetLogo.

For each of the five study reaches (see Section 1.1), spatial grid structures have been developed specific to each of the submodels: link-node segmentation for the QUAL2E water-quality model for the entirety of each river; the nominal 0.25-m curvilinear grid of the study reach for the hydraulic model, and the nominal 1-m grid of the study reach for the SAV and fountain darter models. The first input decision therefore is which reach to study.

The water quality and hydraulic submodels are independent calculations driven by hydrology, and other external variables, as arrayed in the oblong boxes at the top of Fig. 1-8. To facilitate user operation, a file-handling input/output (I/O) structure called the Water-Quality and Temperature Simulation System (WQTSS) has been developed. The user may select one of several pre-run scenarios (see Section 3.1), in which case flat-file results will be selected for input to the SAV and fountain darter submodels. If the user desires to modify the input flows, the WQTSS will automatically rerun the water-quality model and post-process the results for input to the fountain darter submodel.

An alternative model configuration to that depicted in Fig. 1-8, was developed, displayed in Figure 2-11, called the decoupled model. In this configuration, the SAV submodel is replaced with a user-specified distribution of SAV, which can vary in time. This version retains all of the inputs and processes that affect the hydraulics, water quality, and the fountain darter. The objective of the decoupled model is two-fold. First, it offers a vehicle for direct specification of the SAV distribution in a study reach, which is useful for some scenarios. Second, it was useful in the validation and evaluation of the fountain darter submodel, because any errors introduced into the simulation by the SAV part of the model operation under coupled operation (i.e., Figure 1-8) could be eliminated by simply inputting the observed SAV distributions instead. Under this operation, the prediction errors would be ascribed entirely to the fountain darter submodel (along with any residual error that might remain in either the hydraulics or the water quality components).

### **2.2.2 SAV submodel**

The SAV submodel simulates daily accumulation of biomass through photosynthesis, which is controlled by photosynthetically-active (or available) radiation (PAR) and water depth (see Section 2.1.3). The model has a daily time step, but photosynthesis is integrated over both time and the depth profile to determine accumulation of biomass. In addition to the physical and water quality data from the hydrodynamic and water quality submodels (velocity, depth, temperature, and DO), the SAV submodel is initialized with geo-referenced shapefiles of vegetation maps collected during field mapping in 2003 (e.g., see Fig. 2-3).

Irradiance follows daily and seasonal cycles, resulting in spatio-temporal patterns of light availability and growth patterns. These patterns are captured in the model by explicit physical equations for radiation with solar declination and day length as independent variables, determined in turn from position on the earth, season of the year, and clock time (e.g., Sellers, 1965; Peixoto and Oort, 1992, Wallace and Hobbs, 2006). This method uses the terminology and follows the ASTRO and TOTASSIM procedures of Goudriaan and van Laar (1994). PAR ( $\mu\text{E m}^{-2} \text{s}^{-1}$ ) at the water surface is estimated as 50% of the total irradiation given the day of year, hour, declination, and latitude. Light attenuation in the water column follows the Lambert-Beer law (following van Nes et al. 2003). Model equations are presented in Appendix B.

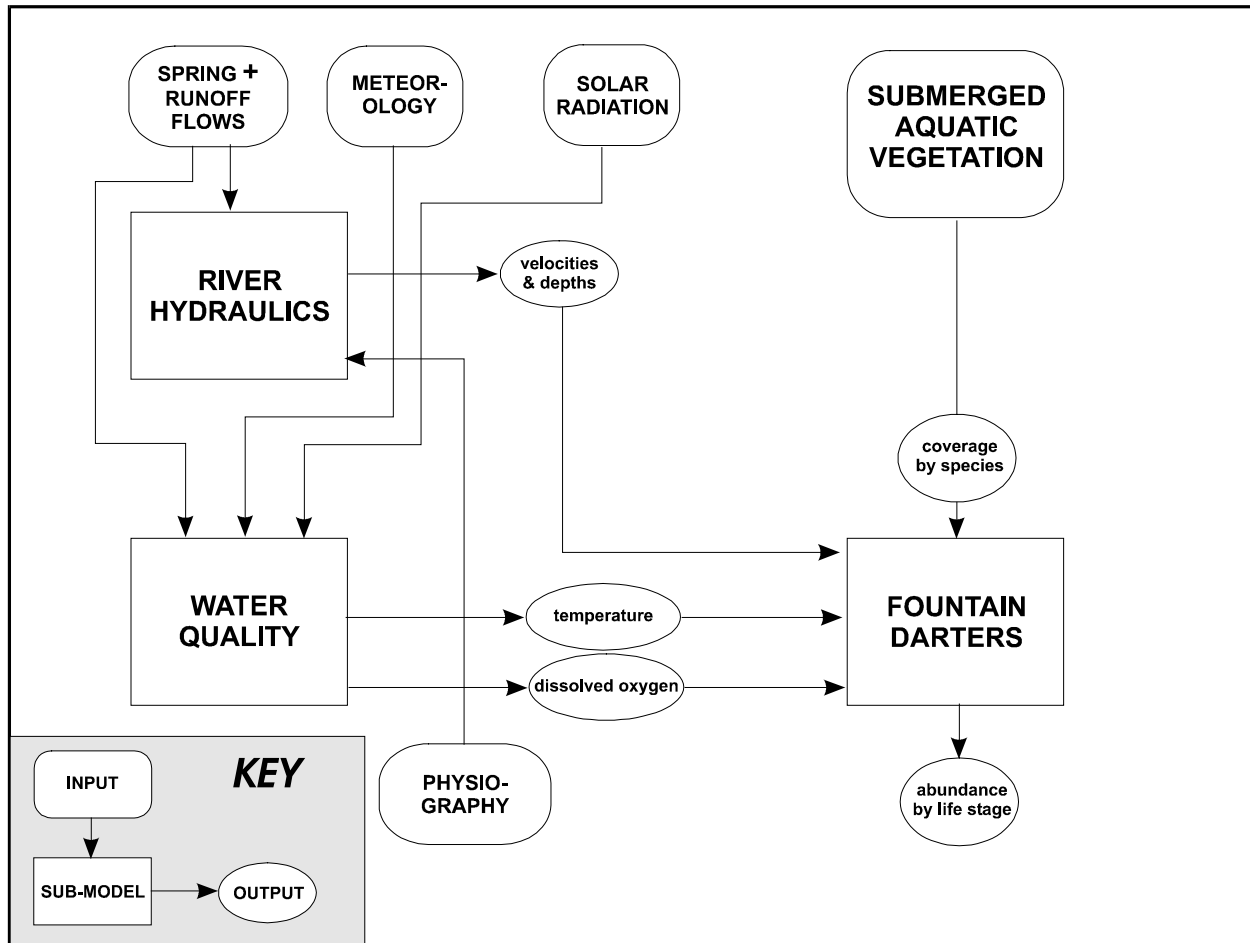


Figure 2-11. Alternative model structure in decoupled configuration, cf. Fig. 1-8

Only one species of SAV is allowed to occur per cell. Colonization of unvegetated cells, or conversion from one species type to another occurs once every ten days, and is based on a series of conditions, including the historical records of particular cells being vegetated, the type of species in a cell, the relative resilience of a species to disturbance, and a matrix of transition probabilities that quantify the probability of a cell transitioning from one species to another. The transition matrix was calculated from thirteen years of field mapping efforts. Details of the transition calculations can be found in Appendix B. (Since SAV's are directly input to the decoupled model, the above does not apply, and the SAV is updated only when a new survey is input, or a modification to the vegetation is specified.)

There are several measurable plant attributes that are important to the growth of aquatic vegetation; these are listed in Appendix B, Table 2. Plant growth, in terms of biomass gained or lost (in grams/day) is modeled on a daily time step and is calculated as net of photosynthetic gain

over respiration and mortality. Photosynthesis is governed by PAR at the water surface, and depth below the surface of the top of the plant (based on Michaelis-Menten saturation functions and a maximum value of photosynthetic accumulation calibrated for different species, see Appendix B). Since light intensity follows a daily cycle, and varies with depth, photosynthesis is calculated at multiple times per day and at multiple depths in the water column through the vegetation, then averaged using Gaussian integration (Goudriaan and van Laar, 1994, see Appendix B). The defaults for maximum photosynthesis per unit biomass is  $0.01 \text{ g g}^{-1} \text{ d}^{-1}$ , but is calibrated to match growth rates of different species. Self-shading is included in the model, and is based on species-specific light attenuation coefficients, which provides a negative feedback for growth (i.e., the more biomass that accumulates the less light reaches the lower layers of the plants).

Maintenance respiration is needed for plants to continue to live. The model estimates maintenance respiration based on daily temperature and the biomass of the aboveground and belowground sections of the plants. For simplicity and computational efficiency, all stems, shoots, and leaves are categorized as aboveground biomass, and roots and other substrate matter as belowground biomass. The difference between gross photosynthesis and maintenance respiration is the amount of assimilate available for growth. In the model this is expressed as the glucose requirement for growth (see Teh, 2006, and Appendix B). Once biomass is converted to glucose it is partitioned to aboveground and belowground parts of the plant.

Morphological maximums are input parameters based on the literature or field data collected during this study, and are set in place to ensure plants sizes do not exceed biological limits. After growth is simulated, if the species-specific aboveground or belowground biomass exceeds the respective user-defined maxima, the model values are truncated to the maximum value. In some cases, the aboveground biomass is less than the user-defined minimum requirement for photosynthesis to occur. This is particularly true for some plants after colonization of new cells. When this happens, the model simulates plant growth by translocating 1% of the root biomass to the aboveground biomass, following methods used by Best and Boyd (2001).

Dispersal by aquatic vegetation can take place through seed deposits, clonal growth, and/or fragments settling and rooting downstream. To model the replacement of one vegetation type with another, which includes the process of dispersal, we focused on the probability that a given

cell transitions from one state to another, i.e., by quantifying the likelihood that a vegetated point within each mapped site remains occupied with the same species, changes to another species, or becomes bare. A cell cannot convert to a different state if it has six neighboring cells of identical states (e.g., a *Hydrilla* cell cannot convert if it has six neighboring cells that are also *Hydrilla*). If a cell has less than six neighbors with the same state, the vegetated cell becomes eligible to convert to another state. State transitions are applied once every 10 days, are probabilistic, and are conditional on the transition probabilities for that species (see Appendix B), and the percent cover within the cell. Percent cover is used to generate a shape parameter for a logistic function that generates a probability of dispersal based on the percent cover of vegetation. This function then generates a probability of dispersal, which is lowest at low values for percent cover, and highest as the cover approaches 100% (Figure 2-12). If the probability of dispersing is large enough, then the transition matrices are used to determine the probability of that cell converting to other states (bare substrate or another species, as explained below).

Vegetation community composition observed within the study reaches was dynamic, and often changed within a given year or across years. Vegetation change was modeled by quantifying the likelihood that a vegetated point within each mapped site remains occupied with the same species, changes to another species or becomes bare. We calculated mean relative transition probabilities for each species using data from all available years and the spring and fall seasons. Transition probabilities were calculated for each study reach independently. The probability of transition was determined for two seasonal passages, spring-fall and fall-spring, and transition probabilities were changed on day 122 for the spring-fall transitions and day 305 for the fall-spring. These transition probabilities are then applied on the 10-day conversion interval in the model. (Sensitivity analyses indicated that such application yielded satisfactory results, obviating any additional transformation of the transition probabilities.)

An example of the transition probabilities for the Old Channel reach is shown in Figure 2-13. These diagrammatic representations (called chord diagrams, inspired by Krzywinski et al., 2009; Holten, 2006) can be used to visualize the relationships among entities, in the present case as tools to elucidate the replacement of one species by another. In these, vegetation species are represented as colored arcs of the circle, called “nodes”.

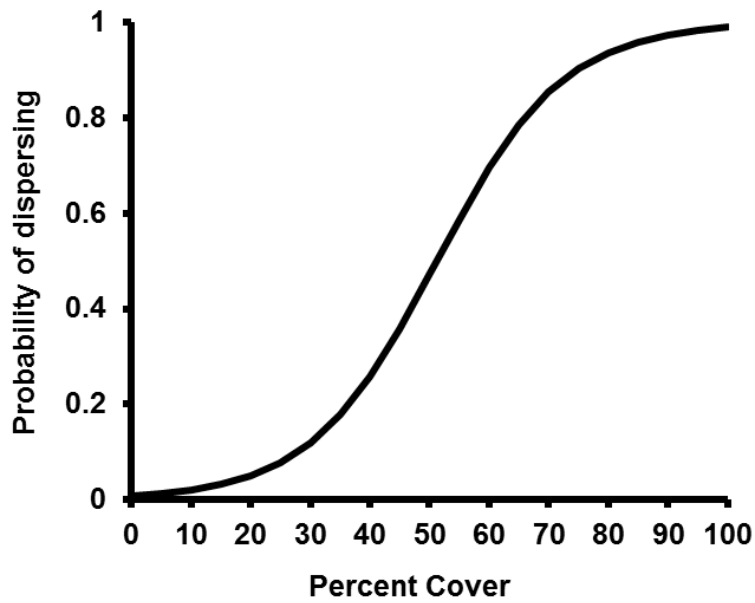


**Figure 2-12. Example of logistic function used to calculate probability of dispersal based on percent cover of vegetation for each cell, following Railsback and Grimm (2014)**

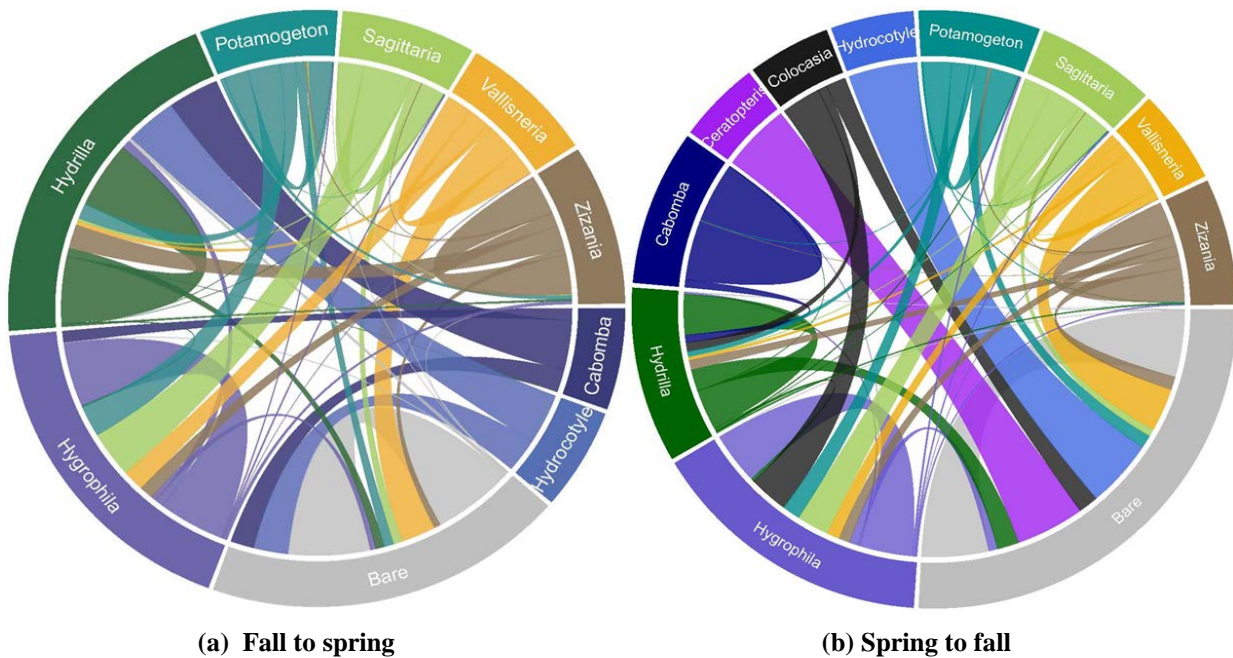


**Figure 2-13. Chord diagrams for City Park reach, showing seasonal transitions between SAV types**

Each species has its own color, and the length of the arc is the relative proportion of that species in the reach at the beginning of the transition. The transition probabilities among species

(including bare substrate) are connected to each other by ribbons, whose areas are proportional to the probability of a given transition (i.e., larger ribbons represent larger probabilities). Each ribbon has the color of the vegetation type that is *replacing* another type. For example, in Figure 2-13(a), *Cabomba* replaces part of the area vegetated by *Hydrilla* and part of the area formerly bare. If a ribbon connects to its node twice, such as “bare” in Figures 2-13(a) and 2-13(b), this represents the likelihood of that species remaining the same (i.e., no change). Generally, highest transition probabilities were found when cells transitioned from vegetated to bare substrate, and when points did not transition to a new vegetated state (i.e., the same species occupied a point through multiple seasons). (See Appendix B for exact values for each transition probability, and for additional chord diagrams.)

### 2.2.3 *Fountain darter submodel*

The computational domain is comprised of a reach-specific number (on the order of thousands) of 1 m<sup>2</sup> habitat patches arrayed in a rectangular grid mapped to the curvilinear grid of the MDSWMS two-dimensional hydrodynamic model calibrated for the reach, see Section 2.1.1 above and citations therein. This horizontal array is populated by a variable number (up to several tens of thousands) of individual fountain darters. Attributes of habitat patches include location, vegetation type (see Section 2.1.3), water temperature (°C), DO concentration (mg/L), depth (m), and current velocity (m s<sup>-1</sup>). Attributes of fountain darters include sex, age (days), life stage (egg, larva, juvenile, young adult, old adult), location (habitat patch currently occupied), and, for adult females, reproductive state (whether or not they are reproductively active, and whether or not they have laid eggs within the last month).

As already noted, the model is programmed and simulations executed in NetLogo (Wilensky and Rand, 2015), the results of which are exported to Excel™ (Microsoft, 2003) for archiving and temporal graphics. During each simulation, the system is initialized by assigning each habitat cell a vegetation type, as well as a water temperature, DO concentration, depth, and velocity, and by assigning each individual fountain darter a sex, age, life stage, and location, as diagrammed in Figure 2-14. The initial number of juvenile plus adult darters is calculated based on the estimated maximum darter density that can be supported by the aquatic vegetation within the reach.

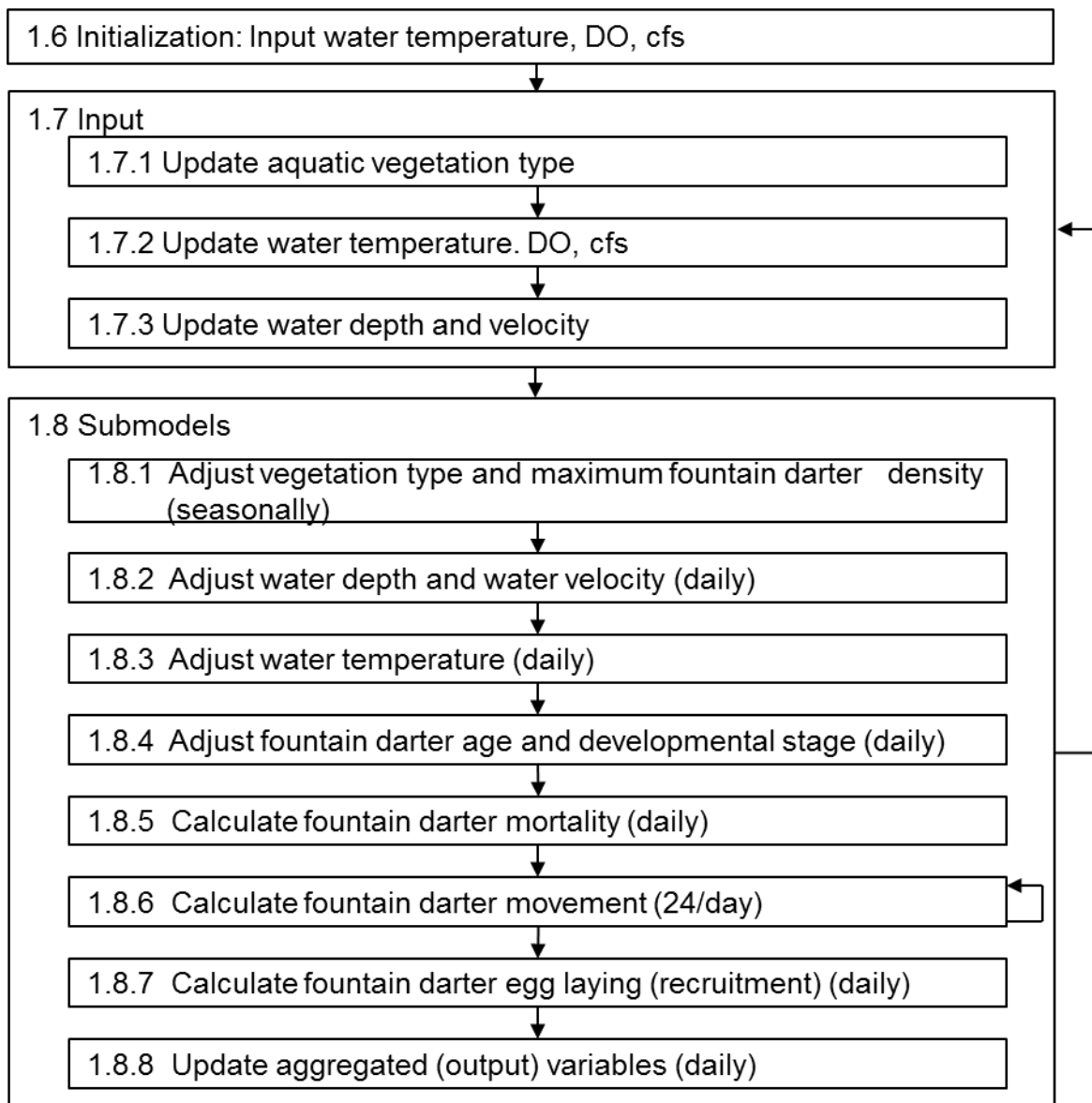


**Figure 2-14. Overview of the sequence of events and processes involved in the execution of the fountain darter submodel**

The maximum darter density associated with each type of aquatic vegetation is based on analyses of drop net data collected from 2003 to 2010 in the particular study reach of the Comal River or the San Marcos River being simulated (BIO-WEST, 2004a – 2014a, BIO-WEST, 2004b – 2014b) in the interim report (BIO-WEST et. al, 2015c).

Simulations are driven by daily time series of values representing estimated historical water discharge, water temperatures and DO concentrations from 1 January 2003 to 31 December

2013. Historical daily water discharges for the given reach are used to assign the associated water depths and water velocities for each habitat cell within the reach for that day. Water depths and velocities associated with various water discharges within each reach are calculated externally to the fountain darter model and formatted for use within the fountain darter model (see Section 2.1.1 and Table 2.1). Next, iteratively during the simulation, (1) values representing estimated daily water discharge, water temperature and DO concentration are adjusted according to their respective input time series, (2) water depth and water velocity in each habitat cell are adjusted based on the estimated daily water discharge, and (3) effects of these changes on the mortality, movement, and egg-laying (recruitment of new individuals) of fountain darters are calculated. Lengths (in days) of developmental life stages are based on data of Simon et al. (1995) and Brandt et al. (1993). Stage-specific daily mortality occurs probabilistically based upon data of Pitcher and Hart (1982) and Brandt et al. (1993), adjusted to represent additional temperature-related mortality based on data of Bonner et al. (1998).

For the decoupled model, estimated historical vegetation changes occur seasonally (spring, summer, and fall of 2003 and 2004; spring and fall of 2005 to 2013). Fountain darters may make up to 24 movements each day, but aging, development (from egg to larva to juvenile to adult), mortality, and egg laying are calculated on a daily basis. During the simulation of each fountain darter activity (move, age, develop, die, lay eggs), individuals are selected in random order, that is, the first randomly selected individual is given the opportunity to perform the given activity, then the second randomly selected individual, then the third, and so on.

Movement rules for the fountain darter are summarized in Figure 2-15. Maximum darter density (MD) represents the number of darters (juveniles plus adults) that can be supported by the vegetation type in the habitat cell,  $\epsilon$  represents the probability of moving to an adjacent habitat cell,  $v'$  represents the number of consecutive moves during which the individual has not occupied a habitat cell that was below its MD (i.e., has not found favorable habitat), and  $v$  represents the maximum number of consecutive moves that the individual can survive in unfavorable habitat.

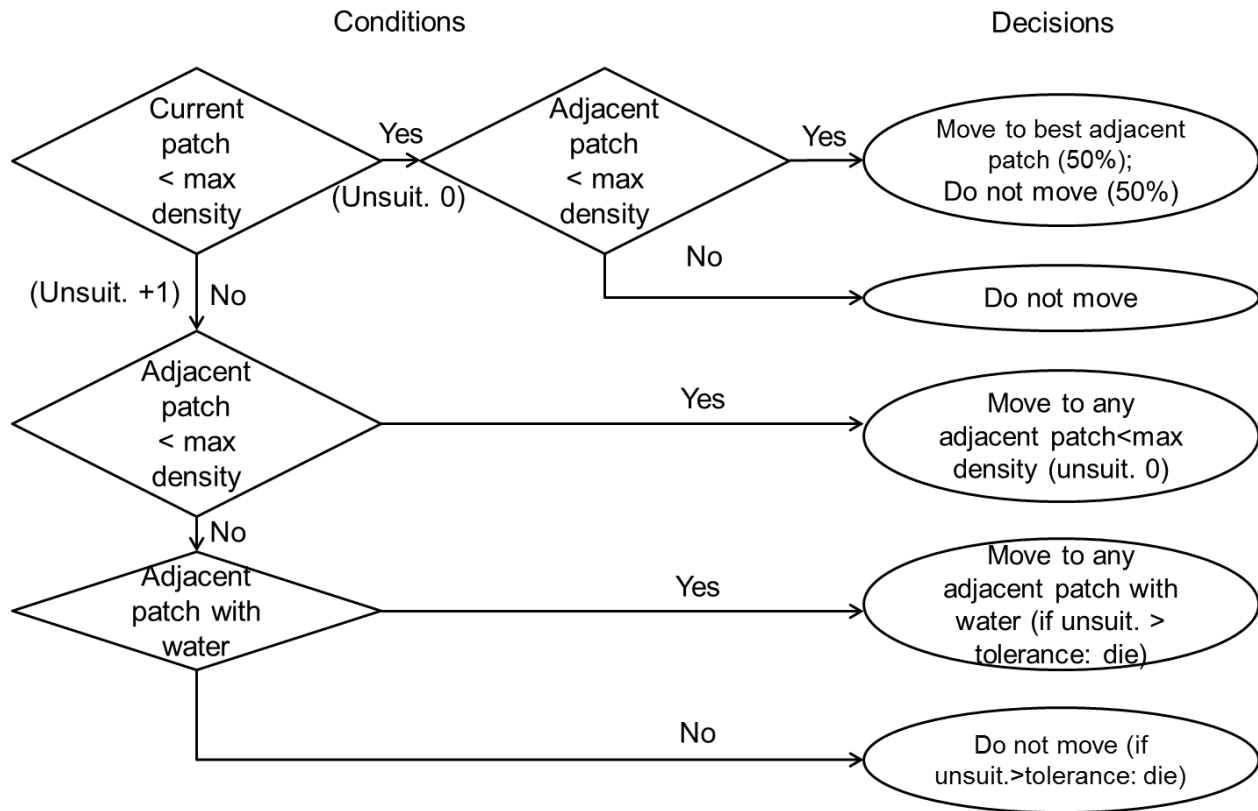


Figure 2-15. Summary of fountain darter movement rules.

The rules are hypothetical, but simple and intuitive:

- (1) If an individual is located in a habitat cell that currently is below its estimated maximum darter density (MD; the number of juveniles plus adults that can be supported by that vegetation type), and there are no adjacent habitat cells below their MD, then the individual will not move from the cell it currently occupies.
- (2) If an individual is located in a habitat cell that currently is below its MD, and one or more of the adjacent habitat cells is below their MD, then the individual has a probability ( $\epsilon = 0.50$ ) of moving to one of those habitat cells (randomly chosen), and a probability ( $1 - \epsilon$ ) of remaining in the cell it currently occupies. This rule allows individuals to move about larger aggregates of suitable habitat cells and prevents situations in which suitable habitat cells near the center of large patches become inaccessible due to “barriers” formed by suitable, fully-occupied habitat cells.

- (3) If an individual is located in a habitat cell that currently is at or above its MD, and one or more of the adjacent habitat cells is below their MD, then the individual moves to one of those habitat cells (randomly chosen).
- (4) If an individual is located in a habitat cell that currently is at or above its MD, and none of the adjacent habitat cells is below their MD, but one or more of the adjacent habitat cells has water, then the individual moves to one of those habitat cells (randomly chosen).
- (5) If an individual is located in a habitat cell that currently is at or above its MD, and none of the adjacent habitat cells is below their MD, and none of the adjacent habitat cells has water, then the individual will not move from the cell it currently occupies. If an individual has not occupied a habitat cell that was below its MD (has not found favorable habitat) within an arbitrarily specified number of consecutive moves ( $v$ ), it dies ( $v = 12$ ).

Fountain darter egg laying is calculated on a daily basis, with the probability that an adult female lays eggs calculated as a function of month-of-year and the presence of aquatic vegetation in the habitat cell in which the individual is located. The monthly proportions of adult females that are reproductively active are modeled by a normal distribution whose mean and standard deviation are taken from the work of Nichols (2015). Each produces a number of eggs following a normal distribution with mean and standard deviation from the data of McDonald et al. (2007). In the model, on the first day of each month, each adult female is identified as reproductively active or not based on a random variate drawn from a normal distribution (truncated at  $+2SD$  and  $-2SD$  or  $0$ ,  $SD$  denoting standard deviation) with the mean and  $SD$  associated with the corresponding month. Each female maintains her status during the entire month. Each day that a reproductively active female is in a habitat cell with aquatic vegetation, she lays a number of eggs based on a random variate drawn from a normal distribution (truncated at  $+2SD$  and  $-2SD$  or  $0$ ) with a mean ( $\pm SD$ ) of  $6.34 (\pm 5.16)$ . Juveniles that become adult females (at 186 days of age) during the month are immediately identified as reproductively active or not in a similar manner.

The aggregated variables that describe the state of the system include the number of habitat patches with each type of aquatic vegetation, the number of fountain darters in each type of

aquatic vegetation, and the numbers and proportions of eggs, larvae, juveniles, young adults, old adults, males, and females in the fountain darter population. All of these aggregated variables are updated daily. Spatial and temporal patterns of abundance of fountain darters in the various life stages emerge as system-level properties, i.e., in the aggregate, as a result of the application of the above processes and movement rules to each individual in the population.

## **2.3 Model performance**

Evaluation of model performance encompasses qualitative assessments of model behavior, quantitative assessments of model response (sensitivity), model operation to assign values to undetermined parameters as necessary (calibration), and comparison of model predictions with data (verification or validation). It is necessary to subject each component submodel (cf. Fig. 1-8) to such an evaluation, to the extent that data permit. In this context, we also note that “prediction” is used in a technical sense, referring to the model output for a given suite of inputs. This suite may represent a completely hypothetical occurrence or a possible future. It frequently is a set of external conditions that occurred in the past for which observations exist for the model variables. Such a set of data is obviously essential for model calibration and validation.

### ***2.3.1 SAV submodel testing and evaluation***

Sensitivity analysis and model validation details are presented in Appendix B and only selected results are summarized here. The SAV model was evaluated across three levels:

- (1) the model’s ability to generate reasonable growth patterns for each of the species modeled. i.e., whether the seasonal patterns were replicated and the modeled values were in the range reported for the species.
- (2) how well the model can recreate the historical distribution of vegetation coverage (that is total number of cells that contained vegetation) in each of the five reaches under two different mortality scenarios.
- (3) how sensitive the model is to changes in input parameters. Preliminary analyses indicated that the largest uncertainties were associated with vegetative dispersal/conversion from one species to another at a given location, how the addition of a constant mortality term impacts the vegetation dynamics, and finally

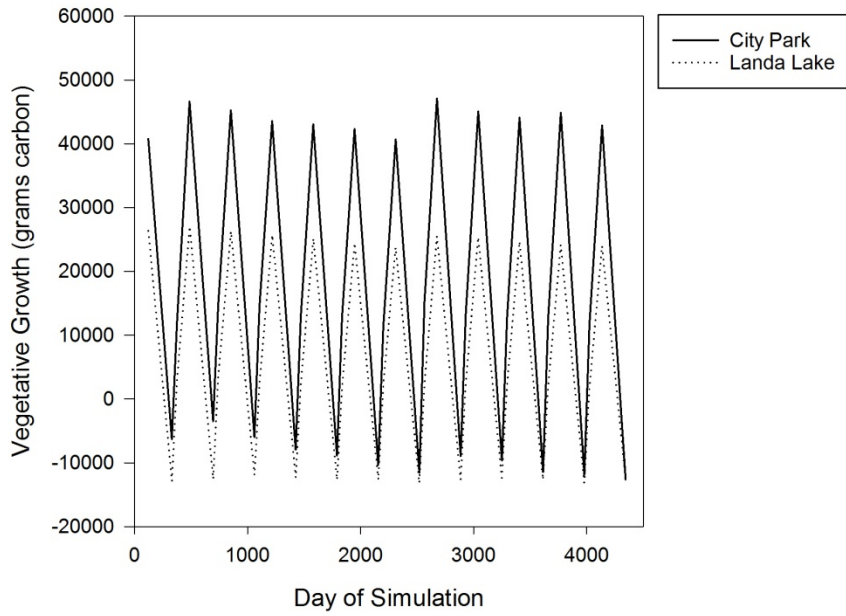
how the temperature induced mortality at a cell level impacts the spatial distribution of the vegetation within the system. We ran sensitivity analyses to determine how different values of temperature, mortality, and frequency of conversion of cells to different states impacted model output.

We ran 10 replicate stochastic iterations for each evaluation scenario. The baseline simulation was a scenario with biomass loss calculated from respiration only, (i.e., no constant mortality), and state conversion at 10 days.

The model simulates realistic seasonal variation in vegetation growth and respiration, similar to the patterns exhibited by Best and Boyd (2001) and van Nes et al. (2003). Plant attributes were cyclical in that the patterns showed increased growth during the spring and summer and decreased growth in the winter (Figure 2-16). Simulated patterns in amount of vegetative cover matched observed patterns of cover in City Park, and Landa Lake relatively well, but underestimated vegetative cover in Old Channel, I35, and Upper Spring Run. (These results are shown in Appendix B.) In the latter three reaches, the underestimation indicates that there are likely processes other than photosynthesis, respiration, and state conversion that drive vegetative cover.

Given the large range of uncertainty associated with quantifying biomass loss for SAV species in general, previous SAV models quantify biomass loss through respiration and a constant biomass-loss term (i.e., a fixed percentage of biomass lost over a specified time step). We conducted a sensitivity analysis to determine how the model responded by including constant loss term (2% per time step) to compare against a scenario parameterized with respiration only. In step with this thinking, we also conducted a sensitivity analysis on how frequent a given cell had the potential to convert to another state by testing how the model responded when state conversions happened once every 3, 15, or 30 days, respectively.

### System-level net growth for City Park and Landa Lake



### System-level net growth for I35, Old Channel, and Upper Spring Run

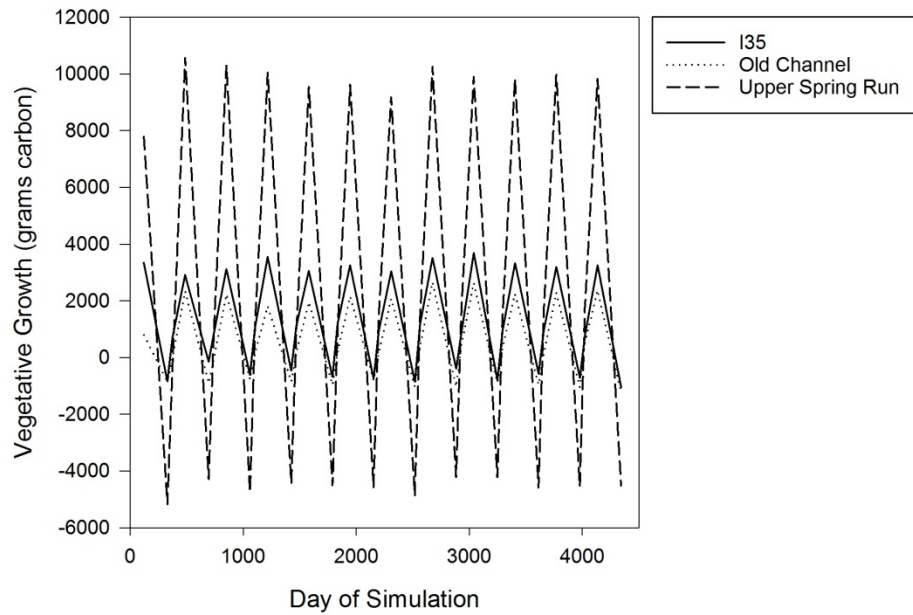


**Figure 2-16. Net Biomass Accumulation over time for each of the five study reaches.**

The results for City Park are shown in Figure 2-17. (Other reaches are shown in Appendix B.) The incorporation of a constant loss term decreased the spatial distribution of vegetation across all five reaches from 25 to 60% compared to baseline. The smallest decrease was exhibited in Old Channel and the largest in Landa Lake. The model proved to be much less sensitive to increases or decreases in temperature, with the total amount of vegetation not changing more than 6% in any reach, compared to baseline.

The sensitivity of model results to changes in the frequency of state conversion depended on the reach. The total amount of vegetation in Old Channel decreased by 90% when state conversion could occur every three days, and by 70% at 30 days. In contrast, City Park did not experience significant losses in total vegetation, with a 2% to 4% decrease when state conversion could occur every three days, and 1% to 6% increase at 30 days. Likewise, total vegetation in Upper Spring Run was not sensitive to changes in the state conversion parameter, with a less than 2% shift from baseline for all parameterizations. Field data indicated that there is a high probability for any given cell to convert to bare substrate. These data also indicate that once a cell converts to bare substrate, it has a high probability of remaining bare. These conditions are not reflected across all study reaches, but were localized to Old Channel.

## City Park Sensitivity Analysis

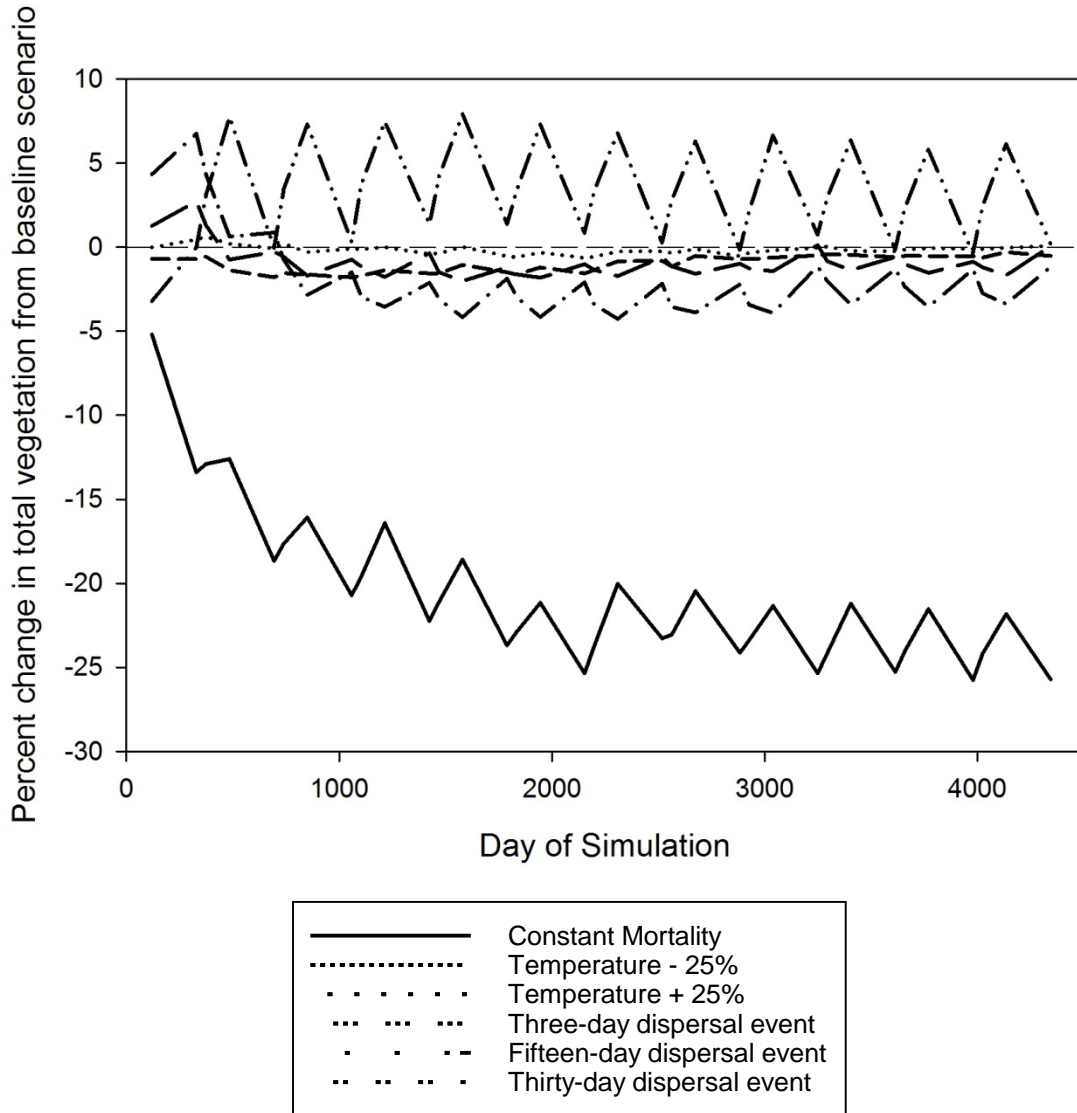


**Figure 2-17. Results from Sensitivity Analyses for total vegetation in City Park study reach**

### ***2.3.2 Fountain darter submodel testing and evaluation***

All model runs for performance evaluation of the fountain darter submodel were made using the decoupled configuration (see Section 2.2.1 and Fig. 2-11), so that actual observations of SAV were used to characterize darter habitat. This strategy separates the performance evaluation of the darter submodel from that of the SAV submodel. Fountain darter population numbers are the sum of juvenile and adult forms. The model has a stochastic element due to the probabilities assigned to darter movement, reproduction, and mortality. For every simulation, three replicate runs were made to provide an indication of the uncertainty latent in the model prediction itself. Three replicates are necessary to estimate the variance. Clearly more replicate runs would be desirable, but the running times and the number of scenarios to be examined precluded this.

Vegetation types are adjusted during the spring (1 March, day-of-year 60), summer (1 July, day 182), and fall (1 October, day 274) of 2003 and 2004, and during the spring (1 March, year 60) and fall (1 September, day 244) of 2005 to 2013, with the vegetation type assigned to each habitat cell based on the input time series of vegetation data. Immediately following the adjustment of the vegetation type within any given habitat, the maximum darter density of that cell (see Section 2.2.3) is adjusted accordingly. Mean water discharges, water depths, water velocities, mean water temperatures, and DO concentrations are adjusted daily. A single discharge, water temperature, and DO concentration are assigned to the entire reach (i.e., as global variables) based on the input time series of these data. Water depths and velocities associated with the daily water discharge then are assigned to the appropriate habitat cells (see Section 2.1.1 and Table 2.1).

The model code was verified to be capable of reproducing the rates of development of fountain darters through egg, larval, juvenile, and adult life stages, as well as the seasonality of reproduction, in accordance with the empirically-estimated life history/demographic input parameters. We then calibrated the model such that simulated abundances of fountain darters responded appropriately to historical changes in habitat conditions from 2003 through 2010. This period was selected to be the “calibration data set,” reserving the 2011-2013 period for “validation.” For model calibration, we used the version of the model that was parameterized to represent the Old Channel study reach of the Comal River. We calibrated this version of the

model by adjusting  $v$  (the number of consecutive moves that a juvenile or adult fountain darter can survive without finding favorable habitat; see Section 2.2.3) such that the simulated number of juveniles plus adults increased toward, but did not markedly exceed, the estimated maximum darter densities that could be supported by the aquatic vegetation. These two criteria were optimally met with  $v = 12$  (see Appendix C for more detail). When we removed the limit on the number of consecutive moves that a fountain darter can survive without finding favorable habitat, the number of fountain darters increased exponentially, and when we replaced the movement rules with random movement the population could not sustain. No other adjustments to model parameters were made.

The comparisons of observed fountain darter density from the drop-net surveys with model predictions for all five reaches for 2003-2010 are shown in Figures 2-18 through 2-22. The three different time plots of darter density correspond to the three replicate runs of the model. It should be emphasized that the model was *calibrated* only with 2003-2010 data from the Old Channel, Figure 2-18. The 2003-2010 comparisons for the other four reaches (Figs. 2-19 – 2-22) represent *validation* against independent data sets for geographically different reaches (two from a different river) for the same time period, each using the calibrated movement rules from the Old Channel study reach simulation. Note, however, that maximum darter densities throughout each simulation were estimated based on analyses of drop-net data collected from 2003 through 2010 in the study reach being simulated.

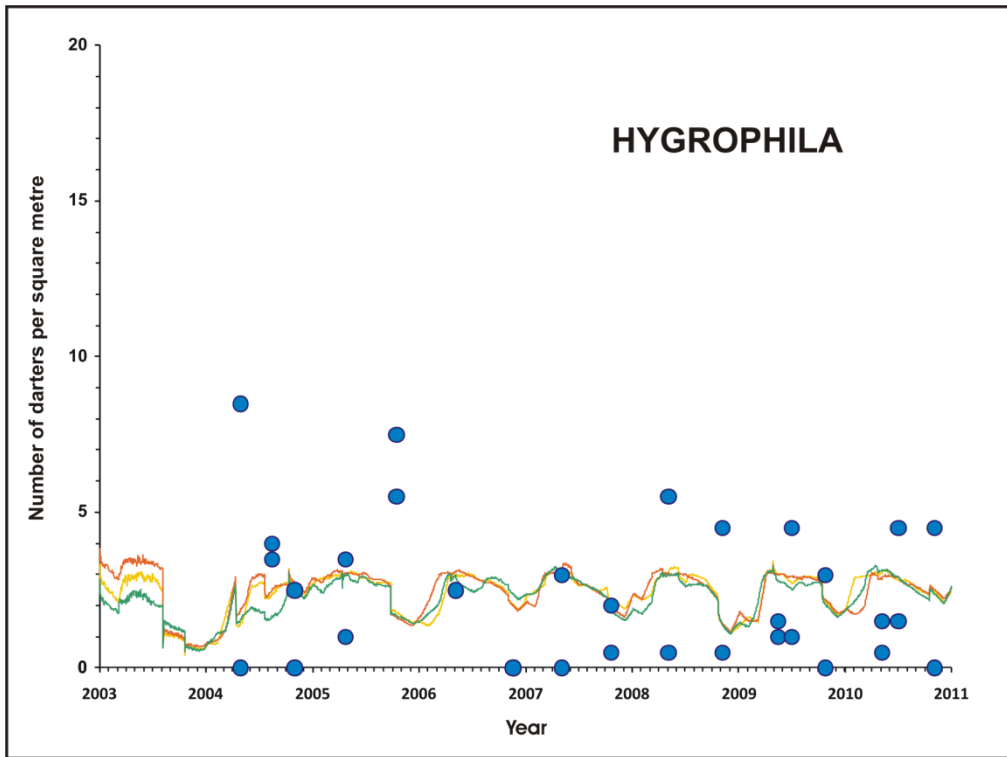


**Figure 2-18(a).** Fountain darter model (continuous traces) and drop-net data (filled circles) in *Hygrophila* for Old Channel study reach of Comal River, 2003-2010

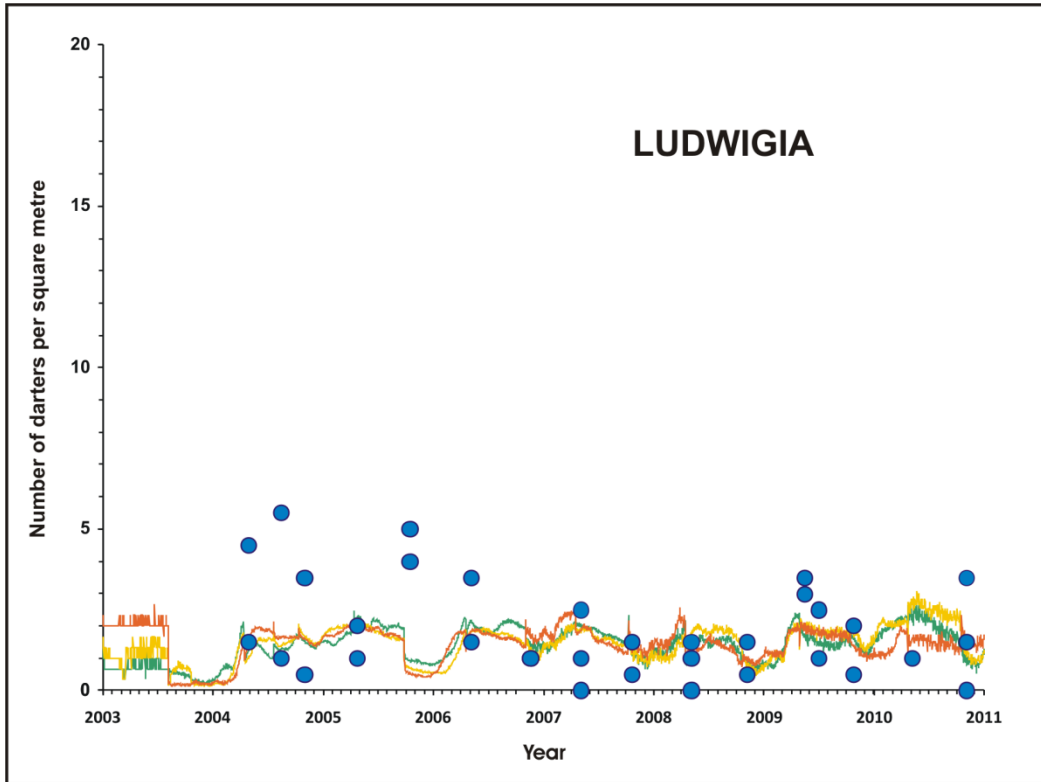


**Figure 2-18(b).** As Figure 2-18(a) in *Ludwigia* for Old Channel study reach of Comal River, 2003-2010

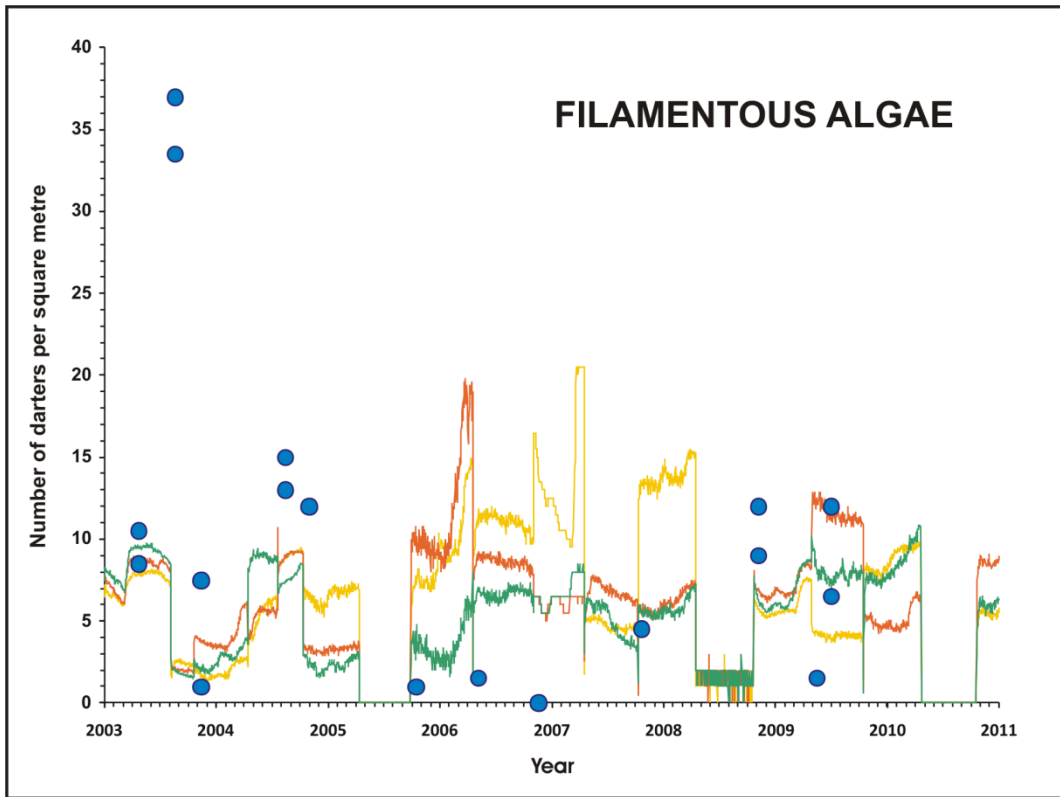


Figure 2-18(c). As Figure 2-18(a) in filamentous algae for Old Channel study reach of Comal River, 2003-2010  
Note change in ordinate axis.

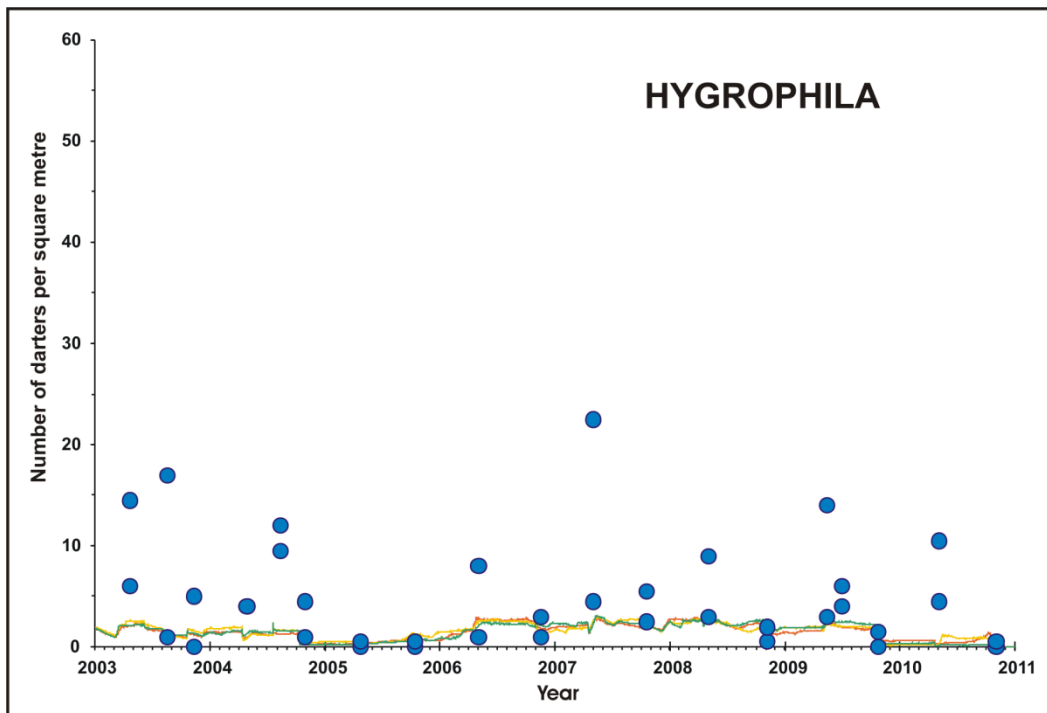


Figure 2-19(a). Fountain darter model (continuous traces) and drop-net data (filled circles) in *Hygrophila* for Upper Spring Run study reach of Comal River, 2003-2010

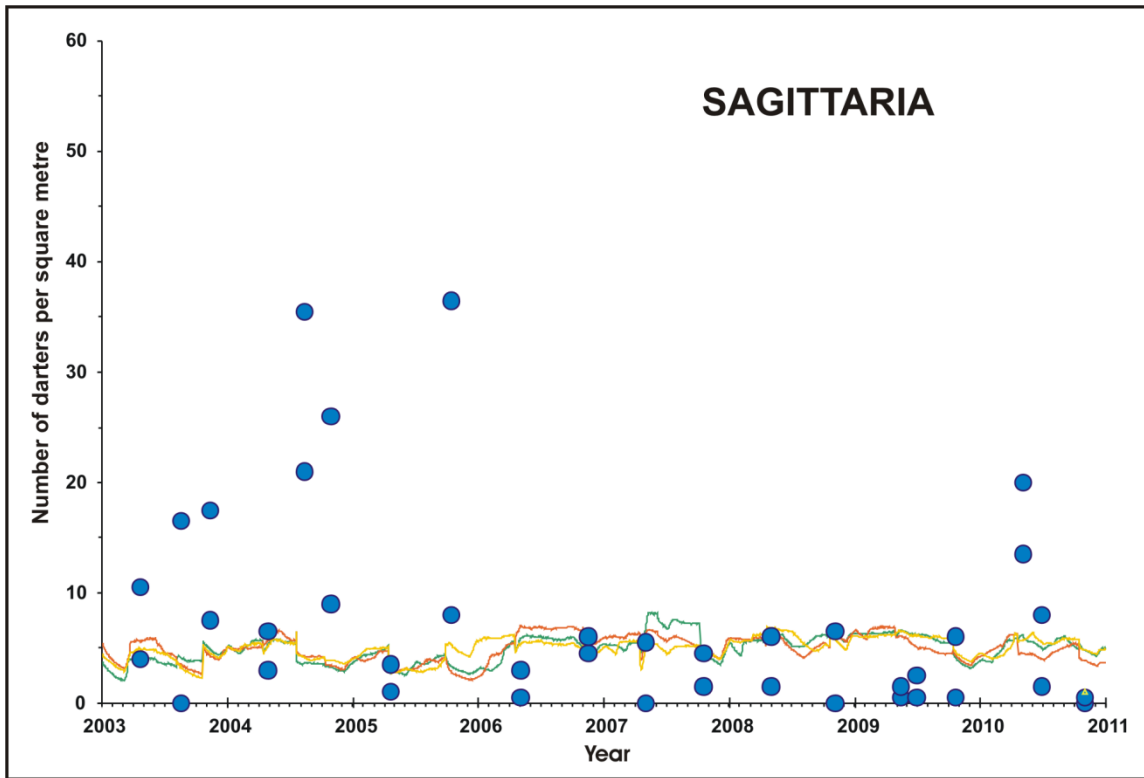


Figure 2-19(b). As Figure 2-19(a) in *Sagittaria* for Upper Spring Run study reach of Comal River, 2003-2010

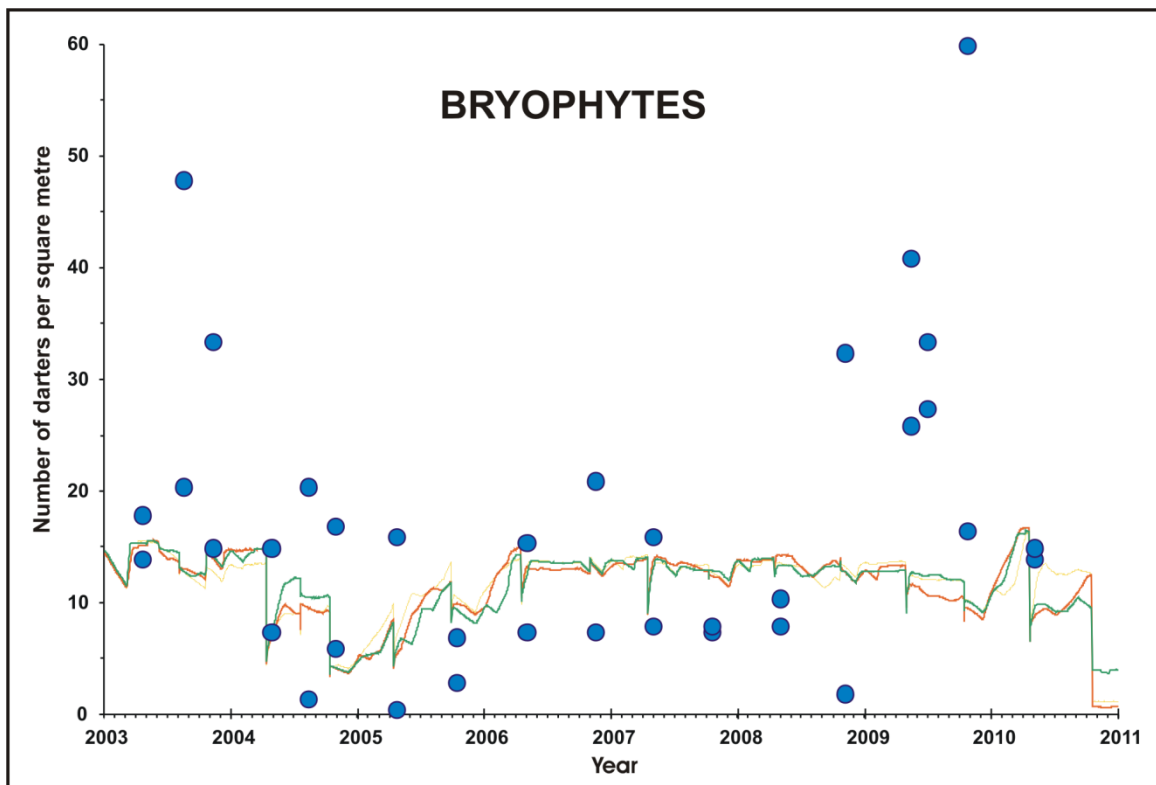
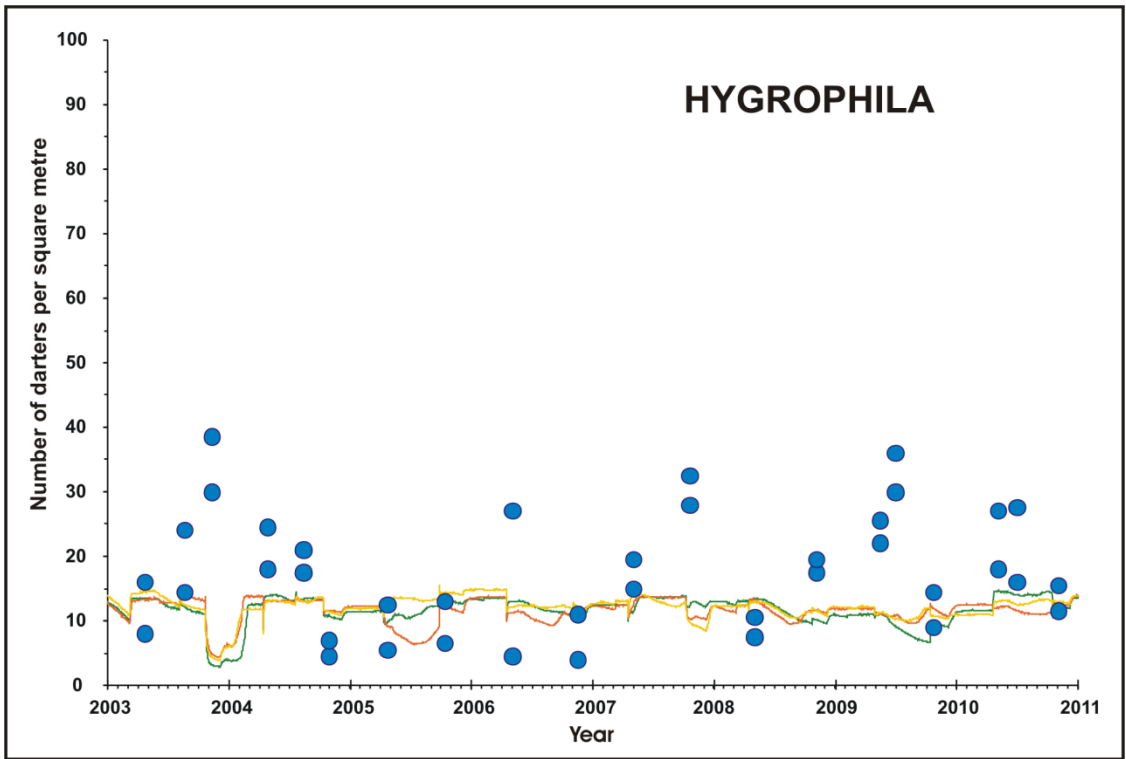
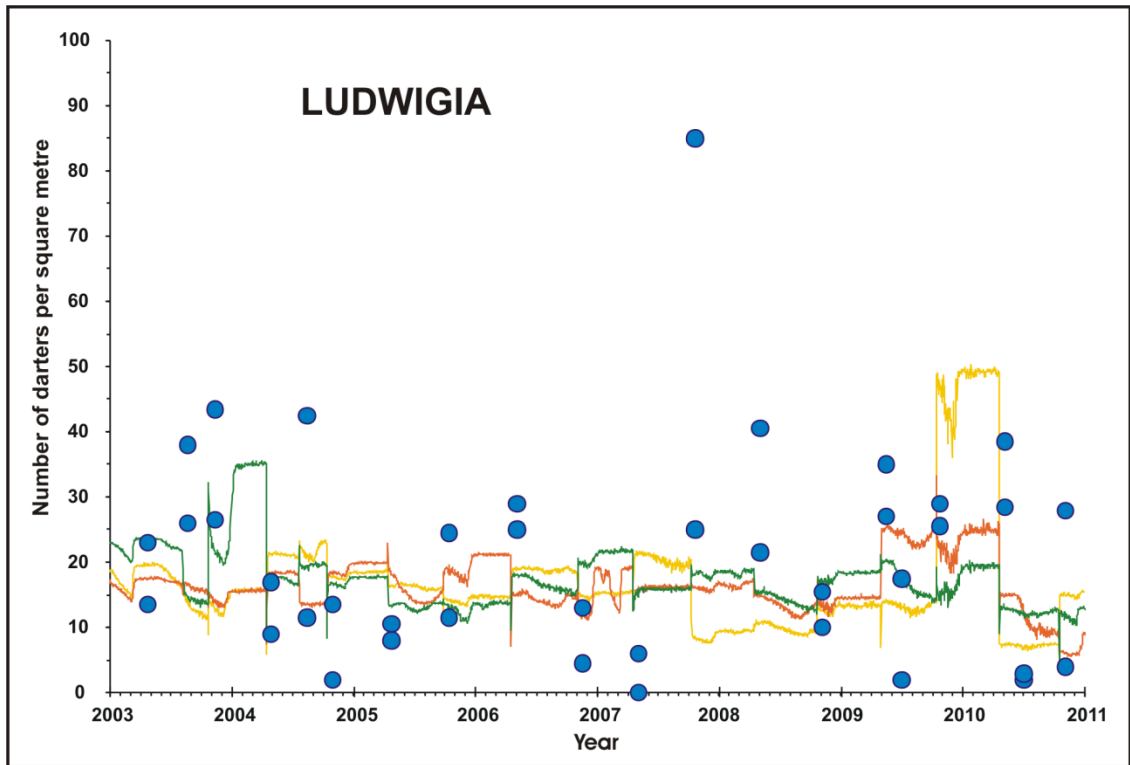


Figure 2-19(c). As Figure 2-19(a) in Bryophytes for Upper Spring Run study reach of Comal River, 2003-2010



**Figure 2-20(a).** Fountain darter model (continuous traces) and drop-net data (filled circles) in *Hygrophila* for Landa Lake study reach of Comal River, 2003-2010



**Figure 2-20(b).** As Fig. 2-20(a) in *Ludwigia* for Landa Lake study reach of Comal River, 2003-2010

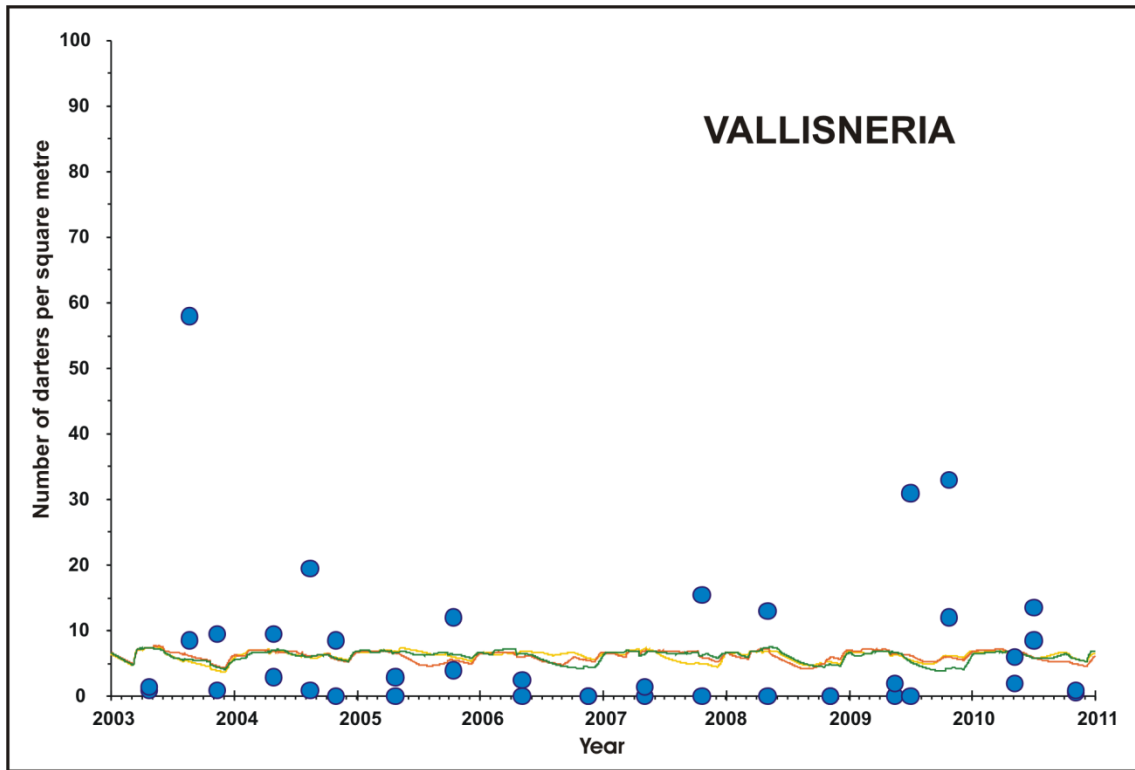


Figure 2-20(c). As Fig. 2-20(a) in *Vallisneria* for Landa Lake study reach of Comal River, 2003-2010

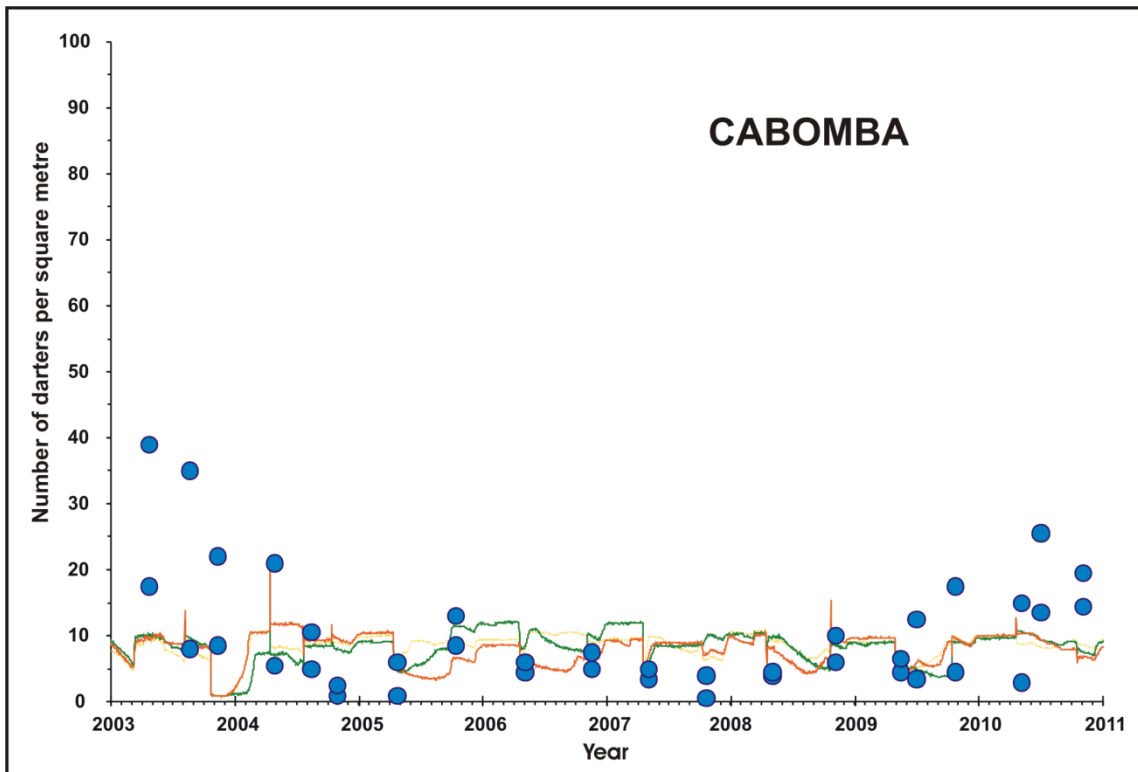


Figure 2-20(d). As Fig. 2-20(a) in *Cabomba* for Landa Lake study reach of Comal River, 2003-2010

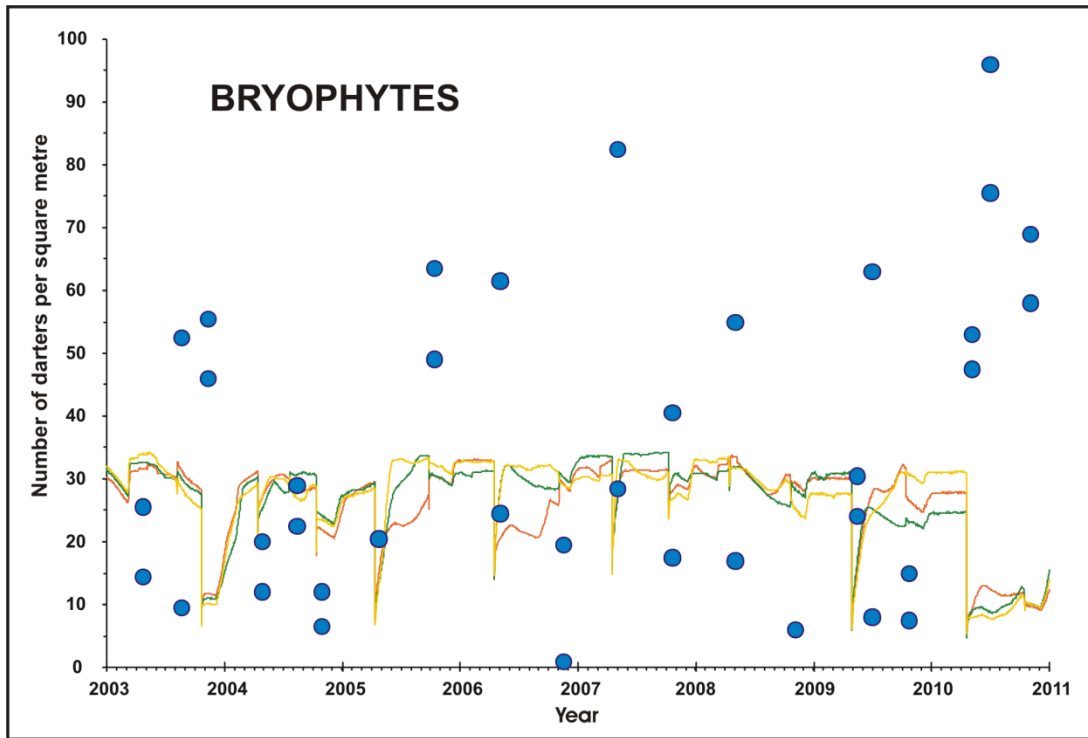


Figure 2-20(e). As Fig. 2-20(a) in Bryophytes for Landa Lake study reach of Comal River, 2003-2010

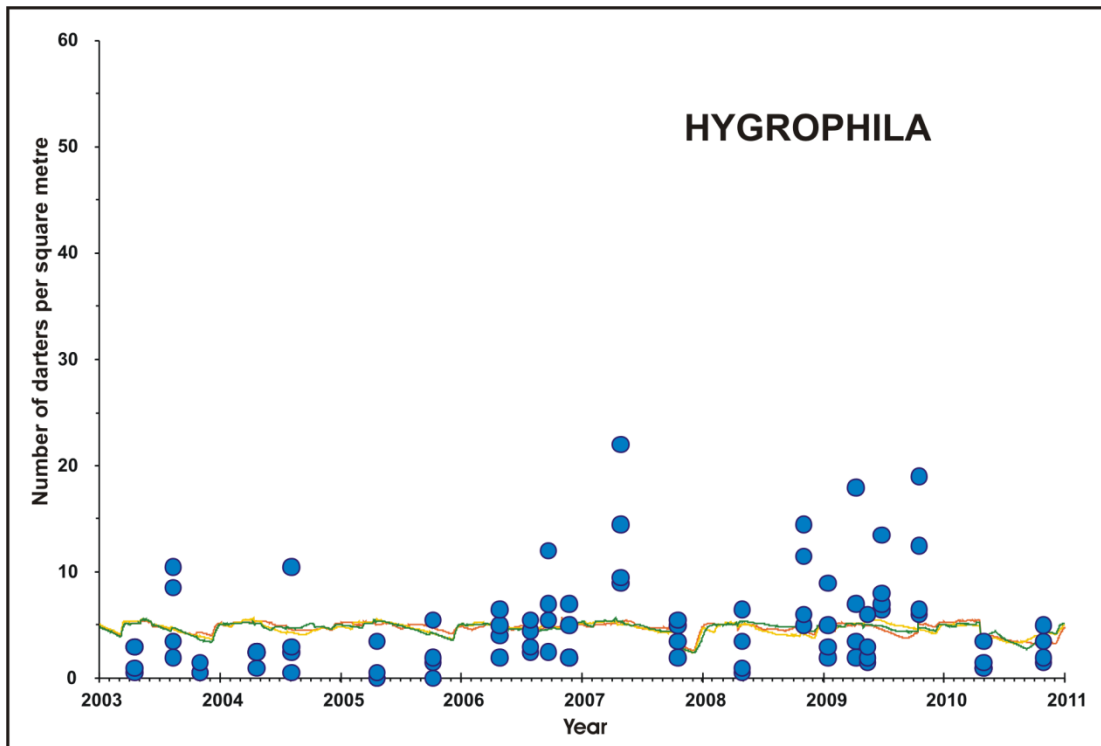


Figure 2-21(a). Fountain darter model (continuous traces) and drop-net data (filled circles) in *Hygrophila* for City Park study reach of San Marcos River, 2003-2010

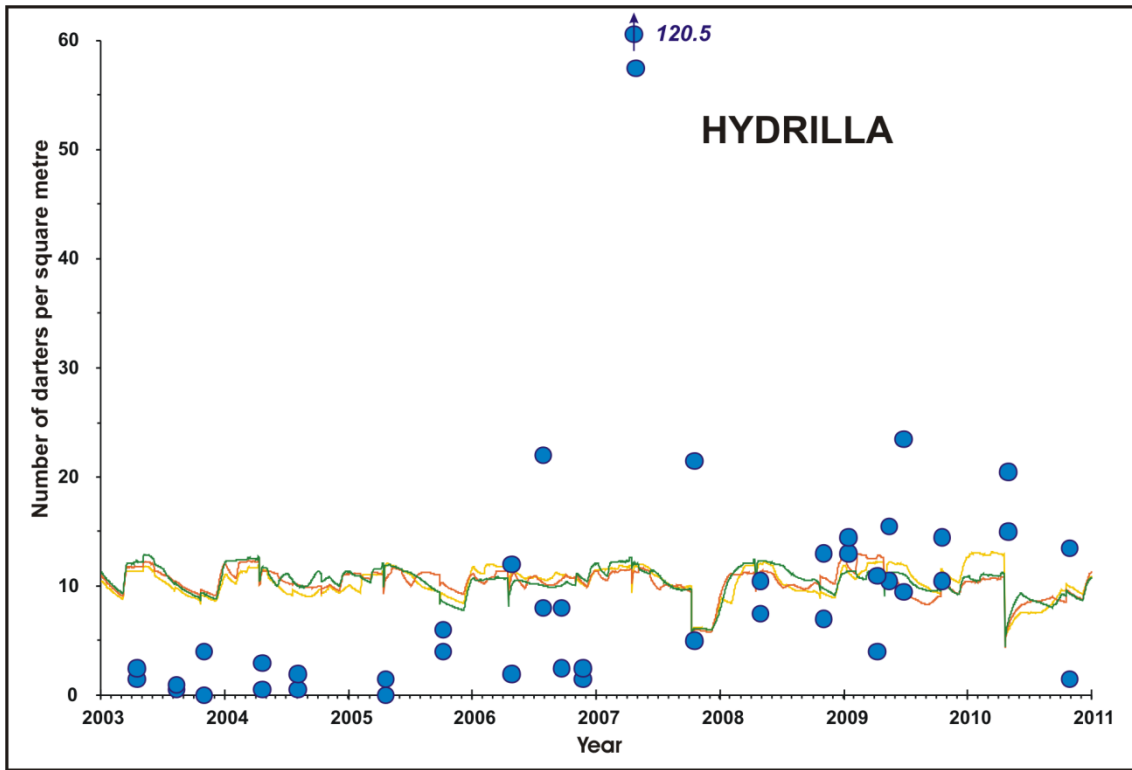


Figure 2-21(b). As Fig. 2-21(a) in *Hydrilla* for City Park study reach of San Marcos River, 2003-2010

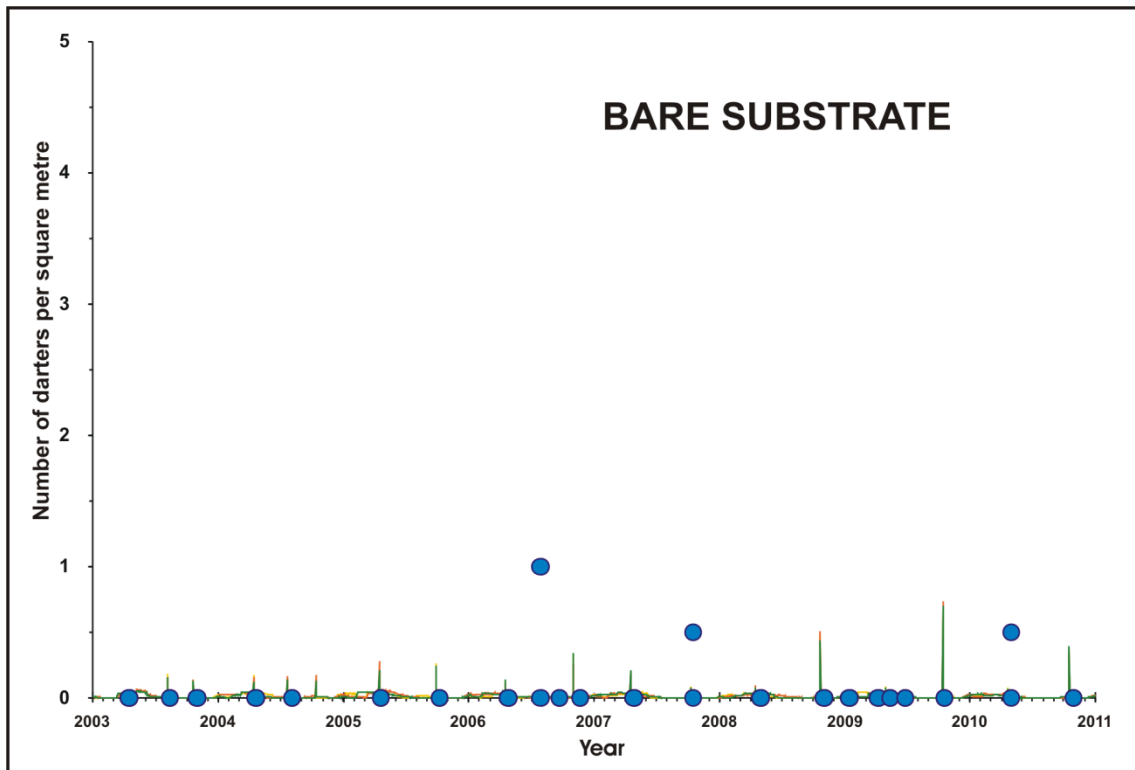


Figure 2-21(c). As Fig. 2-21(a) in bare substrate for City Park study reach of San Marcos River, 2003-2010  
Note change in ordinate axis.

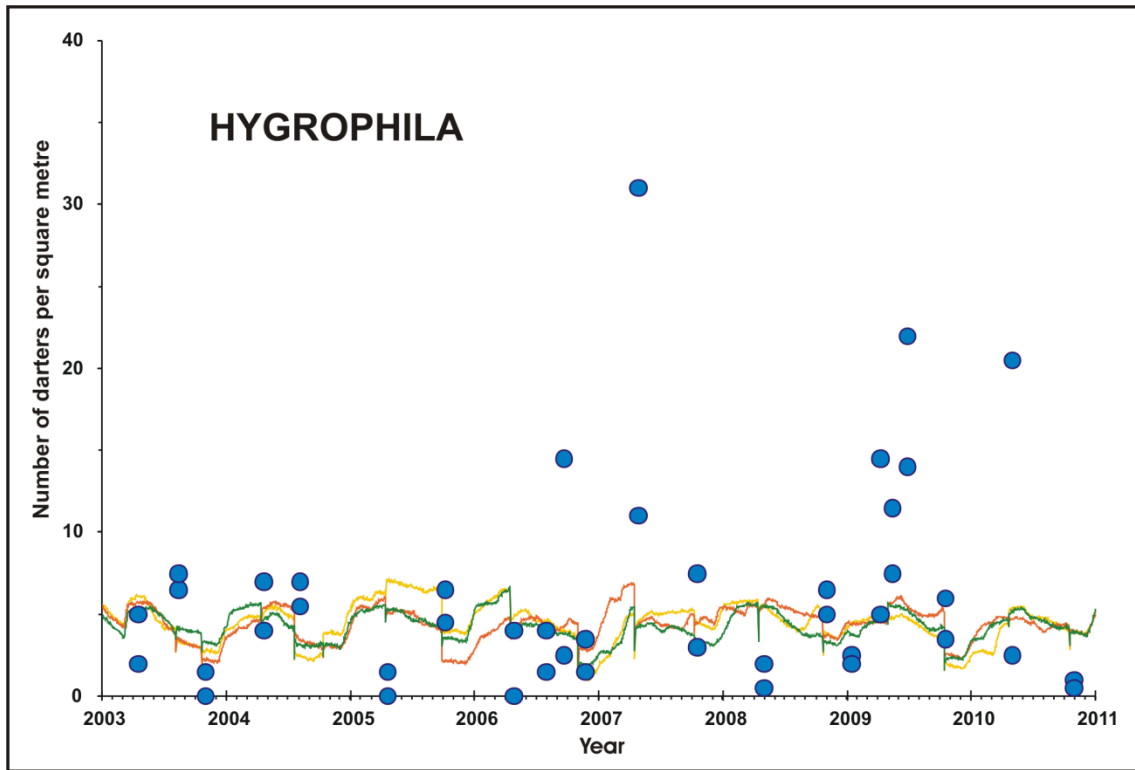


Figure 2-22(a). Fountain darter model (continuous traces) and drop-net data (filled circles) in *Hygrophila* for IH 35 study reach of San Marcos River, 2003-2010

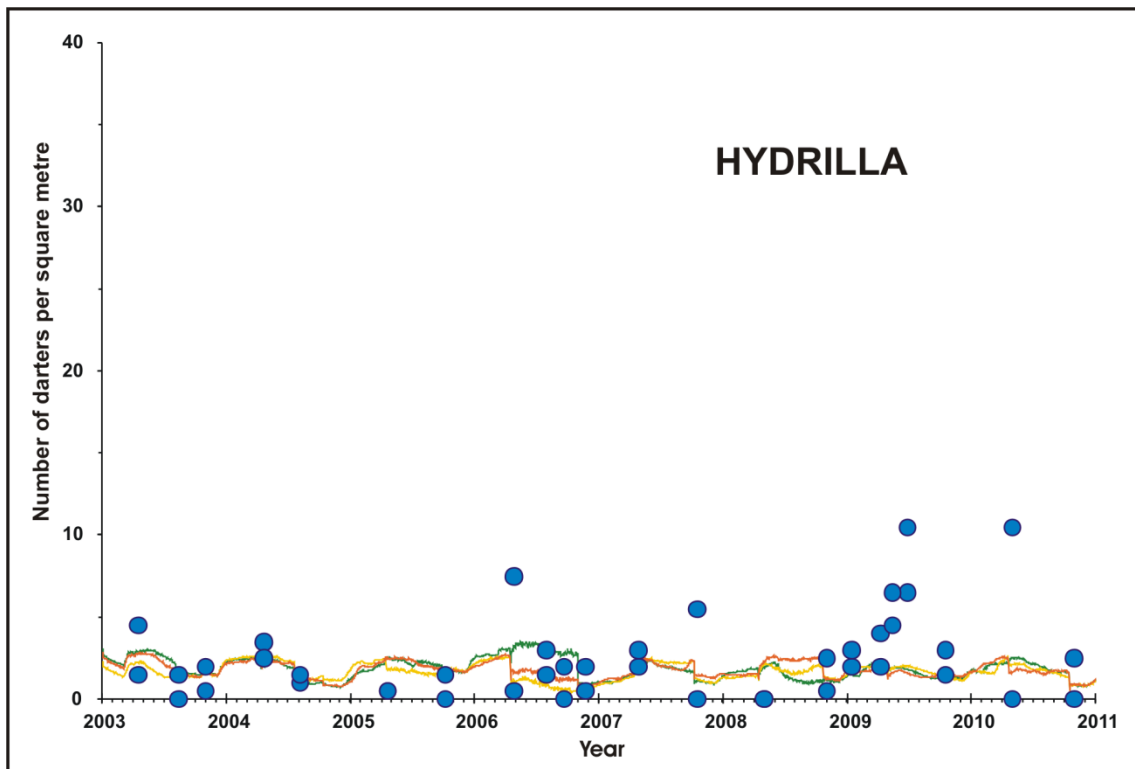


Figure 2-22(b). As Fig. 2-22(a) in *Hydrilla* for IH 35 study reach of San Marcos River, 2003-2010

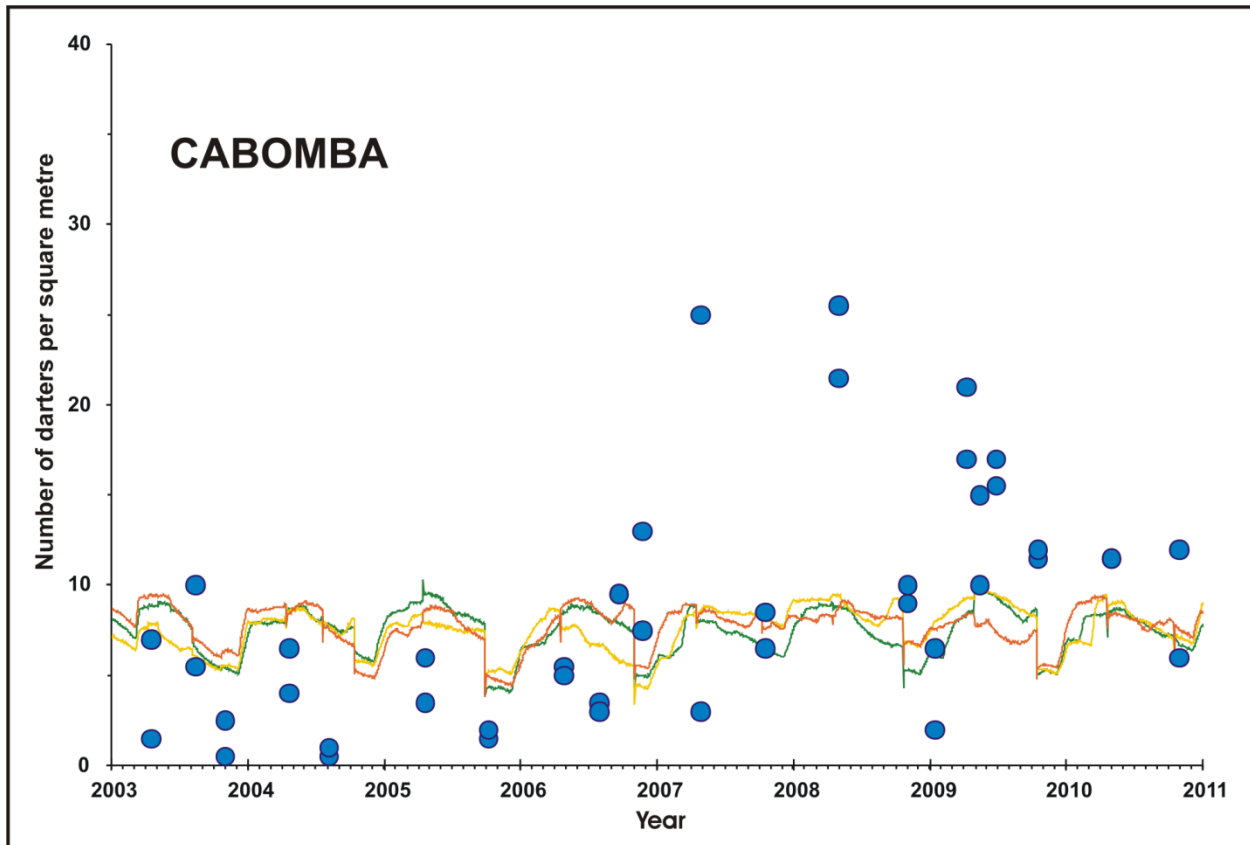


Figure 2-22(c). As Fig. 2-22(a) in *Cabomba* for IH 35 study reach of San Marcos River, 2003-2010

Next, model performance was assessed by comparing simulated fountain darter densities with drop-net observations for all five study reaches for the period 2011-2013. That is, drop-net data collected from 2011 through 2013 were not used in model parameterization. These model-to-data comparisons are shown in Figures 2-23 through 2-27. Judgment of the suitability of the calibrated model and the accuracy of validation is informed by the uncertainty in both model and data. Assuming these uncertainties are independent, a lower bound is the uncertainty in the measurements. A typical value of coefficient of variation of the fountain darter catch, stratified by species and by study reach, is around 70% of the mean density. This means that the uncertainty in the measured density can be stated as a 95% probability that the true density lies within  $\pm 140\%$  of the mean. Simulated densities generally compared well with those observed in the field, considering the variability of field data. However, in the Comal River, simulated densities in bryophytes were lower than those observed in the field in the Upper Spring Run and Landa Lake, Figs. 2-24(d) and 2-25(e), and simulated densities in *Hygrophila* also were lower than those observed in the field in Landa Lake, Fig. 2-25(a).

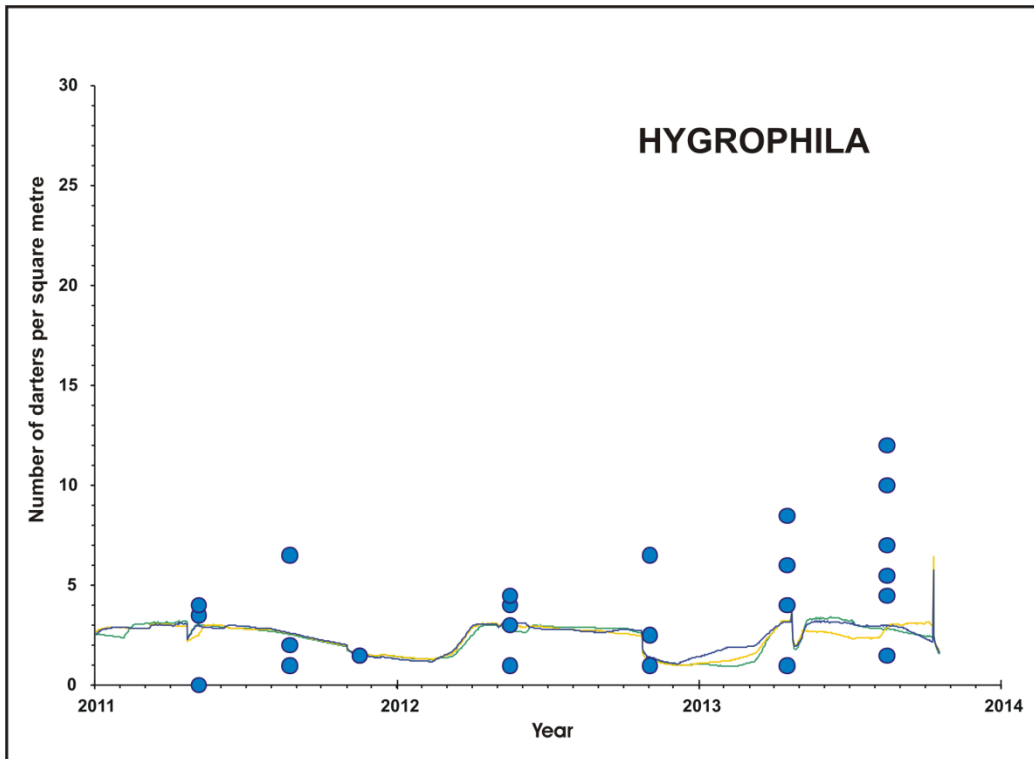


Figure 2-23(a). Fountain darter model (continuous traces) and drop-net data (filled circles) in *Hygrophila* for Old Channel study reach of Comal River, 2011-2013

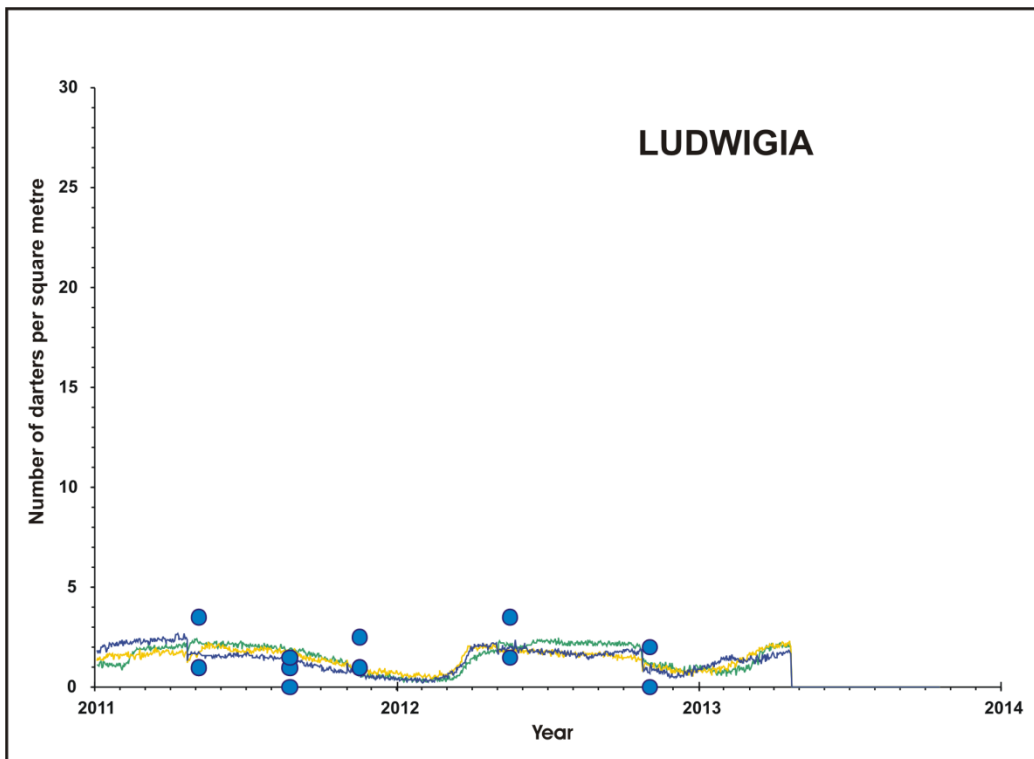


Figure 2-23(b). As Figure 2-23(a) in *Ludwigia* for Old Channel study reach of Comal River, 2011-2013

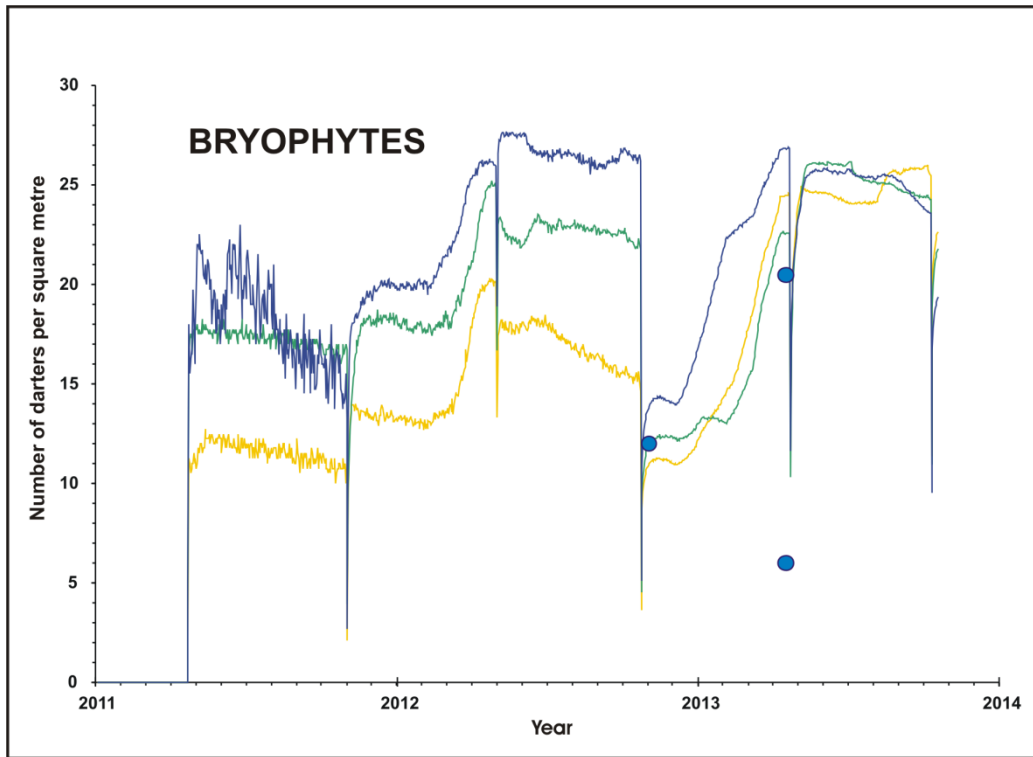


Figure 2-23(c). As Figure 2-23(a) in Bryophytes for Old Channel study reach of Comal River, 2011-2013

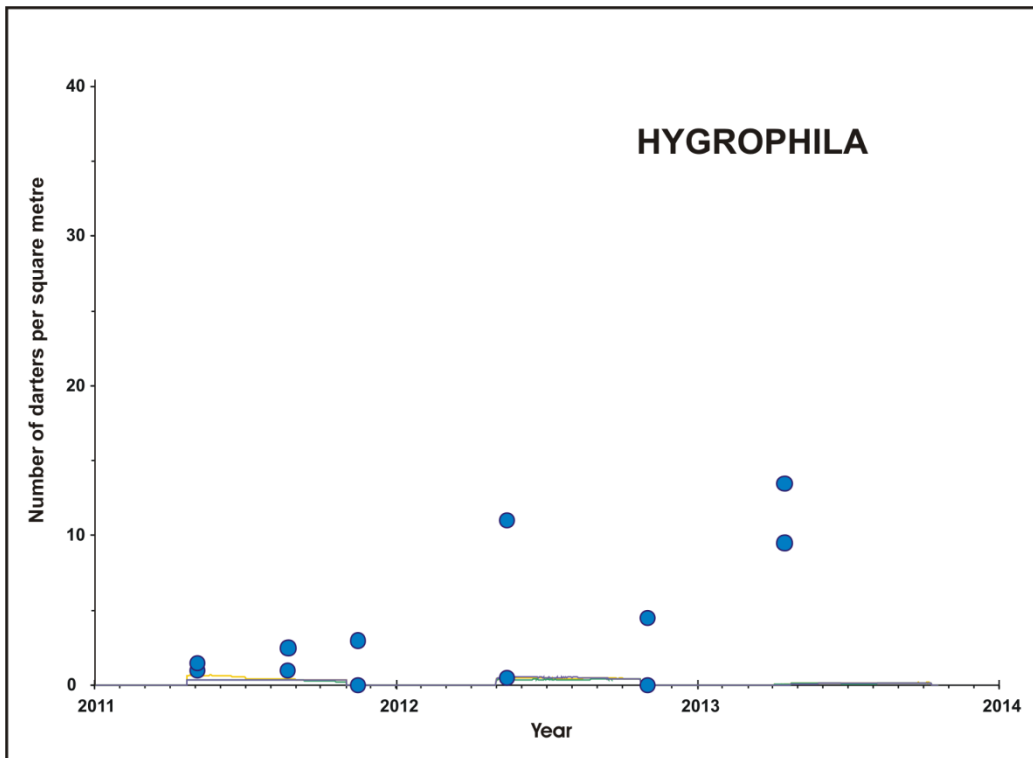


Figure 2-24(a). Fountain darter model (continuous traces) and drop-net data (filled circles) in *Hygrophila* for Upper Spring Run study reach of Comal River, 2011-2013

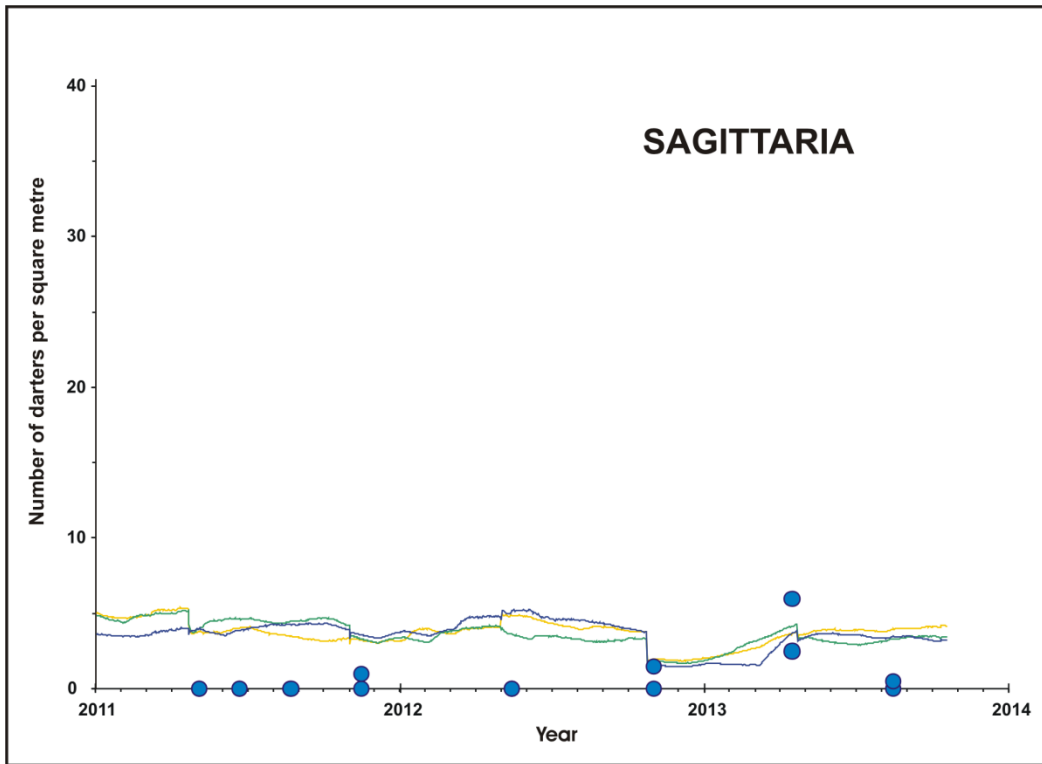


Figure 2-24(b). As Figure 2-24(a) in *Sagittaria* for Upper Spring Run study reach of Comal River, 2011-2013

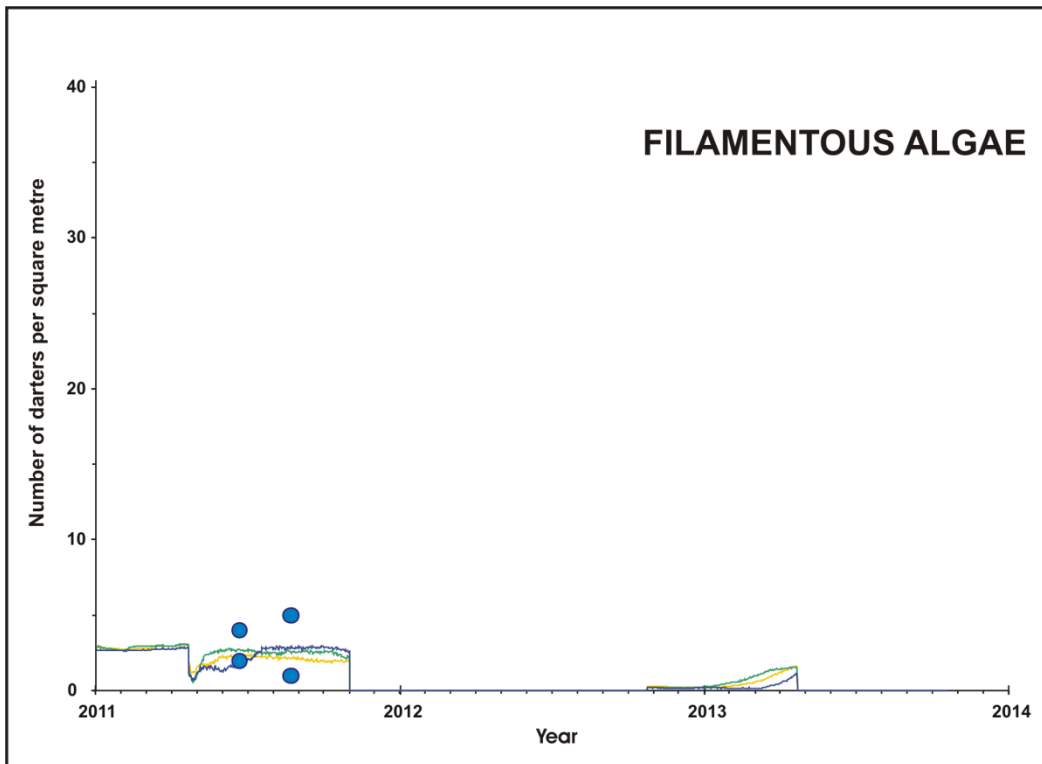


Figure 2-24(c). As Figure 2-24(a) in Filamentous Algae for Upper Spring Run study reach of Comal River, 2011-2013

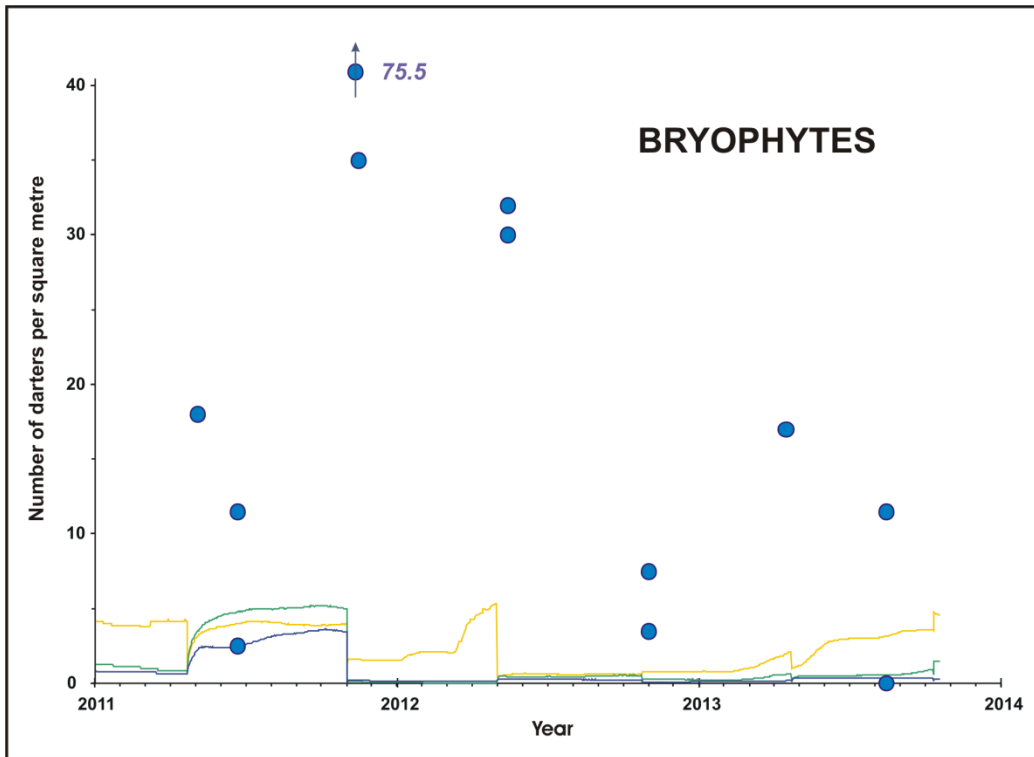


Figure 2-24(d). As Figure 2-24(a) in Bryophytes for Upper Spring Run study reach of Comal River, 2011-2013

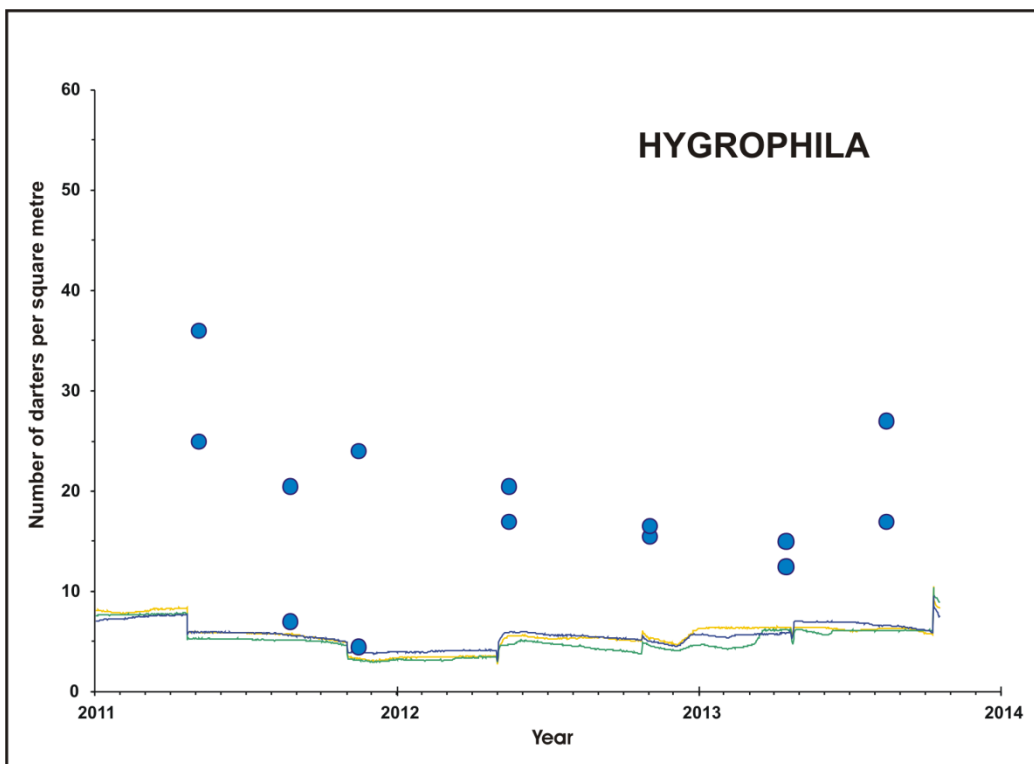


Figure 2-25(a). Fountain darter model (continuous traces) and drop-net data (filled circles) in *Hygrophila* for Landa Lake study reach of Comal River, 2011-2013

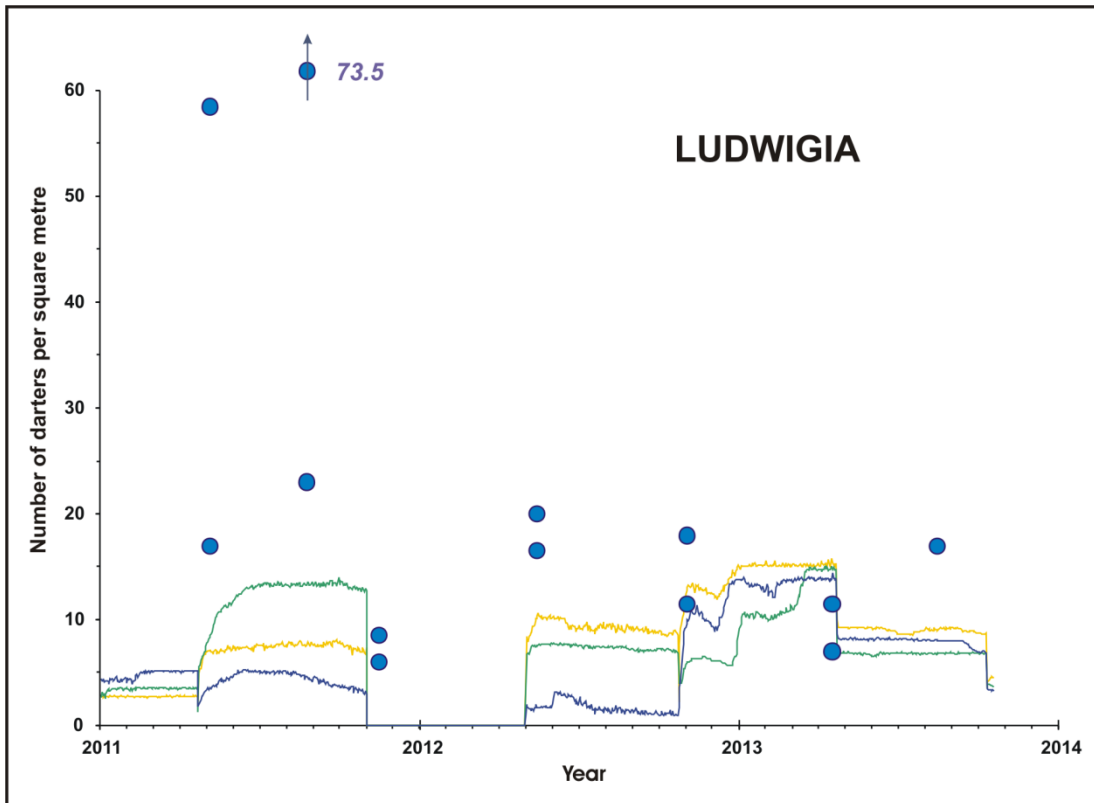


Figure 2-25(b). As Figure 2-25(a) in *Ludwigia* for Landa Lake study reach of Comal River, 2011-2013

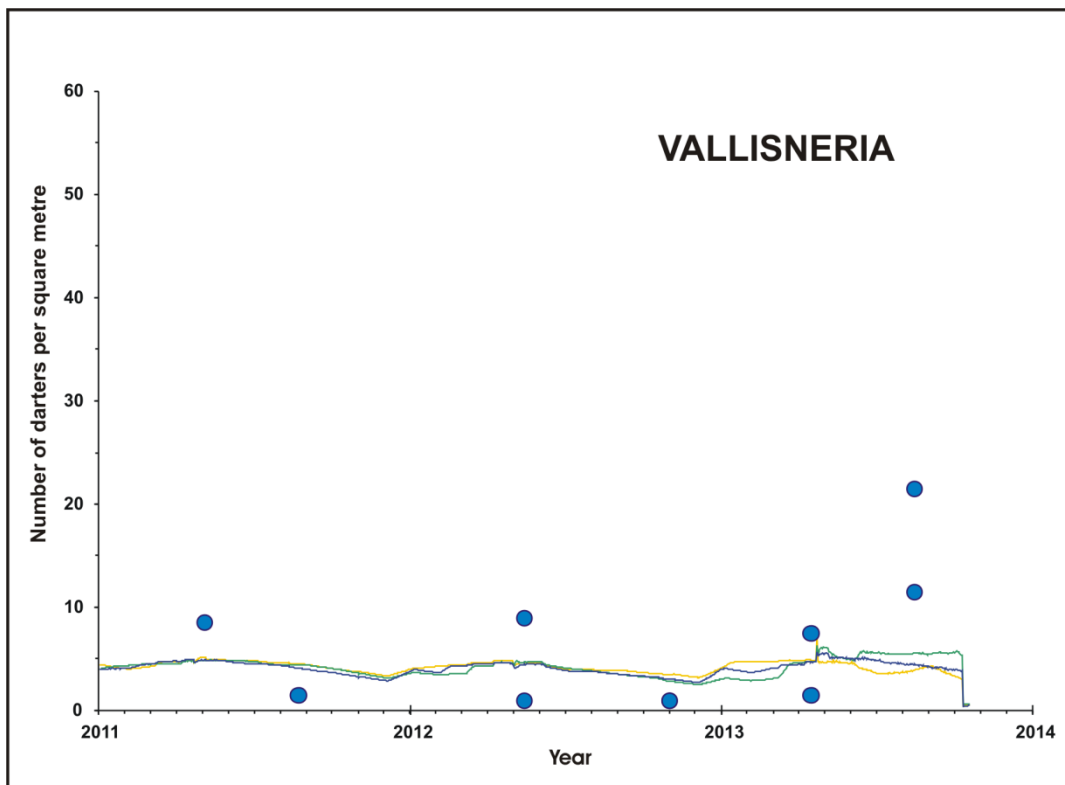


Figure 2-25(c). As Figure 2-25(a) in *Vallisneria* for Landa Lake study reach of Comal River, 2011-2013

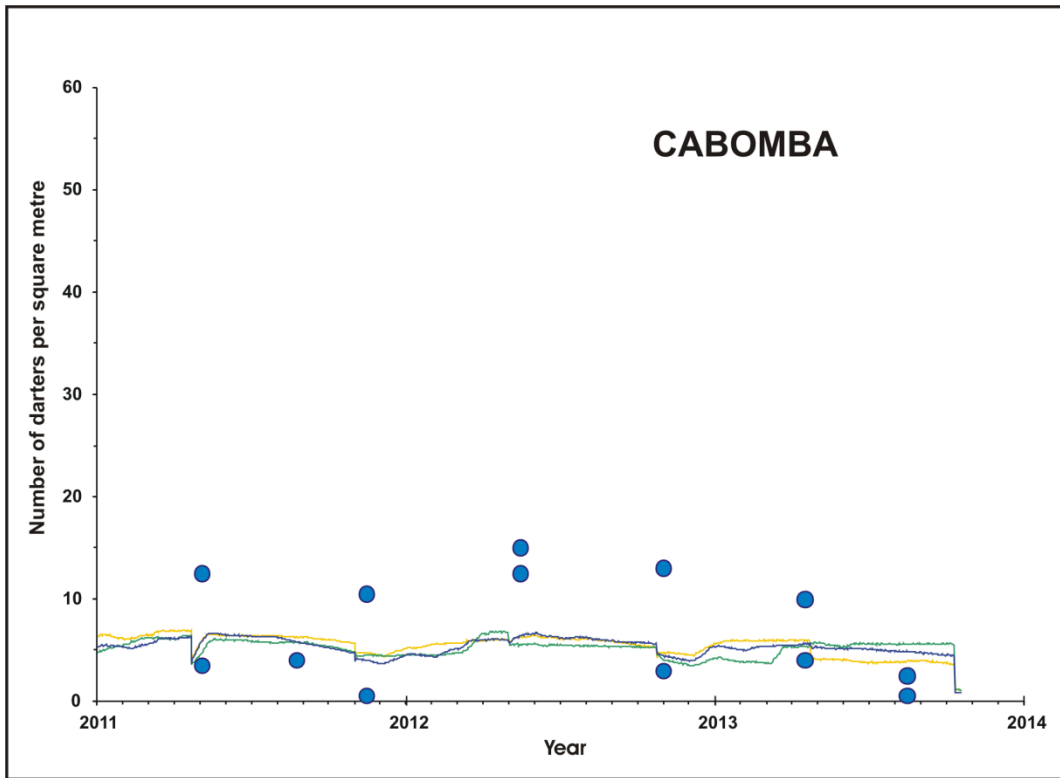


Figure 2-25(d). As Figure 2-25(a) in *Cabomba* for Landa Lake study reach of Comal River, 2011-2013

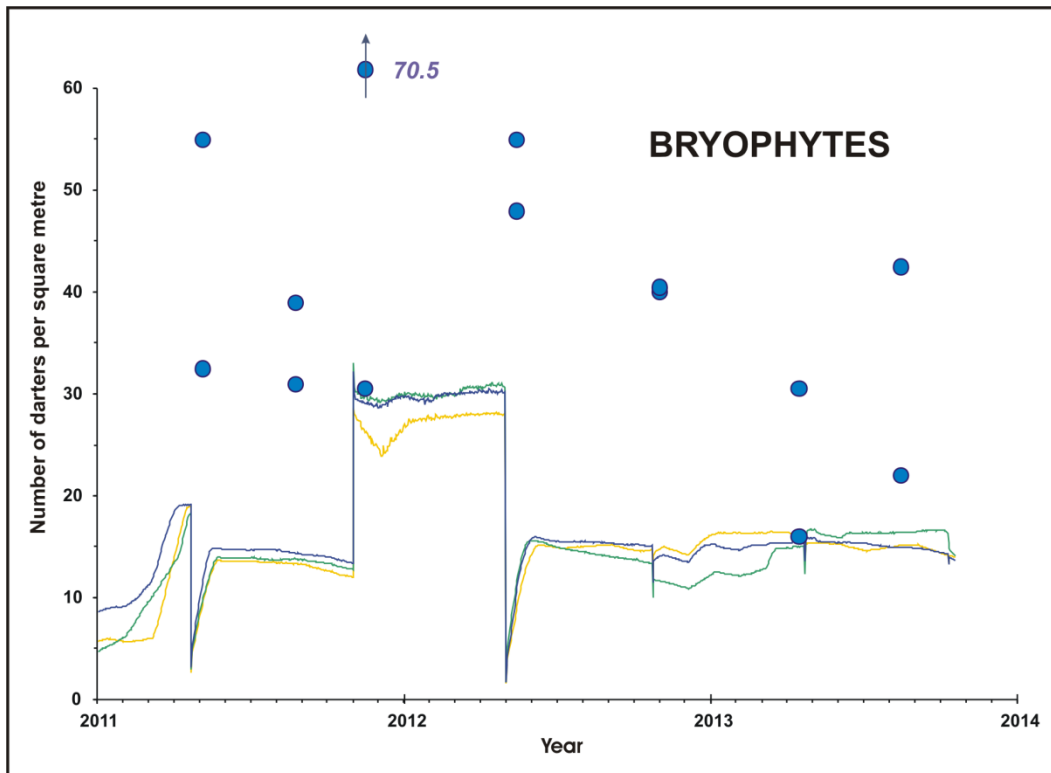
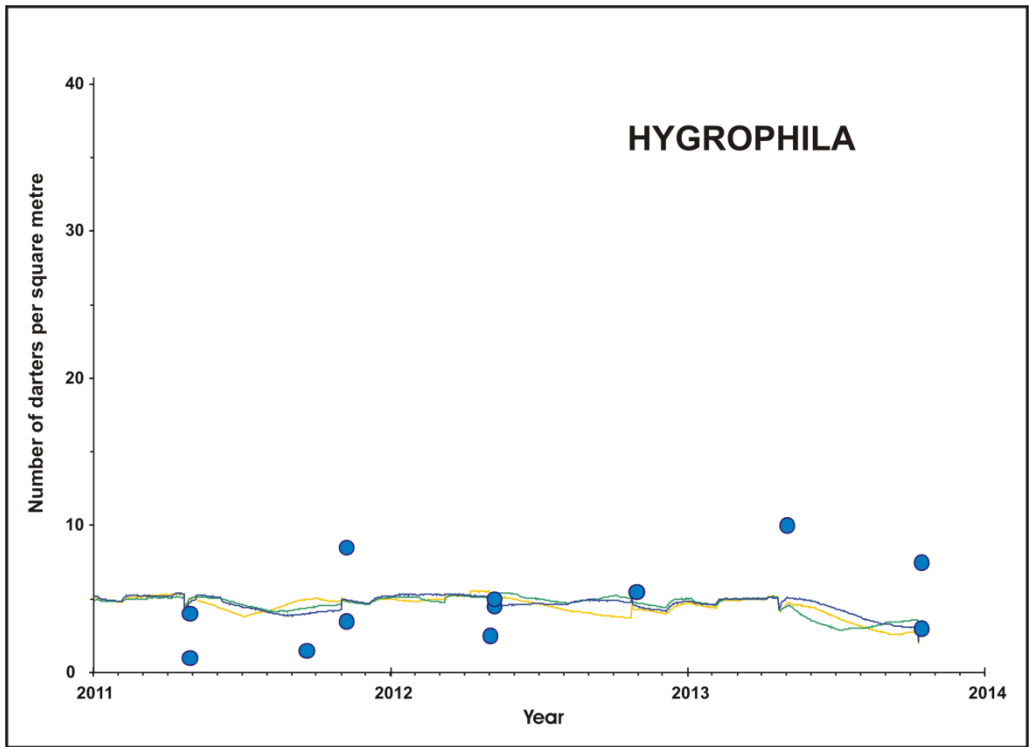
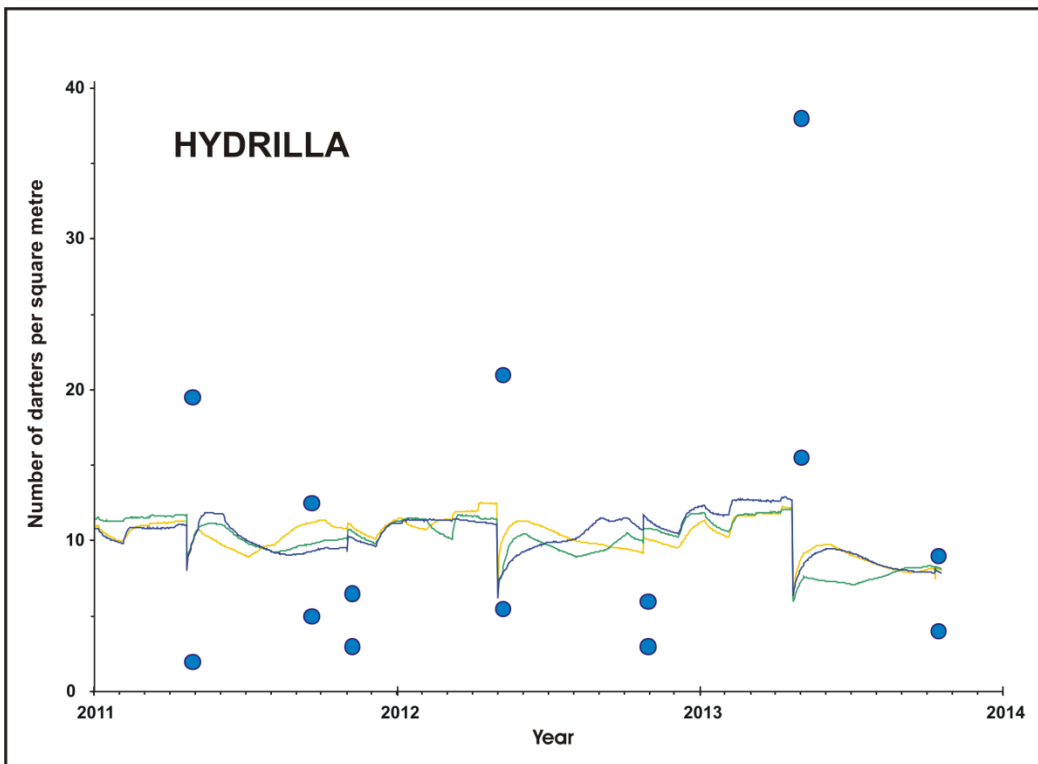


Figure 2-25(e). As Figure 2-25(a) in *Bryophytes* for Landa Lake study reach of Comal River, 2011-2013



**Figure 2-26(a).** Fountain darter model (continuous traces) and drop-net data (filled circles) in *Hygrophila* for City Park study reach of San Marcos River, 2011-2013



**Figure 2-26(b).** As Figure 2-26(a) in *Hydrilla* for City Park study reach of San Marcos River, 2011-2013

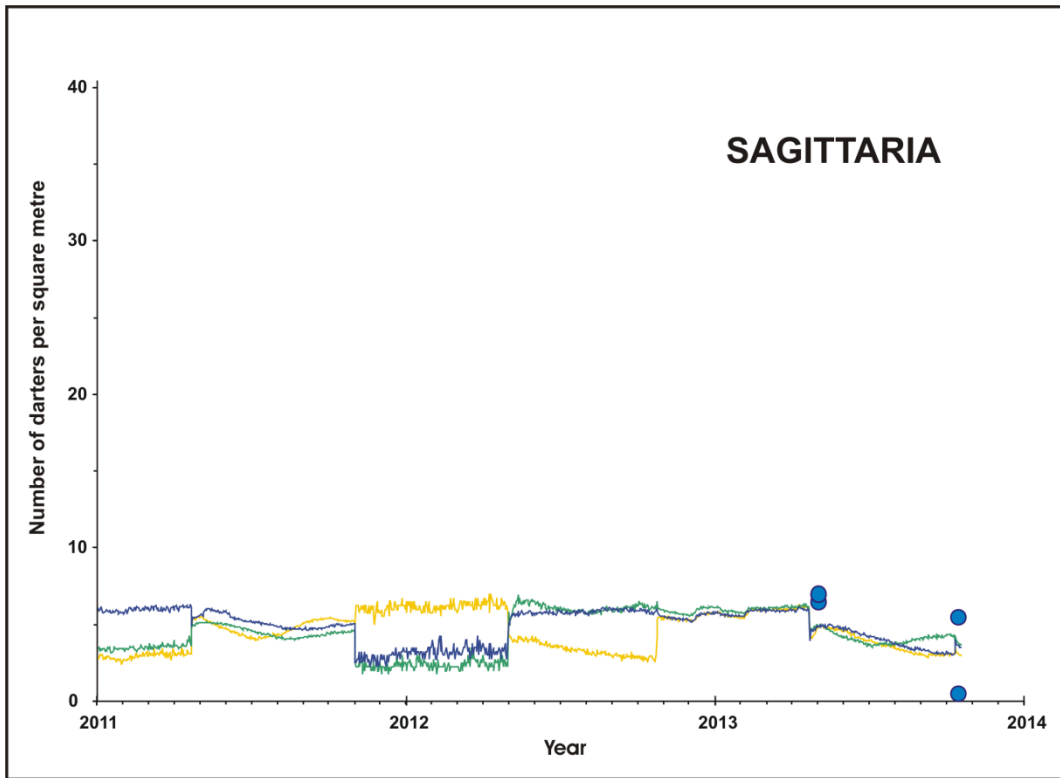


Figure 2-26(c). As Figure 2-26(a) in *Sagittaria* for City Park study reach of San Marcos River, 2011-2013

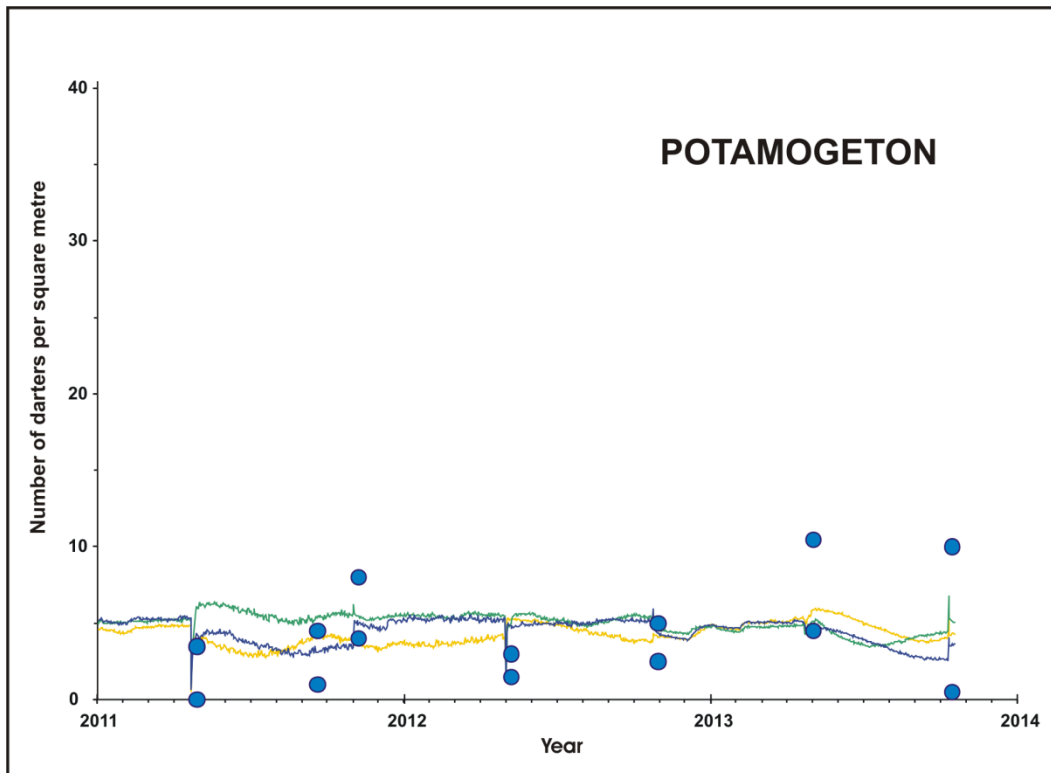


Figure 2-26(d). As Figure 2-26(a) in *Potamogeton* for City Park study reach of San Marcos River, 2011-2013

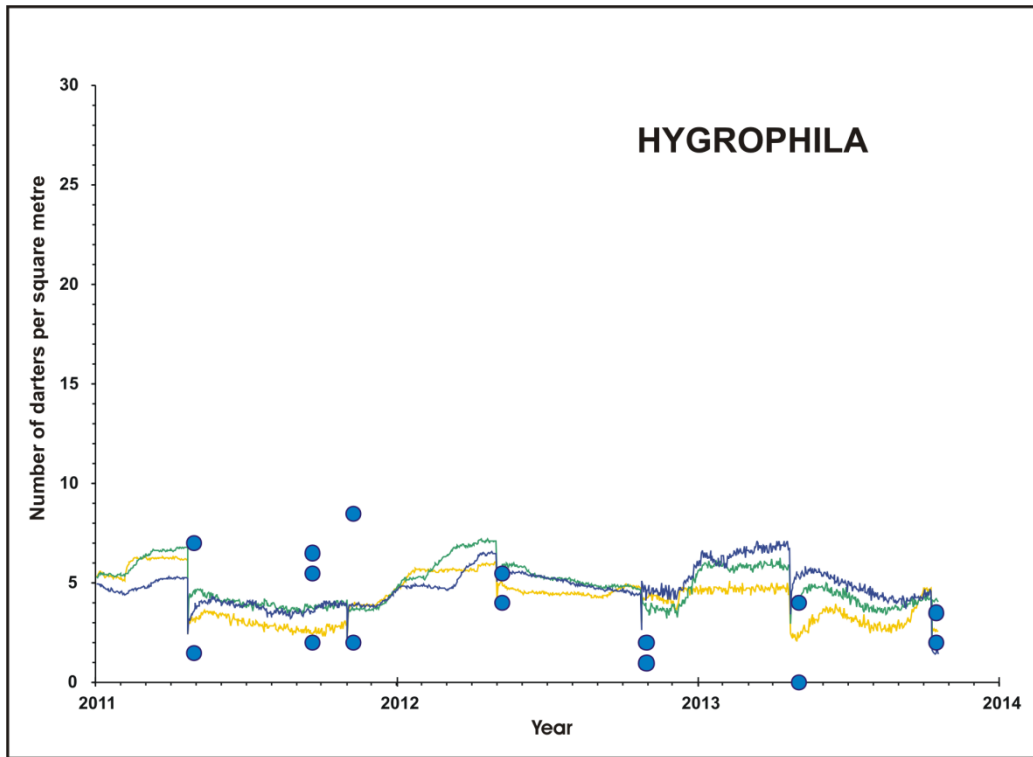


Figure 2-27(a). Fountain darter model (continuous traces) and drop-net data (filled circles) in *Hygrophila* for IH 35 study reach of San Marcos River, 2011-2013

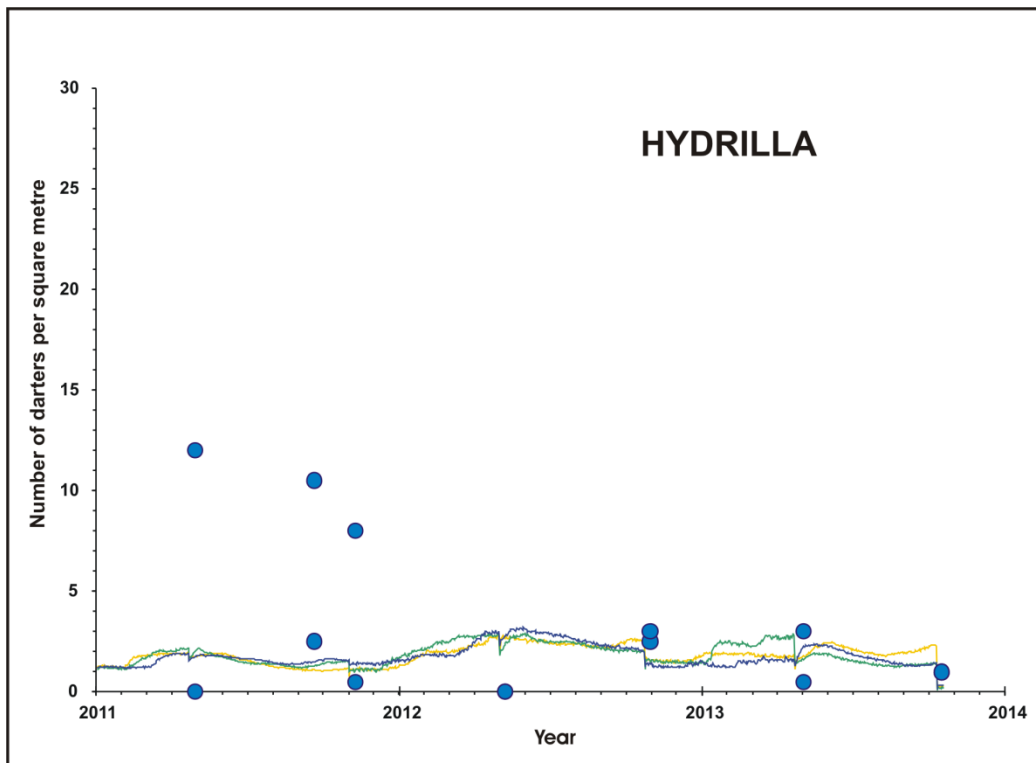


Figure 2-27(b). As Figure 2-27(a) in *Hydrilla* for IH 35 study reach of San Marcos River, 2011-2013

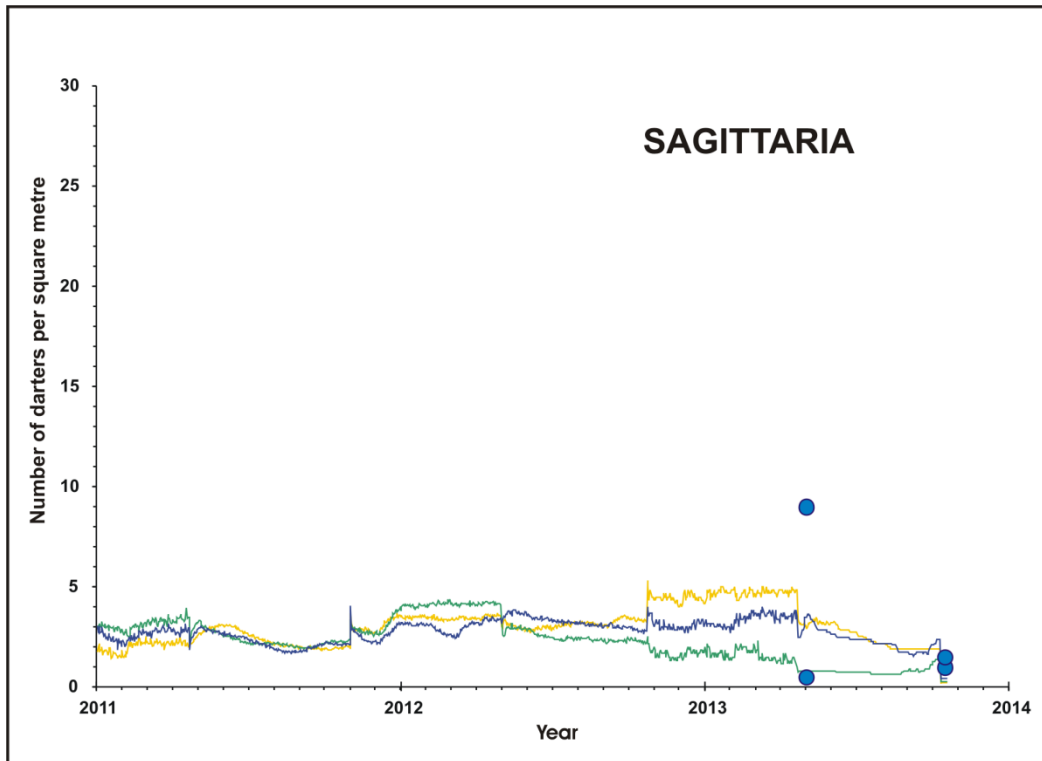


Figure 2-27(c). As Figure 2-27(a) in *Sagittaria* for IH 35 study reach of San Marcos River, 2011-2013

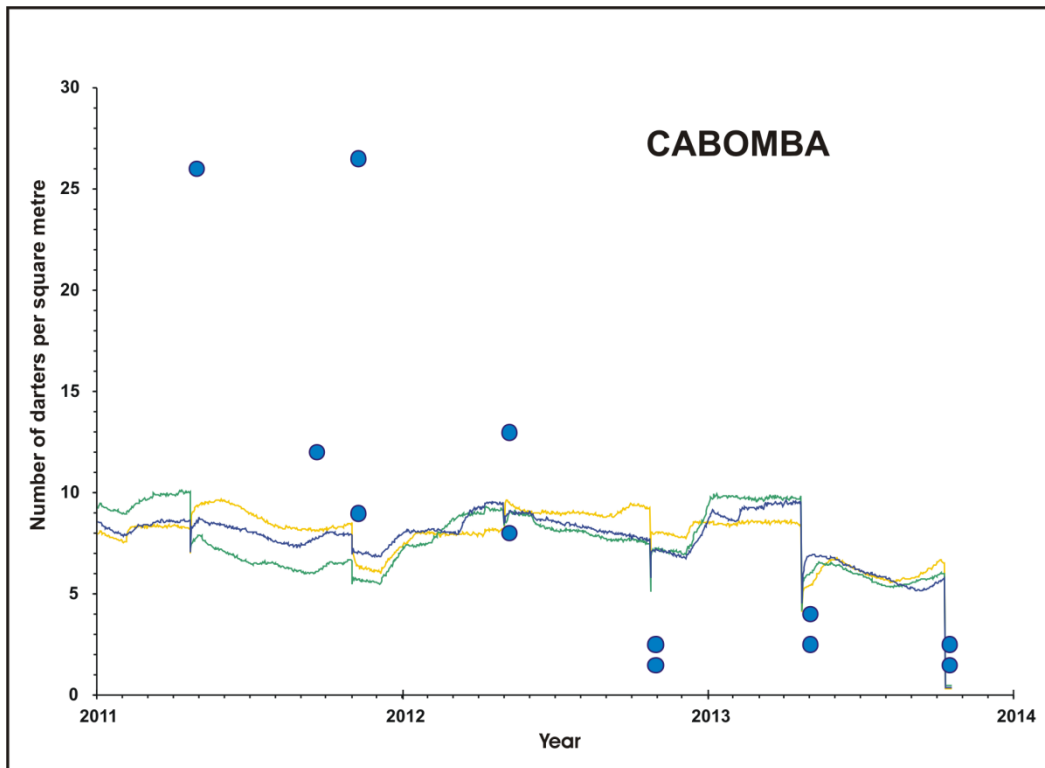


Figure 2-27(d). As Figure 2-27(a) in *Cabomba* for IH 35 study reach of San Marcos River, 2011-2013

Simulated densities in *Ludwigia* were lower than observed densities in Landa Lake during 2011, but simulated and observed densities corresponded well thereafter, Fig. 2-25(b). In the San Marcos River, simulated densities in both *Hydrilla* and *Cabomba* were lower than observed densities in the I35 reach during 2011, but simulated and observed densities corresponded well thereafter, Figs. 2-27(b) and (d). It should be noted in Figs. 2-18 et seq. that generally when the fountain darter submodel is in error, it tends to under-predict darter abundance. This means that the darter model is conservative with respect to depicting impacts on the darter.

We also compared the distances moved by simulated darters under historical habitat conditions from 2003 to 2013 within each of the five reaches to movement distances observed in a recent field study. Relocation data on darters tagged in the Upper Spring Run Reach and Blieders Creek of the Comal River indicated mean movements from their release locations of 20.9 m (BIO-WEST 2014c), whereas fountain darters tagged in the Old Channel of the Comal River moved an average of 10 m ( $\pm 17$  std. dev.) away from their release locations (Dammeyer et al. 2013). Mean movements of simulated darters away from the location where they metamorphosed into mobile juveniles (eggs and larvae are immobile) were 19.9 m in the Upper Spring Run Reach, and 24.6 m, 22.0 m, 26.0 m, and 15.6 m in the Old Channel, Landa Lake, City Park, and I35 reaches, respectively, in excellent agreement with the field observations.

For additional validation, the simulated stock-recruitment relationship was compared to the expected stock-recruitment relationship for fountain darters. Based on their life history, one would expect a Beverton-Holt type spawner-recruit relationship, likely with a weak response (a gradually leveling off curve) characterized by a steepness coefficient of 0.5 to 0.7 (Rose et al. 2001; Kenny Rose, pers. comm.). For these simulations, we used the version of the model of Old Channel study reach of the Comal River, with MD values based on 2003-2010 drop-net data. The model was set up to run a steady-state scenario in order to remove the effect of variable environmental conditions. Inputs were the distribution of aquatic vegetation types observed in the fall of 2012, and mean flow, temperature and DO from the fall period (23 October 2012 – 21 April 2013). (The aquatic vegetation during the fall of 2012 yielded the highest estimated maximum darter density, approximately 11,000 juveniles plus adults, for the Old Channel Reach over the eleven-year period 2003 – 2013.) We initialized the darter population at low densities, ranging from 1 to 20 percent of the estimated MD, which allowed observation of annual stock-

recruitment relationships at a variety of population sizes as the population grew toward the estimated maximum darter density. Stock size was calculated as the mean number of adults alive during a calendar year (i.e., the total number of “adult-days” accumulated during the calendar year divided by 365). Annual recruitment was calculated as the number of eggs laid during a calendar year that reached the adult stage within the same calendar year. These simulations yielded a Beverton-Holt type spawner-recruit relationship with a steepness coefficient of 0.395 ( $r^2 = 0.96$ ), shown in Figure 2-28, in fair agreement with the expected steepness coefficient.

The sensitivity of model fountain darter population dynamics to changes in model parameters was examined by a series of specified runs. Parameters investigated were maximum darter density, demographic/life history attributes, and environmental conditions, as well as several hypothesized forms of density-dependent negative feedback on population growth rate (details on these results in Appendix C). In summary, the sensitivity of simulated population density to how MD is estimated, *viz.* from study reach data only versus from the entire river, was variable (depending in turn on the variation in darter densities in the various study reaches), but both seasonal and longer-term population trends were qualitatively the same regardless of the manner of estimating maximum darter densities. Among the demographic/life history parameters, growth rate was most sensitive to increases in larval mortality rate, decreases in proportion of females laying eggs and mean clutch size, and insensitive to changes in egg, juvenile, and adult mortality rates, as well as duration of juvenile and young adult stages. Among the environmental variables, growth rate was sensitive to both increases in water temperature and decreases in DO.

Model predictions of population dynamics proved most sensitive to density-dependent increases in larval mortality rate, and were insensitive to density-dependent increases in egg, juvenile, and adult mortality rates, as well as to density-dependent decreases in proportion of females laying eggs and mean clutch size. With simultaneous implementation of all six density-dependent effects, model predictions of population dynamics were similar qualitatively to predictions without density-dependent effects, but densities averaged about 60% of those generated without density-dependent effects. Interestingly, with all six density-dependent effects in the model, the resulting stock-recruitment relationship was drawn closer to the expected range of steepness coefficient, 0.5 - 0.7. The best-fit Beverton-Holt type spawner-recruit relationship was found to have a steepness coefficient of 0.487 ( $r^2 = 0.90$ ), see Figure 2-29.

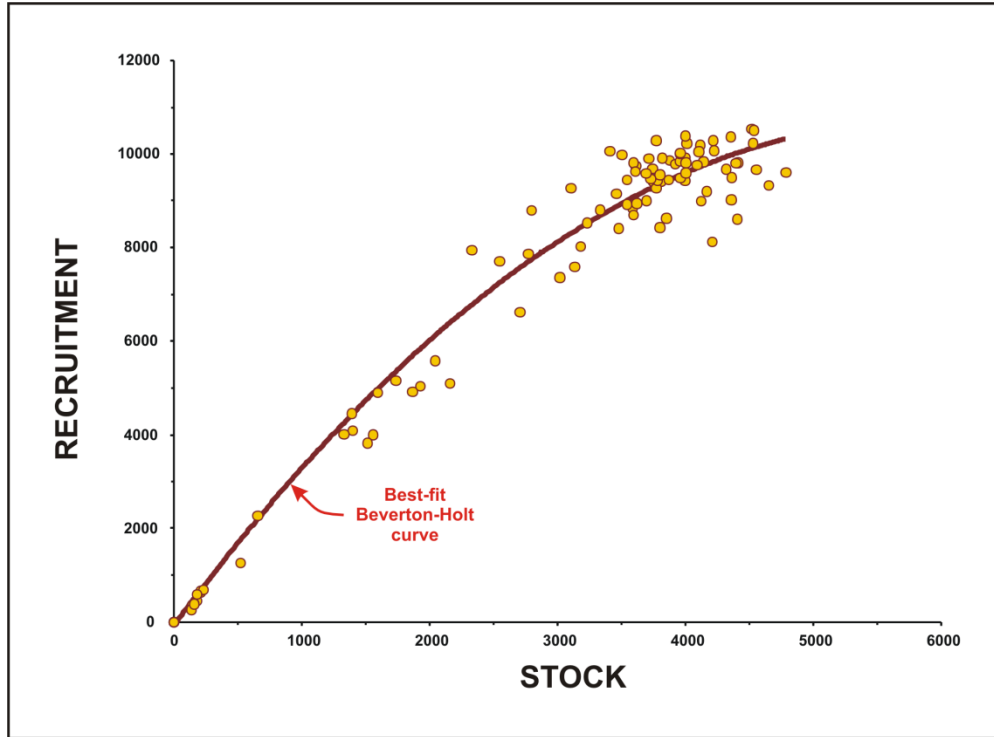


Figure 2-28. Stock recruitment diagram for fountain darter model with best-fit Beverton-Holt relation, no density-dependent feedback

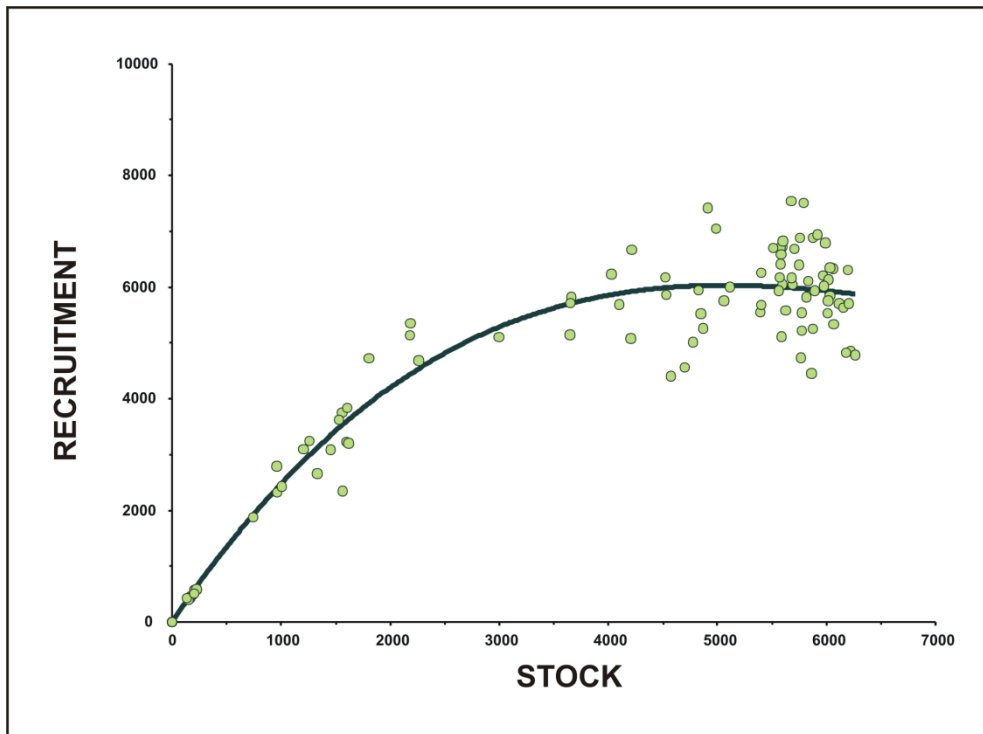


Figure 2-29. Stock recruitment diagram for fountain darter model with best-fit Beverton-Holt relation, six density-dependent feedback mechanisms

### 3 Model Applications

As discussed in the Introduction, the goal of this tool is to be capable of depicting *responses* of the river ecosystem to various external factors (including scenarios of Covered Activities, EARIP, 2012), which can be used to *assist* the management of the Edwards Aquifer. In particular, this model should be capable of addressing the efficacy of the HCP Phase 1 flow regime in terms of the survival and recovery of the fountain darter in the wild. As outlined in the HCP, and consequently understood and adhered to during model development, the intent of this tool from the outset was to assist with management applications in to the future. The model is not designed to be an exhaustive representation of ecological processes or interactions.

#### 3.1 Scenarios

In Section 2.3 above, the operation of the Fountain Darter Modeling System (FDMS) was described in which the user prescribes a suite of inputs whose definition and data specification depend upon the objectives of the model exercise, in that case the evaluation of model performance. In general, the suite of inputs characterizes a *scenario*. In the past half-century, the concept of a scenario has become ensconced in strategic planning and management, and, in particular, environmental assessment (Mahmoud et al., 2009; Rounsevell and Metzger, 2010). A scenario is a plausible timeline of key driving variables that embodies coherent behaviors. It is important that parsimony be exercised in the selection of variables and level of detail, otherwise the scenario becomes bogged down and unwieldy (Schnaars, 1987).

In the present project, the response at issue is the population of fountain darters in the two rivers. The driving variables are streamflow, especially the springflow component, and associated meteorology, together with time sequences of vegetation either from the SAV submodel or by specification, perhaps under altered climate conditions, and perhaps with various anthropogenic activities (e.g., restoration, recreation). In order to facilitate use of the FDMS by EAA staff and EARIP participants, its operation has been set up to be scenario-driven. This means that a series of data sets have been tailored to serve as inputs to the model, and the user interface has been designed to allow the user to select combinations of these inputs to create a model scenario. The principal scenarios evaluated in this report are described in the following sections.

### ***3.1.1 Baseline: 2003-2013 historical flows***

This is one of the fundamental scenarios for model development, because this is the time series of observed flow (and accompanying meteorology) for each river that served as calibration or validation runs of the model. In addition to serving to evaluate the performance of the model, this is a convenient hydrological scenario to examine simulations under a realistic, non-extreme set of conditions. Since this period also encompasses much of the research undertaken in support of the HCP, it could prove useful as a test scenario for future enhancements of the model, such as addressing other classes of organisms.

The total Comal River discharge is recorded at a gauge upstream from its confluence with the Guadalupe River near New Braunfels. For total Comal flows from 160 to 450 cfs (see Table 2 in BIO-WEST et al., 2015c), on average the contribution of the main spring runs to the total Comal River discharge is on the order of 25 percent. The data also suggest that as the total Comal River discharge decreases, the contribution of the main spring runs begins to decrease and that there is a differential reduction between the specific spring runs. The analysis by Guyton Associates (2004) of historical water levels and spring flows was used as a basis for estimating main spring run discharges under lower flow conditions. The percent contributions for each main spring run were initially set to the values associated with a total Comal River flow of 160 cfs. The percent contributions were assumed to linearly decrease to zero at the flow rates where springs were assumed to stop flowing.

In the southern section of Landa Lake, the flow is split between the old channel and the new channel. Flows into the old channel are controlled by manipulation of culverts from Landa Lake and are affected by the volume of flow passing through the spring fed pool downstream in Landa Park. New culverts were added to the old channel bypass from Landa Lake in 2003 as part of a USFWS enhancement project. Estimating the flow in the old channel is problematic due to several factors:

- (1) There is a lack of continuous (daily) gage data within the old channel over the 2003-2013 period.
- (2) The measured flows in the old channel are not a consistent proportion of the total Comal River flows, ranging between 13 and 48 percent of total Comal River flows.

In general, for total Comal River flows less than about 200 cfs, the old channel flows are approximately 45 percent.

- (3) At higher discharges (e.g., floods), flows from Landa Lake overtop the culverts into the old channel.
- (4) Total Comal River flows are often influenced by the contribution of ungauged flows (e.g., Dry Comal drainage) such that flows in the old channel cannot be directly derived by the difference between total Comal River and new channel gauged flows. The range of percentages were derived from 32 actual discharge estimates in the old channel between 2003 and 2013.

Considering these factors, the flows within the old channel were estimated from a linear interpolation of the measured flows. The flows are truncated at 120 cfs, the highest historically measured flow in the old channel. However, the maximum flow through the new culverts restricts controlled flow rates within the old channel to approximately 80 cfs. Flow partitioning between the old channel and new channel are shown in BIO-WEST et. al (2015c, Table 4). For all simulated total flows above 70 cfs in the Comal River, the flow in the Old Channel study reach was maintained at 60 cfs. For computational efficiency, the estimated daily flows in the old channel were aggregated to 7 day averages. This smoothing is justified by the relatively constant daily flow rates through this reach. The time history of flows in the Old Channel study reach is shown in Figure 3-1.

Daily flows for the San Marcos River were taken from the USGS gauge at San Marcos for the period 2003 through 2014, and are shown in Figure 3-2. Individual spring flows within Spring Lake are treated as a single incremental flow, because the study reaches are located downstream from all spring inflows into the lake. This approach assumes that the total discharge is distributed along the entire reach length of Spring Lake, which closely approximates the spatial distribution of springs (Hardy et al., 2010).

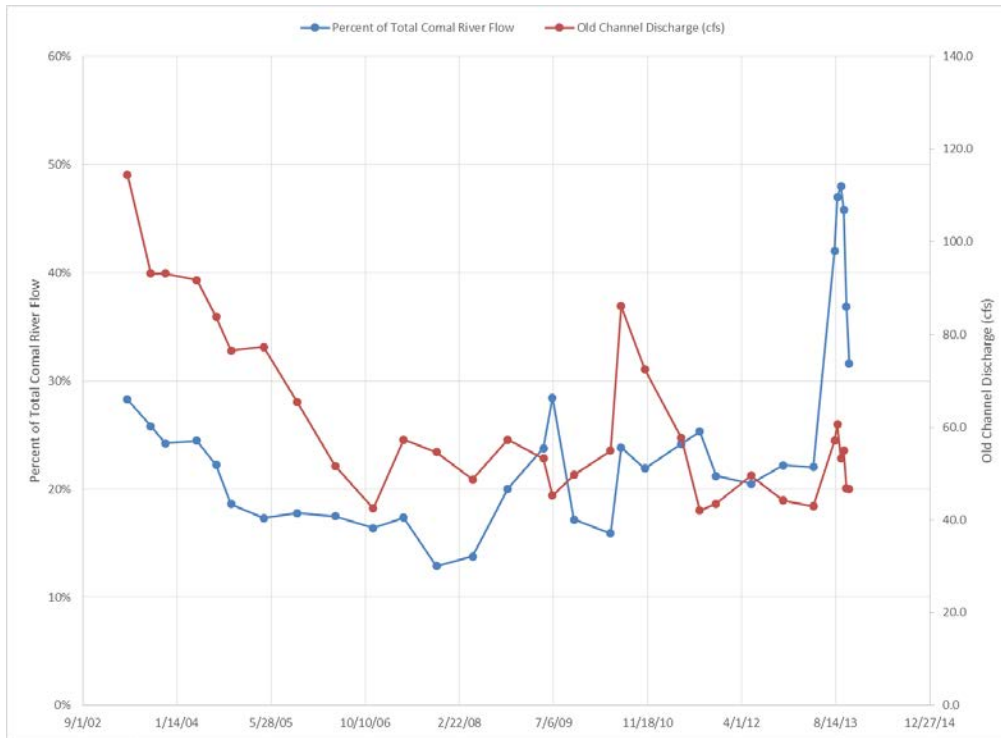


**Figure 3-1. Estimated discharges in the Old Channel reach of the Comal River for 2003-2013 (red) and flows as a percent of total Comal River discharges (blue)**

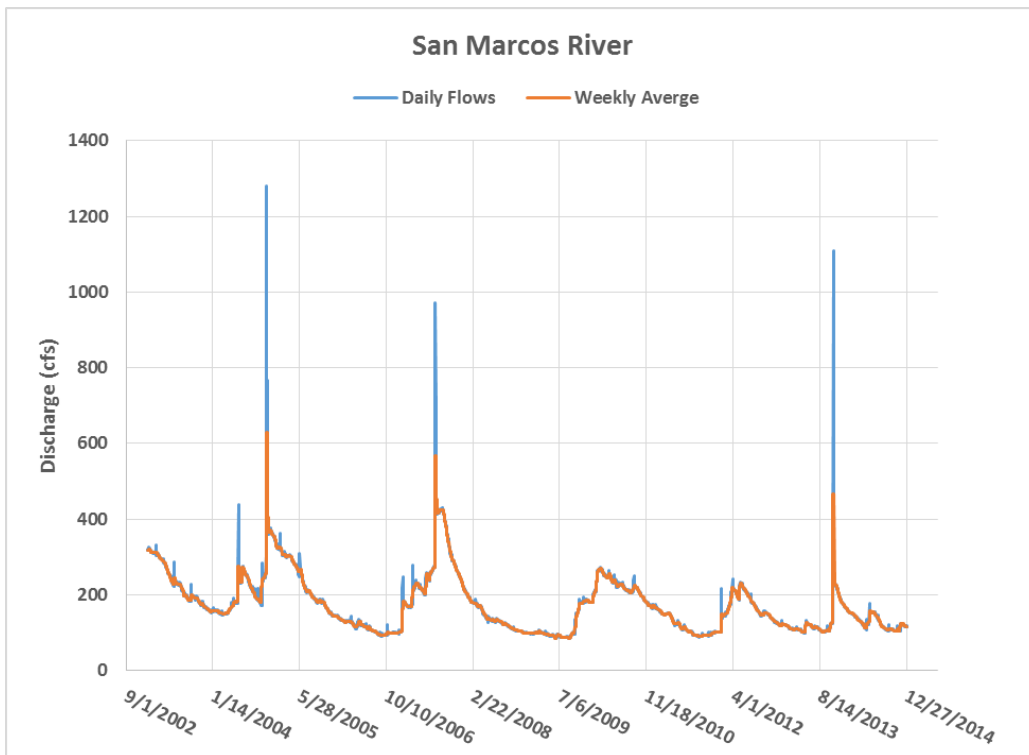


**Figure 3-2. Daily flows and Weekly Average Flows in the San Marcos River**

### ***3.1.2 HCP Flow Regime – Drought: minimum 10-year period flow***

The principal objective of the development of the FDMS is to determine the effects on the fountain darter populations in the two rivers when the magnitudes and time variations in spring flows conform to the HCP Phase 1 specifications. HDR (2011) documents the data, analysis, and modeling used to develop total monthly average springflow projected at Comal and San Marcos Springs for the 1947 - 2000 time-period for the No Action Baseline and HCP Phase 1 – Covered Activities with springflow protection measures. (Further discussions and descriptions of the HCP Phase 1 bottom-up package are presented in Section 4.2 of the HCP and in the EIS.)

Pending receipt of a more formal definition of the HCP Phase 1 flow regime, the modeling team has implemented the flows of Figure 3-3 and 3-4, which follow the HDR bottom-up package results. These are the drought-of-record time period. The meteorology accompanying these flow conditions were developed for the period 2000-2013, because meteorological data from the drought of record are not available at the same level of completeness and temporal detail. (This limits us to running the complete model including water quality and SAV to a 13-year period.)

### ***3.1.3 HCP – LTA: 10-year average flow approximating the HCP LTA***

While the drought scenario of Section 3.1.2 represents the HCP Phase 1 results on a daily average, the HCP flow objectives also specify meeting a long-term average of 225 cfs on the Comal and 140 cfs on the San Marcos. To accomplish this, the project team ran another, separate 13-year window representative of long-term average conditions. To generate this condition, a running average of the HDR (2011) HCP Phase 1 bottom-up package results was calculated and the time period was selected that averaged out to approximately the specified LTA's. This proved to be the period 1966-1979 for the Comal, Figure 3-5, and 1961-1974 for the San Marcos, Figure 3-6.

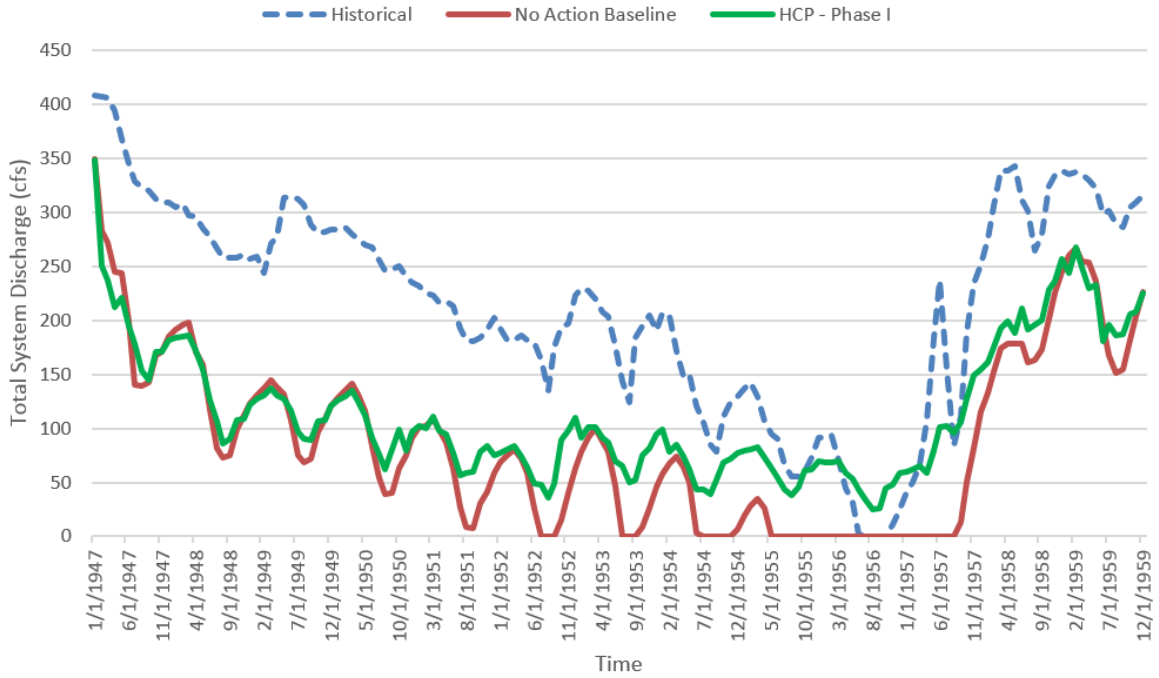


**Figure 3-3. Comal River historical total system discharge (blue) and modeled total system discharge (red [No Action] and green [HCP Phase I bottom up package]) presented in the HCP for time period of 1947 to 1960.**

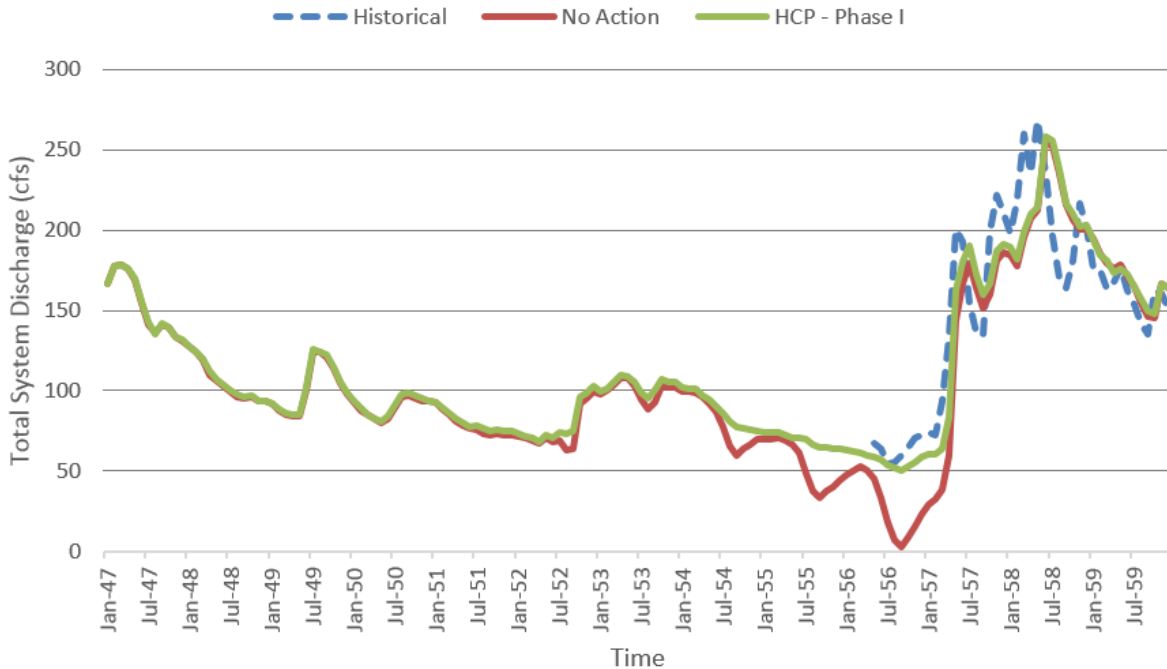


**Figure 3-4. As in Fig. 3-3, for the San Marcos River.**

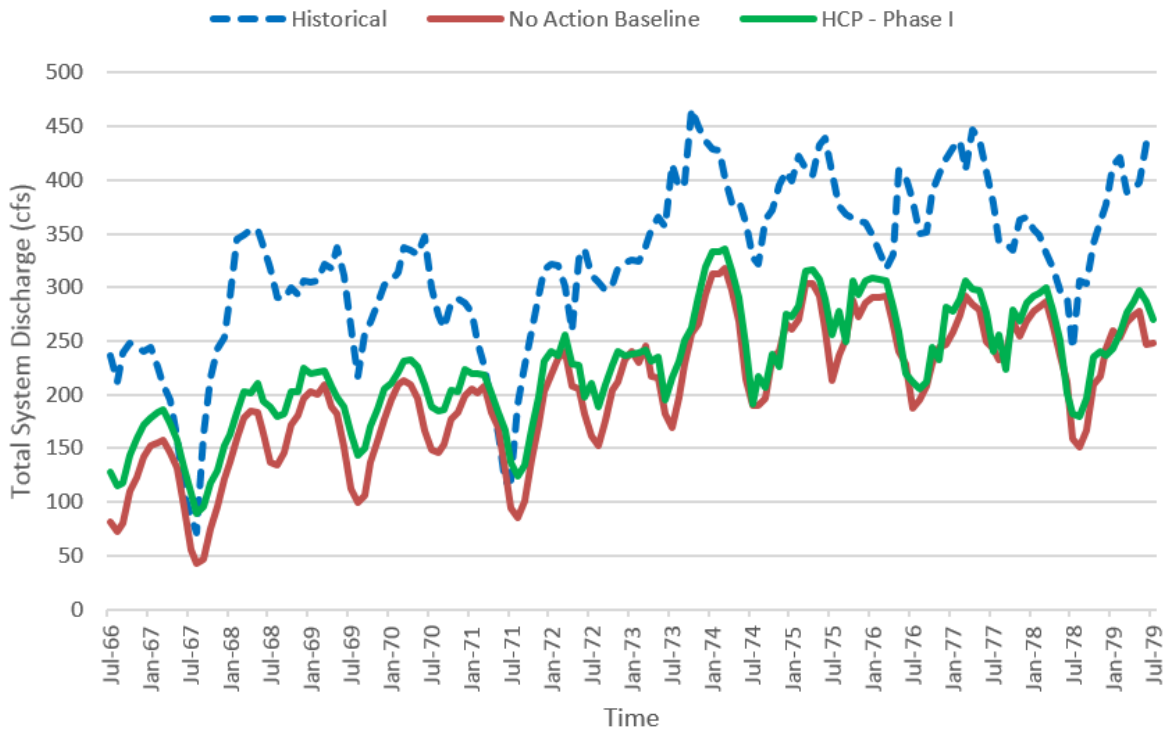


**Figure 3-5. Comal River historical total system discharge (blue) and modeled total system discharge (red [No Action] and green [HCP Phase I bottom up package]) presented in the HCP. Period 1966 to 1979 exhibits mean total system discharge of 225 cfs for HCP Phase I scenario over 13-years.**

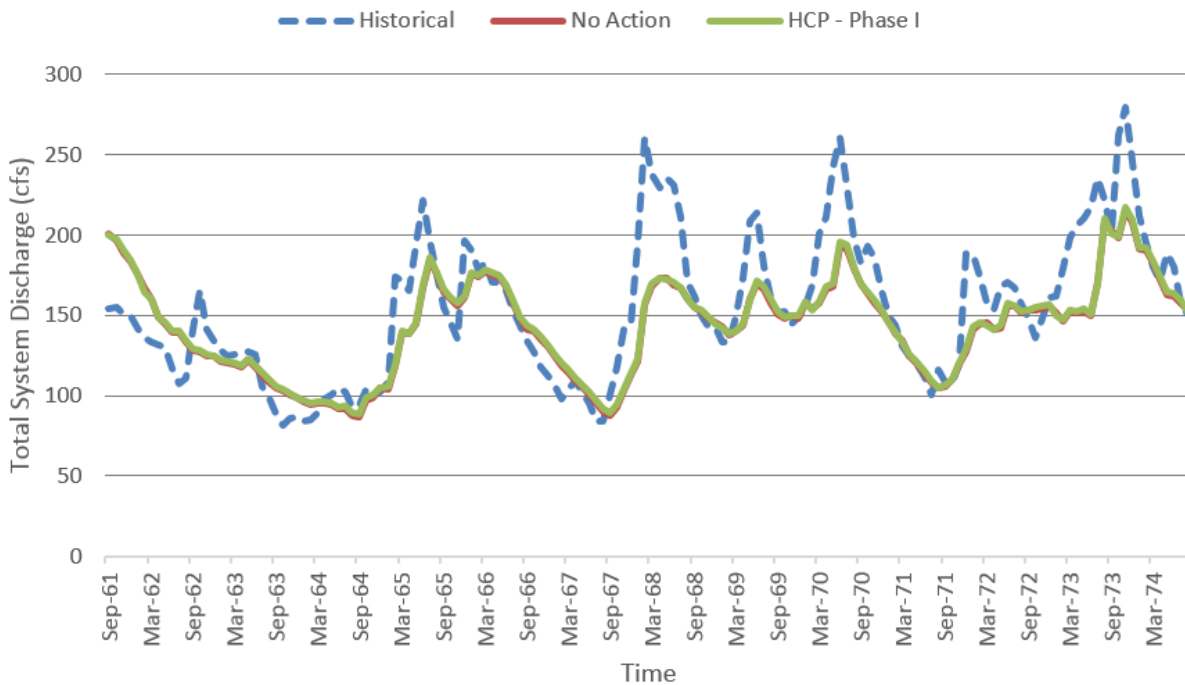


**Figure 3-6. As Fig. 3-5 for San Marcos River. Period 1961 to 1974 exhibits mean total system discharge of 140 cfs for HCP Phase I scenario over 13-years.**

### 3.1.4 Stressed habitat scenarios

To further examine model response, three hypothetical scenarios have been devised to determine the model projections under conditions thought to stress the fountain darter. All of these were created by modifying the baseline scenario (Section 3.1.1) of 2003-2013. The first of these is the **high-temperature scenario**, created by replacing the annual sequence of daily temperatures for the baseline scenario with an annually-repeating sequence of daily water temperatures that represented the year with the highest water temperature observed in the reach during the period 2003-2013 (see Appendix C). Second is the **bad vegetation scenario**, in which the historical sequence of aquatic vegetation changes was replaced with an unchanging aquatic vegetation community that represented the worst fountain darter habitat observed in each respective reach from 2003 to 2013. To represent the worst fountain darter habitat in the Old Channel, Upper Spring Run, Landa Lake, City Park, and I35 study reaches, we used the historical aquatic vegetation from spring 2003, fall 2010, spring 2013, fall 2009, and fall 2012, respectively. Finally, the **combined adverse scenario** applies both the high temperature and bad vegetation together.

## 3.2 Model set-up and operation

A schematic diagram of the operation of the computer program implementing the FDMS is displayed in Figure 3-7. There is a morphological similarity to the conceptual model of Figure 1-8. As the conceptual model indicates, there are four submodels, *viz.* the hydraulic, water quality, SAV and fountain darter submodels. Figure 3-7 applies to the NetLogo program in which the SAV and fountain darter submodels are implemented. The hydraulic and water quality programs will have already been run to create various input files for use by NetLogo, whose outputs are re-formatted for the FDMS by the file utility WQTSS (see Section 2.2.1). The arrows in Figure 3-7 indicate the actual transfer of information from one subunit of the program to another, which in some cases corresponds to the underlying conceptual model (Figure 1-8), but in other circumstances is specific to the functioning of the program.

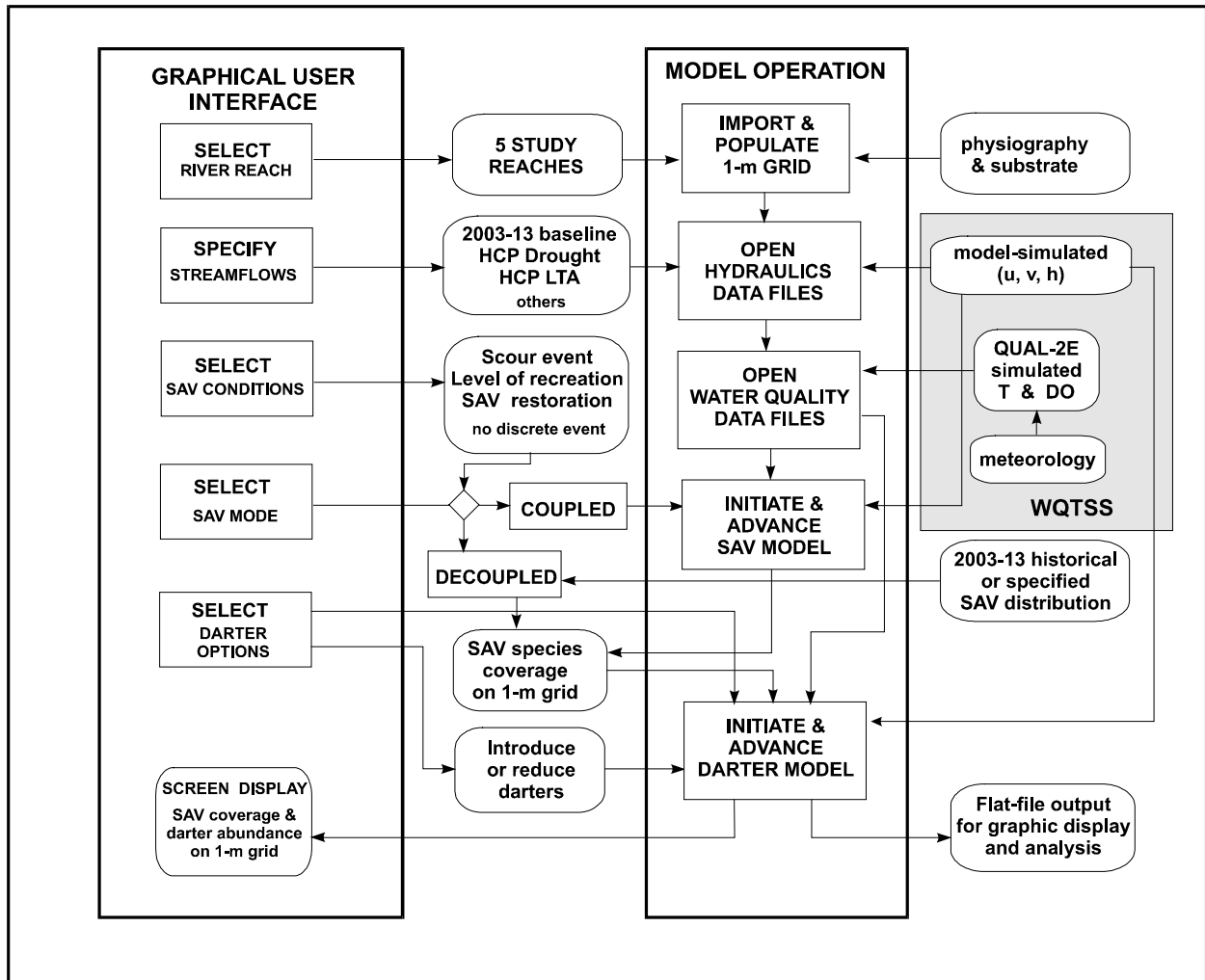


**Figure 3-7. Schematic flow chart of operation of Fountain Darter Modeling System**

The two bold rectangular boxes in Figure 3-7 represent the functioning of the computer. The GRAPHICAL USER INTERFACE (GUI) is the direct interaction between the user and the computer, controlled by entries made in the GUI in response to prompts, during which various stages of model operation are displayed. The prominent role of the GUI in directing various inputs to the model is indicated in Figure 3-7. The MODEL OPERATION represents the actions of the computer in executing the NetLogo program. Oblong boxes are input/output files by which necessary information is transferred to the CPU as needed. The leftmost collection of I/O files, between the GUI and MODEL OPERATION boxes of Figure 3-7, are generated or transferred during the course of the program execution, while the rightmost collection are pre-processed files that are accessed when needed by the program, among which are the output files from the hydraulic and water-quality submodels. The latter are managed by the WQTSS

(Section 2.2.1), which operates in the background to run the submodels and post-process their outputs.

Controls are available for discrete events of SAV modification during model execution. The model may be paused, and any vegetation type converted to any other (including “bare substrate”) throughout the reach. In decoupled operation, the SAV may be “customized” prior to model operation. One of the principal concerns of the team is the impact of loss of aquatic vegetation on the fountain darter population.

After a loss event, the concern is the length of time required for vegetation to recover, and the species that will probably be dominant. The effects of recreation on vegetation will be treated by reducing or eliminating (i.e., zeroing the coverage of) all species in specific areas known to be subjected to heavy recreational use, for time periods every summer corresponding to the tourist season. Upon the termination of the recreation season, the SAV model will re-vegetate these impacted areas by regrowth through rooting of seeds, plant fragments and rhizomes. An even more catastrophic process is the occasional scour event associated with floods in the river. In the present model, a scour event is assumed to remove all SAV's, and the modeling problem is to simulate the re-establishment of vegetation in the affected areas. Scour can be approximated using the species-to-species conversion module on the GUI, replacing a species (the original SAV) with bare substrate (new species).

Considerable latitude is also available for altering darter populations during model execution, whether in coupled or decoupled mode. The input control on darter abundance is used to specify a discrete reduction or a darter increase (“introduction”) at a specified time during the simulation. This allows the user to select a catastrophic die-off of fountain darters, which can be used to simulate such scenarios as sudden disease, a spill of hazardous material, or a DO crash. The same type of alteration can be entered by pausing the model during execution.

## 3.3 Results

### 3.3.1 Baseline and HCP scenarios

The single most important application of the model is to address the question of how protective the HCP Phase 1 flow regimes are to the population of fountain darters in the two rivers. This was addressed by applying the model to three separate scenarios for all five study reaches: (1) HCP long-term average scenario; (2) HCP drought scenario; and, as a standard of comparison, (3) the baseline 2003 – 2013 scenario. Details on these hydrometeorological scenarios are discussed in Section 3.1. Two sets of model runs were carried out, the first without density-dependent effects, and the second with all six density-dependent effects, see Section 2.3.2. All runs were made in the SAV-decoupled mode. We ran three (3) replicate stochastic (Monte Carlo) simulations of each of these scenarios. The results are shown in Figures 3-8 through 3-12 for the five study reaches.

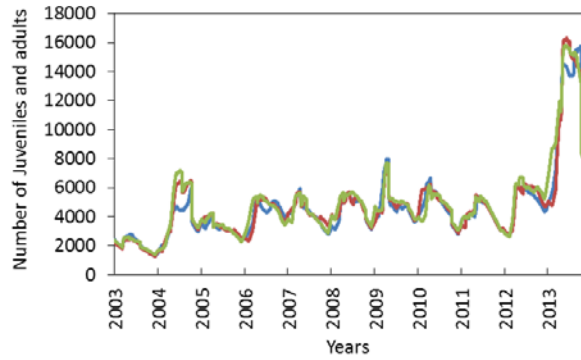
General trends in simulated population dynamics were not noticeably different among the three scenarios within any of the five reaches, based on either the density-independent or density-dependent versions of the model. As would be expected, mean darter total abundances (number of juveniles plus adults in the reach) simulated with the density-dependent version of the model were lower than those simulated with the version of the model without density-dependent negative feedback on population growth. Mean abundances (calculated as the mean of all daily abundances from the three replicate stochastic simulations of a given scenario) simulated under the HCP long-term average scenario and under the HCP drought scenario were all within 12% of abundances simulated under the baseline (historical) scenario, regardless of the reach simulated or the assumed density dependence. The lowest darter abundances (which were produced by the density-dependent version of the model) occurring during simulations of the Old Channel, Upper Spring Run, Landa Lake, City Park, and I35 reaches, were 942, 435, 8387, 10676, and 360 darters in the reach, respectively. These lowest abundances most often occurred during simulations of the HCP drought scenario (Landa Lake, City Park, and I35 reaches), but also occurred during the HCP long-term average scenario (Old Channel Reach) and the baseline (historical) scenario (Upper Spring Run Reach), again emphasizing the lack of noticeable differences among the three scenarios within any of the five reaches.

# OLD CHANNEL STUDY REACH

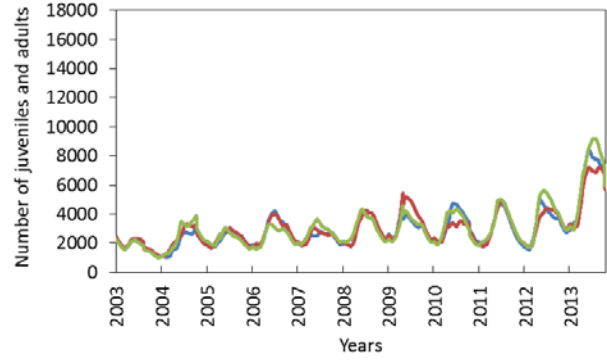
Without density-dependent effect

With density-dependent effects

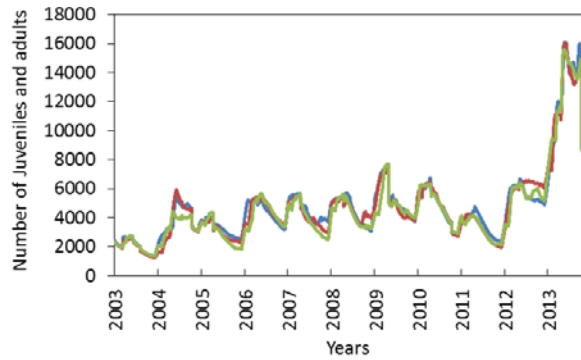
Baseline



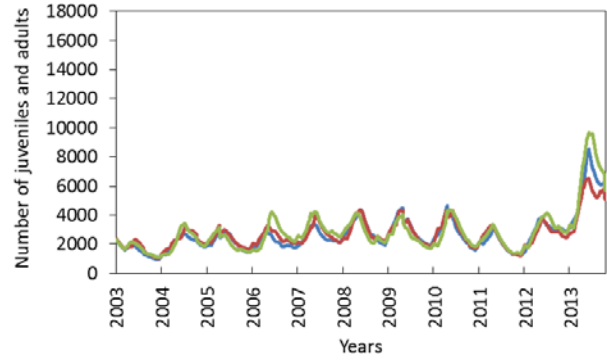
Baseline



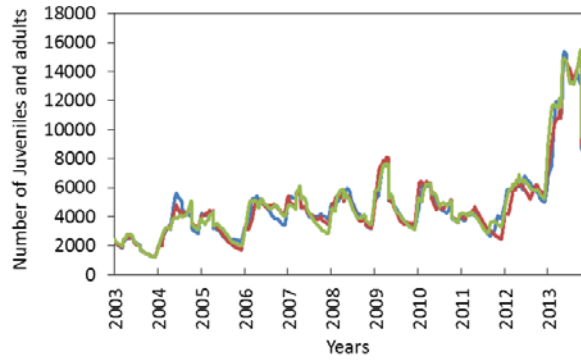
HCP drought



HCP drought



HCP long-term average



HCP long-term average

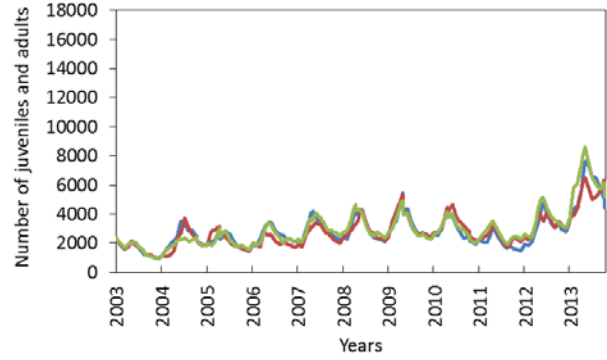


Figure 3-8. Model predictions of number of juvenile + adult fountain darters within the Old Channel Study Reach of the Comal River under baseline, HCP long-term average, and HCP drought scenarios

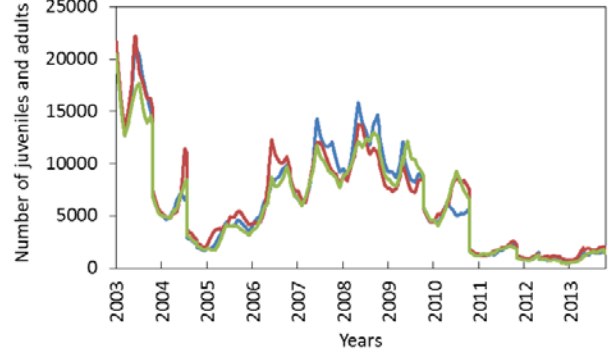
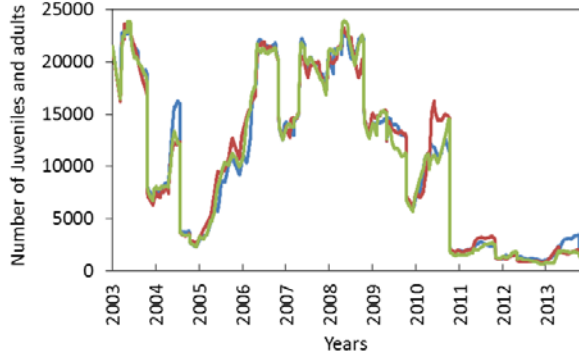
## UPPER SPRING RUN STUDY REACH

**Without density-dependent effect**

**With density-dependent effects**

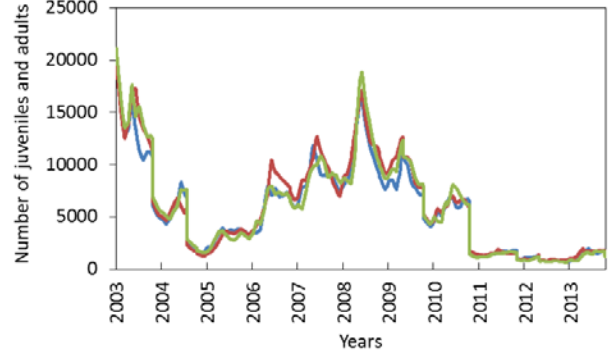
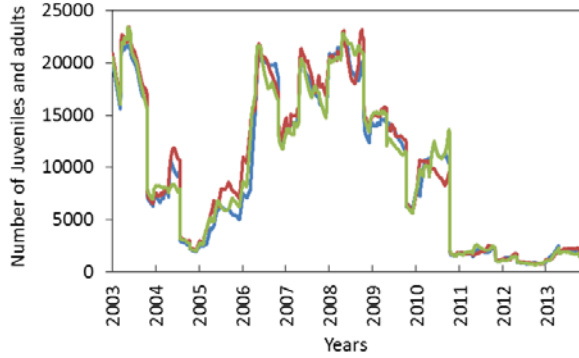
**Baseline**

**Baseline**



**HCP drought**

**HCP drought**



**HCP long-term average**

**HCP long-term average**

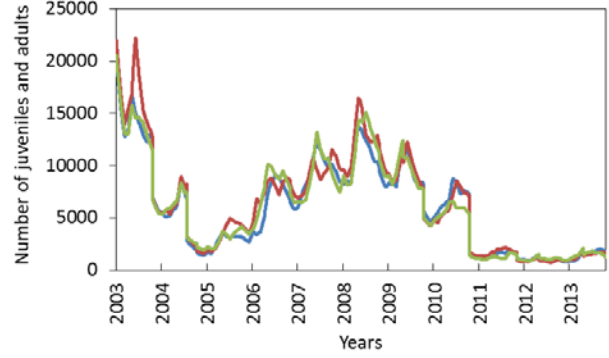
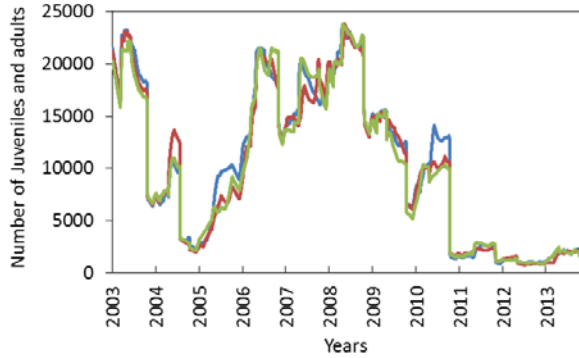


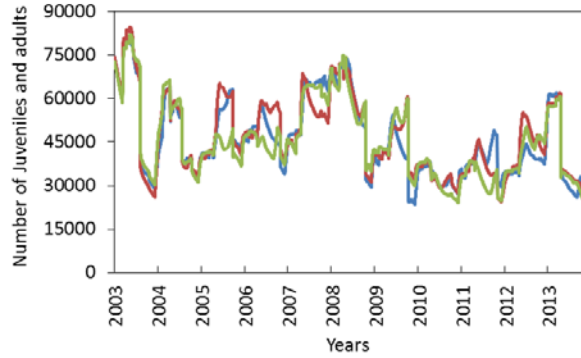
**Figure 3-9. Model predictions of number of juvenile + adult fountain darters within the Upper Spring Run Study Reach of the Comal River under baseline, HCP long-term average, and HCP drought scenarios**

## LANDA LAKE STUDY REACH

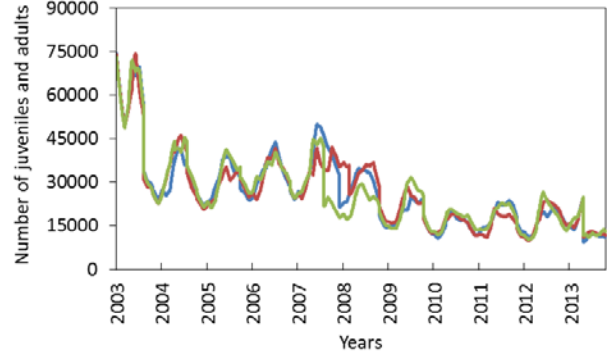
**Without density-dependent effect**

**With density-dependent effects**

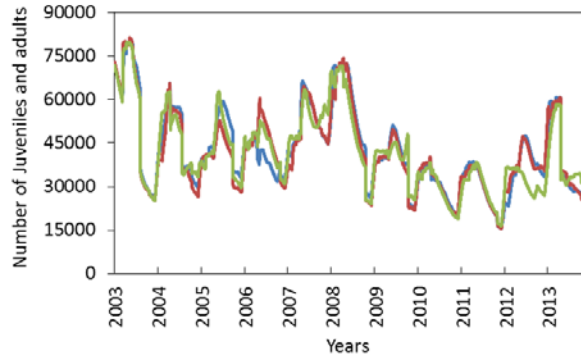
**Baseline**



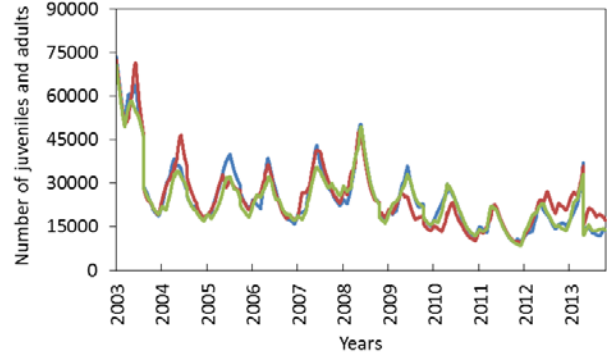
**Baseline**



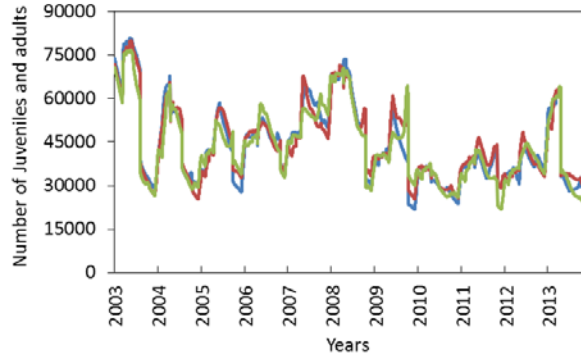
**HCP drought**



**HCP drought**



**HCP long-term average**



**HCP long-term average**

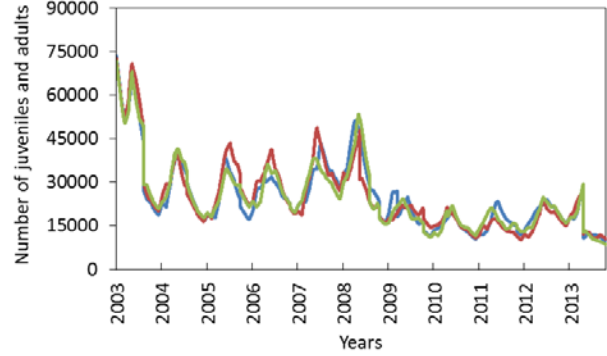


**Figure 3-10. Model predictions of number of juvenile + adult fountain darters within the Landa Lake Study Reach of the Comal River under baseline, HCP long-term average, and HCP drought scenarios**

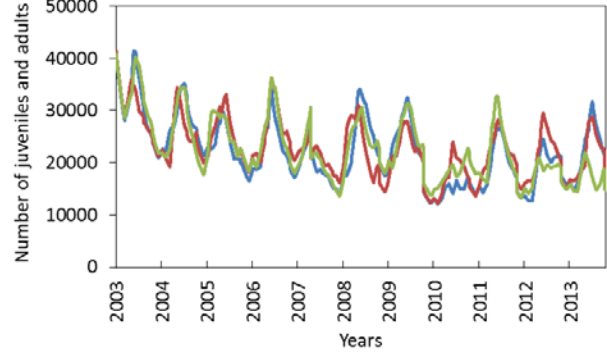
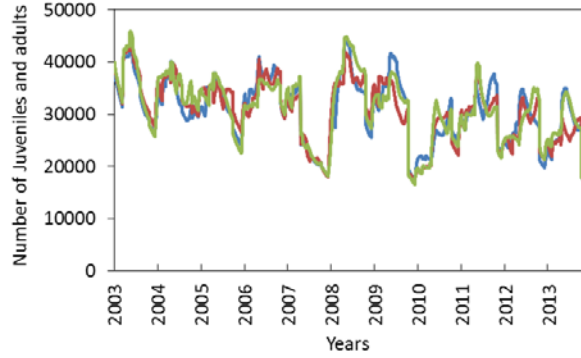
## CITY PARK STUDY REACH

**Without density-dependent effect**

**With density-dependent effects**

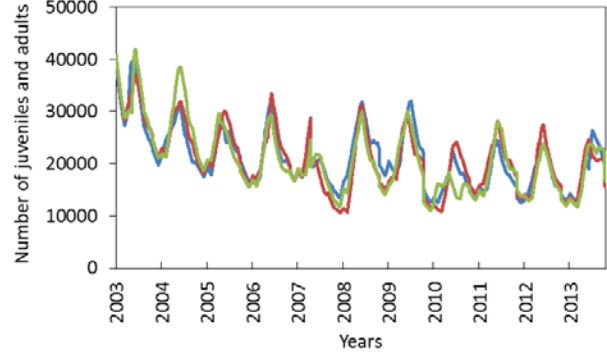
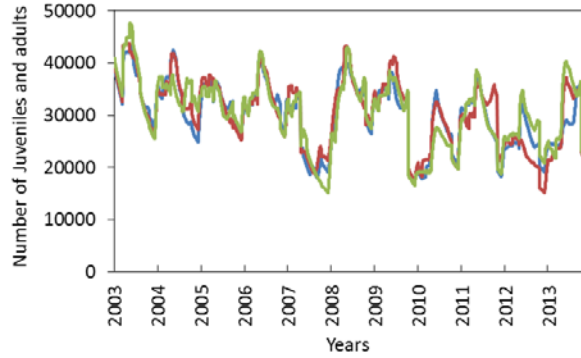
**Baseline**

**Baseline**



**HCP drought**

**HCP drought**



**HCP long-term average**

**HCP long-term average**

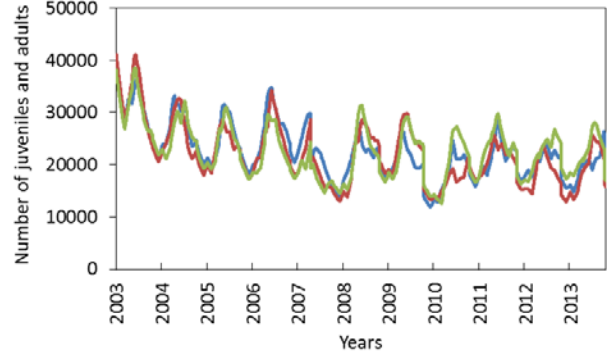
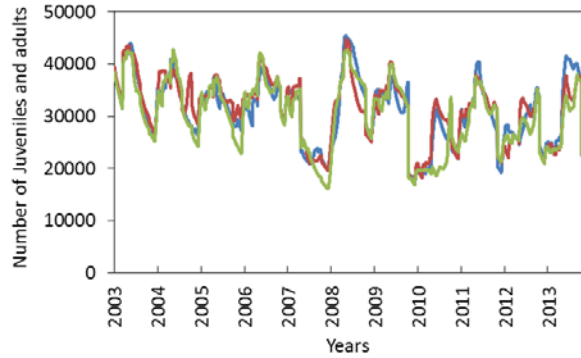


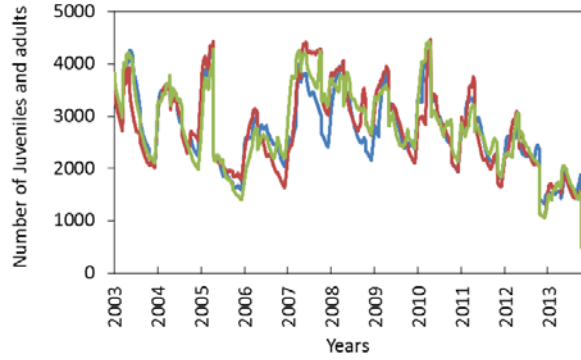
**Figure 3-11. Model predictions of number of juvenile + adult fountain darters within the City Park Study Reach of the San Marcos River under baseline, HCP long-term average, and HCP drought scenarios**

# IH 35 STUDY REACH

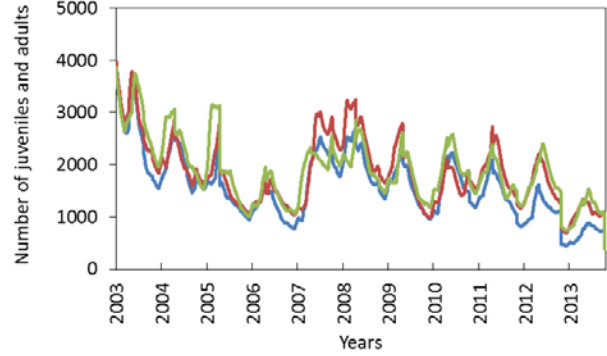
Without density-dependent effect

With density-dependent effects

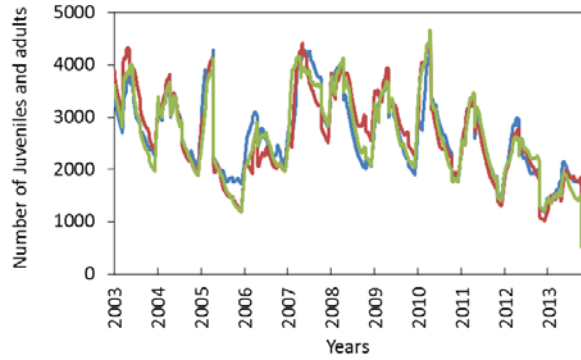
Baseline



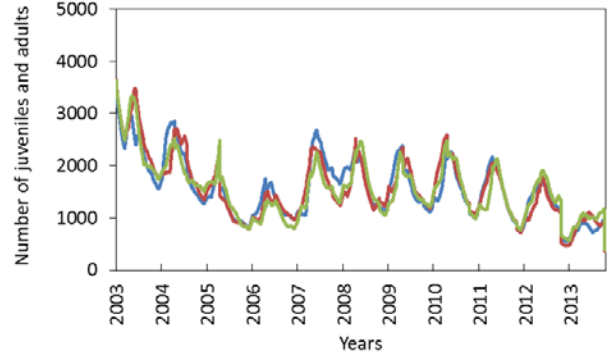
Baseline



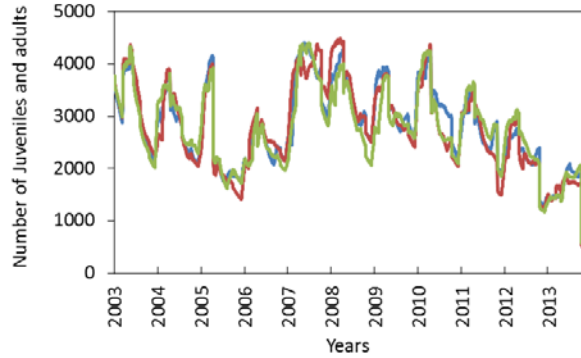
HCP drought



HCP drought



HCP long-term average



HCP long-term average

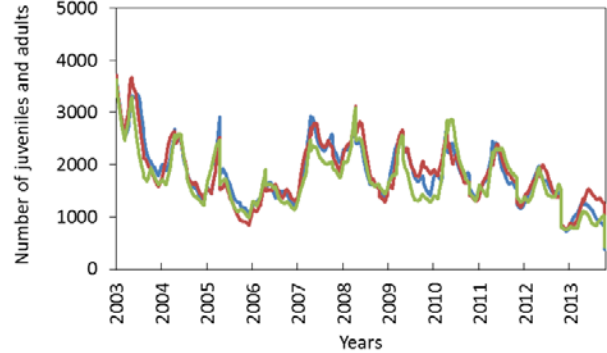


Figure 3-12. Model predictions of number of juvenile + adult fountain darters within the IH 35 Study Reach of the San Marcos River under baseline, HCP long-term average, and HCP drought scenarios

### 3.3.2 *Stressed habitat scenarios*

We next simulated fountain darter population dynamics within each of the five reaches under several adverse scenarios, the high-temperature scenario, bad-vegetation scenario, and combined adverse scenario, see Section 3.1.4, and the results were compared to the baseline scenario. As before, we ran three replicate stochastic (Monte Carlo) simulations of each of these scenarios using versions of the model without any density-dependent effects and with all six density-dependent effects implemented.

The results of these simulations are shown by study reach in Figures 3-13 through 3-17. General trends in population dynamics simulated under the high temperature scenario were not noticeably different than those simulated under the baseline (historical) scenario within any of the five reaches based on either the density-independent or density-dependent versions of the model. Mean darter abundances simulated under the high temperature scenario were within 12% of the abundances simulated under baseline conditions in the Old Channel, Upper Spring Run, and City Park reaches, regardless of the version of the model used. Mean abundances simulated under the high temperature scenario in Landa Lake were 17% lower than baseline, using either version of the model. Mean abundances simulated under the high temperature scenario in the I35 Reach were 22% lower than baseline using the density-dependent version of the model, but only 12% lower using the density-independent version.

There were few noticeable differences between mean darter total abundances simulated under the bad vegetation scenario and those simulated under the combined adverse scenario, although mean abundances decreased to slightly lower levels under the combined scenario in the Landa Lake and I35 reaches. However, mean darter abundances simulated under the bad vegetation scenario and the combined adverse scenario were markedly lower. Mean darter abundances simulated under both the bad vegetation and the combined scenarios were more than 50, 80, 20, 40, and 40% lower than baseline in the Old Channel, Upper Spring Run, Landa Lake, City Park, and I35 reaches, respectively, regardless of the version of the model used.

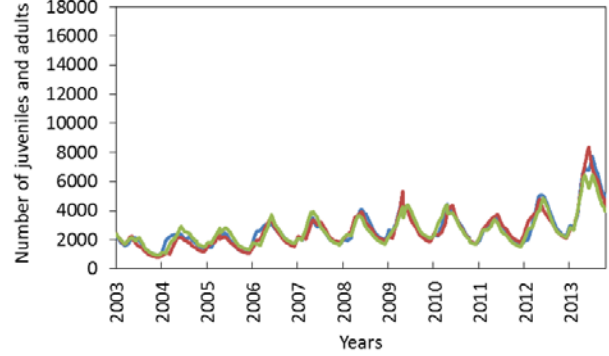
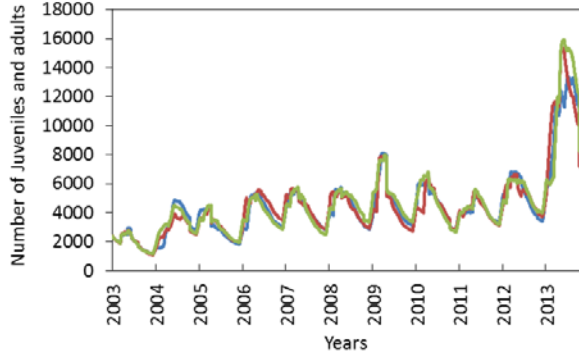
## OLD CHANNEL STUDY REACH

Without density-dependent effect

With density-dependent effect

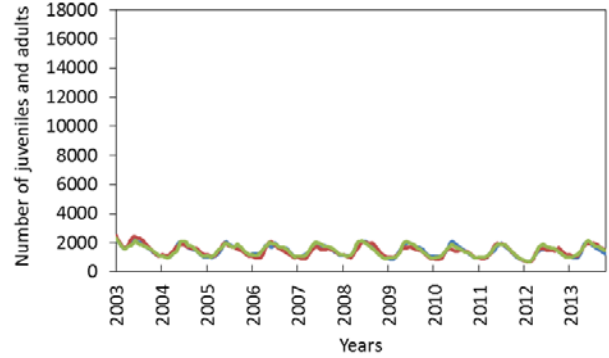
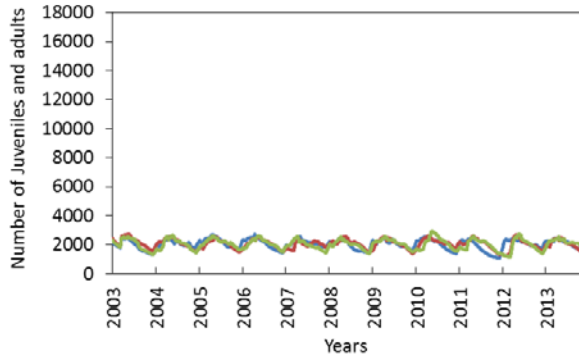
**High Temperature**

**High Temperature**



**Bad Vegetation**

**Bad Vegetation**



**Combined**

**Combined**

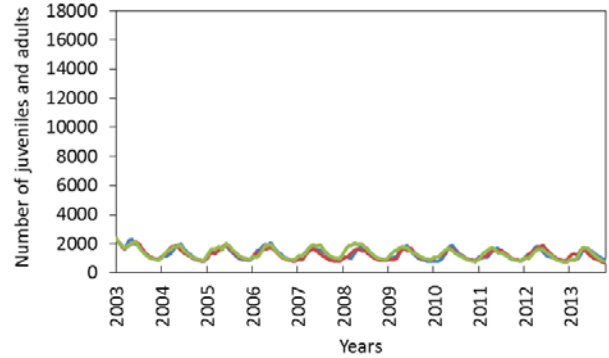
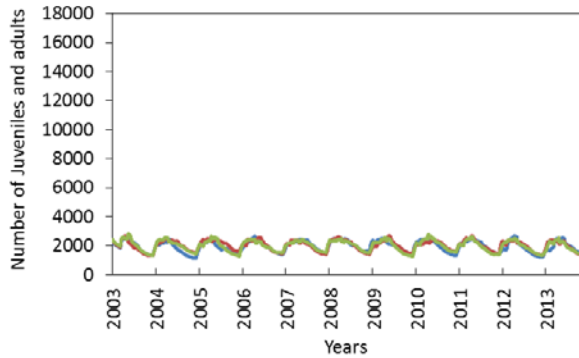


**Figure 3-13. Model predictions of number of fountain darters within the Old Channel Study Reach of the Comal River under high temperature, bad vegetation, and combined adverse scenarios**

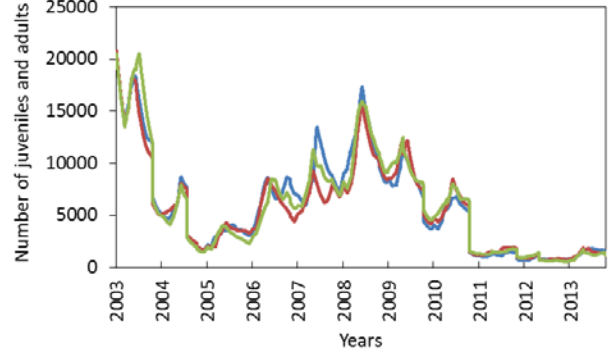
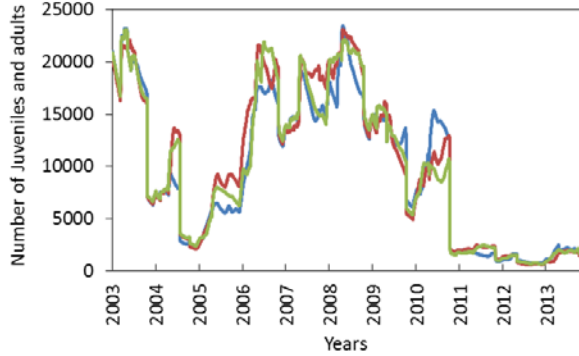
# UPPER SPRING RUN STUDY REACH

Without density-dependent effect

With density-dependent effects

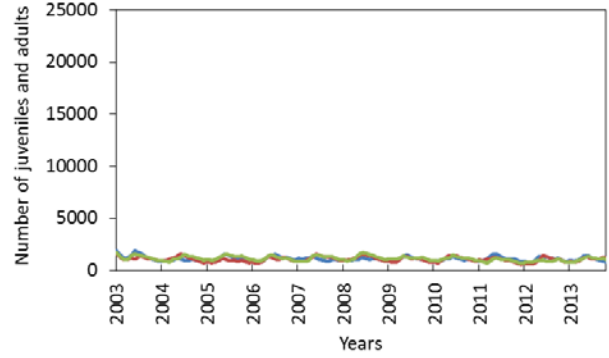
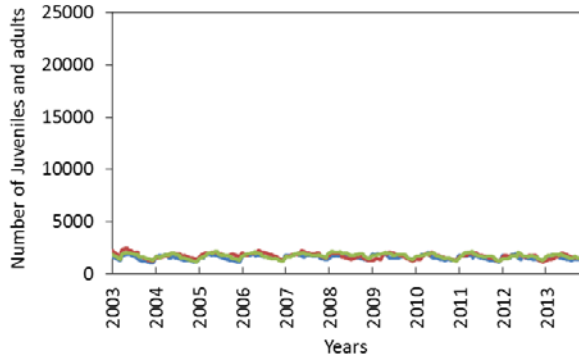
High Temperature

High Temperature



Bad Vegetation

Bad Vegetation



Combined

Combined

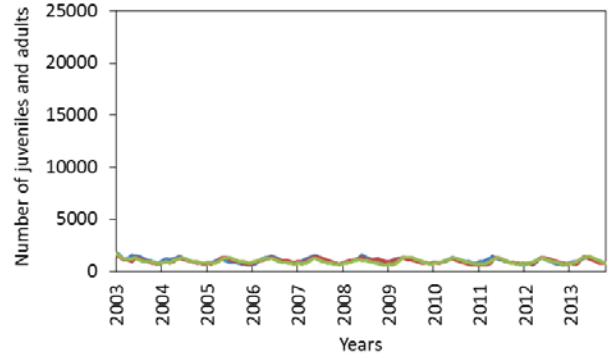
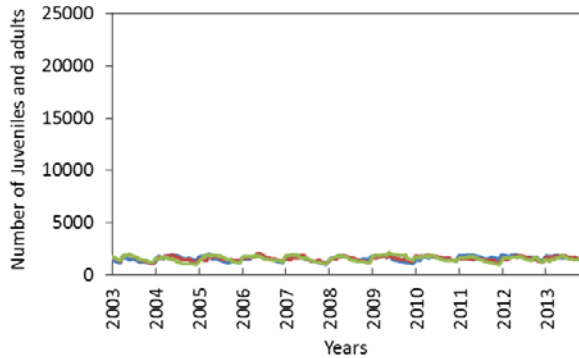


Figure 3-14. Model predictions of number of fountain darters within the Upper Spring Run Study Reach of the Comal River under high temperature, bad vegetation, and combined adverse scenarios

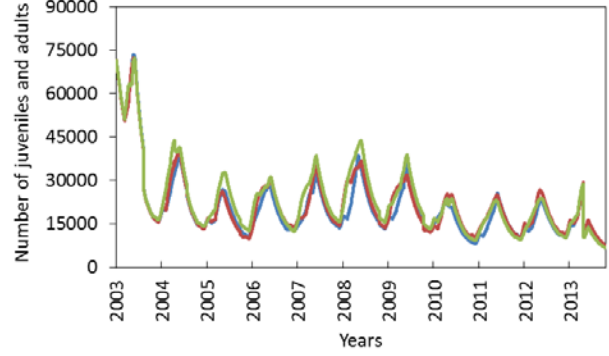
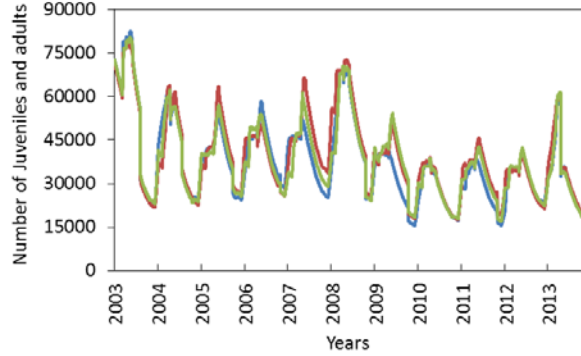
# LANDA LAKE STUDY REACH

Without density-dependent effect

With density-dependent effects

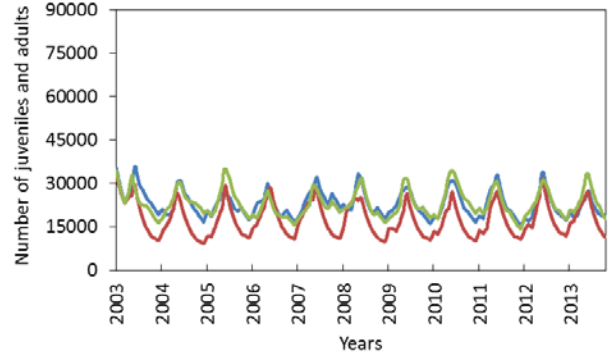
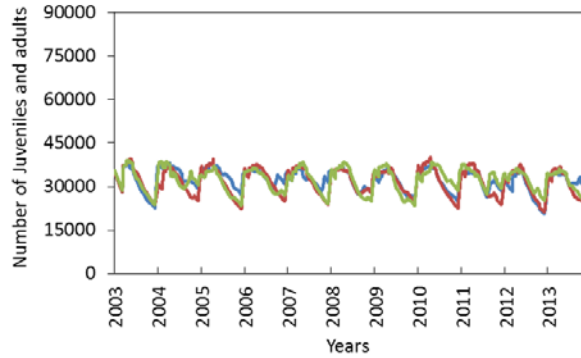
High Temperature

High Temperature



Bad Vegetation

Bad Vegetation



Combined

Combined

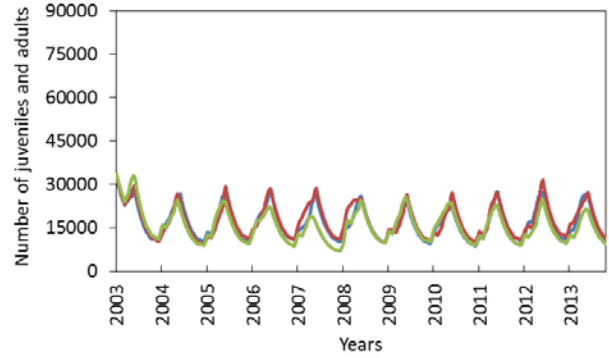
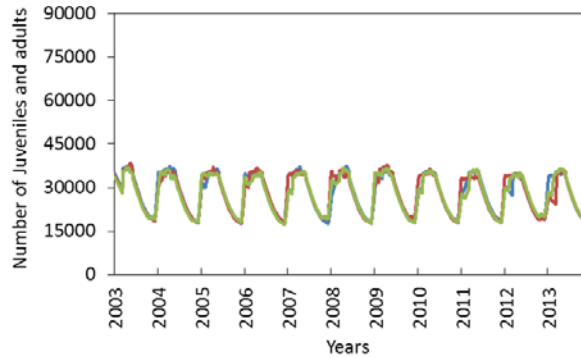


Figure 3-15. Model predictions of number of fountain darters within the Landa Lake Study Reach of the Comal River under high temperature, bad vegetation, and combined adverse scenarios

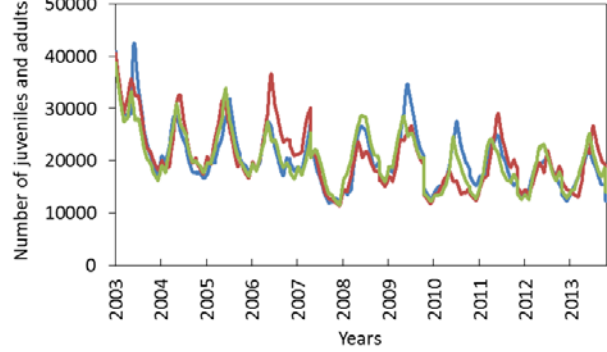
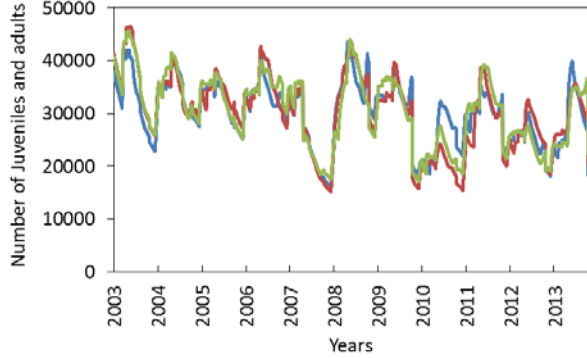
## CITY PARK STUDY REACH

**Without density-dependent effect**

**With density-dependent effects**

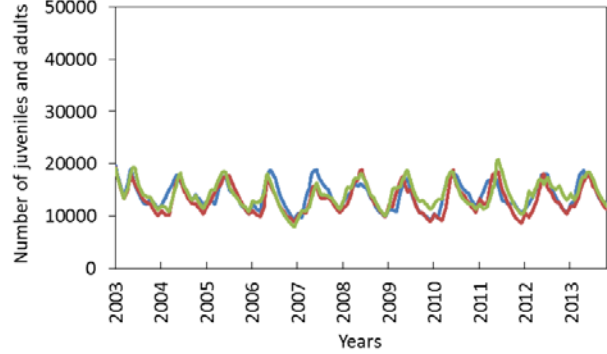
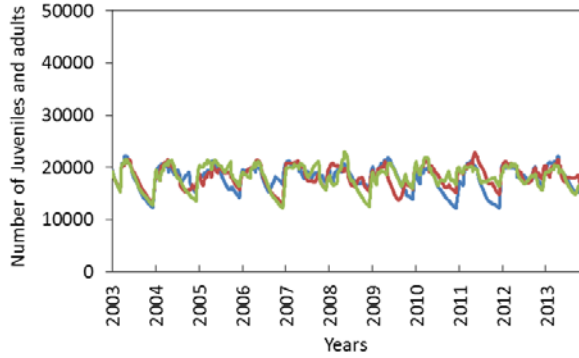
**High Temperature**

**High Temperature**



**Bad Vegetation**

**Bad Vegetation**



**Combined**

**Combined**

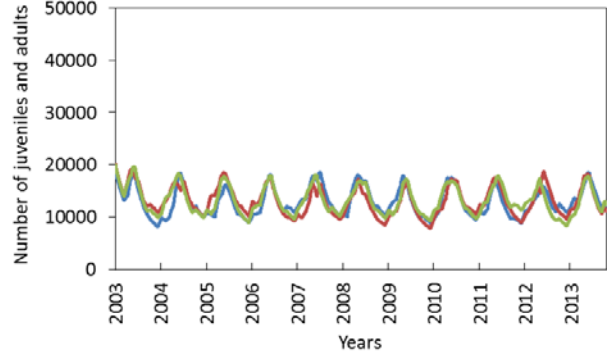
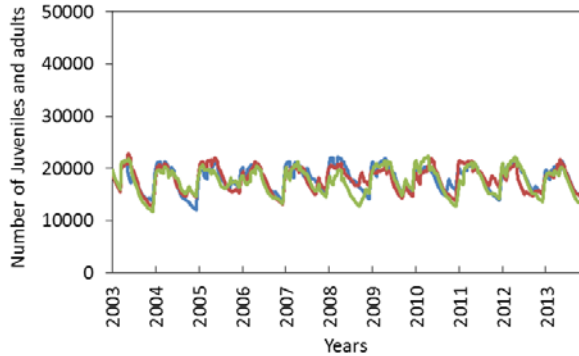


**Figure 3-16. Model predictions of number of fountain darters within the City Park Study Reach of the San Marcos River under high temperature, bad vegetation, and combined adverse scenarios**

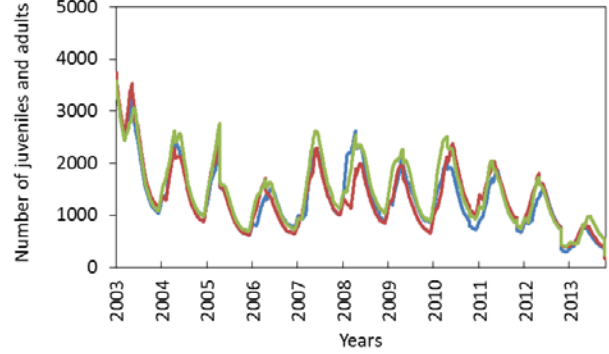
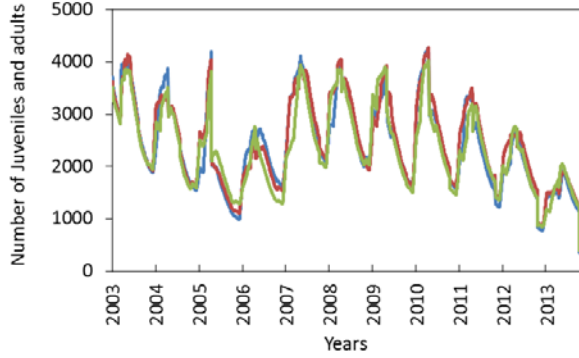
# IH 35 STUDY REACH

Without density-dependent effect

With density-dependent effects

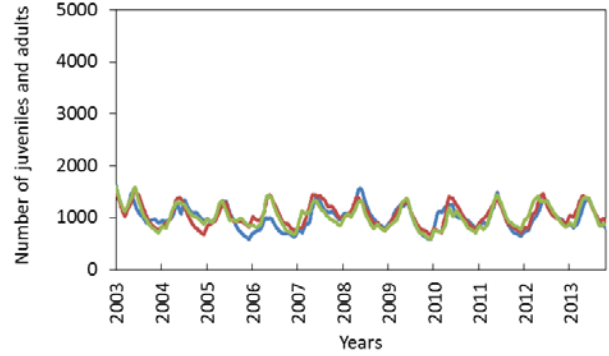
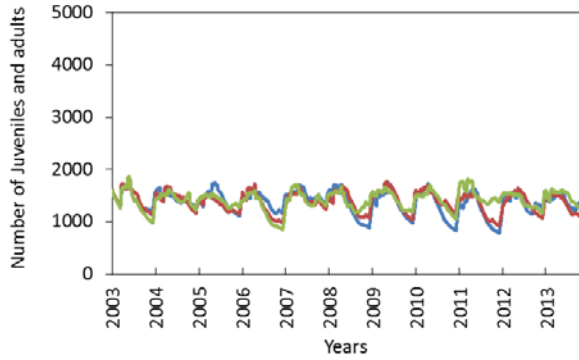
High Temperature

High Temperature



Bad Vegetation

Bad Vegetation



Combined

Combined e

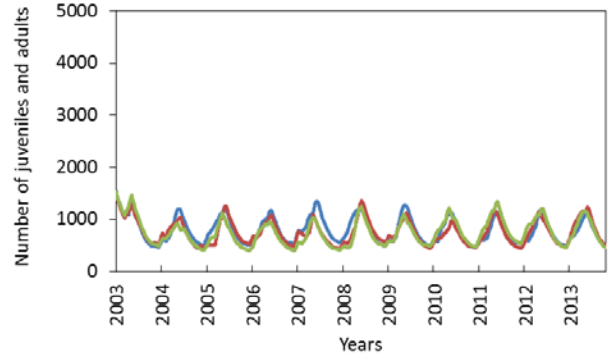
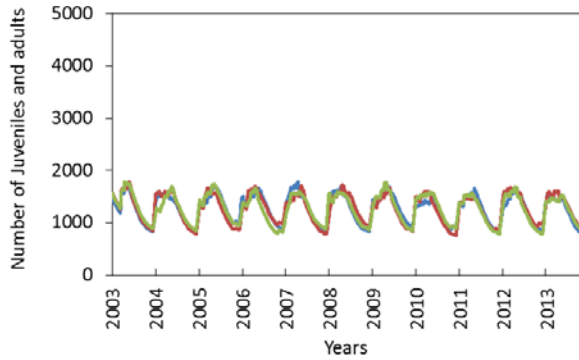


Figure 3-17. Model predictions of number of fountain darters within the IH 35 Study Reach of the San Marcos River under high temperature, bad vegetation, and combined adverse scenarios

The lowest darter abundances (again produced by the density-dependent version of the model) occurring during simulations of the Old Channel, Upper Spring Run, Landa Lake, City Park, and I35 reaches, were 651, 555, 6743, 7829, and 162 darters, respectively. These lowest abundances most often occurred during simulations of the high temperature scenario (Upper Spring Run, Landa Lake, and I35 reaches), but also occurred during the bad vegetation scenario (Old Channel Reach) and the combined scenario (City Park Reach).

The differences among scenarios within reaches with regard to the occurrences of the lowest darter abundances, and, to a lesser extent, the relative levels of the mean darter abundances, are somewhat perplexing at first glance. Nominally, we would expect the lowest abundances and the lowest mean abundances to be associated with the combined adverse scenario in all of the reaches. But the temporal sequencing of changes in aquatic vegetation conditions and water temperature conditions, superimposed on the demographic momentum of the darter population during any given simulation, complicates the issue. Since one of the years in the high temperature scenario coincides with the aquatic vegetation community that represented the worst fountain darter habitat (which was used continuously in the bad vegetation scenario), and one of the years in the bad vegetation scenario coincides with the annually-repeating sequence of daily water temperatures that represented the year with the highest water temperature (which was used repeatedly in the high temperature scenario), there will be a year during both the high temperature scenario and the bad vegetation scenario with the same aquatic vegetation and water temperature conditions that repeat themselves year after year in the combined scenario.

Differences in the size and stage-structure of the darter population entering the “bad vegetation plus high temperature” year will affect the population response to these conditions, and especially will affect the lowest abundance to which the population might fall. Thus, although mean abundances and lowest abundances resulting from the various scenarios are convenient summary metrics that facilitate comparisons among and within scenarios and reaches, the temporal dynamics of darter populations presented in these figures provide a more reliable, albeit perhaps more cumbersome, basis for such comparisons.

### **3.4 Model conclusions and interpretation**

The basic conclusion from the modeling exercise conducted above is that fountain darters survive in all study reaches during each scenario tested. It is evident throughout this report and from these model runs that aquatic vegetation is the primary driver in the fountain darter population size during most conditions with the possible exception at the extremes when water temperature can have an overriding effect.

As discussed throughout this report, the primary purpose of this tool is to provide guidance on future HCP management issues into the future. As such, the interpretation of any model results (like those provided above) need to be extensively vetted amongst the various EARIP tiers before conclusions can be drawn to serve that purpose. It is not within the project team's purview to interpret the above scenarios in an attempt to answer the HCP Phase 1 question regarding survival and recovery of the fountain darter in the wild. Rather, it was our charge to create the tool and provide guidance on interpretation, the latter of which is presented in the following sections.

#### **3.4.1 Assumptions**

Several assumptions were made in the development of this management tool that need to be considered from an ecological standpoint during any interpretation of model results. Some, such as fountain darter food being sufficient or gill parasites being under control, are backed by specific HCP applied research results and/or long-term monitoring. Nonetheless, they remain assumptions at this time that may require more focused research to better establish their applicability.

Another assumption made because of the complexities and resources necessary to study ecological interactions is that behavior, competition, predation, etc. are inherently represented within the drop-net density data results. One can argue this is supported by years of long-term monitoring, but, again, this remains an assumption. Other potential impactors such as disease and pollution were not addressed because of lack of data or because they would require major

efforts in hydrology and water quality and dynamic modeling far beyond the scope of this project.

### ***3.4.2 Existing Model Shortcomings***

It also needs to be clear that, in addition to the assumptions considered above, the model in its present state has shortcomings. For instance, air temperature data from the drought of record was not incorporated into the aforementioned runs. The high temperature run took the annual sequences of daily temperatures from the year with the highest water temperature observed in the reach during the model baseline period (2003-2013) and repeated those for 10 years straight.

Secondly, the DO model is not calibrated because of the lack of long-term DO data during low-flow conditions and because of complexities within QUAL2E. The version of the model used in the runs described above did not project DO conditions during low-flow conditions to be a concern. Based on empirical observations in the Upper Spring Run during 2013 and 2014 drought conditions in the Comal systems, DO conditions were not a concern. However, we are not confident in the specific DO values produced in the model runs for those scenarios. It is the conclusion of the project team that more DO data is needed and a more sophisticated water quality model will likely be required (see Section 5.2) to address specific DO values and potential DO concerns during low-flow conditions beyond what is presented in the HCP Phase 1 flow regime.

As described in this report the coupled model provides the ability to explicitly simulate aquatic vegetation growth. The coupled model, particularly its dispersal algorithms, represents important new science, but has not been adequately tested and evaluated. It should therefore be regarded as a “beta” release. It is expected that this version of the model will require a number of user specified scenarios to be run and evaluated rigorously in order to update and refine the modeling system as part of any normal software development cycle. Until this step is completed, we do not believe that the coupled modeling system should be used for arbitrary scenario evaluations unless the user has a complete understanding of the various modeling components and the existing limitations of the coupled modeling system. Coupled model runs should not be interpreted in isolation, and should only be interpreted relatively compared to other

scenarios. For this reason, we recommend use of the decoupled model for management purposes, though the depiction of aquatic vegetation responses based on historical vegetation maps will require careful interpretation. This is also a topic for directed research suggested in Section 5.2.

### ***3.4.3 Cumulative reach or full system consideration***

Another key consideration in answering HCP Phase 1 questions will be the interpretation of the study reach results in a cumulative fashion or some type of full system analysis. One might assume that if darters survive and recover at both model reaches in the San Marcos River, then they could be summed together for still a very conservative answer, in that there is considerable fountain darter habitat between those reaches and above the City Park reach, not to mention the large population of fountain darters in Spring Lake.

A similar assumption could be made in the Comal system, but with a slightly less conservative nature. This is because the system overall, and downstream areas in the old channel and the majority of the new channel, are predicted as having unacceptable water temperature conditions during the HCP Phase 1 minimums. With that said, the Old Channel study reach represents only a small (and downstreammost) portion of the ERPA, and the Landa Lake study reach upstream to Spring Island encompasses the deepest parts of the lake.

## 4 Validation and Lessons Learned

Applied-research findings, long-term monitoring, and early fountain darter modeling results exhibit a higher level of resilience than previously hypothesized for the fountain darter in the two river systems. Analysis of the field data shows limited to no dependence of darters on flow or on the associated water velocities. This will come to a surprise for many as much of the research and model formulation was based upon an assumed dependence on current velocities (consistent with the usual assumption underlying environmental flow determinations). The survival and recovery of the fountain darter in the Upper Spring Run study reach (described further below) support this higher level of resiliency. The topic of validation and observation is presented below in a more untraditional, integrated approach, specifically because of the potential HCP-designated management application of this tool.

### 4.1 Validation

Validation work presented herein has judged the decoupled model performance satisfactory in terms of HCP Phase 1 development for the five study reaches for the purposes of a management tool. As discussed in Section 2.2, this involved specific reach validation activities as well as cross comparison of the key parameterizations over the five reaches. Validation to date has also considered uncertainty in both data and model, and its use in interpreting model results. Though the operational FDMS designated for Phase 1 is technically complete, the HCP specified that this not be the conclusion of model validation and testing for the Comal and San Marcos springs ecosystems.

Section 6.3.4 of the HCP laid out a specific plan for Applied Research to be conducted during Phase 1. This plan included a tiered approach based on the progression of activities undertaken by the HCP. Section 6.3.4.2 of the HCP describes these tiers as,

“Tier A will focus on habitat requirements and responses; Tier B will focus on low-flow impacts directly on the fountain darter and Comal Springs riffle beetle; and Tier C will investigate the implications of the timing, frequency, and duration of multiple events in

varying sequences and include specific research efforts designed to assess ecological model predictions (e.g., model validation).”

Within this same section, Ecological Model Validation was specifically referenced as follows:

***“Ecological Model Validation***

Existing information and data gathered during Tiers A and B applied research and through continued ecological monitoring and on-site studies will be entered into the ecological models developed for these ecosystems. Towards the end of Phase I, specific studies will be designed and conducted to test the validity of ecological model results. This may involve simple or complex parameters and single or multiple low-flow events depending on Phase II questions that may be relevant at that time.”

Tier A and B applied research has been conducted over the first four years of Phase 1 as appropriate and with solicited input from the HCP Science Committee as mandated by the HCP Funding and Management Agreement (FMA Section 7.13.2). This applied research has proved extremely valuable for many aspects of the HCP including the development of the FDMS.

Finally, Section 6.3.4.2 of the HCP states, “Tier C will investigate the implications of the timing, frequency, and duration of multiple events in varying sequences and include specific research efforts designed to assess ecological model predictions (e.g., model validation).” Tier C concepts highlighted in the HCP include assessing “simple or complex parameters and single or multiple low-flow events” within the context of controlled experimentation in applied research channels. With the completion of this potential management tool, the HCP is well positioned to embark upon this second stage of model validation and experimentation.

## ***4.2 Lessons Learned***

As anticipated in the HCP, Tier A and tier B applied research along with continued biological monitoring has provided a wealth of information in regards to assisting with fountain darter model development. In fact, when coupled with the direct observation of the extended drought

from 2013 through 2014 in the Comal system, one could contend that the primary question laid out for the ecomodel of

“Is the HCP Phase 1 flow regime sufficient to support the survival and recovery of the fountain darter?”

could possibly be answered using the Upper Spring Run as a surrogate for the system without any modeling at all. Of course, the worst drought for the Comal system in nearly a quarter of a century was not something forecasted in the HCP. Through applied research, monitoring, and HCP mitigation activities the following key observations were established, expanded or confirmed.

- *Aquatic vegetation tolerance* - the springs-adapted aquatic vegetation in the Comal and San Marcos systems are more resilient to extreme water quality conditions – primarily temperature and carbon dioxide than previously hypothesized;
- *Fountain darter food source (abundance and tolerance)* – macroinvertebrate monitoring coupled with applied research has shown an abundance of fountain darter food and a high temperature tolerance of amphipods;
- *Fountain darter movement* – ranges and conditions for movement have been established and/or confirmed;
- *Fountain darter fecundity* – the ability for this species to reproduce in all types of habitat and flow conditions including bare substrate and near zero flow expands the resiliency factor for this species beyond that previously hypothesized;
- *Aquatic vegetation restoration* – the restoration projects in both systems have demonstrated that the reduction of non-native aquatic vegetation and subsequent establishment of native vegetation is achievable, in most cases beyond what was hypothesized leading into the HCP;
- *Gill parasites* – gill parasite concentrations remain low in these systems and at present are not a significant threat.

Key information gleaned from the extended drought conditions of 2013 and 2014 in the Comal system include:

- Low total discharge conditions not witnessed in over 25 years were observed and offered fairly minimalistic impacts to the system as a whole, with the key areas specified in the HCP (Landa Lake and Old Channel ERPA) left mostly unaffected;
- Bryophytes in the Upper Spring Run study reach died off as anticipated and consistent with applied research results;
- Rooted aquatic vegetation exhibited more resilience in the wild than anticipated but consistent with applied research results;
- Algae that is common each summer caused initial problems with coating of plants as typical, but did not take over during the extended period of low flow as previously hypothesized;
- Fountain darters survived and recovered in the Upper Spring Run study reach even with limited habitat, higher temperatures and no measurable flow at times;
- Gill parasite concentrations and infected snail populations did not rapidly increase or cause any distinguishable impacts.

To provide the framework for comparison with FDMS results (for a quasi-validation exercise), the following summary of conditions and impacts relative to the 2013-2014 drought in the Comal system are noted. Several years of an exceptional drought in Texas culminated in the lowest total system discharge (65 cfs) observed in the Comal River in 2014 since the inception of the EAA biological monitoring program in 2000. For context, total system discharge in the Comal system has declined below 150 cfs seven times and below 100 cfs five times over the past 40 years (BIO-WEST, 2015a). The lowest daily level recorded during this time period was 26 cfs in 1984, which was a year that, like 2014, experienced eight consecutive months below 150 cfs. Although the lowest total system discharge recorded in 2014 was 65 cfs, the number of consecutive days below 150 cfs was greater than was experienced in 1984: specifically, the duration of the low-flow event experienced in 2014 is the longest recorded since the drought of record in the 1950s. In terms of scale, lowest level, timing, and duration, 2014 was very similar to 1989. Essentially, the Comal system had not observed those springflow conditions for almost a quarter century.

In breaking total system discharge down to study reaches, this translates into the Upper Spring Run reach experiencing less than 3 cfs for over nine consecutive months starting in April 2014.

By August 2014, the Upper Spring Run study reach discharge had declined to 1 cfs and stayed at or below this value through September. During this two-month period, no measurable discharge was recorded in late August. Discharge in the Landa Lake study reach equivalates with the total system discharge recorded because the vast majority of upwelling springs and major spring runs all flow into this reach. As such, Landa Lake experienced less than 80 cfs for most of August and September, declining to a low of 65 cfs. The Old Channel study reach is manipulated via culverts for the protection of the ERPA and thus, discharge through the Old Channel was controlled around 50 cfs during the 2014 hot summer months.

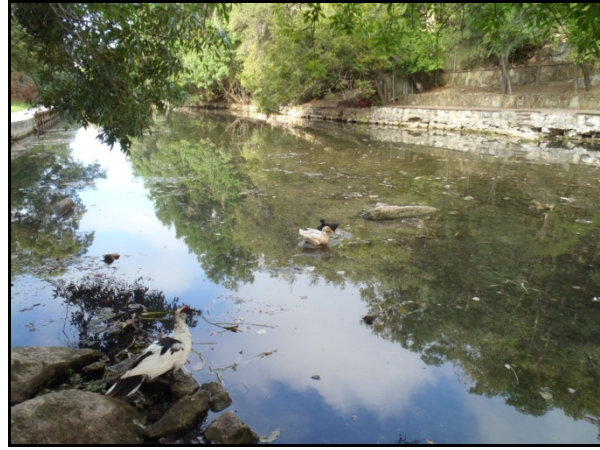
Figures 4-1 through 4-3 give a visual overview of typical conditions, and those observed during August and November 2014 in the Comal System ecomodel study areas. Fountain darter habitat conditions within the Upper Spring Run study reach deteriorated over the course of the year primarily due to the following reasons:

- blooms of green algae covered and killed native bryophytes early in the year,
- this alga itself died off later in the summer exposing additional bare substrate,
- stagnant conditions that caused decreased water clarity and increased water temperatures in non-upwelling influenced areas,
- summertime recreational pressure, and
- declining water levels that caused the typically submerged *Sagittaria* in this reach to become emergent, resulting in vegetation mat build-up and restricting water flow to lower reaches.

Remarkably, water temperatures continued to be maintained in this uppermost reach for most of the year, as spring openings were still evident during periods of zero measured discharge throughout this portion of the reach in late August. The Upper Spring Run study reach did experience water temperatures above 29°C for a brief period in late August and early September. Data from all three HCP biological sampling techniques (drop net, dip net, and fish community sampling) showed declines in fountain darter numbers in this reach over the course of 2014 (BIO-WEST, 2015a). However, it is important to note that in late December 2014, after nearly 9 months of reach-specific discharge of less than 3 cfs, fountain darters were observed to still utilize this reach of the Comal system.



(A) Typical



(B) August 2014



(C) November 2014

**Figure 4-1. Upper Spring Run reach**

Impacts to fountain darter habitat did occur downstream in Landa Lake, but to a much lesser extent than witnessed in the Upper Spring Run reach. Impacts were primarily due to shallow water depths enabling aquatic vegetation to become emergent, which resulted in floating vegetation mats (Figure 4-2), leading to shading and subsequent die-off of underlying vegetation. Although low DO measurements were recorded at the fixed water quality sonde in the center of the lake throughout most of the summer, there has not been a corresponding biological response documented. Neither drop-net nor dip-net sampling data have shown discernible declines in fountain darter abundance in Landa Lake during 2014.



(A) Typical



(B) August 2014



(C) November 2014

**Figure 4-2. Landa Lake Floating Vegetation Mats**

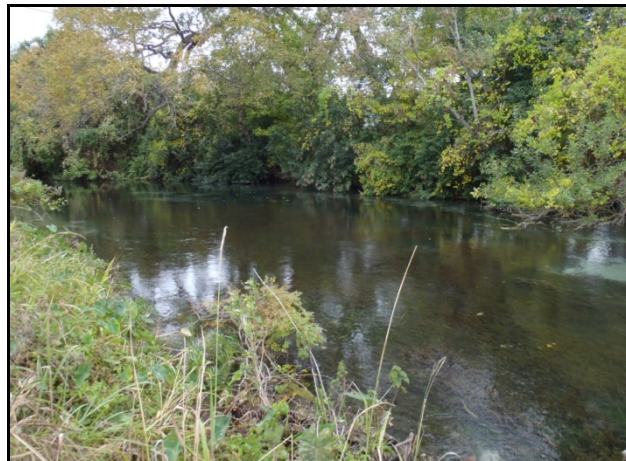
By HCP design, the old channel of the Comal River did not experience the changes in spring flow or water levels observed in 2014 at other locations in the Comal system. Consequently, the Old Channel ERPA supported high quality fountain darter habitat with thriving restored native aquatic vegetation throughout the year. Although water temperature shows more daily variability in the Old Channel relative to sites closer to the spring discharge, it was maintained within the ranges necessary to support the fountain darter throughout 2014. There were no changes in fountain darter populations observed within the Old Channel during 2014 biological monitoring activities.



**(A) Pre-restoration 2013 with all nonnative vegetation of one species**



**(B) August 2014 with five species of restored native vegetation**



**(C) November 2014 restored**

**Figure 4-3. Old Channel Environmental Restoration and Protection Area**

### ***4.3 Lessons Learned: 2013-14 drought impacts compared to FDMS results***

As discussed throughout this document, caution must be taken when interpreting successful model validation. It can also be informative to conduct high-level comparisons to investigate trends or similarities with observed ecological data. To that extent, a brief discussion on simulated model trends and observed drought information is presented. The 2013-14 drought period and the subsequent recovery occurred after the 13-year period identified for model validation, too late to be included in the model-development work. However, in view of the intense drought conditions, this qualitative comparison of observations and modeling is useful.

As described above, the modeled Upper Spring Run reach during the drought of record simulations involved discharge conditions (1.7 cfs) similar to what was measured in 2014. When those simulations were conducted with the time-series of observed vegetation (2003 to 2013), the model predicted fountain darter populations between approximately 1,000 and 25,000 total darters. However, during the “bad vegetation” simulations in which the worst aquatic vegetation conditions were maintained for 10 consecutive years, the population of darters remained consistently around 1,000 individuals. The total numbers are of no consequence for this examination, but the trends are intriguing. First, fountain darters were not extirpated in the FDMS under extremely low flows, poor vegetation conditions, and high temperatures in the Upper Spring Run study reach. Similarly, fountain darters persisted in the wild during 2014 under similar flow, vegetation, and temperature conditions. The model predicted essentially a 90% reduction in darters in the Upper Spring Run reach from typical conditions to this scenario. A cursory comparison of biological data shows considerable declines in the Upper Spring Run reach (e.g., dip net data showed large reductions in darters in Fall 2014). Second, when aquatic vegetation recovers in the model, darter populations rebound quickly. This response was also witnessed in the wild in the Upper Spring Run study reach during 2015 and 2016.

Not surprisingly, fountain darter populations in Landa Lake react very differently compared to those in the Upper Spring Run study reach under similar conditions to those observed in 2014. Discharge in Landa Lake (49.99 cfs modeled and 65 cfs observed) during that time period, coupled with the consistency of aquatic vegetation over time, resulted in predicted (FDMS) darter reductions during these conditions on the order of 20 to 30%. Similarly, biological data collected during that period indicate smaller levels of reductions in Landa Lake when compared to the Upper Spring Run study reach. In the case of the Old Channel ERPA, when flow, temperature, and aquatic vegetation are sustained in the model, fountain darters excel. The same was observed in nature. It is our opinion that the timed fountain darter dip net data provides an independent indicator of population trends. The fact that the magnitudes of the changes are consistent in nature and in the model serves to bolster confidence in the FDMS. That is, for small changes, no changes, and considerable changes in the dip net (timed) observations, the FDMS predicted changes in the same directions and at similar magnitudes.

As an additional test against empirical data, we computed the mean fountain darter densities in the model and collected in the drop net surveys over time, per reach, multiplied by the areal coverage in vegetation alone, for an observed versus FDMS-predicted comparison. The observed-versus-predicted results tracked well with respect to trends and with appropriate scaling, for fountain darter abundances. However, one must bear in mind that the drought of record conditions in the model only approximate in some respects those occurring in nature during the 2013-14 period. Also, one must bear in mind that the observed SAV distributions and associated fountain darter densities are not entirely independent, because the observed abundances by aquatic vegetation type are used in defining the habitat suitability, which influences the population growth and movement of the darters, so that the maximum observed abundances act as a sort of carrying-capacity constraint. There is considerable population/life-stage dynamics occurring in the model, and therefore opportunity for the modeled fountain darter population to evolve in different directions, so the agreement between model and data, even acknowledging this lack of independence, provides support that the model is functioning satisfactorily for its intended purpose. Moreover, the important applications of the model are to scenarios that we have not observed in the field, for which this issue of independence is moot.

The above discussion was a common-sense qualitative comparison of the model performance to observations during the recent drought. However, with a view to subsequent research, one proposed Tier C validation study is to run the calibrated decoupled FDMS for the Upper Spring Run reach, Landa Lake, and Old Channel study reaches with detailed accurate hydrometeorological inputs for 2013 through 2016 for comparison with actual observations properly reduced and organized from that time period.

## 5 Next Steps and Future Considerations

As discussed in Section 3.4 the current state of the FDMS is built upon several assumptions and, at present, has some notable shortcomings. It also needs to be re-emphasized that this model was built specifically for a management tool, not an academic representation of all ecological processes in these two complex springs / river systems. With that understanding, should the EARIP wish to enhance this tool or expand its use beyond the HCP Phase 1 flow regime conditions, it is our opinion that two key areas for further work revolve around DO and SAV predictability. Brief descriptions of future work for consideration are presented below.

### 5.1 Dissolved oxygen kinetics and modeling

Dissolved oxygen has not been a major focus of the monitoring and modeling activities to date in either river. With respect to the Comal River, except for continuous monitoring directly in spring orifices / runs with limited variability or a few sporadic monitors in DO-problematic areas, such as Landa Lake, there has been no systematic DO observation program focused on ecological impacts. As a consequence, the available data did not support the validations of QUAL2E as a DO model. During this project, one of the major causal pathways potentially connecting spring flows to the maintenance of the fountain darter was considered to be **SPRING FLOWS → CURRENT VELOCITY & WATER DEPTHS → WATER TEMPERATURE → DO BUDGET → DO THRESHOLD FOR DARTER SURVIVAL**. Under low spring flows and drought conditions, solubility would be reduced, lower velocities would limit aeration and promote water stagnation, whereupon respiration from submerged plants as well as planktonic algae would drive down nocturnal concentrations of DO. Incorporation of these processes in the darter model requires monitoring data on DO under summer low flows, field or lab determinations of SAV respiration rates in the submerged structures of the plants, and enhancement of the model to include plant production processes.

### ***5.1.1 DO monitoring***

Technology for automated field measurement of DO and related water parameters has evolved significantly in the past several decades. Now, inexpensive, reliable monitors with internal digital datalogging capabilities are widely available, and capable of recording time series of measurements at frequent intervals. We recommend several such monitors be deployed at key spatial locations in the Comal River. One of the challenges of operation of such robot sondes is instrument drift, arising from slow loss of calibration and from biofouling of the sensor. A systematic rigorous strategy of data collection will be necessary, including recovery of instruments after about a week of deployment (two weeks at the most), laboratory calibrations both before deployment and after recovery, and careful servicing and re-calibration in the laboratory. The program should include uploading and inspection of the data on the same service cycle.

Analysis of the data should be carried out by first modeling the observed drift during the deployment period and correcting the data for this drift. When this is done accurately, the diurnal swings in DO may be used to extract daily-mean values of gross production and respiration. (A lagniappe of this procedure is the determination of the DO reaeration coefficient, which is also needed in the DO model.) Procedures were outlined and subjected to field testing in the Texas estuaries by Ward (2003a, 2003b), and have been used recently in a five-year program of detailed monitoring of the Klamath River in northern California (Ward and Armstrong, 2006, 2010). The same computational protocols can be applied to the study rivers.

### ***5.1.2 DO modeling including SAV influence***

Utilization of QUAL2E to simulate DO dynamics in the Comal and San Marcos Systems did not produce calibration or simulation results that were considered viable for use within the modeling framework. Primarily this was attributed to the underlying model formulation and analytical subroutines in QUAL2E that were developed for pelagic algae dynamics and not the process mechanisms representative of submerged rooted aquatic vegetation dynamics, which is more characteristic of the Comal and San Marcos systems.

We recommend that the existing SAV modules developed for the FDMS be extended to simulate photosynthesis and respiration on a sub-daily time step (e.g., hourly). This has the inherent advantage of maintaining the linkage between the spatially explicit SAV simulation dynamics that is then coupled to the DO simulations.

## **5.2 Advanced SAV modeling**

The SAV model developed herein represents a step forward in spatially-explicit modeling for submerged aquatic vegetation. Most SAV models are spatially-implicit, and do not model both growth and dispersal. While growth is modeled mechanistically via photosynthesis and respiration, we did make some simplifying assumptions compared to existing models. First, we simplified the equation used for photosynthesis by removing a nutrient component. Future research should focus on the extent to which the river systems are nutrient limited for SAV. Second, it might be possible to model this suite of SAV species as functional groups rather than individual species. Future efforts should determine if structural similarities in species translate to similarities in growth and in darter preference. Dispersal and competition (i.e., state conversion of SAV) are poorly understood. We were unable to develop a mechanistic model of these processes, but were able to capture some of the spatio-temporal variation in vegetative cover using transition probabilities calculated from the empirical mapping data. Detailed studies should be conducted to determine the mechanisms that drive spatio-temporal dynamics of these species.

The SAV model captures the seasonal mechanics of vegetation growth. The state transition algorithm provides a mechanism to explore spatial dynamics and patterns of SAV species in riverine systems. This algorithm was parameterized with transition matrices developed from 13 years of mapped data. Our evaluation of this algorithm indicates that further refinement is necessary for it to be a truly predictive tool. The distribution and abundance of SAV in the San Marcos and Comal Rivers are dynamic, and are likely driven by complex interactions of physical and environmental factors not currently represented in the model. Future research should explicitly focus on determining how those factors control vegetative transitions, and how to best parameterize those processes in a quantitative framework that can be incorporated into mechanistic, spatially explicit models.

### **5.3 Future Considerations**

Though the completed, validated and operational FDMS will complete this contracted effort, for reasons highlighted in this report, this should not mark the end of model development for the Comal and San Marcos springs ecosystems. There are numerous other aspects (e.g., nutrients, scour, disease, pollution, recreation, etc.), that would be of direct interest to the HCP and likely useful in the further development of this tool specific to the fountain darter. Additionally, other management scenarios may present themselves as being desirable for inclusion in the model operation. However, at this time we feel the prudent approach is for the EARIP to evaluate (1) the tool at hand, (2) potential management applications as is, (3) potential validation exercises as prescribed in the HCP, and (4) whether and what other studies might be warranted to accomplish the goals of the HCP, such as the development of a similar tool for assessment of other HCP covered species.

## 6 References

- Batchelor, G. K., 1967: *An introduction to fluid dynamics*. Cambridge, U.K.: Cambridge University Press.
- Behen, K. 2013. *Influence of connectivity and habitat on fishes of the upper San Marcos River*. M.S. Thesis, Texas State University.
- Best, E.P.H. and W. A. Boyd. 1996. *A simulation model for growth of the submerged aquatic macrophyte Hydrilla verticillata L.* Technical Report A-96-8, US Army Corps of Engineers Waterways Experiment Station.
- Best, E.P.H. and W. A. Boyd. 1999. *A simulation model for growth of the submersed aquatic macrophyte Myriophyllum spicatum L.* Technical Report A-99-3, US Army Engineer Research and Development Center, Vicksburg, Mississippi.
- Best, E.P.H. and W. A. Boyd. 2001. *A simulation model for growth of the submersed aquatic macrophyte American wildcelery (Vallisneria americana Michx.)*. ERDC/EL TR-01-5, U.S. Army Engineer Research & Development Center, Environmental Laboratory, Vicksburg, Mississippi.
- Best, E.P.H. and W. A. Boyd. 2007. *Expanded simulation models (Version 3.0) for growth of submersed aquatic plants American wildcelery, sago pondweed, hydrilla, and Eurasian watermilfoil*. ERDC TN-SWRRP-07-10.
- Best, E.P.H. and W. A. Boyd. 2008. A carbon flow-based modeling approach to ecophysiological processes and biomass dynamics of submersed aquatic plants using *Vallisneria americana* as an example. *Ecol. Model.* 217, 117-131.
- Best, E.P.H. and W. A. Boyd. 2003. *A simulation model for growth of the submersed aquatic macrophyte Sago pondweed (Potamogeton pectinatus L.)*. ERDC/EL TR-03-6. U.S. Army Engineer Research & Development Center, Environmental Laboratory, Vicksburg, Mississippi.
- Best, E.P.H., Boyd, W.A., and K. P. Kenow. 2011. *A generic modeling approach to biomass dynamics of Sagittaria latifolia and Spartina alterniflora*. Report ERDC TN-SWRRP-11-1.
- BIO-WEST. 2003a. *Comprehensive and critical period monitoring program to evaluate the effects of variable flow on biological resources in the Comal Springs/River aquatic ecosystem*. Final 2003 annual report. Round Rock, Texas, USA.
- BIO-WEST. 2003b. *Comprehensive and critical period monitoring program to evaluate the effects of variable flow on biological resources in the San Marcos Springs/River aquatic ecosystem*. Final 2003 annual report. Round Rock, Texas, USA.

- BIO-WEST. 2004a. *Comprehensive and critical period monitoring program to evaluate the effects of variable flow on biological resources in the Comal Springs/River aquatic ecosystem*. Final 2004 annual report. Round Rock, Texas, USA.
- BIO-WEST. 2004b. *Comprehensive and critical period monitoring program to evaluate the effects of variable flow on biological resources in the San Marcos Springs/River aquatic ecosystem*. Final 2004 annual report. Round Rock, Texas, USA.
- BIO-WEST. 2005a. *Comprehensive and critical period monitoring program to evaluate the effects of variable flow on biological resources in the Comal Springs/River aquatic ecosystem*. Final 2005 annual report. Round Rock, Texas, USA.
- BIO-WEST. 2005b. *Comprehensive and critical period monitoring program to evaluate the effects of variable flow on biological resources in the San Marcos Springs/River aquatic ecosystem*. Final 2005 annual report. Round Rock, Texas, USA.
- BIO-WEST. 2006a. *Comprehensive and critical period monitoring program to evaluate the effects of variable flow on biological resources in the Comal Springs/River aquatic ecosystem*. Final 2006 annual report. Round Rock, Texas, USA.
- BIO-WEST. 2006b. *Comprehensive and critical period monitoring program to evaluate the effects of variable flow on biological resources in the San Marcos Springs/River aquatic ecosystem*. Final 2006 annual report. Round Rock, Texas, USA.
- BIO-WEST. 2007a. *Comprehensive and critical period monitoring program to evaluate the effects of variable flow on biological resources in the Comal Springs/River aquatic ecosystem*. Final 2008 annual report. Round Rock, Texas, USA.
- BIO-WEST. 2007b. *Comprehensive and critical period monitoring program to evaluate the effects of variable flow on biological resources in the San Marcos Springs/River aquatic ecosystem*. Final 2008 annual report. Round Rock, Texas, USA.
- BIO-WEST. 2007c. *Variable flow study: seven years of monitoring and applied research*. Round Rock, Texas, USA, 70 pp.
- BIO-WEST. 2008a. *Comprehensive and critical period monitoring program to evaluate the effects of variable flow on biological resources in the Comal Springs/River aquatic ecosystem*. Final 2008 annual report. Round Rock, Texas, USA.
- BIO-WEST. 2008b. *Comprehensive and critical period monitoring program to evaluate the effects of variable flow on biological resources in the San Marcos Springs/River aquatic ecosystem*. Final 2008 annual report. Round Rock, Texas, USA.
- BIO-WEST. 2009a. *Comprehensive and critical period monitoring program to evaluate the effects of variable flow on biological resources in the Comal Springs/River aquatic ecosystem*. Final 2009 annual report. Round Rock, Texas, USA.
- BIO-WEST. 2009b. *Comprehensive and critical period monitoring program to evaluate the effects of variable flow on biological resources in the San Marcos Springs/River aquatic ecosystem*. Final 2009 annual report. Round Rock, Texas, USA.

- BIO-WEST. 2010a. *Comprehensive and critical period monitoring program to evaluate the effects of variable flow on biological resources in the Comal Springs/River aquatic ecosystem.* Final 2009 annual report. Edward Aquifer Authority.
- BIO-WEST. 2010b. *Comprehensive and Critical Period Monitoring Program to Evaluate the Effects of Variable Flow on Biological Resources in the San Marcos/River Aquatic Ecosystem.* Final 2009 Annual Report.
- BIO-WEST. 2011a. *Comprehensive and critical period monitoring program to evaluate the effects of variable flow on biological resources in the Comal Springs/River aquatic ecosystem.* Final 2010 annual report. Edward Aquifer Authority.
- BIO-WEST. 2011b. *Comprehensive and Critical Period Monitoring Program to Evaluate the Effects of Variable Flow on Biological Resources in the San Marcos/River Aquatic Ecosystem.* Final 2010 Annual Report.
- BIO-WEST. 2012a. *Comprehensive and critical period monitoring program to evaluate the effects of variable flow on biological resources in the Comal Springs/River aquatic ecosystem.* Final 2011 annual report. Edward Aquifer Authority.
- BIO-WEST. 2012b. *Comprehensive and Critical Period Monitoring Program to Evaluate the Effects of Variable Flow on Biological Resources in the San Marcos/River Aquatic Ecosystem.* Final 2011 Annual Report.
- BIO-WEST. 2013a. *Comprehensive and critical period monitoring program to evaluate the effects of variable flow on biological resources in the Comal Springs/River aquatic ecosystem.* Final 2012 annual report. Edward Aquifer Authority.
- BIO-WEST. 2013b. *Comprehensive and Critical Period Monitoring Program to Evaluate the Effects of Variable Flow on Biological Resources in the San Marcos/River Aquatic Ecosystem.* Final 2012 Annual Report.
- BIO-WEST. 2014a. *Comprehensive and critical period monitoring program to evaluate the effects of variable flow on biological resources in the Comal Springs/River aquatic ecosystem.* Final 2013 annual report. Edward Aquifer Authority.
- BIO-WEST. 2014b. *Comprehensive and Critical Period Monitoring Program to Evaluate the Effects of Variable Flow on Biological Resources in the San Marcos/River Aquatic Ecosystem.* Final 2013 Annual Report.
- BIO-WEST. 2014c. *Fountain darter movement under low-flow conditions in the Comal springs/river ecosystem.* Final Report. San Antonio, TX: Edwards Aquifer Authority.
- BIO-WEST. 2015a. *Habitat conservation plan biological monitoring program: Comal Springs/River aquatic ecosystem.* Final 2014 Annual Report submitted to the Edwards Aquifer Authority, San Antonio, Texas.
- BIO-WEST. 2015b. *Habitat conservation plan biological monitoring program: San Marcos Springs/River aquatic ecosystem.* Final 2014 Annual Report submitted to the Edwards Aquifer Authority, San Antonio, Texas

- BIO-WEST et al. (Ecomodel Project Team) 2015c. *Predictive Ecological Model for the Comal and San Marcos Ecosystems Project*. Interim report submitted to Edwards Aquifer Authority, San Antonio, Texas.
- BIO-WEST. 2016a. *Habitat conservation plan biological monitoring program: Comal Springs/River aquatic ecosystem*. Final 2015 Annual Report submitted to the Edwards Aquifer Authority, San Antonio, Texas.
- BIO-WEST. 2016b. *Habitat conservation plan biological monitoring program: San Marcos Springs/River aquatic ecosystem*. Final 2015 Annual Report submitted to the Edwards Aquifer Authority, San Antonio, Texas.
- BIO-WEST. 2017a. *Habitat conservation plan biological monitoring program: Comal Springs/River aquatic ecosystem*. Final 2016 Annual Report submitted to the Edwards Aquifer Authority, San Antonio, Texas.
- BIO-WEST. 2017b. *Habitat conservation plan biological monitoring program: San Marcos Springs/River aquatic ecosystem*. Final 2016 Annual Report submitted to the Edwards Aquifer Authority, San Antonio, Texas.
- Bonner, T., T. Brandt, J. Fries, and B. Whiteside. 1998. Effects of temperature on egg production and early life stages of the Fountain Darter. *Trans. Am. Fish. Soc.* 127, 971-978.
- Brandt T., K. Graves, C. Berkhouse, T. Simon and B. Whiteside. 1993. Laboratory spawning and rearing of the endangered Fountain Darter. *Progressive Fish-Culturist* 55, 149-156.
- Carr G., H. Duthie and W. Taylor. 1997. Models of aquatic plant productivity: a review of the factors that influence growth. *Aquatic Botany* 59, 195-215.
- Chapra, S.C. 1997. *Surface water-quality modeling*. Boston: McGraw-Hill Companies.
- Colorado and Lavaca Rivers and Matagorda and Lavaca Bays Basin and Bay Expert Science Team. [CL BBEST]. 2011. *Environmental Flow Regime Recommendations Report*. Final Submission to the Colorado and Lavaca Rivers and Matagorda and Lavaca Bays Basin and Bay Area Stakeholder Committee, Environmental Flows Advisory Group, and Texas Commission on Environmental Quality. March 1, 2011.
- Committee on Review of Methods for Establishing Instream Flows for Texas Rivers, 2005: *The science of instream flows: a review of the Texas Instream Flow Program*. Publ. 11197, National Academies Press, Washington, D.C.
- Dammeyer, N. T., C. Phillips, and T. Bonner. 2013. Site fidelity and movement of the smallest theostomine darter with implications for endangered species management. *Trans. Am. Fish. Soc.* 142:1049-1057.
- Dingman, S. L. 2002. *Physical hydrology*. Upper Saddle River, NJ: Prentice-Hall.
- Doyle, R., M. Francis and R. Smart. 2003. Interference competition between *Ludwigia repens* and *Hygrophila polysperma*: two morphologically similar aquatic plant species. *Aquat. Bot.*, 77, 223-234.

- Doyle, R., S. Hester and C. Williams. 2014. *Edwards Aquifer Authority: 2014 - Ecomodeling: vegetation percent cover to biomass*. Technical Report Prepared for Edwards Aquifer Authority. Baylor University, Waco.
- EARIP (Edwards Aquifer Recovery Implementation Program). 2012. *Habitat Conservation Plan and Appendices*. November 2012.
- Erdogan, B., C. Abbott, G. Aouad and A. Kazi. 2009. Construction IT in 2030: a scenario planning approach. *J. Inform. Tech. Constr.* 14, 539-555.
- Gilbert, N., and S. Bankes. 2002. Platforms and methods for agent-based modeling. *Proc. Natl. Acad. Sci.* 99 (suppl 3), 7197-7198.
- Goudriaan, J., and H. van Laar. 1994. *Modelling Potential Crop Growth Processes: Textbook with Exercises*. Dordrecht, Netherlands: Kluwer Academic Publishers.
- Grant, W., and T. Swannack. 2008. *Ecological modeling: a common-sense approach to theory and practice*. Malden, MA: Blackwell Publishing.
- Grimm, V. and S. Railsback. 2005. *Individual-based modeling and ecology*. Princeton, NJ: Princeton University Press.
- Grimm, V., U. Berger, F. Bastiansen, S. Eliassen, V. Ginot, J. Giske, J. Goss-Custard, T. Grand, S. K. Heinz, G. Huse, A. Huth, J. U. Jepsen, C. Jørgensen, W. M. Mooij, B. Müller, G. Pe'er, C. Piou, S. F. Railsback, A. M. Robbins, M. M. Robbins, E. Rossmannith, N. Rüger, E. Strand, S. Souissi, R. A. Stillman, R. Vabø, U. Visser, and D. L. DeAngelis. 2006. A standard protocol for describing individual-based and agent-based models. *Ecological Modelling* 198, 115-126.
- Grimm V., U. Berger, D. DeAngelis, G. Polhill, J. Giske, and S. F. Railsback. 2010. The ODD protocol: a review and first update. *Ecological Modelling* 221: 2760-2768
- Guadalupe, San Antonio, Mission, and Aransas Rivers and Mission, Copano, Aransas, and San Antonio Bays Basin and Bay Expert Science Team. [GSA BBEST] 2011. *Environmental Flows Recommendations Report*. Final Submission to the Guadalupe, San Antonio, Mission, and Aransas Rivers and Mission, Copano, Aransas, and San Antonio Bays Basin and Bay Area Stakeholder Committee, Environmental Flows Advisory Group, and Texas Commission on Environmental Quality.
- Guyton, W.F. and Associates. 2004. *Evaluation of Augmentation Methodologies in Support of In-Situ Refugia at Comal and San Marcos Springs, Texas*. 192 pp.
- Hardy, T.B. 2010. Technical assessments in support of the Edwards Aquifer science committee “J Charge” flow regime evaluation for the Comal and San Marcos River systems. River Systems Institute, Texas State University. 159 pp

- Hardy, T., K. Kollaus and K. Tower. 2010. *Evaluation of the proposed Edwards Aquifer recovery implementation program drought of record minimum flow regimes in the Comal and San Marcos River systems*. River Systems Institute, Texas State University. 81 pp.
- HDR Engineering, Inc. (HDR). 2011. *Evaluation of Water Management Programs and Alternatives for Springflow Protection of Endangered Species at Comal and San Marcos Springs*. Prepared for the Edwards Aquifer Recovery Implementation Program. October 2011.
- Holten, D. 2006. "Hierarchical Edge Bundles: Visualization of Adjacency Relations in Hierarchical Data" (PDF). *IEEE Trans. on Visualization and Computer Graphics*. IEEE Computer Society. 12 (5). ISSN 1077-2626
- Jowett, I.G. 1997. Instream flow methods: a comparison of approaches. *Regul. Rivers 13*, 115-127.
- Krzywinski, M. et al. Circos: An Information Aesthetic for Comparative Genomics. *Genome Res* (2009) 19:1639-1645
- Mahmoud, M., Y. Liu, H. Hartmann, S. Stewart, T. Wagener, D. Semmens, R. Stewart, H. Gupta, D. Dominguez, F. Dominguez, D. Hulse, R. Letcher, B. Rashleigh, C. Smith, R. Street, J. Ticehurst, M. Twery, H. van Delden, R. Waldick, D. White and L. Winter. 2009. A formal framework for scenario development in support of environmental decision-making. *Env. Modelling Software 24*, 798-808.
- McDonald, R.R., J.M. Nelson, and J.P. Bennett. 2005. *Multi-dimensional surface-water modeling system user's guide*. U.S. Geological Survey Techniques and Methods, 6-B2.
- McDonald, R.R., J.M. Nelson, P.J. Kinzel, and J.S. Conaway. 2006. Modeling surface-water flow and sediment mobility with the multi-dimensional surface water modeling system. U.S. Geological Survey Fact Sheet 2005-3078.
- McDonald, D., T. Bonner, E. Oborny Jr. and T. Brandt. 2007. Effects of fluctuating temperatures and gill parasites on reproduction of the Fountain Darter, *Etheostoma fonticola*. *Journal of Freshwater Ecology 22*, 311-318.
- Milhous, R., D. Wegner, and T. Waddle. 1984. *User's guide to the physical habitat simulation system*. FWS/OBS-81/43, Biological Services Program, U.S. Fish & Wildlife Service, Washington, D.C.
- Mora, M., W. Grant, L. Wilkins and H.-H. Wang. 2013. Simulated effects of reduced spring flow from the Edwards Aquifer on population size of the fountain darter (*Etheostoma fonticola*). *Ecological Modelling 250*, 235-243.
- Peixoto, J., and A. Oort. 1992. *Physics of climate*. New York: American Institute of Physics.
- Railsback, S., and V. Grimm. 2014. *Agent-based and individual-based modeling: A practical introduction*. Princeton University Press, Princeton, New Jersey. 2014.

- Rounsevell, M., and M. Metzger. 2010. Developing qualitative scenario storylines for environmental change assessment. *Wiley Interdisciplinary Review: Climate change* 1, 606-619.
- Scheffer, M., Bakema, A. and Wolterboer, F. 1993. MEGAPLANT: a simulation model of the dynamics of submerged plants. *Aquatic Botany* 45(4), 341-356.
- Schenk, J., and Whiteside, B. 1977. Food habits and feeding behavior of the fountain darter, *Etheostoma fonticola* (Osteichthyes: Percidae). *The Southwestern Naturalist*, 487-492.
- Schnaars, S.P. 1987. How to develop and use scenarios. *Long Range Planning* 20 (1), 105-114.
- Schulman, A., D. McKinney, and P. John. 1995. Stochastic recharge model for Edwards Aquifer in Central Texas. *Journal of Water Resources Planning and Management* 121, 479-489.
- Sellers, W.D. 1965. *Physical climatology*. Chicago: University of Chicago Press.
- Teh, C. B. S., 2006. *Introduction to Mathematical Modeling of Crop Growth: How the Equations are Derived and Assembled into a Computer Model*. Boca Raton, FL: Brown Walker Press.
- van Nes, E., M. Scheffer, M. van den Berg, and H. Coops. 2003. Charisma: a spatial explicit simulation model for submerged macrophytes. *Ecological Modelling* 150,103-116.
- Wallace, J., and P. Hobbs. 2006. *Atmospheric Science*, 2nd ed. San Diego, CA: Academic Press.
- Ward, G.H. 2003a. *Primary productivity in the Coastal Bend bays in space and time*. Report to Texas General Land Office, Center for Research in Water Resources, University of Texas.
- Ward, G.H. 2003b. *Eutrophication state of Corpus Christi Bay*. Report to Texas General Land Office, Center for Research in Water Resources, University of Texas.
- Ward, G. and N. Armstrong. 2006. *Estimation of dissolved oxygen kinetic parameters from Klamath sonde data*. Report to U.S. Fish & Wildlife Service, Arcata, CA.
- Ward, G., and N. Armstrong. 2010. *Assessment of Community Metabolism and Associated Kinetic Parameters in the Klamath River*. Report to Arcata Office, U.S. Fish & Wildlife Service.
- Waters, T. F. 1969. The turnover ratio in production ecology of freshwater invertebrates. *The American Naturalist*, 103(930). 172-185.
- Wilensky, U, and W. Rand, 2015: *An introduction to agent-based modeling: Modeling natural, social and engineered complex systems with NetLogo*. Cambridge, MA: MIT Press.

## **APPENDIX A: Key Decision Points**

Throughout the process of model development, a series of decisions on model formulation and implementation were confronted. Some of these decisions were matters of technical detail and were resolved or informed by a series of specifically targeted HCP applied research projects. These specific projects were summarized in the Interim Report (BIO-WEST, 2015c) with full reports provided as appendices. In other cases, upon further evaluation and sensitivity analysis it was revealed that certain decisions did not have a crucial impact on model development. However, some remain key decisions that represent forks in the road of model development. The major decisions are summarized below.

### *Water quality parameters*

The suite of water-quality variables to be included in the model was limited to water temperature and dissolved oxygen (DO). The darters and, to a lesser extent, aquatic vegetation are primarily sensitive to water temperature, especially its stability during extreme low flows, so this is a necessary water quality variable. Although there has been limited oxygen depletion in the study rivers, under drought conditions it is conceivable that DO may drop below the limits of toleration for darters. Therefore, this variable was also included in the model. Moreover, to simplify the linkage between the water quality submodel and the darter submodel, the key variables selected were daily maximum temperature and daily minimum DO.

### *Water quality model*

To model temperature and DO, the QUAL2E models already developed for the Comal and San Marcos rivers (Hardy et al., 2010) were adopted for use in this project. Both river models were validated to the extent that suitable data existed for model testing. Each river system is modeled in its entirety as a complete link-node system. Adoption of this model meant that the spatial resolution of water quality would be limited to the underlying link-node segmentation for the river (nominally, 100 foot computational cells for both systems). In this model, the computed temperature and DO are cross-section mean values representing (i.e., averaged over) major segment reaches.

### *Hydraulic modeling*

Since the outset of the project, the necessity was accepted that a highly-resolved simulation of fluid velocity was needed to better depict the currents that vegetation and darters were exposed to in the various physiographies in the two rivers. The two-dimensional hydraulic model already developed for the river systems (Hardy et al., 2010) was adopted, an implementation of the U.S. Geological Survey (USGS) Multidimensional Surface Water Modeling System (MDSWMS) hydrodynamic software. The model grid is a vertically-integrated boundary-following curvilinear coordinate system, with nominal resolution of 0.25 m (25 cm, 10 in).

### *Sediment transport and turbidity*

In the past fifteen years (at least), dramatic scour and deposition of sediment have occurred within the two river systems, and even under relatively quiescent conditions. Turbidity due to sediment suspension can play a significant role in primary production. Therefore, consideration was given to expanding the existing model capabilities to include sedimentary processes. While this may be desirable to pursue in future research, given the present emphasis upon HCP flows under drought conditions, it was the judgment of the scientific team that sedimentary processes were less likely to be controlling on darter populations, and the effort to produce a sophisticated sediment transport model was unwarranted at this stage of model development.

### *Submerged aquatic vegetation (SAV) model*

The project team had access to the SAV models developed by the U.S. Army Engineer Research and Development Center (Vicksburg) in support of its program of wetlands management (Best and Boyd, 1996; 1999; 2001; 2003; 2007; 2008). While it was anticipated at the outset that one of these might be adopted for application to the San Marcos and Comal Rivers, upon careful review of the capabilities of these models and the properties of the SAV's in the study rivers, the decision was made to develop a model specific to the species in these rivers.

### *Agent-based modeling*

The conceptual model (Figure 1-8) focuses on the fountain darter because the sustainability of the present population of this species is the central motivation for the HCP (Phase 1) flow prescriptions. While traditional instream flow modeling approaches have been used in the past for evaluation of flow requirements for a particular fish species, it was the consensus of the

EARIP that a fresh modeling approach would take better advantage of the considerable data resources available to the project. An Agent-based Model (ABM, a.k.a. Individual-based Model, IBM) framework was selected (Grimm and Railsback, 2005; Grimm et al., 2007; Railsback and Grimm, 2014). This was considered to afford a viable means of simulating the time evolution of darter distributions in space, subject to time-varying external factors, and also enable the incorporation of random variation into the model.

#### *NetLogo modeling environment*

The fundamental choice for implementing an ABM is whether to create the code oneself or to rely upon an existing software product. The modeling team considered the latter to be the most efficient and selected NetLogo (Gilbert and Bankes, 2002; Wilensky and Rand, 2015). NetLogo is a fully open source, freely available software language specifically designed for simulating complex systems developing over time. It excels at spatially-explicit, agent-based modeling where users and modelers can give instructions to hundreds or thousands of "agents" that operate independently, based on their individual experience. This makes it possible to model the fine-scale interactions among individuals that results in system-scale patterns (e.g., how individual fish interact to create a population).

#### *Combination of the SAV and fountain darter submodels into a single NetLogo code*

A spatially explicit computation was needed to depict the spatial complexity of the rivers. The complexity of the computer codes and the differences between space-time discretization of the hydraulic and water quality submodels led to the conclusion that these model operations should be kept separate, using input/output text files to communicate model results to the SAV and fountain darter submodels. Both the SAV and fountain darter submodels employ the same underlying grid, which is a subsampled version of the hydraulic model grid. Because of this geometric coincidence and the intimate connection anticipated between SAV and darter abundance, the decision was made to combine the two submodels.

#### *Coverage-biomass conversion in aquatic vegetation model*

Almost all computational vegetation models employ biomass (measured in grams) as the basic dependent variable. The formulation of the present model is no exception. Because the field data is measured as areal coverage by species, the need to explore whether such observations

could be converted to equivalent biomass was recognized early in the project and led to recommendation for an applied research study. The results of that study indicated that conversions could be formulated relating the two measures of vegetation density. These conversions (unique to each SAV species) were incorporated into the SAV model code.

#### *Vegetation scour*

Review of the observations of river vegetation since 2000 identified several occasions when high stream velocities scoured substantial quantities of SAV. It was judged that this scour process would benefit the capabilities of the model. Unfortunately, the detailed hydraulic data for the plants specific to the San Marcos and Comal rivers were not available in the literature, so a research project was requested to perform the necessary measurements in laboratory flumes. While a contractor was selected, the contract could not be consummated, and this work was not carried out. Given that this data could not be available to the modeling team within the project time frame, it was decided that this process would not be included in the model. Instead scour processes would be represented as discrete events, in which pre-existing stands of SAV would be set to zero coverage at a specified point in time. This strategy would limit the model to depicting re-growth after the scour event, and excluded the ability to predict sites and quantities of SAV scoured by high-flow events. It would be desirable to address this as a future model refinement.

#### *Plant dispersal and competition in aquatic vegetation model*

Based upon examination of field observations of SAV coverage, the decision was made that dispersal (i.e., propagation) needed to be depicted in the SAV model. The need to explicitly model plant dispersal meant developing new vegetation model components based upon current literature and analysis of field data. This represents new science, and would be a major advance over present SAV models, the majority of which are spatially-implicit (Best and Boyd, 1996; 1999; 2001; 2003; 2007; 2008; Scheffer et al., 1993; van Nes et al., 2003). This entailed several subordinate decisions, highlighted later in the report. Most important was the recognition that it might not be possible to achieve this objective within the present project time frame, therefore it was necessary to formulate an alternate plan by which alterations in plant coverage could be accommodated in the fountain darter model. (See the de-coupled model, below.)

### *Fountain darter model grid*

The spatial resolution of each of the submodels is different, determined by the intrinsic variability of the physical relationships underlying the model, the resolution of field data, and the demands on computing capacity. Selection of a grid resolution for the fountain darter model was postponed until sufficient experience had been obtained with the early versions of the darter model. After this experimentation, a grid resolution of 1 meter was selected as being a satisfactory compromise between detailed SAV distributions, the incremental steps of darter movement, and computational demands and execution times.

### *Prey component in darter model*

Darters eat a variety of invertebrates, and inclusion of these food sources would necessitate separate submodels for each prey species. Based upon estimates of standing crop of categories of invertebrates and the daily requirements for darters, it was determined that availability of food was not a limiting factor for the darter populations. The decision was made to disregard food availability in the current version of the darter model.

### *Fully coupled SAV-darter model*

This is the designation for the full model depicted in Fig. 1-8 in which the SAV model component includes propagation capabilities (see *Plant dispersal*, above). This model configuration is fully predictive, in the sense that the user need only input initial conditions and a scenario of hydrology and meteorology (as well as management actions such as recreation or restoration), whereupon the model will produce a time history of SAV and darter abundance. This type of operation is the ultimate goal of model development.

### *De-coupled SAV-darter model*

The de-coupled model removes the projection of SAV growth and dispersal from the computation, and instead employs a user-defined time scenario of the space-time distribution of SAV in the model reach. The de-coupled model was first formulated to facilitate calibration and verification of the fountain darter submodel, by using the observed temporal and spatial distributions of SAVs as input to the darter model, based on field mapping efforts. (This strategy removes error propagation to the fountain darter model from uncertainties in SAV formulation.) Since the new science involved in creating a predictive SAV submodel was not proven, the de-

coupled model—relying on input distributions of SAVs— provided an alternative to the fully coupled model.

## APPENDIX B: Submerged Aquatic Vegetation Modeling – Technical Supplement

### Model Overview and Description

#### *Model Overview*

The model simulates vegetation growth, density, and colonization of several SAV species found in the spring-fed Comal and San Marcos rivers of Central Texas (for a list of species see Table 1). The formulations for the SAV submodel are based on earlier models (Best and Boyd, 2001), but have been modified for clear water, spring-fed, temperature-constant systems.

**Table 1. List of species being modeling in the Comal and San Marcos systems.**

<b>Species</b>
Cabomba
Hydrilla
Hygrophila
Ludwigia
Potamogeton
Sagittaria
Vallisneria
<u>Zizania (Texas Wild Rice)</u>

The model is spatially-explicit (i.e., geo-referenced and grid-based with a cell size of 1m<sup>2</sup>), stochastic, process-based, and programmed in Netlogo v5.3.1. The model simulates daily accumulation of biomass through photosynthesis, which is controlled by photosynthetically-active solar radiation and water depth. The model has a daily time step, but biomass accumulation is calculated using three-point Gaussian integration over both time and the depth profile for photosynthetic accumulation of biomass, growth to be estimated in more detail (Best and Boyd, 2001). We did not include the effects of temperature or nutrients because these systems are spring-fed and have a relatively constant temperature (ranging from 21 - 24°C annually), and are not nutrient limited.

Colonization of unvegetated cells, or conversion from one species type to another occurs once a month and is based on a series of conditions, including the historical records of particular cells being vegetated, the type of species in a cell, the relative resilience of a species to disturbance, and a matrix of transition probabilities that quantify the probability of a cell transitioning from one species to another. The transition matrix was calculated from thirteen years of field mapping efforts. For computational efficiency, the model allows one species type to occur per cell.

### *Model Initialization*

In addition to the physical and water quality data from the hydrodynamic submodel (velocity, depth, temperature, and DO), the SAV submodel is initialized with geo-referenced shapefiles of vegetation maps collected during field mapping in 2000 (Figures 1A and 1B), monthly extraterrestrial radiation<sup>1</sup>, and a user-defined latitude in degrees<sup>2</sup>.

### *Model Description*

Plant growth, in terms of biomass gained or lost (in grams/day) is modeled (Table 2) on a daily timestep and is calculated as

$$\Delta W = W_s P - W(R_m + M) \quad (1)$$

Where  $\Delta W$  is the change in plant weight for a given day,  $W_s$  is the weight of the sprout,  $P$  is the amount of biomass gained through photosynthesis per unit weight of the plant,  $W$  is the weight of individual plant,  $R_m$  is respiration, and  $M$  is mortality.

---

<sup>1</sup> Monthly radiation can be found at <http://w2.weather.gov/climate/> or <http://www.fao.org/docrep/x0490e/x0490e0j.htm>

<sup>2</sup> For the Comal and San Marcos Rivers, 29.7° N latitude was used

**Table 2. Parameter table for growth model**

Parameter	Description	Unit	Vegetation Species	
			Potamogeton	Vallisneria
$S_D$	Average stem density per plant	count	3 <sup>1</sup>	35 <sup>1</sup>
$H_{Max}$	Maximum stem height	cm	80 <sup>1,2,3</sup>	34.7 <sup>2</sup>
$S_M$	Maximum mass of each stem	g	6 <sup>1</sup>	0.09 <sup>3</sup>
$RL_{Max}$	Maximum root length	cm	60 <sup>4</sup>	30 <sup>4</sup>
$P_{D-Max}$	Maximum plant density per 0.5 m <sup>2</sup>	count	11.23 <sup>5</sup>	3.15 <sup>3</sup>
$CSA_{Average}$	Average cross-sectional area of a stem	cm <sup>2</sup>	0.231 <sup>6</sup>	0.155 <sup>5</sup>
$R_{RAB}$	Root-to-aboveground biomass ratio	ratio	0.429 <sup>7</sup>	1.128 <sup>4</sup>
$R_{RS}$	Root-to-shoot ratio	ratio	0.95 <sup>8</sup>	1.10 <sup>4</sup>
MinRoot	Minimum root size	g	0.001 <sup>b</sup>	0.001 <sup>b</sup>
MinSize	Minimum size for photosynthesis	g	0.5 <sup>b</sup>	0.5 <sup>b</sup>
Dispersal	# of 0.5 m increments traversed per year	count	8 <sup>9</sup>	1 <sup>6</sup>
Season <sub>Begin</sub>	First day of growing season	Julian day	107 <sup>10</sup>	121 <sup>4</sup>
Season <sub>End</sub>	Last day of growing season	Julian day	226 <sup>11</sup>	274 <sup>3</sup>
LeafDO	First day of leaf die off	Julian day	163 <sup>11</sup>	244 <sup>4</sup>
k	Plant tissue light extinction coefficient	m <sup>-2</sup> g <sup>-1</sup>	0.0235 <sup>a</sup>	0.0235 <sup>a</sup>
$H_I$	Half-saturation constant for light	μEm <sup>-2</sup> s <sup>-1</sup>	14 <sup>a</sup>	14 <sup>a</sup>
$P_{max}$	Maximum daily production	g <sup>-1</sup> hr <sup>-1</sup>	0.01 <sup>a</sup>	0.01 <sup>a</sup>
WintStor	Winter storage of biomass	proportion	0.33 <sup>b</sup>	0.33 <sup>b</sup>
WintDie	Additional winter die off	proportion	0.05 <sup>b</sup>	0.05 <sup>b</sup>
$F_{greenleaves}$	Biomass allocation to leaves	proportion	0.50 <sup>7</sup>	0.27 <sup>b</sup>
$F_{stem}$	Biomass allocation to stem	proportion	0.20 <sup>7</sup>	0.20 <sup>b</sup>
$F_{roots}$	Biomass allocation to roots	proportion	0.30 <sup>7</sup>	0.53 <sup>4</sup>

**Figure 1A. Shapefiles of vegetative coverage for the Old Channel in the Comal River System**

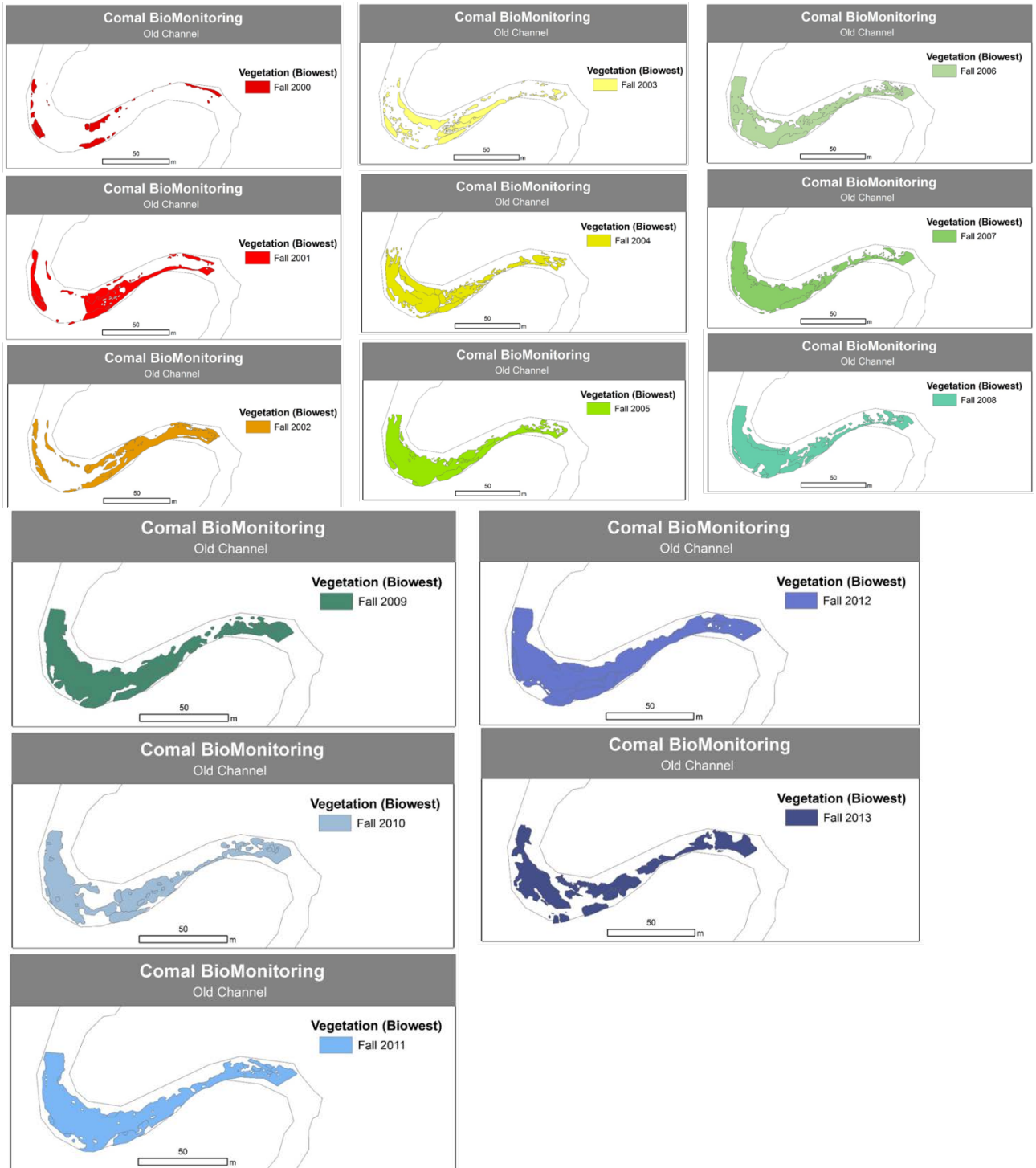
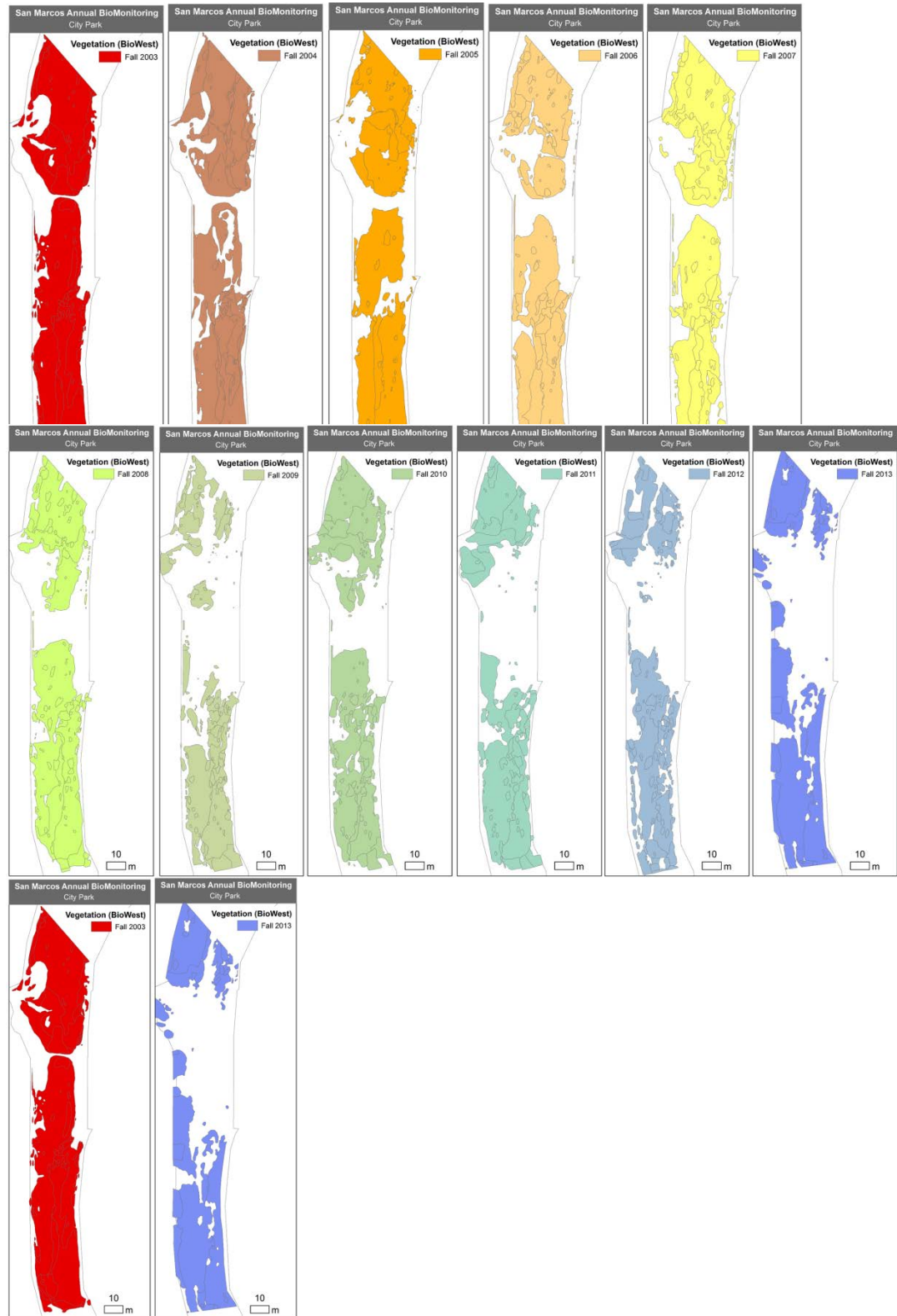


**Figure 1B. Shapefiles of vegetative coverage for the City Park Reach in the San Marcos River System.**



### *Photosynthesis*

Photosynthesis is affected by in-situ light ( $I$ ), and distance from the top of the plant ( $D$ ) using Michaelis-Menten saturation functions and a maximum value of photosynthetic accumulation ( $P_{max}$ ), which can be calibrated for different species. The Michaelis-Menten function for light assimilation provides a good approximation of photosynthetic response to light (Carr *et al.* 1997). Since light intensity follows a daily cycle, and varies with depth, photosynthesis is calculated at multiple times per day and at multiple depths in the vegetation, and is then integrated into a total daily value using Gaussian integration (Goudriaan and van Laar (1994), explained in section 2.2.2). Photosynthesis is calculated as

$$P = P_{max} * \frac{I}{I + H_I} \quad (2)$$

Where  $P_{max}$  represents the daily production of the plant top at 20°C (which assumes no resource limitation). The defaults for  $P_{max}$  is 0.01 g g<sup>-1</sup> d<sup>-1</sup>, but is calibrated to match growth rates of different species.  $I$  is the daily value photosynthetically available radiation (PAR),  $H_I$  is the half-saturation coefficient of light (100 μE m<sup>-2</sup> s<sup>-1</sup>),  $D$  is the distance from the top of the plant, and  $H_D$  is the half-saturation coefficient of depth (1m). Since these rivers are not nutrient or temperature limited, we did not model their effects on growth.

### *In situ light*

In aquatic systems, the availability of light is the driving factor controlling photosynthesis (Carr *et al.* 1997). Irradiance follows daily and seasonal cycles, resulting in spatio-temporal patterns of light availability and growth patterns. These patterns are captured by including solar declination (eq. 3) and day length (eq. 4) to calculate PAR. This method uses the terminology and follows the ASTRO and TOTASSIM procedures of Goudriaan and van Laar (1994). Briefly, day of year ( $day$ ) is used as an input to calculate solar declination (eq. 3), which is then combined with latitude ( $lat$ ) in intermediate equations ( $i_1$  through  $i_3$ ) to calculate day length (eq. 4). *Daylength* is then used to calculate a specific hour when photosynthesis occurs (eq. 5). Finally, PAR (μE m<sup>-2</sup> s<sup>-1</sup>) at the water

surface is estimated as 50% of the total irradiation given the day of year, hour, declination, and latitude (intermediate calculations  $i_4$  through  $i_6$ ).

$$\text{Declination} = -\text{asin}(\sin(23.45) * \left(\cos(2 * \pi * \frac{\text{day} + 10}{365})\right)) \quad (3)$$

$$\text{sinld} = \sin(\text{lat}) * \sin(\text{declination}) \quad i_1$$

$$\text{cosld} = \cos(\text{lat}) * \cos(\text{declination}) \quad i_2$$

$$\text{aob} = \frac{\text{sinld}}{\text{cosld}} \quad i_3$$

$$\text{daylength} = 12 * \left(1 + 2 * \frac{\text{asin}(\text{aob})}{\pi}\right) \quad (4)$$

$$\text{hour}_i = 12 + (\text{daylength} * 0.5 * \text{gaussian weight}_j) \quad (5)$$

$$\text{dsinB} = 3600 * (\text{daylength} * \text{sinld} + 24 * \text{cosld} * \sqrt{(1 - \text{aob}^2) / \pi}) \quad i_4$$

$$\text{dsinBE} = 3600 * (\text{daylength} * (\text{sinld} + 0.4 * (\text{sinld}^2 + \text{cosld}^2 * 0.5)) + 12 * \text{cosld} * (2 + 3 * 0.4 * \text{sinld}) * \sqrt{(1 - \text{aob}^2) / \pi}) \quad i_5$$

$$\text{sinb} = \max(0, (\text{sinld} + \text{cosld} * \cos(2 * \pi * (\text{hour}_i + 12) / 24)) \quad i_6$$

$$\text{PAR} = 0.5 * \text{dailyradiation} * \text{sinb} * (1 + 0.4 * \text{sinb}) / \text{dsinBE} \quad (6)$$

Light attenuation in the water column follows the Lambert-Beer law (following van Nes et al. 2003). Self-shading is included, and is based on species -specific light attenuation coefficients ( $K_p$ ), which provides a negative feedback for growth (i.e., the more biomass that accumulates the less light reaches the lower layers of the plants. Irradiance at a given depth ( $z$ ) is calculated as

$$I_z = \text{PAR} * e^{(-0.12 * z) - (K_p * \text{biomass}_{>z})} \quad (7)$$

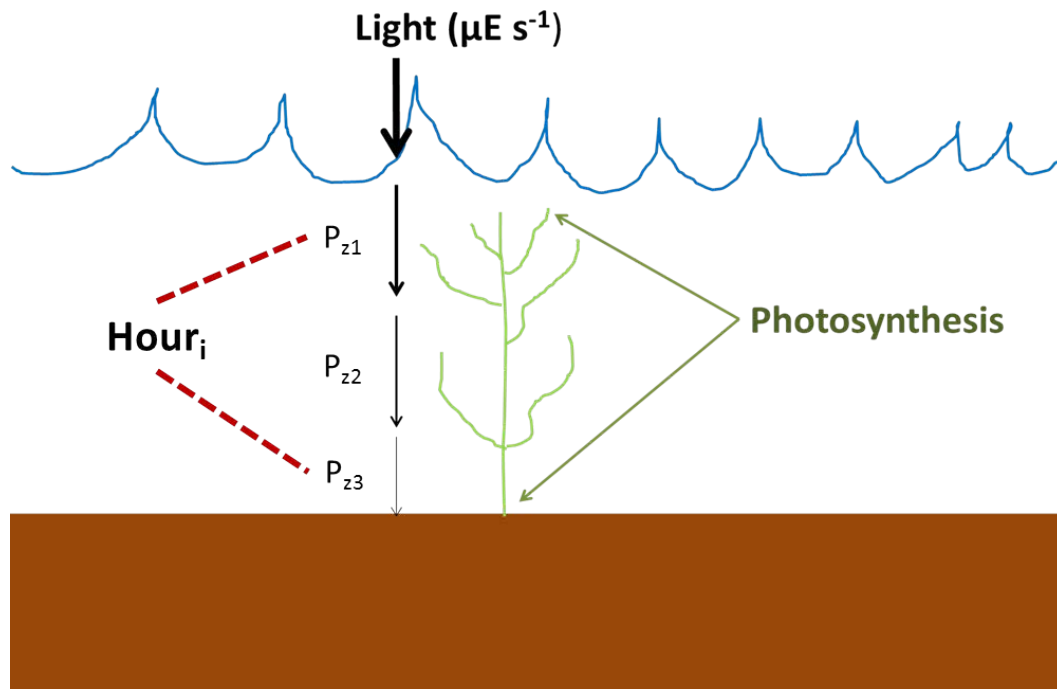
Where  $PAR$  represents the photosynthetically available radiation at the surface,  $-0.12$  is the light attenuation coefficient of the water<sup>3</sup>,  $z$  is the depth of the water at which photosynthesis is occurring, and  $\text{biomass}_{>z}$  is the biomass above depth  $z$ .

<sup>3</sup> <http://www.lakeaccess.org/ecology/lakeecologyprim3.html>

### Gaussian Integration

Since photosynthesis occurs throughout daylight hours, and irradiance changes throughout the day, PAR is calculated three times at three different depths per plant (Figure 2), and then integrated using three point Gaussian integration, which has been shown to provide accurate estimates of daily accumulation of biomass (Goudriaan and van Laar (1994)).

**Figure 2. Conceptual model of Gaussian integration of photosynthesis (see Photosynthesis section)**



Total daily gross assimilation (*TDGA*) in grams (*g*) is calculated as

$$TDGA = \text{daylength} * \sum_{h=1}^3 \left( GW_h * \sum_{z=1}^3 P_{z_i} \right) \quad (8)$$

Where *daylength* is the length of a given day, in hours (*h*), *GW* is the Gaussian weight used to weight the hourly photosynthesis (*P*) that was accumulated at depth *z* with irradiance (*i*). Gross assimilation is needed for growth and maintenance of the plant, which are based on their glucose requirement. Therefore, the *TDGA* was converted into

the weight of glucose for potential plant growth ( $W_{glucose}$ ) by multiplying it by the aboveground biomass of the plant and  $\frac{30}{44}$  (Teh, 2006). Once biomass is converted to glucose it is partitioned to above-ground and below-ground parts of the plant.

### *Respiration*

Maintenance respiration is needed for plants to continue to live. The model estimates maintenance respiration based on daily temperature and the biomass of the in the above and below ground sections of the plants. Maintenance respiration rates ( $R$ ) for above-ground ( $AG$ ) and below-ground ( $BG$ ) biomass were based on a  $Q_{10}$  formulation (i.e., the measure of the rate of change of a by increasing the temperature by  $10^{\circ}\text{C}$ ), and are calculated as

$$R_{AG} = 0.0225 * (Q_{10}^{(temp-25)/10}) \quad (9)$$

$$R_{BG} = 0.015 * (Q_{10}^{(temp-25)/10}) \quad (10)$$

where  $Q_{10}$  is a constant and set at 2, temp is daily temperature, and 0.0225 and 0.015 are the maintenance respiration coefficients for  $AG$  and  $BG$  biomass, respectively (based on values in Table 7.1 Teh, 2006).

### *Plant growth*

The difference between gross photosynthesis and maintenance respiration is the amount of assimilate available for growth. The glucose requirement for growth ( $G_{Growth}$ ) is calculated using the following equation from Teh (2006):

$$G_{Growth} = F_{AG} G_{AG} + F_{BG} G_{BG} \quad (12)$$

where  $F$  is the fraction of dry matter allocated to each plant part and  $G$  is the glucose requirement for growth of each plant part. The  $G$  estimates used for each plant part are from Table 7.4 of Teh (2006), with aboveground biomass being the sum of the above ground plant sections. The incremental plant part biomass gain per day is then estimated as

$$BM_{t+1} = BM_t + F * \left( \frac{W_{glucose} - R}{G_{growth}} \right) \quad (13)$$

If  $R$  is greater than the weight of glucose for potential plant growth, no growth occurs.

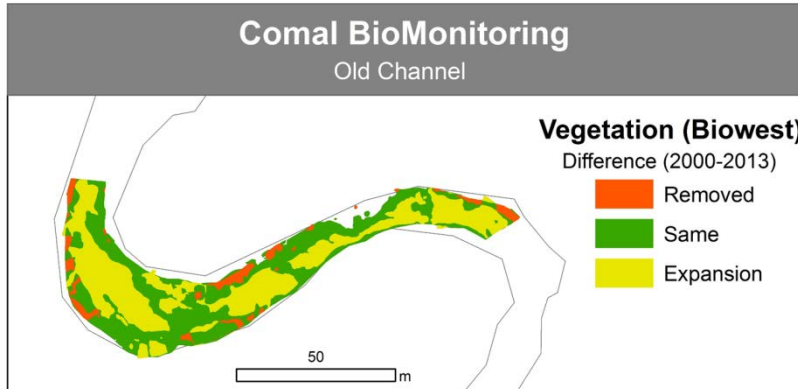
Morphological maximums are input parameters based on the literature or field data collected during this study, and are set in place to ensure plants sizes do not exceed biological limits. If after growth is simulated the species specific aboveground biomass exceeds the user-defined maximum aboveground biomass ( $BM_{AG-Max}$ ), the aboveground biomass is truncated to the maximum value. If after growth is simulated the species-specific root mass exceeds the user-defined maximum root mass ( $R_{M-Max}$ ), the root mass is truncated to the maximum value.

In some cases, the aboveground biomass is less than the user-defined minimum requirement for photosynthesis to occur. This is particularly true for some plants after colonization of new cells. When this happens, the model simulates plant growth by translocating 1% of the root biomass to the aboveground biomass, following methods used by Best and Boyd (2001).

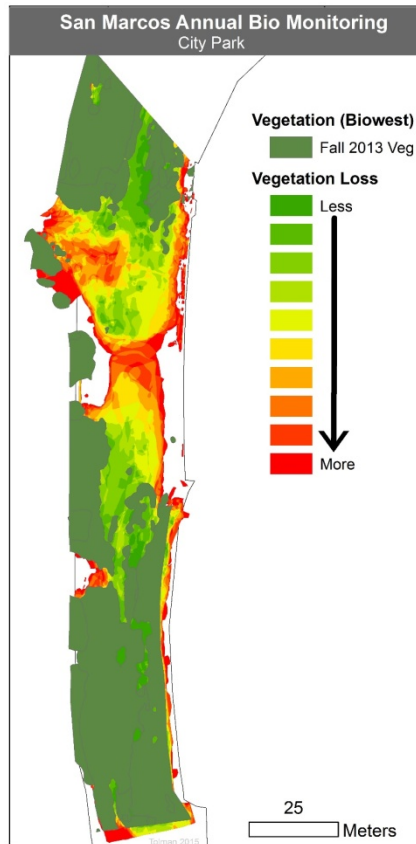
### *Conversion and dispersal*

Currently, there are few models that explicitly quantify the relationship between environmental conditions, and the ability of a plant to colonize new areas or be replaced by another species. We have developed an approach that simulates changes in vegetative cover over time based ecological dispersal theory and on empirical estimates gathered from 13 years of vegetation mapping. Vegetation coverage for each reach was mapped at least twice a year for thirteen years (e.g. Figures 1A and 1B). Spatial analysis indicated that both vegetation coverage and species composition were highly variable. Within each reach, there were specific areas that were never vegetated, others that remained vegetated, and other locations that oscillated between vegetated and unvegetated (Figures 3A and 3B).

**Figure 3. Depiction of frequency of occupancy of a given cell over time in the Old Channel (A), and City Park (B) reaches. Red and orange colors indicate that locations oscillated between vegetated and unvegetated during the course of the 13-year study, while green colors indicate those locations remained mostly vegetated.**



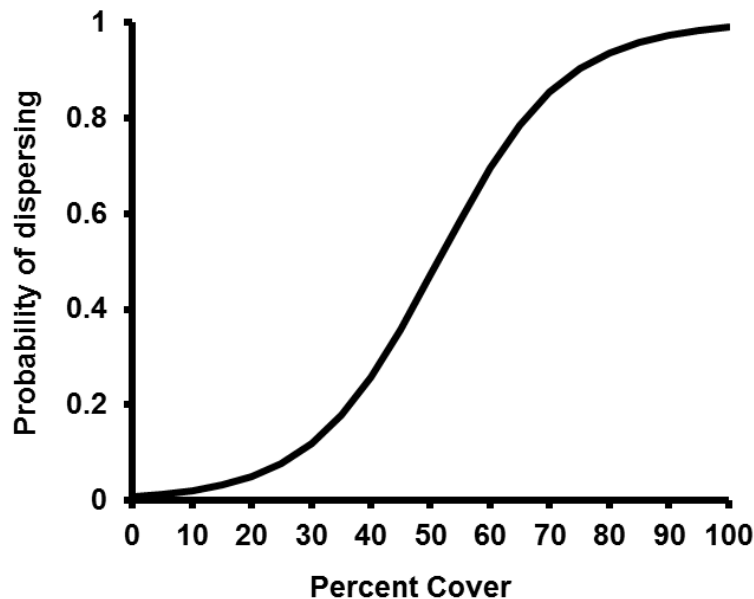
**A**



**B**

Dispersal by aquatic vegetation can take place through seed deposits, clonal growth, and/or fragments settling and rooting downstream. We did not model specific dispersal mechanisms, rather, we focused on modeling the probability that a given cell transitions from one state to another. Transition states included no change, convert to another species, or convert to bare. A cell cannot convert to a different state if it has six neighboring cells of identical states (e.g., a *Hydrilla* cell cannot convert if it has six neighboring cells that are also *Hydrilla*). If a cell has less than six neighbors with the same state, the model creates shape parameters for a logistic distribution based on the percent cover of vegetation for each of vegetated cell. This function then generates a probability of dispersal, which is lowest at low values for percent cover, and highest as the cover approaches 100% (Figure 4). Conversion to another species is calculated by comparing the probability of dispersal to a random number drawn from a uniform distribution between 0 and 1; conversion occurs if the random number is less than the probability of converting.

**Figure 4. Diagrammatic representation of logistic function used to calculate probability of dispersal based on percent cover of vegetation for each cell. Logistic algorithm can be found in Railsback and Grimm, 2014.**



Vegetation community composition within the study reaches was dynamic, and would often change within a given year or across years. Vegetation change was modeled by quantifying the likelihood that a vegetated point within each mapped site remains occupied with the same species, changes to another species or becomes bare. We calculated mean relative transition probabilities for each species using data from all available years and the spring and fall seasons. Transition probabilities were calculated for each reach independently. We calculated the probability of transition through two seasons (spring-fall and fall-spring), and transition probabilities were changed on day 122 for the spring-fall transitions, and day 305 for the fall-spring. An example of the transition probabilities for the Old Channel reach is shown in Figure 5. (See Appendix B supplement for exact values for each transition probability). Generally, highest transition probabilities were found when points became unoccupied and returned to bare space, and when points did not transition to a new vegetated state (i.e. the same species occupied a point through multiple seasons).

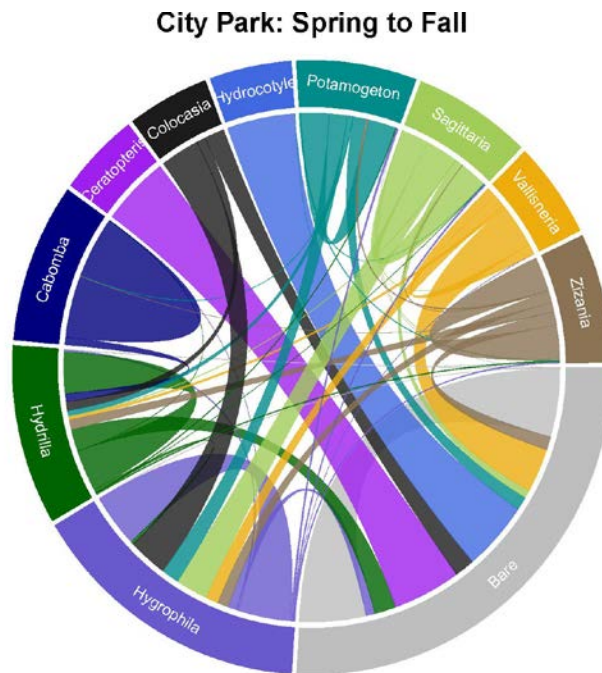
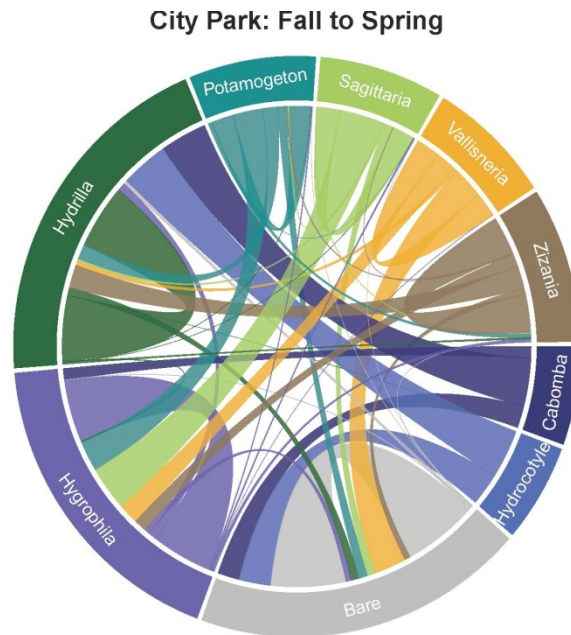
### *Mortality*

Senescence is based on overall growth patterns and temperature. It is lowest in the summer, and highest in the winter. Death rates and their corresponding temperatures were based on Best and Boyd (2001). Senescence was integrated into the equation for incremental plant part biomass gain per day (see equation 13) such that

$$BM_{t+1} = BM_t + F * \left( \frac{W_{glucose} - R}{G_{growth}} \right) - d * BM_t \quad (14)$$

The City Park reach also includes a recreation mortality based on observed human recreation patterns within the reach. The model assumes disturbance associated with a recreation event causes direct mortality to plants through excess flow, or human-mediated disturbance. Therefore, any plants within cells that are impacted by these events die.

**Figure 5. Chord chart representing transition probabilities from converting from one state to another in the City Park reach.**



The depletion in plant parts or in some cases the mortality of a plant occurred other plant parts were depleted. For example, if at any point the below-ground biomass was depleted, or if the above ground biomass falls below a user-defined threshold then entire plant died. This might occur if the annual senescence for a plant part consistently exceeded the incremental plant part biomass gain.

#### 2.2.8. Plant attributes

There are several measurable plant attributes that are important to the growth of aquatic vegetation. For simplicity, and computational efficiency we categorized all stems, shoots, and leaves as aboveground biomass, and roots and other below-ground matter as belowground biomass.

Aboveground height ( $H$ ) is calculated based on biomass: root ratio, following Best and Boyd (2001), and it cannot exceed the water depth of its cell. Root length (RL) is calculated as

$$RL = R_{RS} * H \quad (15)$$

where  $R_{RS}$  is a user-defined root-to-shoot ratio. If the root length overshoots a user-defined, maximum root length, the root length is truncated to the user-defined maximum root length. Maximum root biomass ( $R_{M-Max}$ ) was then calculated as a portion of  $BM_{max}$ , such that

$$R_{M-Max} = R_{RAB} * BM_{max} \quad (16)$$

where  $R_{RAB}$  is the root to aboveground biomass ratio.

#### *Model validation and sensitivity analysis*

Each function for the SAV model was verified independently in MS Excel, R, and Matlab. The implementation across platforms had to match exactly before it was implemented into the final version of the model. The SAV model was evaluated across three levels: (1) the model's ability to generate reasonable growth patterns for each of the

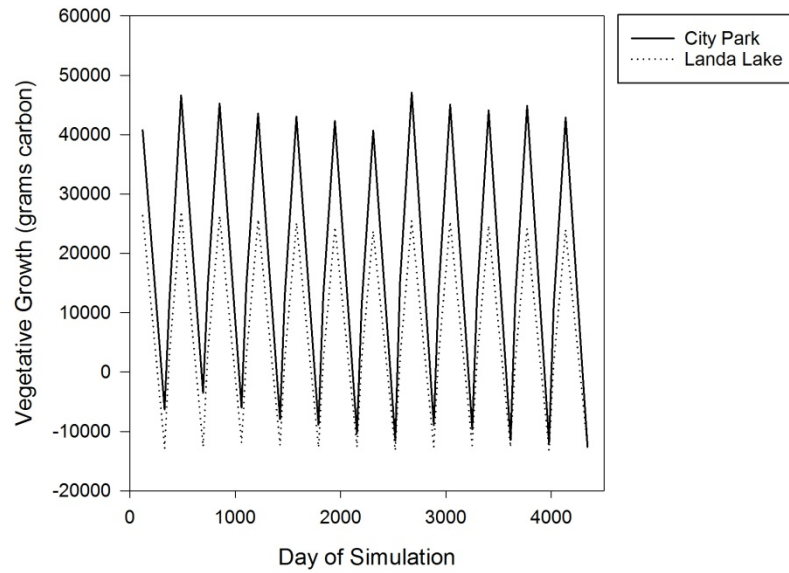
species modeled, (2) how well the model can recreate the historical distribution of vegetation coverage in each of the five reaches under two different mortality scenarios, and (3) how sensitive the model is to changes in input parameters, specifically how different values of temperature and frequency of conversion of cells to different states impacted model output. Due to limitations in computing time the latter was only performed on three reaches (City Park, Old Channel, and Upper Spring Run. We ran 10 replicate stochastic iterations for each evaluation scenario. The baseline simulation was a scenario with no constant biomass loss term, and state conversion at 10 days.

The model simulates realistic seasonal variation in vegetation growth and respiration, similar to the patterns exhibited by Best and Boyd (2001) and van Nes et al. (2003). Plant attributes were cyclical in that the patterns showed increased growth during the spring and summer and decreased growth in the winter (Figure 6). Simulated patterns in amount of vegetative cover matched observed patterns of cover in City Park, and Landa Lake relatively well, but underestimated vegetative cover in Landa Lake, I35, and Upper Spring Run. In the latter three reaches, the underestimation indicates that there are likely processes other than photosynthesis, respiration, and state conversion that drive vegetative cover. Future research should explore how processes not included in the model affect SAV distribution and abundance.

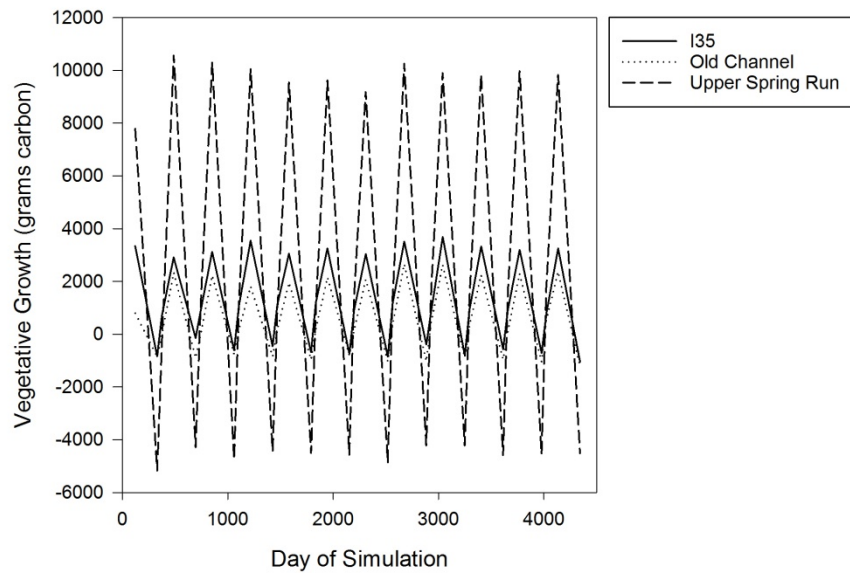
Given the large range of uncertainty associated with quantifying biomass loss for SAV species in general, previous SAV models quantify biomass loss through respiration and a constant biomass-loss term (i.e., a fixed percentage of biomass lost over a specified time step). We conducted a sensitivity analysis to determine how the model responded by including constant loss term (2% per time step) to compare against a scenario parameterized with respiration only. In step with this thinking, we also conducted a sensitivity analysis on how frequent a given cell had the potential to convert to another state by testing how the model responded when state conversions happened once every 3, 15, or 30 days, respectively.

**Figure 6. Net biomass accumulation over time for each of the five reaches. Reaches were modeled independently. The oscillations are a result of seasonal differences in water temperature and depth.**

System-level net growth for City Park and Landa Lake



System-level net growth for I35, Old Channel, and Upper Spring Run

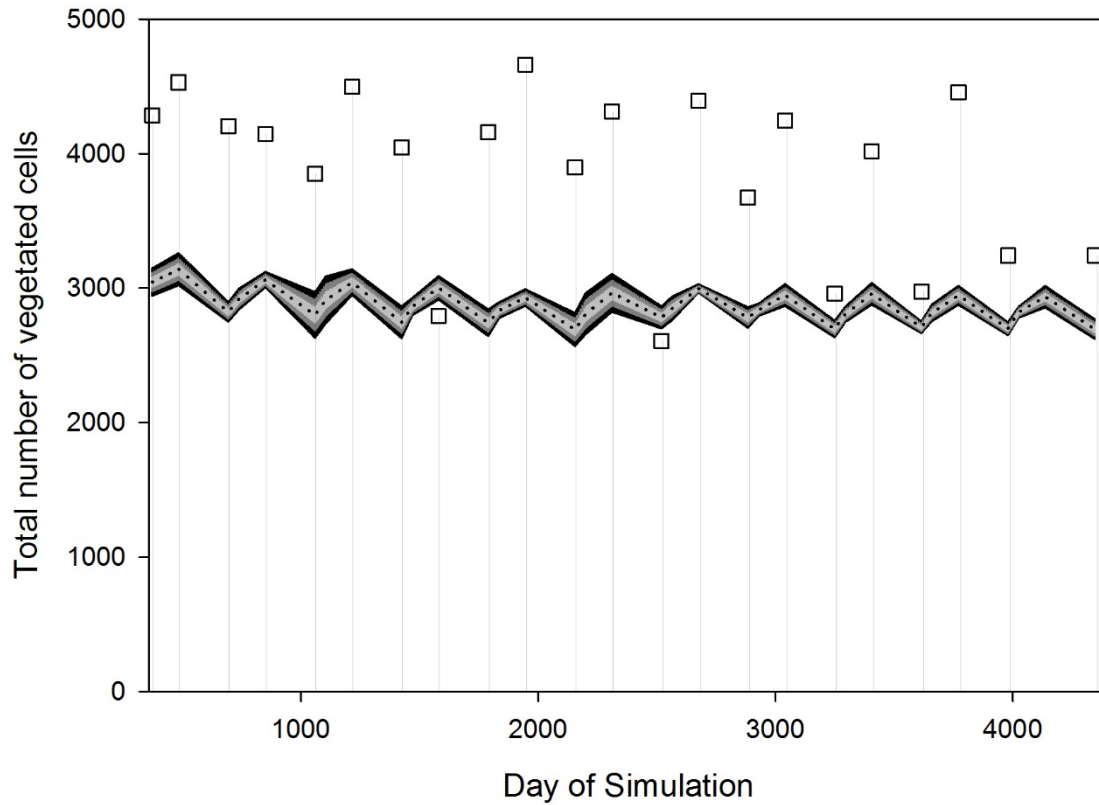


The incorporation of a constant loss term decreased the spatial distribution of vegetation across all five reaches from 25 to 60% compared to baseline (Figure 7). Old Channel decreased the least and Landa Lake the most. The model was much less sensitive to increases or decreases in temperature, with the total amount of vegetation not changing more than 6% in any reach when compared to baseline. In general, there was an inverse relationship between the total number of vegetated cells and temperature change. When temperature decreased, the total number of cells occupied by vegetation increased, and when temperature increased the number of vegetated cells decreased (Figure 8)

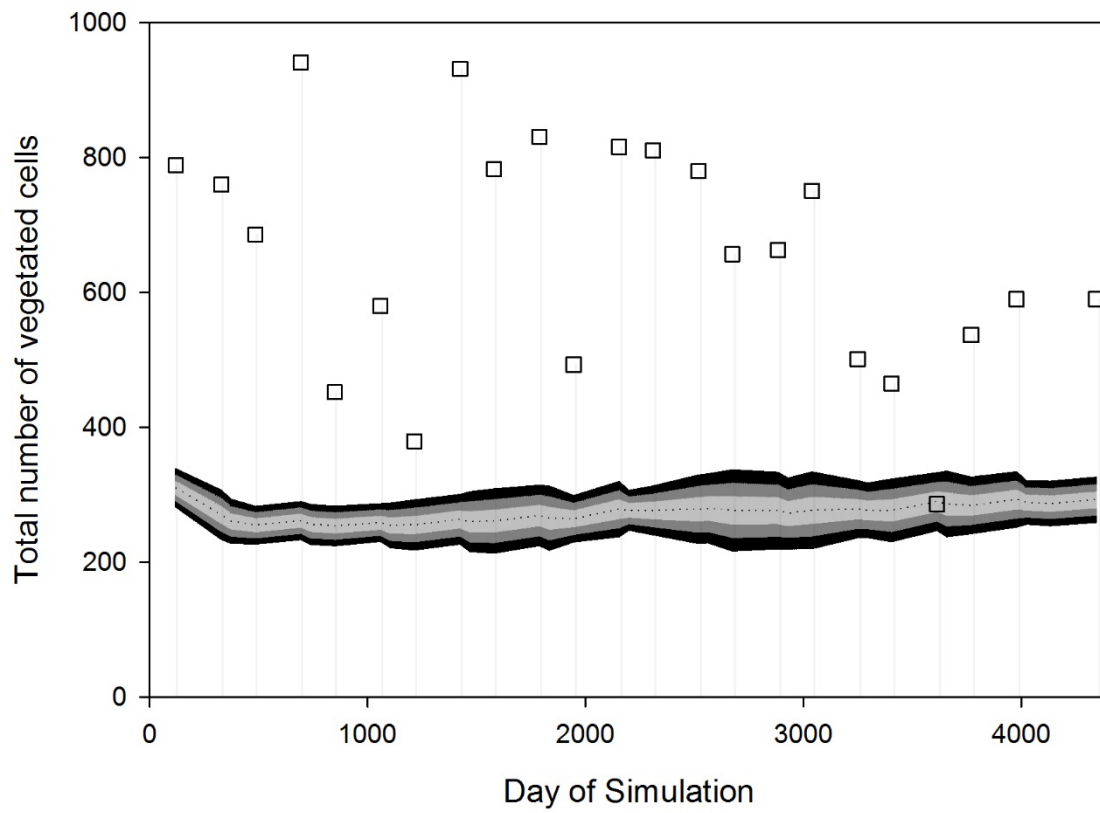
The sensitivity of model results to changes in the frequency of state conversion depended on the reach. The total amount of vegetation in Old Channel decreased by 90% when state conversion could occur every three days, and by 70% at 30 days. Conversely, City Park did not experience significant losses in total vegetation, with a 2% to 4% decrease when state conversion could occur every three days, and 1% to 6% increase at 30 days. Likewise, total vegetation in Upper Spring Run was not sensitive to changes in the state conversion parameter, with a less than 2% shift from baseline for all parameterizations). Figure 8). However, total reach biomass decreased significantly for all reaches for all three different parameterizations of state conversion (approximately 70% loss of total biomass in each reach) (Figure 8). This indicates that vegetation occupying cells is significantly smaller compared to baseline values.

**Figure 7.** Comparison of total number of vegetated cells (m<sup>2</sup>) from baseline simulations to field mapped data points collected from 2003 – 2013 for each of the five simulated reaches. Baseline simulations are represented as a mean (dotted line) ± one (light gray), two (dark gray), and three (black) standard deviations. Field mapped data are represented as open boxes with drop-lines added for ease of comparison.

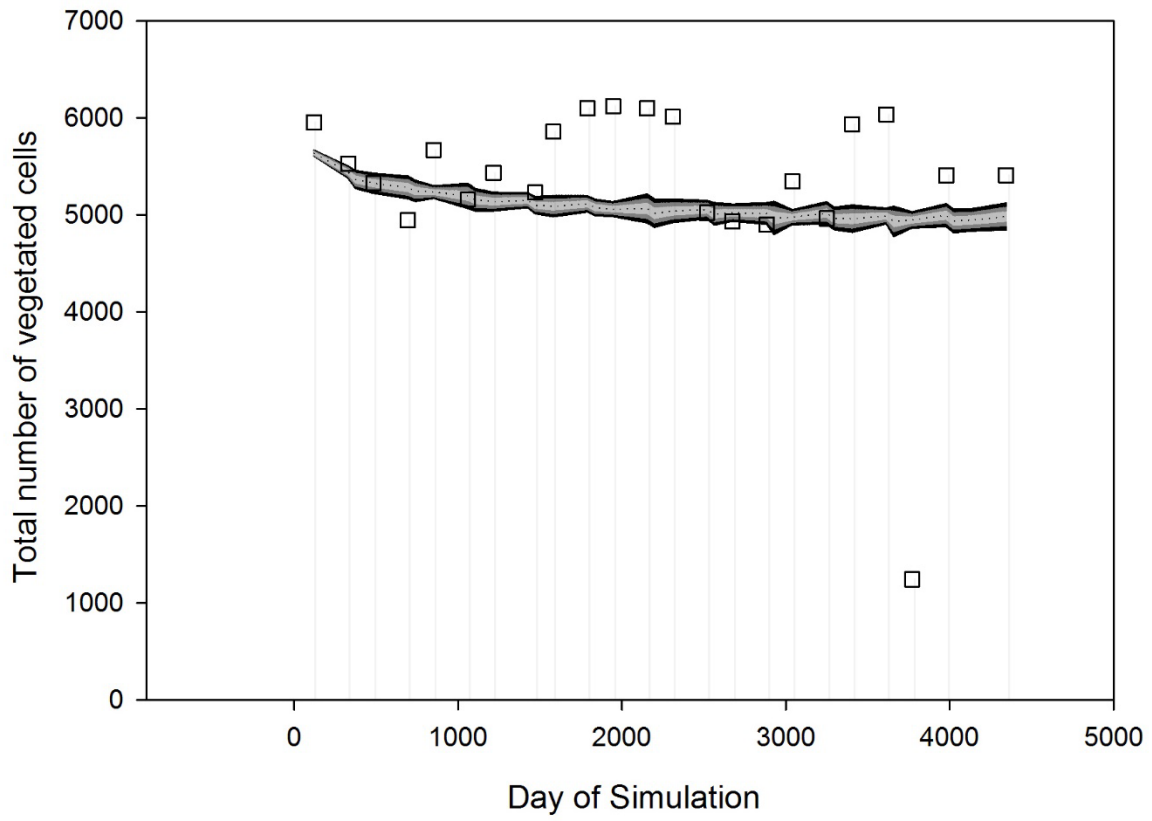
### City Park Reach



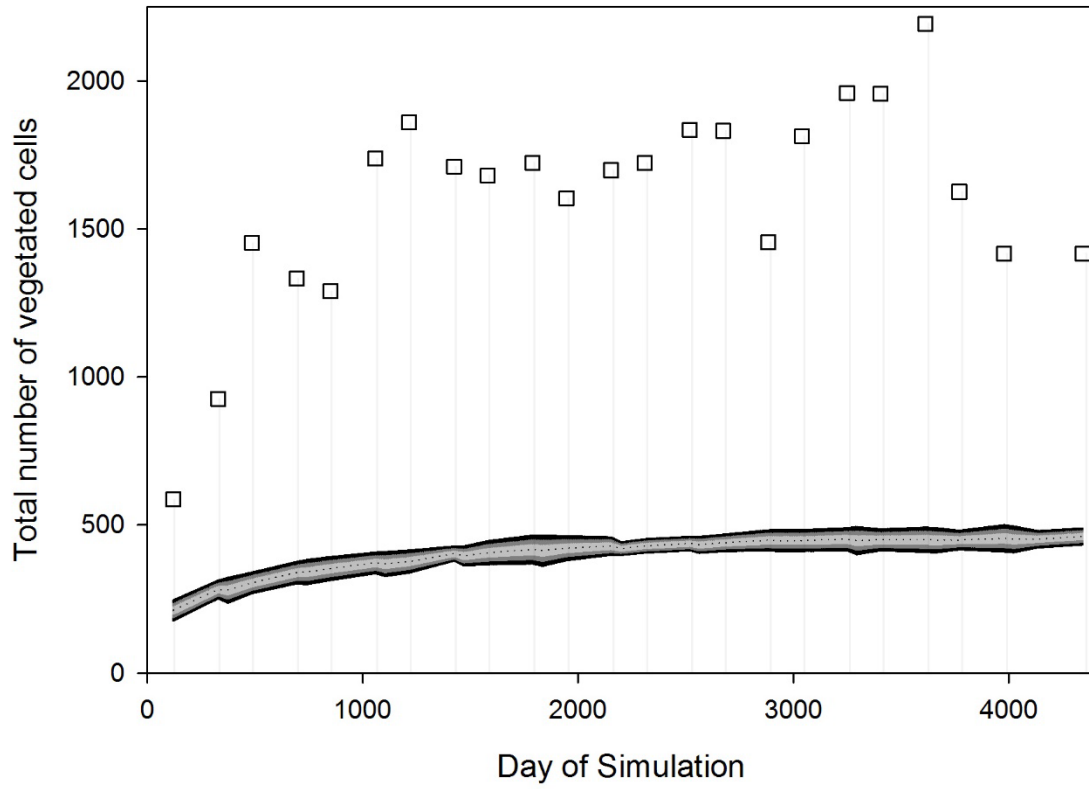
### I-35 Reach



## Landa Lake Reach



### Old Channel Reach



## Upper Spring Run Reach

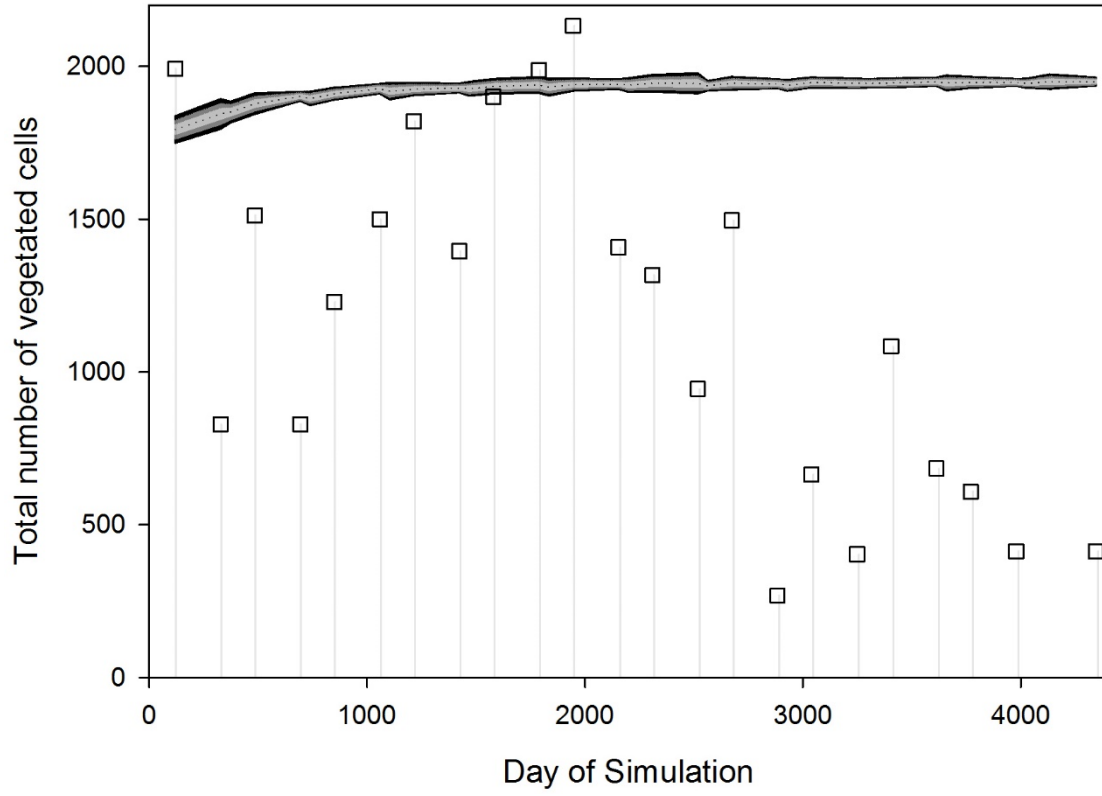
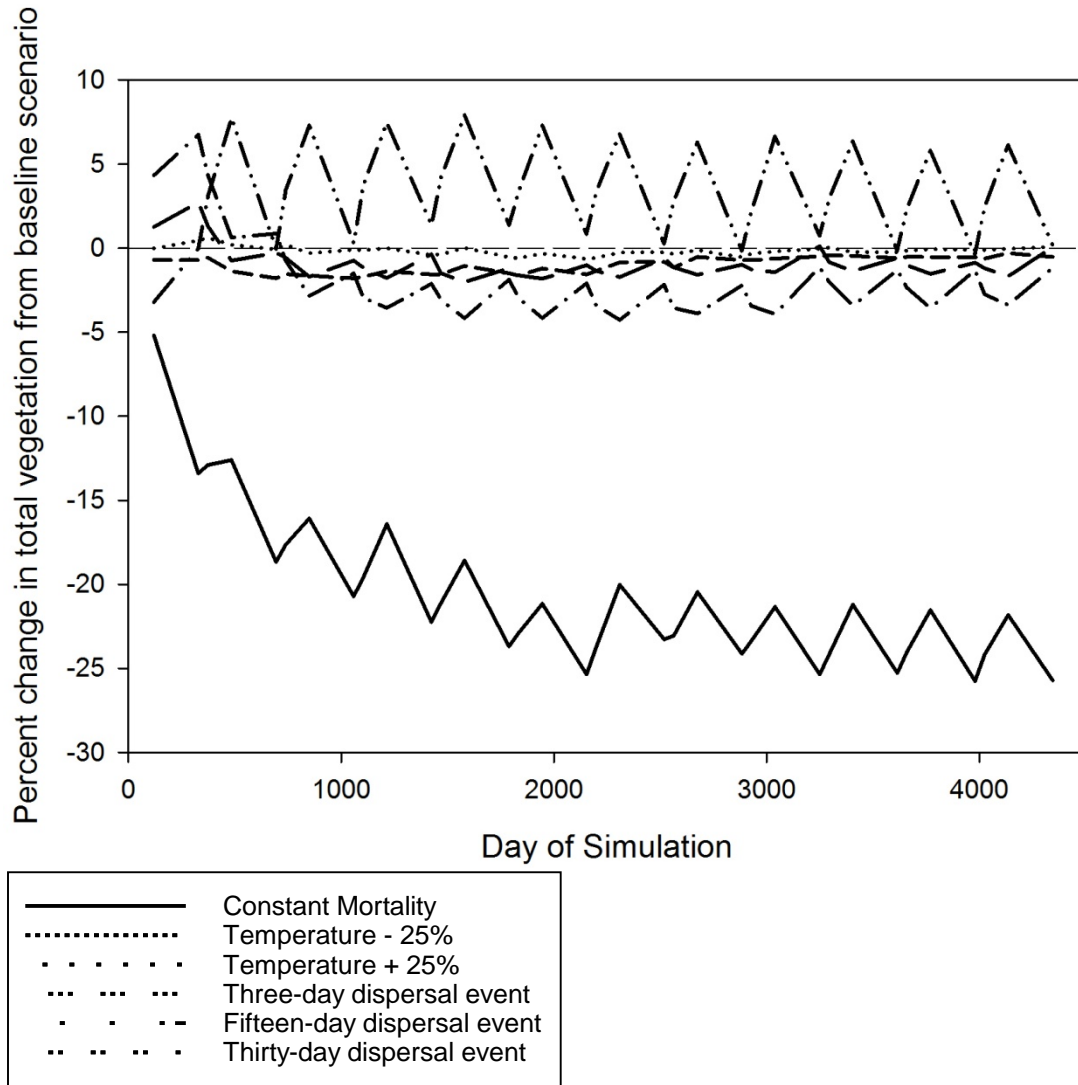
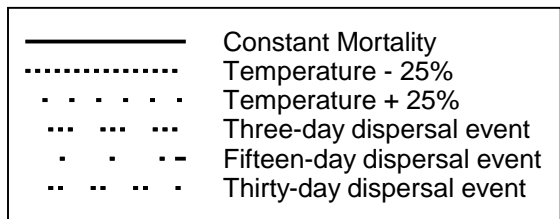
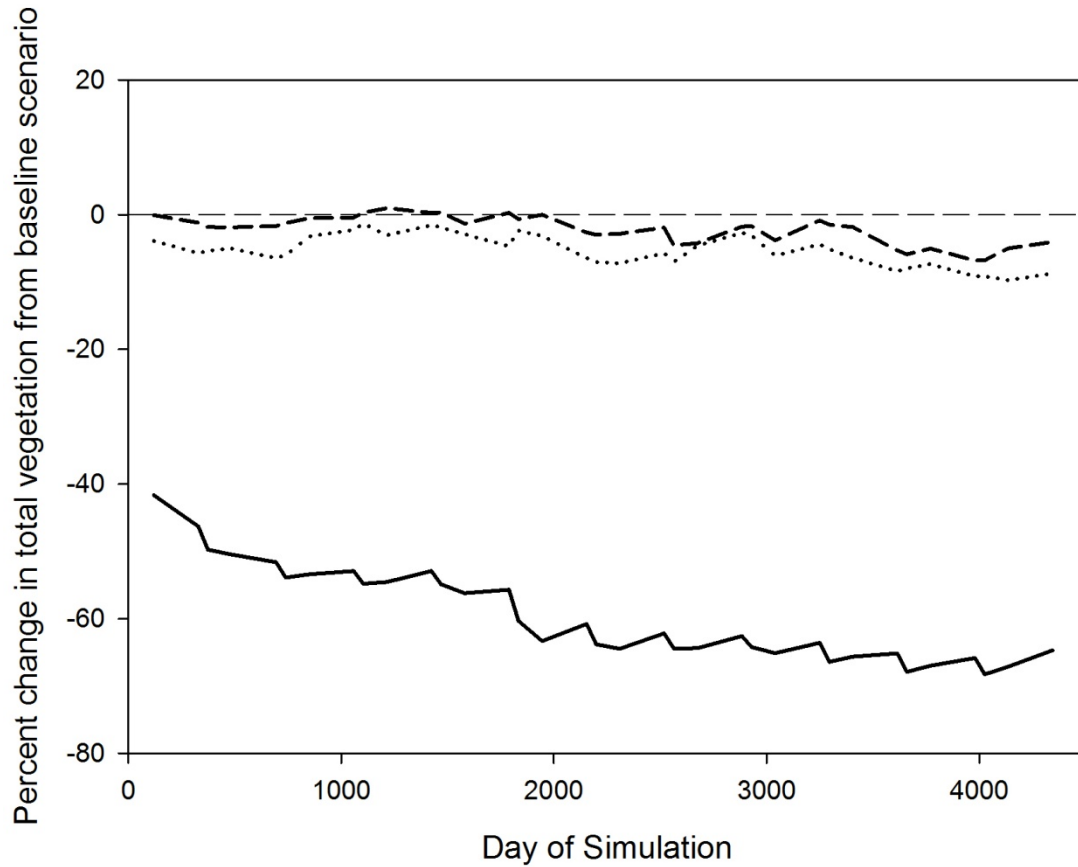


**Figure 8. Results from Sensitivity Analyses for total vegetation in each reach (note that analysis for state conversion was only applied to three reaches. Values are reported as Percent difference from baseline (represented at  $y = 0\%$ ). *MinusTemp* and *PlusTemp* represent scenarios where daily temperature was decreased or increased by 25%, respectively. *Constant Mort* represents the scenario when a constant percentage of biomass was lost each time step. *D03*, *D15*, and *D30* represent scenarios when state conversions happened once every 3, 15, or 30 days, respectively (Baseline value for conversion is 10 days).**

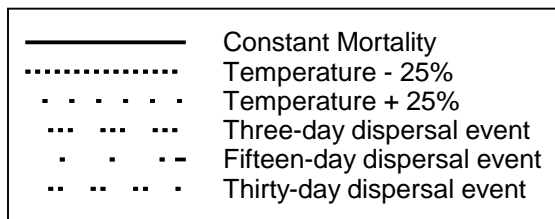
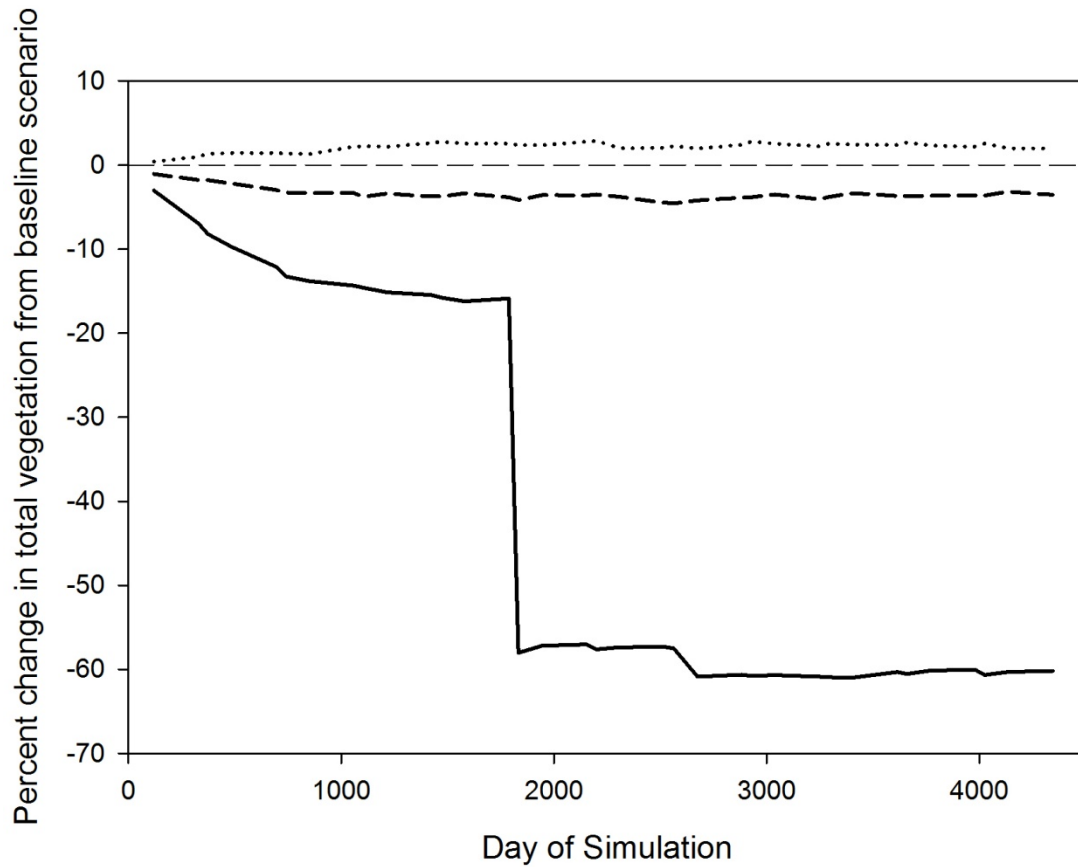
### City Park Sensitivity Analysis



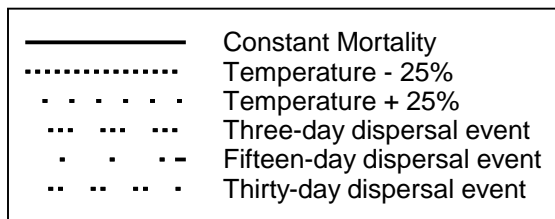
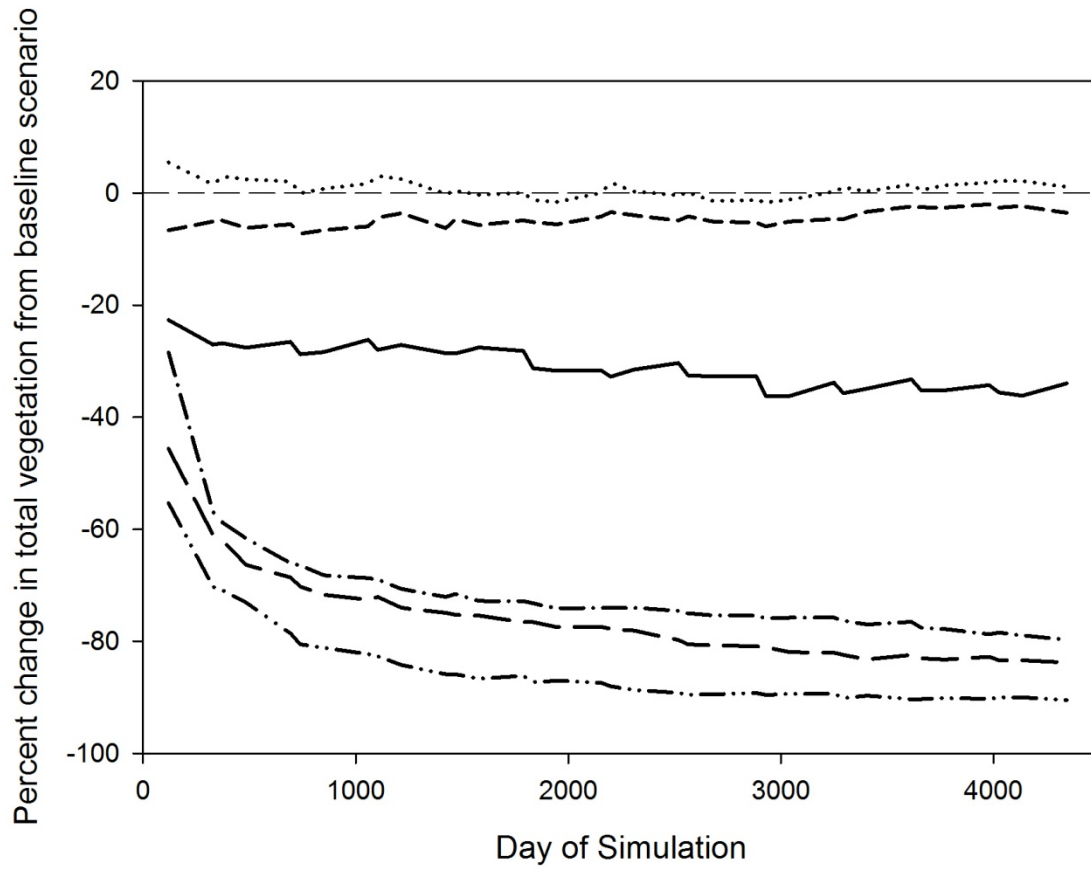
### I35 Sensitivity Analysis



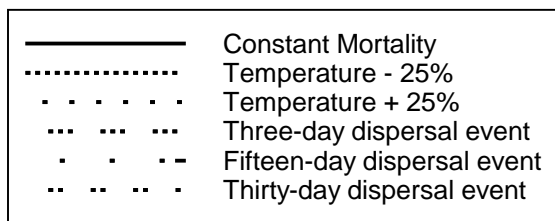
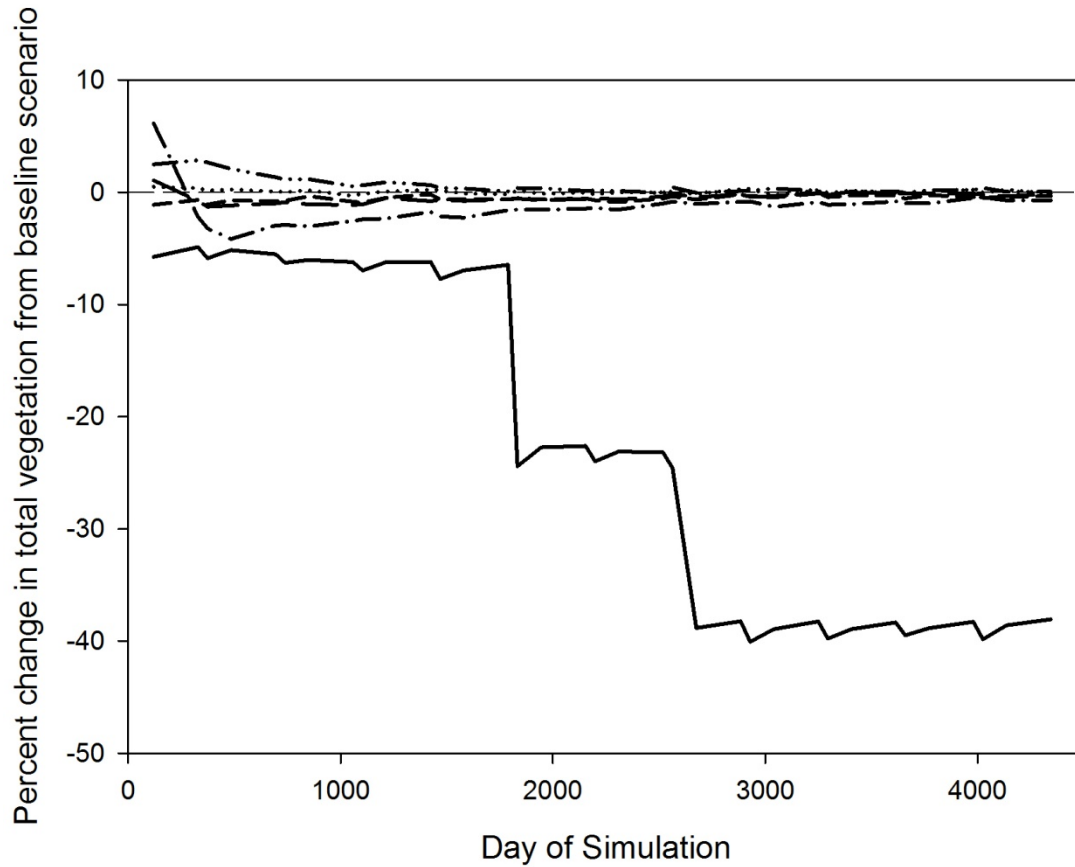
### Landa Lake Sensitivity Analysis



### Old Channel Sensitivity Analysis



### Upper Spring Run Sensitivity Analysis



**References**

- Best, E. P. H., and Boyd, W. A., 2001. A simulation model for growth of the submersed aquatic macrophyte American wildcelery (*Vallisneria americana Michx.*). ERDC/EL TR-01-5, U.S. Army Engineer Research and Development Center, Vicksburg, Mississippi.
- de Witt, C. T., 1965, Photosynthesis of leaf canopies. Agricultural Research Reports 663. Pudoc, Wageningen.
- Goudriaan, J., 1986. A simple and fast numerical method for the computation of daily totals of crop photosynthesis. Agricultural and Forest Meteorology 38, 249–254.
- Goudriaan, J., and van Laar, H. H., 1994. Modelling Potential Crop Growth Processes: Textbook with Exercises. Kluwer Academic Publishers. Dordrecht, The Netherlands.
- Scheffer, M., Baveco, J. M., DeAngelis, D. L., Rose, K. A., and van Nes, E. H., 1995. Super-individuals a simple solution for modelling large populations on an individual basis. Ecological Modelling 80: 161–170.
- Teh, C. B. S., 2006, Introduction to Mathematical Modeling of Crop Growth: How the Equations are Derived and Assembled into a Computer Model. Brown Walker Press. Boca Raton, Florida.
- van Nes, E. H., Scheffer, M., van den Berg, M. S., and Coops, H., 2003. Charisma: a spatial explicit simulation model for submerged macrophytes. Ecological Modelling 150:103–116.

## Appendix B – Supplemental materials

**Tables B1. Mean transition probability from spring to fall and fall to spring for all species sampled and bare space across 12 years of sampling at all five reaches.**

### City Park Spring to Fall

Mean Transition Probability		Spring (current)										
		Bare	<i>Cabomba</i>	<i>Ceratopteris</i>	<i>Colocasia</i>	<i>Hydrilla</i>	<i>Hydrocotyle</i>	<i>Hygrophila</i>	<i>Potamogeton</i>	<i>Sagittaria</i>	<i>Vallisneria</i>	<i>Zizania</i>
Previous Fall	Bare	0.94	0.00	0.00	0.00	0.04	0.00	0.01	0.00	0.00	0.00	0.00
	<i>Cabomba</i>	0.27	0.00	0.00	0.00	0.59	0.00	0.14	0.00	0.00	0.00	0.00
	<i>Hydrilla</i>	0.10	0.00	0.00	0.00	0.80	0.00	0.01	0.00	0.00	0.00	0.02
	<i>Hydrocotyle</i>	0.40	0.00	0.00	0.00	0.60	0.00	0.00	0.00	0.00	0.00	0.00
	<i>Hygrophila</i>	0.07	0.00	0.00	0.00	0.10	0.00	0.76	0.01	0.02	0.00	0.04
	<i>Potamogeton</i>	0.11	0.00	0.00	0.00	0.19	0.00	0.38	0.28	0.00	0.00	0.05
	<i>Sagittaria</i>	0.10	0.00	0.00	0.00	0.03	0.00	0.55	0.02	0.28	0.00	0.01
	<i>Vallisneria</i>	0.40	0.00	0.00	0.00	0.05	0.00	0.25	0.00	0.00	0.30	0.00
	<i>Zizania</i>	0.07	0.00	0.00	0.00	0.28	0.00	0.16	0.01	0.00	0.00	0.47
Standard Dev Transition Probability		Spring (current)										
		Bare	<i>Cabomba</i>	<i>Ceratopteris</i>	<i>Colocasia</i>	<i>Hydrilla</i>	<i>Hydrocotyle</i>	<i>Hygrophila</i>	<i>Potamogeton</i>	<i>Sagittaria</i>	<i>Vallisneria</i>	<i>Zizania</i>
Previous Fall	Bare	0.00	0.00	0.00	0.00	0.00	0.00	0.00	0.00	0.00	0.00	0.00
	<i>Cabomba</i>	0.08	0.00	0.00	0.00	0.06	0.00	0.09	0.00	0.00	0.00	0.00
	<i>Hydrilla</i>	0.01	0.01	0.00	0.01	0.00	0.00	0.01	0.01	0.01	0.01	0.01
	<i>Hydrocotyle</i>	0.35	0.00	0.00	0.00	0.28	0.00	0.00	0.00	0.00	0.00	0.00
	<i>Hygrophila</i>	0.01	0.00	0.01	0.00	0.01	0.01	0.00	0.01	0.01	0.01	0.01
	<i>Potamogeton</i>	0.02	0.00	0.00	0.00	0.02	0.00	0.02	0.02	0.03	0.00	0.03
	<i>Sagittaria</i>	0.04	0.00	0.00	0.00	0.04	0.00	0.03	0.04	0.04	0.00	0.04
	<i>Vallisneria</i>	0.17	0.00	0.00	0.00	0.22	0.00	0.19	0.00	0.00	0.19	0.00
	<i>Zizania</i>	0.02	0.00	0.00	0.00	0.02	0.00	0.02	0.02	0.02	0.00	0.02

### City Park Fall to Spring

Mean Transition Probability		Fall (current)										
		Bare	<i>Cabomba</i>	<i>Ceratophyllum</i>	<i>Hydrilla</i>	<i>Hydrocotyle</i>	<i>Hygrophila</i>	<i>Meriophyllum</i>	<i>Potamogeton</i>	<i>Sagittaria</i>	<i>Vallisneria</i>	<i>Zizania</i>
Previous Spring	Bare	0.98	0.00	0.00	0.01	0.00	0.01	0.00	0.00	0.00	0.00	0.00
	<i>Cabomba</i>	0.00	0.89	0.00	0.11	0.00	0.00	0.00	0.00	0.00	0.00	0.00
	<i>Ceratopteris</i>	1.00	0.00	0.00	0.00	0.00	0.00	0.00	0.00	0.00	0.00	0.00
	<i>Colocasia</i>	0.29	0.00	0.00	0.13	0.00	0.58	0.00	0.00	0.00	0.00	0.00
	<i>Hydrilla</i>	0.32	0.00	0.00	0.60	0.00	0.04	0.00	0.01	0.00	0.00	0.02
	<i>Hydrocotyle</i>	1.00	0.00	0.00	0.00	0.00	0.00	0.00	0.00	0.00	0.00	0.00
	<i>Hygrophila</i>	0.13	0.00	0.00	0.03	0.00	0.77	0.00	0.03	0.02	0.00	0.02
	<i>Potamogeton</i>	0.19	0.01	0.02	0.08	0.00	0.27	0.00	0.41	0.01	0.00	0.01
	<i>Sagittaria</i>	0.11	0.00	0.00	0.01	0.00	0.47	0.00	0.00	0.40	0.00	0.00
	<i>Vallisneria</i>	0.63	0.00	0.00	0.04	0.00	0.18	0.00	0.00	0.00	0.14	0.00
	<i>Zizania</i>	0.19	0.00	0.00	0.14	0.00	0.16	0.00	0.03	0.00	0.00	0.49
Std Deviation Transition Probability		Fall (current)										
		Bare	<i>Cabomba</i>	<i>Ceratophyllum</i>	<i>Hydrilla</i>	<i>Hydrocotyle</i>	<i>Hygrophila</i>	<i>Meriophyllum</i>	<i>Potamogeton</i>	<i>Sagittaria</i>	<i>Vallisneria</i>	<i>Zizania</i>
Previous Spring	Bare	0.00	0.00	0.00	0.00	0.00	0.00	0.00	0.00	0.00	0.00	0.00
	<i>Cabomba</i>	0.00	0.08	0.00	0.22	0.00	0.00	0.00	0.00	0.00	0.00	0.00
	<i>Ceratopteris</i>	0.00	0.00	0.00	0.00	0.00	0.00	0.00	0.00	0.00	0.00	0.00
	<i>Colocasia</i>	0.06	0.00	0.00	0.07	0.00	0.05	0.00	0.00	0.00	0.00	0.00
	<i>Hydrilla</i>	0.01	0.01	0.01	0.00	0.01	0.01	0.01	0.01	0.01	0.01	0.01
	<i>Hydrocotyle</i>	0.00	0.00	0.00	0.00	0.00	0.00	0.00	0.00	0.00	0.00	0.00
	<i>Hygrophila</i>	0.01	0.01	0.00	0.01	0.00	0.00	0.01	0.01	0.01	0.01	0.01
	<i>Potamogeton</i>	0.02	0.03	0.03	0.03	0.03	0.02	0.00	0.02	0.03	0.00	0.03
	<i>Sagittaria</i>	0.04	0.00	0.00	0.04	0.00	0.03	0.00	0.00	0.03	0.04	0.04
	<i>Vallisneria</i>	0.09	0.00	0.00	0.14	0.00	0.13	0.00	0.00	0.00	0.13	0.00
	<i>Zizania</i>	0.02	0.02	0.00	0.02	0.00	0.02	0.00	0.02	0.02	0.00	0.01

### I35 Spring to Fall

Mean Transition Probability		Fall (current)								
		Bare	<i>Cabomba</i>	<i>Hydrilla</i>	<i>Hygrophila</i>	<i>Justicia</i>	<i>Ludwigia</i>	<i>Potamogeton</i>	<i>Sagittaria</i>	<i>Zizania</i>
	<i>Bare</i>	0.99	0.00	0.01	0.00	0.00	0.00	0.00	0.00	0.00
	<i>Cabomba</i>	0.32	0.59	0.00	0.03	0.00	0.01	0.00	0.05	0.01
	<i>Hydrilla</i>	0.58	0.02	0.25	0.06	0.03	0.01	0.00	0.01	0.04
	<i>Hygrophila</i>	0.51	0.09	0.04	0.24	0.01	0.03	0.00	0.05	0.03
	<i>Justicia</i>	0.26	0.00	0.13	0.00	0.61	0.01	0.00	0.00	0.00
	<i>Ludwigia</i>	0.26	0.12	0.03	0.16	0.00	0.39		0.03	0.01
	<i>Sagittaria</i>	0.36	0.13	0.00	0.09	0.00	0.00	0.00	0.36	0.07
	<i>Zizania</i>	0.40	0.01	0.04	0.03	0.00	0.01	0.00	0.00	0.51
Std Deviation Transition Probability		Fall (current)								
		Bare	<i>Cabomba</i>	<i>Hydrilla</i>	<i>Hygrophila</i>	<i>Justicia</i>	<i>Ludwigia</i>	<i>Potamogeton</i>	<i>Sagittaria</i>	<i>Zizania</i>
Previous Spring	<i>Bare</i>	0.00	0.00	0.00	0.00	0.00	0.00	0.00	0.00	0.00
	<i>Cabomba</i>	0.02	0.02	0.00	0.02	0.00	0.02	0.00	0.02	0.02
	<i>Colocasia</i>	0.00	0.00	0.00	0.00	0.00	0.00	0.00	0.00	0.00
	<i>Hydrilla</i>	0.01	0.02	0.02	0.02	0.02	0.02	0.02	0.02	0.02
	<i>Hydrocotyle</i>	0.00	0.00	0.00	0.00	0.00	0.00	0.00	0.00	0.00
	<i>Hygrophila</i>	0.02	0.03	0.03	0.03	0.03	0.03	0.00	0.03	0.03
	<i>Justicia</i>	0.05	0.00	0.06	0.00	0.04	0.06	0.00	0.00	0.00
	<i>Ludwigia</i>	0.10	0.11	0.12	0.11	0.00	0.09	0.00	0.12	0.12
	<i>Rorippa</i>	0.00	0.00	0.00	0.00	0.00	0.00	0.00	0.00	0.00
	<i>Sagittaria</i>	0.03	0.04	0.04	0.04	0.00	0.04	0.00	0.03	0.04
<i>Zizania</i>	0.02	0.03	0.03	0.03	0.03	0.03	0.00	0.03	0.02	

### I35 Fall to Spring

Mean Transition Probability		Spring(current)							
		Bare	Cabomba	Hydrilla	Hygrophila	Justicia	Ludwigia	Sagittaria	Zizania
Previous Fall	Bare	0.99	0.00	0.00	0.00	0.00	0.00	0.00	0.00
	<i>Cabomba</i>	0.28	0.61	0.01	0.03	0.00	0.00	0.00	0.06
	<i>Hydrilla</i>	0.59	0.00	0.23	0.02	0.01	0.00	0.00	0.00
	<i>Hygrophila</i>	0.47	0.03	0.09	0.30	0.00	0.00	0.01	0.06
	<i>Justicia</i>	0.31	0.00	0.03	0.03	0.59	0.00	0.00	0.00
	<i>Ludwigia</i>	0.33	0.14	0.07	0.19	0.00	0.19	0.00	0.02
	<i>Sagittaria</i>	0.32	0.12	0.02	0.06	0.00	0.00	0.01	0.46
	<i>Zizania</i>	0.40	0.00	0.05	0.02	0.00	0.00	0.00	0.00
Std Deviation Transition Probability		Spring(current)							
		Bare	Cabomba	Hydrilla	Hygrophila	Justicia	Ludwigia	Sagittaria	Zizania
Previous Fall	Algae	0.15	0.00	0.00	0.19	0.00	0.00	0.00	0.00
	Bare	0.00	0.00	0.00	0.00	0.00	0.00	0.00	0.00
	<i>Cabomba</i>	0.02	0.01	0.02	0.02	0.00	0.02	0.02	0.02
	<i>Hydrilla</i>	0.01	0.02	0.02	0.02	0.02	0.02	0.02	0.02
	<i>Hydrocotyle</i>	0.00	0.00	0.00	0.00	0.00	0.00	0.00	0.00
	<i>Hygrophila</i>	0.02	0.03	0.03	0.02	0.03	0.03	0.03	0.03
	<i>Justicia</i>	0.04	0.00	0.05	0.05	0.03	0.00	0.00	0.00
	<i>Ludwigia</i>	0.07	0.08	0.08	0.08	0.00	0.08	0.08	0.09
	<i>Sagittaria</i>	0.04	0.04	0.05	0.04	0.00	0.05	0.05	0.03
	<i>Zizania</i>	0.02	0.03	0.03	0.03	0.00	0.00	0.00	0.03

### Landa Lake Spring to Fall

Mean Transition Probability		Fall (current)							
		Bare	<i>Cabomba</i>	<i>Hygrophila</i>	<i>Ludwigia</i>	<i>Nuphar</i>	<i>Riccia</i>	<i>Sagittaria</i>	<i>Vallisneria</i>
Previous Spring	Bare	0.91	0.00	0.00	0.00	0.00	0.01	0.01	0.06
	<i>Cabomba</i>	0.10	0.78	0.00	0.00	0.01	0.03	0.04	0.05
	<i>Hygrophila</i>	0.28	0.00	0.63	0.03	0.00	0.03	0.02	0.01
	<i>Ludwigia</i>	0.53	0.00	0.01	0.32	0.00	0.06	0.00	0.08
	<i>Nuphar</i>	0.11	0.01	0.00	0.00	0.80	0.02	0.01	0.04
	<i>Riccia</i>	0.45	0.01	0.00	0.00	0.00	0.44	0.02	0.04
	<i>Sagittaria</i>	0.10	0.00	0.00	0.00	0.00	0.14	0.70	0.05
	<i>Vallisneria</i>	0.03	0.00	0.00	0.00	0.00	0.01	0.00	0.96
Std Deviation Transition Probability		Fall (current)							
		Bare	<i>Cabomba</i>	<i>Hygrophila</i>	<i>Ludwigia</i>	<i>Nuphar</i>	<i>Riccia</i>	<i>Sagittaria</i>	<i>Vallisneria</i>
Previous Spring	Bare	0.00	0.00	0.00	0.00	0.00	0.00	0.00	0.00
	<i>Cabomba</i>	0.03	0.02	0.00	0.00	0.04	0.04	0.04	0.03
	<i>Hygrophila</i>	0.02	0.00	0.01	0.02	0.00	0.02	0.02	0.02
	<i>Ludwigia</i>	0.05	0.00	0.07	0.05	0.00	0.06	0.00	0.06
	<i>Nuphar</i>	0.02	0.03	0.00	0.00	0.01	0.02	0.03	0.02
	<i>Riccia</i>	0.01	0.01	0.01	0.01	0.01	0.01	0.01	0.01
	<i>Sagittaria</i>	0.01	0.01	0.01	0.01	0.01	0.01	0.01	0.01
	<i>Vallisneria</i>	0.00	0.00	0.00	0.00	0.00	0.00	0.00	0.00

### Landa Lake Fall to Spring

Mean Transition Probability		Spring (current)						
		Bare	<i>Cabomba</i>	<i>Hygrophila</i>	<i>Ludwigia</i>	<i>Nuphar</i>	<i>Sagittaria</i>	<i>Vallisneria</i>
Previous Fall	Bare	0.91	0.00	0.01	0.00	0.00	0.01	0.01
	<i>Cabomba</i>	0.19	0.52	0.00	0.00	0.02	0.05	0.07
	<i>Hygrophila</i>	0.06	0.00	0.90	0.00	0.00	0.01	0.01
	<i>Ludwigia</i>	0.34	0.00	0.01	0.46	0.00	0.00	0.09
	<i>Nuphar</i>	0.06	0.01	0.00	0.00	0.91	0.01	0.01
	<i>Riccia</i>	0.33	0.00	0.01	0.00	0.00	0.10	0.04
	<i>Sagittaria</i>	0.08	0.00	0.00	0.00	0.00	0.85	0.04
	<i>Vallisneria</i>	0.12	0.00	0.00	0.00	0.00	0.00	0.87
Std Deviation Transition Probability		Spring (current)						
		Bare	<i>Cabomba</i>	<i>Hygrophila</i>	<i>Ludwigia</i>	<i>Nuphar</i>	<i>Sagittaria</i>	<i>Vallisneria</i>
Previous Fall	Bare	0.00	0.00	0.00	0.00	0.00	0.00	0.00
	<i>Cabomba</i>	0.03	0.02	0.03	0.00	0.03	0.03	0.03
	<i>Hygrophila</i>	0.02	0.00	0.01	0.00	0.00	0.03	0.03
	<i>Ludwigia</i>	0.07	0.00	0.09	0.06	0.00	0.00	0.08
	<i>Nuphar</i>	0.03	0.03	0.00	0.00	0.01	0.03	0.03
	<i>Riccia</i>	0.01	0.01	0.01	0.01	0.01	0.01	0.01
	<i>Sagittaria</i>	0.02	0.02	0.02	0.02	0.02	0.01	0.02
	<i>Vallisneria</i>	0.00	0.00	0.00	0.00	0.00	0.00	0.00

## Old Channel Spring to Fall

Mean Transition Probability		Current Fall				
		Bare	<i>Ceratopteris</i>	<i>Hygrophila</i>	<i>Ludwigia</i>	<i>Nuphar</i>
Previous Spring	Bare	0.90	0.05	0.04	0.01	0.00
	<i>Ceratopteris</i>	0.25	0.61	0.08	0.00	0.00
	<i>Hygrophila</i>	0.18	0.01	0.77	0.01	0.01
	<i>Ludwigia</i>	0.35	0.00	0.26	0.39	0.00
	<i>Nuphar</i>	0.16	0.26	0.09	0.00	0.45
Std Deviation Transition Probability		Current Fall				
		Bare	<i>Ceratopteris</i>	<i>Hygrophila</i>	<i>Ludwigia</i>	<i>Nuphar</i>
Previous Spring	Bare	0.01	0.00	0.00	0.00	0.00
	<i>Ceratopteris</i>	0.02	0.01	0.02	0.00	0.02
	<i>Hygrophila</i>	0.00	0.01	0.00	0.01	0.01
	<i>Ludwigia</i>	0.03	0.00	0.03	0.03	0.00
	<i>Nuphar</i>	0.03	0.03	0.03	0.00	0.20

## Old Channel Fall to Spring

Mean Transition Probability		Current Spring				
		Bare	<i>Ceratopteris</i>	<i>Hygrophila</i>	<i>Ludwigia</i>	<i>Nuphar</i>
Previous Fall	Bare	0.95	0.01	0.04	0.01	0.00
	<i>Ceratopteris</i>	0.60	0.26	0.05	0.01	0.09
	<i>Hygrophila</i>	0.12	0.00	0.85	0.01	0.00
	<i>Ludwigia</i>	0.27	0.00	0.28	0.44	0.00
	<i>Nuphar</i>	0.61	0.00	0.24	0.05	0.91
Std Deviation Transition Probability		Current Spring				
		Bare	<i>Ceratopteris</i>	<i>Hygrophila</i>	<i>Ludwigia</i>	<i>Nuphar</i>
Previous Fall	Bare	0.01	0.00	0.03	0.00	0.04
	<i>Ceratopteris</i>	0.00	0.01	0.00	0.01	0.03
	<i>Hygrophila</i>	0.00	0.01	0.01	0.00	0.00
	<i>Ludwigia</i>	0.03	0.00	0.03	0.02	0.04
	<i>Nuphar</i>	0.00	0.04	0.04	0.00	0.05

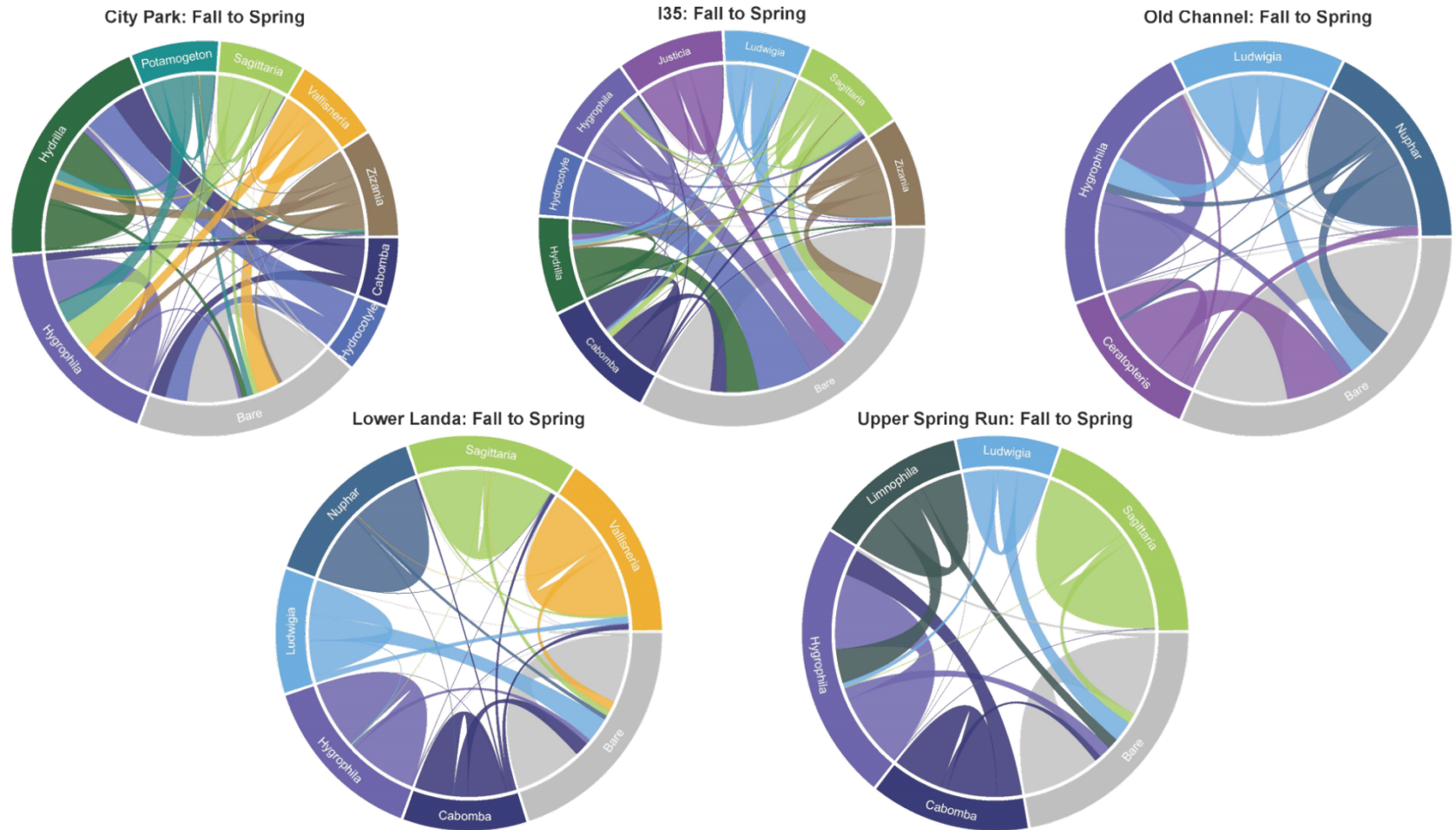
### Upper Spring Run Spring to Fall

Mean Transition Probability		Fall (current)						
		Bare	<i>Cabomba</i>	<i>Hygrophila</i>	<i>Limnophila</i>	<i>Ludwigia</i>	<i>Riccia</i>	<i>Sagittaria</i>
Previous Spring	Bare	0.91	0.00	0.02	0.00	0.00	0.05	0.02
	<i>Cabomba</i>	0.27	0.57	0.03	0.03	0.00	0.10	0.00
	<i>Hydrocotyle</i>	0.00	0.00	1.00	0.00	0.00	0.00	0.00
	<i>Hygrophila</i>	0.37	0.00	0.51	0.00	0.00	0.09	0.02
	<i>Limnophila</i>	0.39	0.00	0.11	0.50	0.00	0.00	0.00
	<i>Ludwigia</i>	0.43	0.00	0.04	0.00	0.29	0.24	0.00
	<i>Nuphar</i>	1.00	0.00	0.00	0.00	0.00	0.00	0.00
	<i>Sagittaria</i>	0.12	0.00	0.00	0.00	0.00	0.02	0.85
	Unknown Veg	0.50	0.00	0.00	0.00	0.00	0.00	0.50
Std Deviation Transition Probability		Fall (current)						
		Bare	<i>Cabomba</i>	<i>Hygrophila</i>	<i>Limnophila</i>	<i>Ludwigia</i>	<i>Riccia</i>	<i>Sagittaria</i>
Previous Spring	Bare	0.00	0.01	0.01	0.01	0.01	0.01	0.01
	<i>Cabomba</i>	0.16	0.12	0.18	0.18	0.00	0.17	0.00
	<i>Hydrocotyle</i>	0.00	0.00	0.00	0.00	0.00	0.00	0.00
	<i>Hygrophila</i>	0.02	0.02	0.01	0.00	0.00	0.02	0.02
	<i>Limnophila</i>	0.15	0.00	0.18	0.13	0.00	0.00	0.00
	<i>Ludwigia</i>	0.08	0.00	0.11	0.00	0.09	0.10	0.00
	<i>Nuphar</i>	0.00	0.00	0.00	0.00	0.00	0.00	0.00
	<i>Sagittaria</i>	0.02	0.02	0.02	0.00	0.00	0.02	0.01
	Unknown Veg	0.29	0.00	0.00	0.00	0.00	0.00	0.29

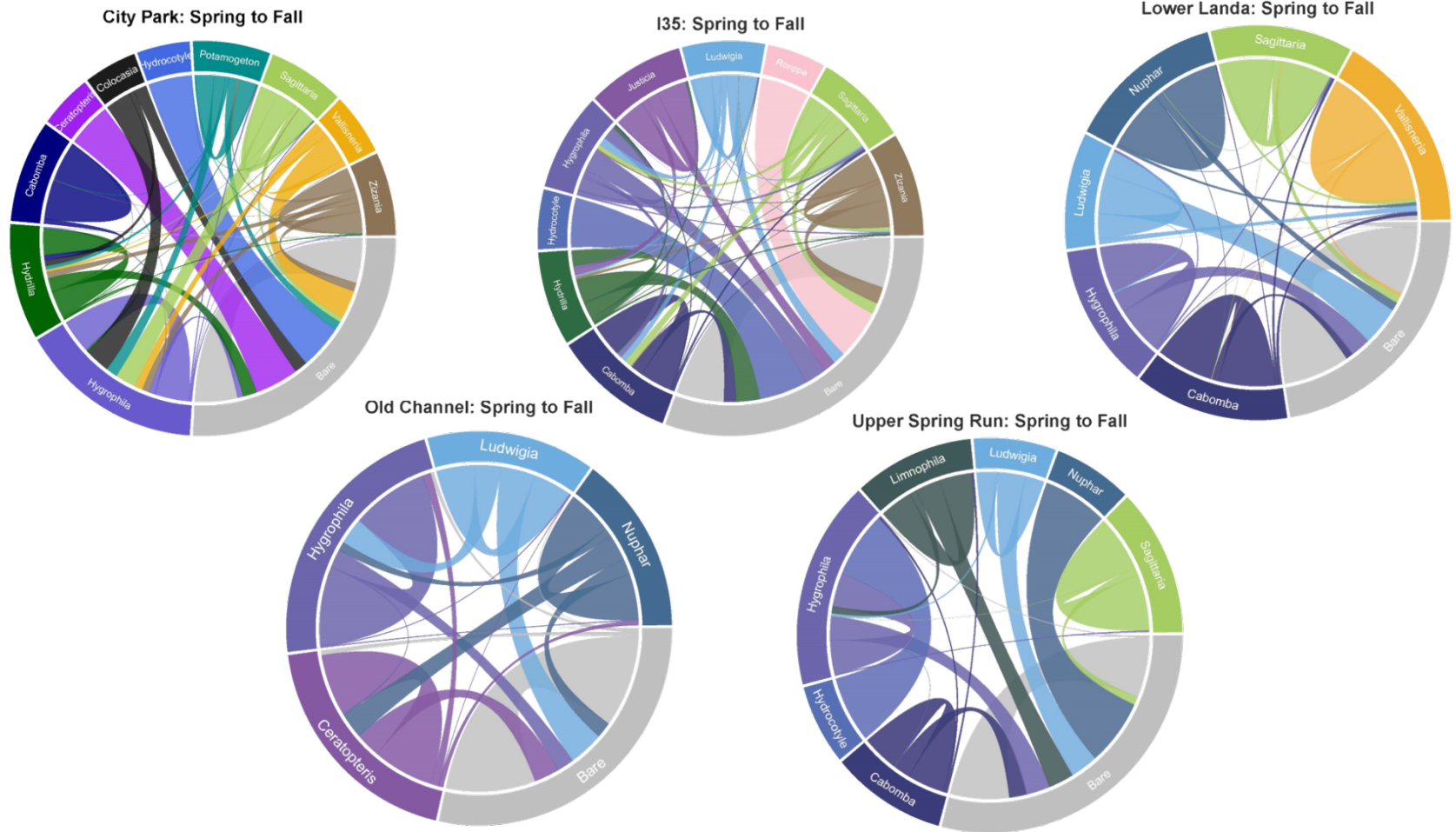
## Upper Spring Run Fall to Spring

Mean Transition Probability		Spring (current)							
		Bare	<i>Cabomba</i>	<i>Hydrocotyle</i>	<i>Hygrophila</i>	<i>Limnophila</i>	<i>Ludwigia</i>	<i>Riccia</i>	<i>Sagittaria</i>
Previous Fall	Bare	0.75	0.00	0.00	0.02	0.00	0.00	0.19	0.01
	<i>Cabomba</i>	0.06	0.48	0.00	0.24	0.00	0.00	0.21	0.00
	<i>Hygrophila</i>	0.11	0.00	0.00	0.72	0.00	0.00	0.16	0.01
	<i>Limnophila</i>	0.11	0.00	0.00	0.32	0.39	0.00	0.18	0.00
	<i>Ludwigia</i>	0.20	0.00	0.00	0.05	0.00	0.29	0.47	0.00
	<i>Sagittaria</i>	0.09	0.00	0.00	0.00	0.00	0.00	0.04	0.86
Std Deviation Transition Probability		Spring (current)							
		Bare	<i>Cabomba</i>	<i>Hydrocotyle</i>	<i>Hygrophila</i>	<i>Limnophila</i>	<i>Ludwigia</i>	<i>Riccia</i>	<i>Sagittaria</i>
Previous Fall	Bare	0.00	0.01	0.01	0.01	0.01	0.01	0.01	0.01
	<i>Cabomba</i>	0.17	0.12	0.00	0.15	0.00	0.00	0.15	0.00
	<i>Hygrophila</i>	0.02	0.02	0.00	0.01	0.02	0.02	0.02	0.02
	<i>Limnophila</i>	0.18	0.00	0.00	0.16	0.15	0.00	0.17	0.00
	<i>Ludwigia</i>	0.11	0.00	0.00	0.12	0.00	0.10	0.09	0.00
	<i>Sagittaria</i>	0.02	0.00	0.00	0.02	0.00	0.00	0.02	0.01

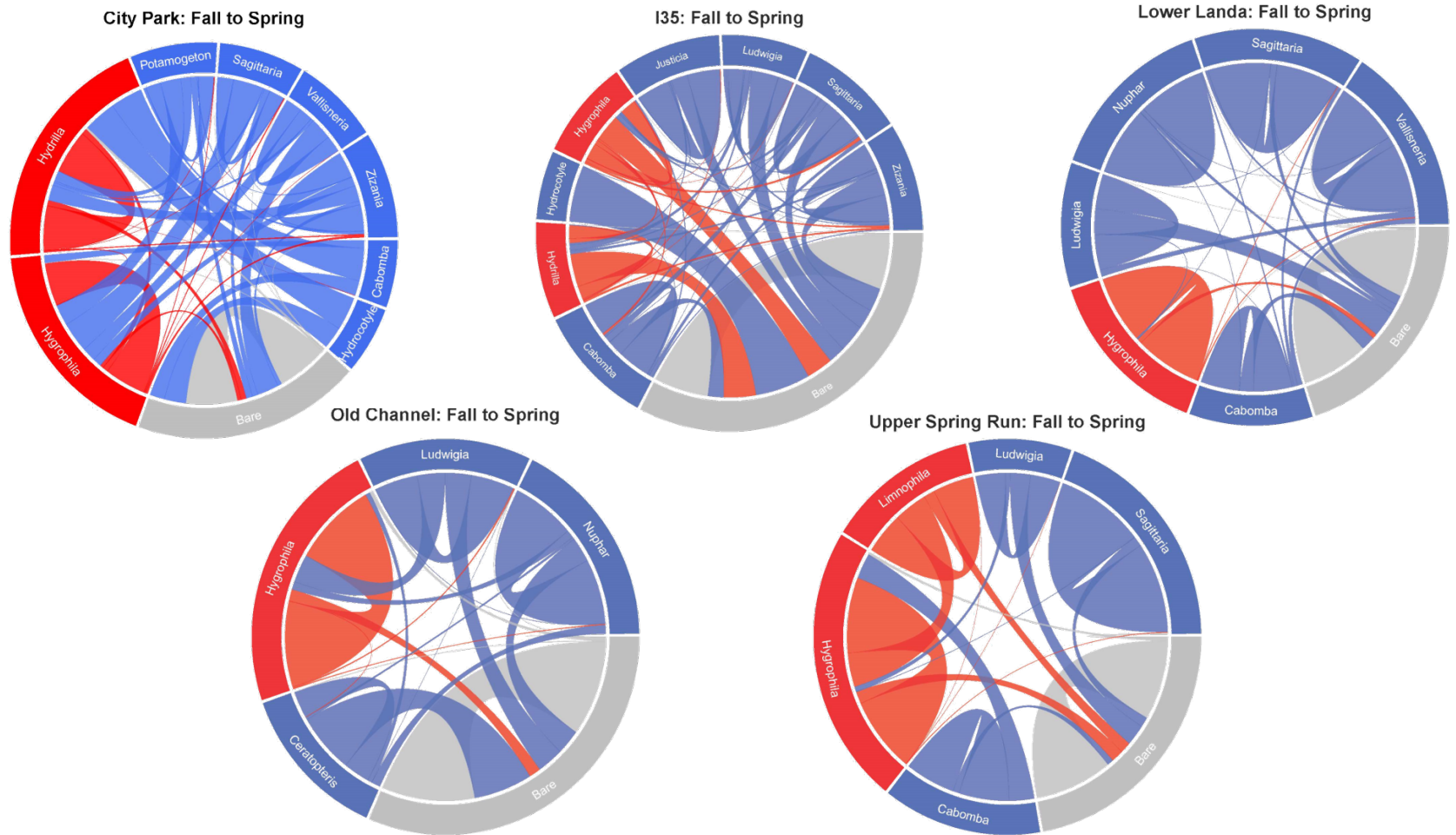
Chord chart diagrams depicting seasonal vegetation transitions from one species to another for each of five reaches. Multi-colored charts reflect species-to-species transitions, and red/blue charts reflect invasive (red) to native (blue) transitions. Bare substrate is gray in both sets of figures.



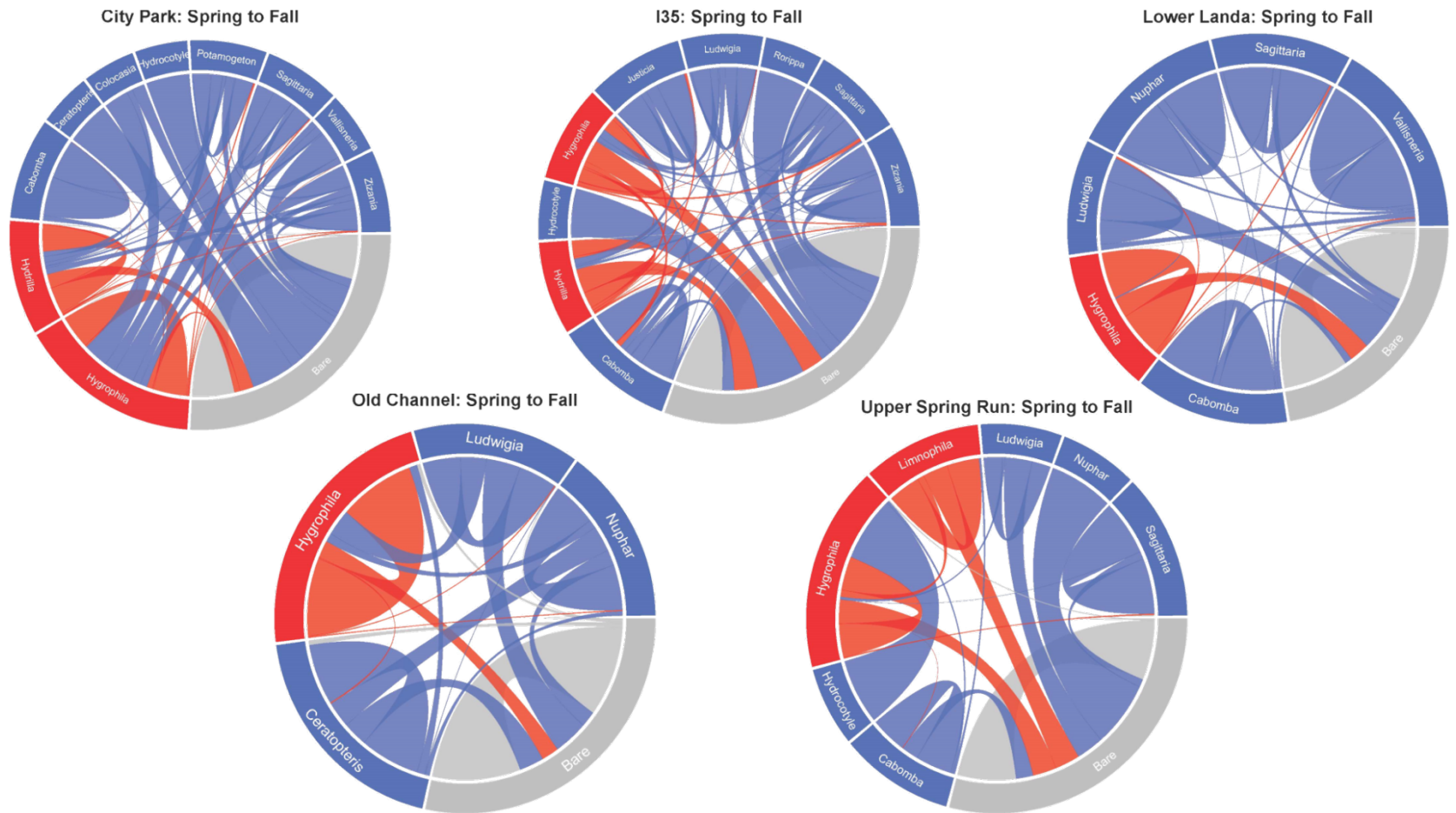
Appendix B



Appendix B



Appendix B



## APPENDIX C: Fountain Darter Submodel – Technical Supplement

(Table and Figures presented at conclusion of text)

### 1. Model description

#### 1.1 Overview

We developed a spatially-explicit, individual-based, model to investigate fountain darter population dynamics in response to changes in aquatic vegetation and hydrological conditions (Fig. 1). Input data for each reach included time series of water depth, velocity, temperature, and dissolved oxygen (DO) concentration, as well as the spatial distribution of aquatic vegetation types, from 2003 through 2013 for the particular reach of the river being simulated (the Old Channel, Upper Spring Run, or Landa Lake reach of the Comal River, or the City Park or I35 reach of the San Marcos River). The model simulates fountain darter the reproduction, development through egg, larval, juvenile, and adult life stages, mortality, and movement among the various types of aquatic vegetation. In the sections that follow, we present details of the model following the protocol suggested by Grimm et al. (2006, 2010) for describing individual-based models.

#### 1.2 Purpose

The purpose of the model is to simulate the population dynamics of fountain darters in response to changes in habitat conditions that might result directly or indirectly from changes in water flow within the Comal River and the San Marcos River. The ability to simulate fountain darter population responses to spatial-temporal changes in the distribution and species composition of aquatic vegetation, as well as water temperature, DO concentration, depth, and velocity, as they pass through egg, larval, juvenile, and adult life stages is of particular interest.

#### 1.3 Entities, state variables and scales

Entities include (1) a reach-specific number (tens of thousands) of  $1\text{m}^2$  habitat patches arrayed in a rectangular grid representing the area of, and immediately adjacent to the given reach, derived from the MD-SWMS (USGS 2013) 2-dimensional hydrodynamic model calibrated for the reach (Hardy et al., 2010)), and (2) a variable number (up to several tens of thousands) of individual fountain darters. State variables, or attributes, of habitat patches include location (latitude, longitude), vegetation type, water temperature (C), DO concentration (mg/L), depth (m), and

velocity ( $\text{m}^3 \text{sec}^{-1}$ ). Attributes of fountain darters include sex, age (days), life stage (egg, larva, juvenile, young adult, old adult), location (habitat patch currently occupied), and, for adult females, reproductive state (whether or not they are reproductively active, and whether or not they have laid eggs within the last month). Attributes of habitat patches that can change over time include vegetation type, water temperature, DO concentration (mg/L), depth, and velocity. Attributes of fountain darters that can change over time include age, life stage, and location.

#### *1.4 Process overview and scheduling*

We programmed the model and executed simulations in NetLogo (Wilensky, 1999), exported simulation results to Excel© (Microsoft, 2003) for archiving and temporal graphics. During each simulation, the system is initialized by assigning each habitat cell a vegetation type, as well as a water temperature, DO concentration, depth, and velocity, and by assigning each individual fountain darter a sex, age, life stage, and location (Fig. 2). Simulations are driven by daily time series of values representing estimated historical water discharge (cfs), and water temperatures and DO concentrations from the 1 January 2003 to 31 December 2013. Historical daily water discharges for the given reach are used to estimate the associated water depths and water velocities for each habitat cell within the reach for that day. Next, iteratively during the simulation, (1) values representing estimated daily water discharge, and water temperature and DO concentration are adjusted according to their respective input time series, (2) water depth and water velocity in each habitat cell are adjusted based on the estimated daily water discharge, and (3) effects of these changes on the mortality, movement, and egg-laying (recruitment of new individuals) of fountain darters are calculated. Estimated historical vegetation changes occur seasonally (spring, summer, and fall of 2003 and 2004; spring and fall of 2005 to 2013).

Fountain darters may make up to 24 movements each day, but aging, development (from egg to larva to juvenile to adult), mortality, and egg laying are calculated on a daily basis. During the simulation of each fountain darter activity (move, age, develop, die, lay eggs), individuals are selected in random order, that is, the first randomly selected individual is given the opportunity to perform the given activity, then the second randomly selected individual, then the third, and so on. The aggregated variables that describe the state of the system include the number of habitat patches with each type of aquatic vegetation, the number of fountain darters in each type of aquatic vegetation, and the numbers and proportions of eggs, larvae, juveniles, young adults, old

adults, males, and females in the fountain darter population. All of these aggregated variables are updated daily.

### *1.5 Design concepts*

*Basic principles:* Motivation for development of such a model came from the perceived need to refine the representation, both functionally and spatially, of the response of fountain darters to changes in spring flow and/or changes in the amount of habitat provided by aquatic vegetation potentially resulting from future water demands of an increasing human population (Mora et al., 2013). Although hydrological models of the Edwards Aquifer (Schulman et al., 1995; Lindgren et al., 2004; EAA, 2006a and b) are available, as is a framework for assessing levels of spring flow needed to maintain fountain darter habitat (INSE, 2004, Hardy et al., 2012), to our knowledge the only population dynamics model for the fountain darter was developed quite recently by Mora et al. (2013). Their model is a compartment model based on difference equations representing the effect of spring flow and water temperature on fountain darter recruitment and survival, which they used to project fountain darter population sizes under various scenarios of reduced spring flows. In the present study, we describe development of a spatially-explicit, individual-based, population dynamics model for the fountain darter emphasizing more mechanistic connections among spring flow, the distribution of aquatic vegetation, and fountain darter recruitment, survival, and development.

*Emergence:* Spatial and temporal patterns of abundance of fountain darters in the various life stages (egg, larvae, juvenile, young adult, old adult) emerge as system-level properties as a result of empirically-based spatial and temporal patterns of habitat characteristics (vegetation type, water temperature, water depth, water velocity), empirically-based rates of fountain darter egg-laying, development, and survival, and hypothesized rules governing fountain darter movement.

*Adaptation:* Individual hosts do not possess adaptive traits, the rules for their behavior (movement) are fixed.

*Objectives:* Individual hosts do not adapt their behavior to achieve specific objectives.

*Learning:* Individual hosts do not learn, that is, they do not change their behavior as a result of past experience.

*Prediction:* Individual hosts do not predict the future, that is, they do not estimate future conditions nor judge the consequences of their behavior.

*Sensing:* Fountain darters are “aware” of their age and life stage, the characteristics of the habitat cell in which they currently are located, and the number of consecutive time steps that they have been in habitat cells without aquatic vegetation.

*Interaction:* Habitat cells and fountain darters interact implicitly in that movement, survival, and egg-laying of fountain darters is affected by the characteristics of the habitat cell in which they currently are located.

*Stochasticity:* During initialization of the model, age and life stage of fountain darters are assigned randomly based on empirical probabilities that result in age- and stage-class distributions approximating those observed in the field. During simulations, movement, survival, and egg-laying of fountain darters are determined probabilistically.

*Collectives:* The model does not contain collectives.

*Observation:* Output from the model includes time series of daily values of water discharge, the numbers and proportions of habitat patches containing each type of aquatic vegetation, the vegetation-based, estimated carrying capacity of the reach for fountain darters (juveniles and adults only), and the numbers and proportions of eggs, larvae, juveniles, and adults in the fountain darter population.

## 1.6 Initialization

The system is initialized by assigning each habitat cell an aquatic vegetation type, and a water temperature, DO concentration, depth, and velocity such that the resulting simulated habitat patterns resemble those observed during the spring of 2003 in the particular reach of the Comal River or the San Marcos River being simulated, and by assigning each individual fountain darter an age and life stage such that the resulting age- and stage-class distributions and sex ratio of the simulated population approximate those observed in the field during 2003 (Bio-West 2004a in interim final report), and such that all simulated darters are located in habitat cells with aquatic vegetation (Fig. 2). The initial number of juvenile plus adult darters is calculated based on the estimated maximum darter density that can be supported by the aquatic vegetation within the reach. The maximum darter density associated with each type of aquatic vegetation is based on analyses of drop-net data collected from 2003 to 2010 in the particular reach of the Comal River or the San Marcos River being simulated (BIO-WEST, 2004a – 2014a, BIO-WEST, 2004b – 2014b in interim final report). The maximum darter density of each habitat cell ( $MD_i$ ; the

number of juveniles plus adults that can be supported by the vegetation type in habitat cell *i*) is assigned probabilistically based on the cumulative frequency distribution of the density of darters (individuals / m<sup>2</sup>) collected in drop nets placed in that vegetation type in the field.

### *1.7 Input data*

Input data include time series of values representing, for the particular reach of the Comal River or the San Marcos River being simulated, (1) the aquatic vegetation type within each habitat cell, (2) the water discharge, temperature, and DO concentration for the entire reach, and (3) the water depth and velocity in each habitat cell associated with the specific water discharge rates (Fig. 2).

#### *1.7.1 Aquatic vegetation type*

Aquatic vegetation maps were developed by physically delineating the vegetation polygons in the field using GPS (BIO-WEST, 2004a – 2014a, BIO-WEST, 2004b – 2014b in interim final report). The corresponding vegetation polygons were spatially mapped to the hydrodynamic computational grid using ArcMap 9.3 (ESRI 2014).

#### *1.7.2 Water discharge, temperature, and DO concentration*

Mean daily water discharge was estimated based on data from a gauge as described in Section 2.2 (in interim final report). Mean daily water temperatures and mean daily DO concentrations were estimated based on hydrodynamic simulations using Qual-2E as described in Section 2.3 (in interim final report).

#### *1.7.3 Water depth and velocity*

Results of hydraulic simulations of water depth and velocity for various water discharge rates within and beyond historical ranges (0.28 to 2.26 m<sup>3</sup> sec<sup>-1</sup> ; 10 to 80 cfs) using the U.S. Geological Survey Multi-dimensional Surface Water Modeling System (MDSWMS) hydraulic model (Hardy et al., 2010 in interim final report) were used to interpolate the depth and velocity at each habitat cell. Water depths and velocities associated with discharge rates not simulated using MDSWMS were estimated by linear interpolation. Interpolated values at known water discharges showed less than a 3.0 percent variation in interpolated depth and velocities when compared to the simulated hydraulic attributes, as described in Section 2.2 (in interim final report).

## 1.8 Submodels

### 1.8.1 Adjust vegetation type and maximum darter density

Vegetation types are adjusted during the spring (1 March, day-of-year 60), summer (1 July, day-of-year 182), and fall (1 October, day-of-year 274) of 2003 and 2004, and during the spring (1 March, day-of-year 60) and fall (1 September, day-of-year 244) of 2005 to 2014, with the vegetation type assigned to each habitat cell based on the input time series of vegetation data. Immediately following the adjustment of the vegetation type within any given habitat cell  $i$ , the maximum darter density of that cell ( $MD_i$ ) is adjusted accordingly (as described in Section 1.6).

### 1.8.2 Adjust water discharge, temperature, and DO concentration

Mean water discharges, and mean water temperatures and DO concentrations are adjusted daily, with a single discharge, water temperature, and DO concentration assigned to the entire reach (global variables) based the input time series of discharge, temperature, and DO concentration data.

### 1.8.3 Adjust water depth and water velocity

Water depths and velocities are adjusted daily, with the water depth and velocity assigned to each habitat cell based on the water depth and velocity data input file associated with the mean water discharge being simulated for that day.

### 1.8.4 Adjust fountain darter age and developmental stage

Fountain darter ages are updated daily, with developmental stages updated from egg to larva at 6 days of age (Simon et al., 1995), from larva to juvenile at 66 days of age, from juvenile to young adult at 186 days of age, and from young adult to old adult at 736 days of age (Brandt et al., 1993).

### 1.8.5 Calculate fountain darter mortality

Fountain darter mortality related to water temperature is calculated on a daily basis, with the probability of dying ( $pd$ ) of each individual calculated as a function of its stage of development and the water temperature in the habitat cell in which the individual is located. For eggs, larvae, juveniles, young adults, and old adults, respectively:

$$pd_{eggs} = (\text{base-mort-egg} + \text{egg-mort-temp})$$

where egg-mort-temp = 0.025 if temp <= 23C

$$= -0.6075 + 0.0275 * \text{temp if } 23\text{C} < \text{temp} \leq 27$$

$$= 0.135 \text{ if temp} > 27\text{C}$$

$$pd_{larvae} = (\text{base-mort-lar} + \text{lar-mort-temp})$$

where  $\text{lar-mort-temp} = 1 / (1 + \exp(-7.31 + 5.43 * \ln \text{temp}))$  if  $\text{temp} \leq 22\text{C}$

$$= 1 / (1 + \exp(310.96 - 89.83 * \ln \text{temp})) \text{ if temp} > 22\text{C}$$

$$pd_{juv- yng adu} = (\text{base-mort-juv- yngadu} * \text{juv-adu-mort-temp})$$

where  $\text{juv-adu-mort-temp} = 3$  if  $\text{temp} \leq 0\text{C}$

$$= 3 - 0.025 * \text{temp if } 0\text{C} < \text{temp} \leq 8\text{C}$$

$$= 1 \text{ if } 8\text{C} < \text{temp} \leq 22\text{C}$$

$$= -4.5 + 0.25 * \text{temp if } 22\text{C} < \text{temp} \leq 30\text{C}$$

$$= 3 \text{ if temp} > 30\text{C}$$

$$pd_{old adults} = (\text{base-mort-oldadu} * \text{juv-adu-mort-temp})$$

The base mortality rates for eggs, larvae, juveniles/young adults, and old adults, were 0.03, 0.031, 0.00149, and 0.00545, respectively, were based on information in Pitcher and Hart (1982) and Brandt et al. (1993), and the water temperature effects on mortality were based on information in Bonner et al. (1998).

Fountain darter mortality related to DO concentration (mg/l) is calculated on a daily basis, with the probability of dying ( $pd$ ) of each individual calculated as a function of its stage of development and the current DO concentration in the reach. For eggs/larvae, and juveniles/adults, respectively:

$$pd_{egg/larDO} = 1 - (1 / (1 + \exp(-5.3 * (\text{DO} - 3))))$$

$$pd_{juv-aduDO} = 1 - (1 / (1 + \exp(-10.6 * (\text{DO} - 2.5))))$$

These equations were estimated based on information in Hlohowskyj and Wissing (1987), Behen (2013), and Hartline (2013). Eggs and larvae also die if the habitat cell in which they are located loses its aquatic vegetation, juveniles and adults also die if they fail to find suitable habitat (see next section on darter movements), and old adults also die when they reach 1100 days of age (about 3 years old).

### 1.8.6 Calculate fountain darter movement

Juvenile and adult fountain darters may make up to 24 movements per day, whereas eggs and larvae are immobile. Movement rules, which are hypothetical, but which result in movement patterns generally consistent with those based on field data collected from marked individuals (Bio-West, unpublished data), are summarized in Fig. 3. (1) If an individual is located in a habitat cell that currently is below its estimated maximum darter density (MD; the number of juveniles plus adults that can be supported by that vegetation type), and there are no adjacent habitat cells below their MD, then the individual will not move from the cell it currently occupies. (2) If an individual is located in a habitat cell that currently is below its MD, and one or more of the adjacent habitat cells is below their MD, then the individual has a probability ( $\epsilon = 0.50$ ) of moving to one of those habitat cells (randomly chosen), and a probability  $(1 - \epsilon)$  of remaining in the cell it currently occupies. This rule allows individuals to move about larger aggregates of suitable habitat cells and prevents situations in which suitable habitat cells near the center of large patches become inaccessible due to “barriers” formed by suitable, fully-occupied habitat cells. (3) If an individual is located in a habitat cell that currently is at or above its MD, and one or more of the adjacent habitat cells is below their MD, then the individual moves to one of those habitat cells (randomly chosen). (4) If an individual is located in a habitat cell that currently is at or above its MD, and none of the adjacent habitat cells is below their MD, but one or more of the adjacent habitat cells has water, then the individual moves to one of those habitat cells (randomly chosen). (5) If an individual is located in a habitat cell that currently is at or above its MD, and none of the adjacent habitat cells is below their MD, and none of the adjacent habitat cells has water, then the individual will not move from the cell it currently occupies. If an individual has not occupied a habitat cell that was below its MD (has not found favorable habitat) within an arbitrarily specified number of consecutive moves ( $v$ ), it dies ( $v = 12$ ; see model calibration section below).

### 1.8.7 Calculate fountain darter egg laying (recruitment)

Fountain darter egg laying is calculated on a daily basis, with the probability that an adult female lays eggs calculated as a function of month-of-year and the presence of aquatic vegetation in the habitat cell in which the individual is located. The mean ( $\pm$  1SD) proportions of adult females that are reproductively active during the months of January through December are 0.1913 (0.0345), 0.2893 (0.0850), 0.3104 (0.1968), 0.1000 (0.2000), 0.1133 (0.0585), 0.1774 (0.0863),

0.1528 (0.0991), 0.0192 (0.0385), 0.0 (0.0), 0.1007 (0.0208), 0.0385 (0.0769), and 0.0948 (0.0478), respectively (Nichols, 2015). Actively reproducing females produce a mean ( $\pm$  1SD) of 6.34 (5.16) healthy (fertilized with embryo development underway) eggs per day (based on data collected at 24C in McDonald et al., 2007). In the model, on the first day of each month, each adult female is identified as reproductively active or not based on a random variate drawn from a normal distribution (truncated at +2SD and -2SD or 0) with the mean and SD associated with the corresponding month. Each female maintains her status during the entire month. Each day that a reproductively active female is in a habitat cell with aquatic vegetation, she lays a number of eggs based on a random variate drawn from a normal distribution (truncated at +2SD and -2SD or 0) with a mean ( $\pm$ SD) of 6.34 ( $\pm$  5.16). Juveniles that become adult females (at 186 days of age) during the month are immediately identified as reproductively active or not in a similar manner.

#### *1.8.8 Update aggregated (output) variables*

Aggregated variables describing the state of the system that are calculated daily and written to output files include: (1) the total number of habitat patches with aquatic vegetation, (2) the numbers of habitat patches with each type of aquatic vegetation, (3) the maximum fountain darter density, (4) the total number of juvenile plus adult fountain darters, (5) the number of juvenile plus adult fountain darters in each type of aquatic vegetation, and (6) the proportions of eggs, larvae, juveniles, young adults, old adults, males, and females in the fountain darter population.

## **2. Model evaluation**

We preface our presentation of model evaluation with a somewhat lengthy explanation of our use of terminology. To illustrate our terminology, we have excerpted examples, out of context, from subsequent sections of the present report. Thus, we present the examples here exclusively to clarify our use of terminology. We will return to the points associated with each example, within the appropriate contexts, later in this section on model evaluation.

Considerable confusion often arises regarding the terminology associated with the “validation” of ecological simulation models (see Rykiel, 1996, for a classic treatment of the subject which

still is relevant today). In the early days of ecological modeling, Holling (1978) suggested that “model validation” was an unfortunate choice of terms and that we might more appropriately refer to the process as “model invalidation.” This analogy to the process of attempting to refute a hypothesis via the scientific method has merit in that a model can be viewed as a collection of hypotheses about the structure and function of the system we are modeling. Nonetheless, validation remains the most commonly-used term. Other terms such as verification, calibration, assessment of performance, and sensitivity analysis, which are used frequently in conjunction with validation, also continue to be defined and applied in a variety of ways.

We prefer to use “model evaluation” when referring to the multifaceted process of deciding under what circumstances we should use a model and how much confidence we should place in simulation results, or, stated more simply, the process of evaluating the relative usefulness of a model for a given purpose (Grant and Swannack 2008). This includes verification, calibration, assessment of performance, and sensitivity analysis of the model.

We use “model verification” to refer to the process of confirming that execution of the model’s computer code representing mathematical and logical relationships yields appropriate numerical results. For example, we have verified that the computer code intended to generate a uniform random variate on the interval from 0 to 1 and assign “male” to an individual if that variate has a value  $<0.58$  and “female” to an individual if that variate has a value  $\geq 0.58$  actually does generate a 0.58 to 0.42 sex ratio among individuals when executed relatively many times. In a similar fashion, we have verified that the computer code intended to generate the literature-based development rates of individuals through egg, larval, juvenile, and adult life stages, as well as the computer code intended to generate empirically-observed seasonal patterns of reproduction, actually does generate these literature-based and empirically-observed values. Thus, mathematical components and formal logical structures can be verified.

We use “model calibration” to refer to the process of adjusting estimates of model parameters to improve agreement between model output and *a priori* expectations we have regarding certain aspects of model behavior. These expectations may be based on theory, data, expert opinion, or

may arise from hypotheses relevant to the questions at hand. For example, after the darter population dynamics model had been parameterized based on the best information available, it generated fluctuations in abundance of individuals that were similar qualitatively to the fluctuations expected based on historical data and expert opinion. However, quantitatively, the simulated abundances were not sufficiently close to the expected abundances. A legitimate procedure in such cases is to consider adjusting the values of model parameters to improve agreement between simulated and expected abundances. But this procedure must be confined strictly to parameters whose initial values were estimated with relatively high uncertainty and only a very few parameters should be calibrated (Grant and Swannack 2008). For example, the hypothetical darter movement rules that we coded into the computer include a parameter ( $v$ ) that represents the number of consecutive moves an individual can make without encountering favorable habitat (a cell with aquatic vegetation that has room for more darters) before it dies. This code serves to limit darter population size based on habitat availability, which ensures the appropriate theoretical (and commonsensical) form of population growth in a limited environment. The larger the value of  $v$ , the higher will be the limit on population abundance. But the value of  $v$  has no empirical basis and, *per se*,  $v$  has no theoretical interpretation, thus making it a prime candidate for calibration, and, in fact, the only parameter that we adjusted during model calibration.

We use “assessment of performance” to refer to the process of assessing the degree to which model output meets the performance standards required for the model’s purpose. This is what Rykiel (1996) referred to as “operational validation,” or “whole model validation,” which is a pragmatic approach concerned primarily with how well the model mimics the real system regardless of the mechanisms built into the model. For example, we compared (1) simulated darter densities within various aquatic vegetation types to densities of darters captured in drop-net samples collected from the corresponding vegetation types in the real system, (2) distances moved by simulated darters to movement distances observed in a recent field study, and (3) the simulated stock-recruitment relationship to the stock-recruitment relationship expected for fountain darters based on their life history attributes

We use “sensitivity analysis” to refer to the general process of determining the degree of response of model behavior to changes in the representation of model components. There is a huge scientific literature on sensitivity analysis methodologies and, to state the obvious, the methodology employed depends on the specific objectives of the analysis. We focused our three-part analysis on the sensitivity of model predictions of darter population dynamics to changes in parameters representing (1) maximum darter densities supported by different types of aquatic vegetation, (2) demographic/life history and environmental factors, and (3) density-dependent effects of these factors on population growth rate ( $\lambda$ ). The first part might be perceived as “data validation” (Rykiel 1996), in that it involved changes in the manner in which we estimated model parameters from field data. That is, we estimated maximum darter densities using reach-specific data on aquatic vegetation versus data from an entire river. The idea being that we cannot assume that a particular data set accurately represents the real system and thereby constitutes the best test of a model. The second part of our analysis might be thought of as quantifying the parametric uncertainty (resulting from changes in 11 demographic/life history parameters) and environmental uncertainty (resulting from changes in 2 environmental factors) associated with population growth rates. The third part might be perceived as “event validation” (Rykiel 1996), in that it focused primarily on the ability of the model to represent qualitatively appropriate relationships among model variables (hypothesized forms of density-dependent negative feedback on population growth rate) which generated qualitatively reasonable model behavior (population growth rate was most sensitive to density-dependent increases in larval mortality rate).

## 2.1 Overview

To evaluate the capability of the model to provide useful information regarding possible responses of fountain darter populations to changes in habitat conditions, we first verified the model code was capable of reproducing the historical aquatic vegetation and hydrological conditions within each of the five reaches being simulated (the Old Channel, Upper Spring Run, and Landa Lake reaches of the Comal River and the City Park and I35 reaches of the San Marcos River) from 2003 through 2013. We also verified the model code was capable of reproducing the rates of development of fountain darters through egg, larval, juvenile, and adult life stages, as well as the seasonality of reproduction, in accordance with the empirically-estimated life

history/demographic input parameters. We then calibrated the model such that simulated abundances of fountain darters responded appropriately to historical changes in habitat conditions within one of the reaches (the Old Channel Reach of the Comal River) from 2003 through 2010. Next, we assessed model performance by comparing simulated fountain darter densities within each of the various aquatic vegetation types within each of the five reaches from 2011 through 2013 to density estimates based on field data from the corresponding aquatic vegetation types within the corresponding reach from 2011 through 2013. We also compared the distances moved by simulated darters under historical habitat conditions from 2003 to 2013 within in each of the five reaches to movement distances observed in a recent field study, as well as the simulated stock-recruitment relationship to the expected stock-recruitment relationship for fountain darters. Finally, we analyzed the sensitivity of model predictions of fountain darter population dynamics to changes model parameters representing maximum darter densities, demographic/life history attributes, and environmental conditions, as well as to the implementation of several hypothesized forms of density-dependent negative feedback on population growth rate.

## *2.2 Verification*

We first verified the model code appropriately generated historical habitat conditions for each of the reaches of the Comal River and the San Marcos River by simulating spatial-temporal dynamics of aquatic vegetation, as well as the temporal dynamics of water discharge, temperature, and DO concentration from 2003 through 2013 for each reach and comparing simulation outputs to the corresponding time series of input data. We then verified that the model code generated appropriate spatial distributions of water depth and velocity over a range of different water discharges for each of the reaches by comparing simulated depth and velocity patterns with those generated by MDSWMS at the corresponding discharges. Finally, we verified the model code represented the development of individual fountain darters through egg, larval, juvenile, young adult, and old adult life stages, as well as the seasonality of reproduction, in accordance with the empirically-estimated life history/demographic input parameters.

## *2.3 Calibration*

For model calibration, we used the version of the model that was parameterized to represent the Old Channel Reach of the Comal River. We calibrated this version of the model by adjusting  $v$  (the number of consecutive moves that a juvenile or adult fountain darter can survive without

finding favorable habitat; see Section 1.8.6) such that the simulated number of juveniles plus adults increased toward, but did not markedly exceed, the estimated maximum darter densities that could be supported by the aquatic vegetation ( $\sum MD_i$ ; where  $MD_i$  is the number of juveniles plus adults that can be supported by the vegetation type in habitat cell  $i$ ; see Section 1.6. and Section 1.8.1) within the Old Channel reach from 2003 to 2010. These two criteria were met with  $v = 12$ , whereas with higher and lower values of  $v$ , the number of juveniles plus adults increased beyond, and failed to reach, the estimated maximum darter density, respectively. When we removed the limit on the number of consecutive moves that a juvenile or adult fountain darter can survive without finding favorable habitat ( $v = 99999$ ), the number of juveniles plus adults increased exponentially, and when we replaced the movement rules with random movement the population could not sustain.

#### *2.4 Assessment of performance*

To assess model performance, we first simulated historical habitat conditions from 2003 to 2013 within each of the reaches of the Comal and San Marcos rivers and compared both graphically and statistically, simulated fountain darter densities within each of the various aquatic vegetation types from 2011 through 2013 to the densities of fountain darters captured in drop-net samples collected from the corresponding aquatic vegetation types in the corresponding reaches from 2011 through 2013. (Note that we did not recalibrate  $v$  for simulations of the Upper Spring Run and Landa Lake reaches of the Comal River or for simulations of the City Park and I35 reaches of the San Marcos River. Also, note that maximum darter densities throughout each simulation were estimated based on analyses of drop-net data collected from 2003 through 2010 in the reach being simulated. That is, drop-net data collected from 2011 through 2013 were not used in model parameterization.) Simulated densities generally compared well with those observed in the field, considering the variability and sparsity of field data (Fig. 4, Table 1). However, in the Comal River, simulated densities in Bryophytes were lower than those observed in the field in the Upper Spring Run and Landa Lake, and simulated densities in *Hygrophila* also were lower than those observed in the field in Landa Lake (Fig. 4b and c). Simulated densities in *Ludwigia* were lower than observed densities in Landa Lake during 2011, but simulated and observed densities corresponded well thereafter (Fig. 4c). In the San Marcos River, simulated densities in both *Hydrilla* and *Cabomba* were lower than observed densities in the I35 reach during 2011, but simulated and observed densities corresponded well thereafter (Fig. 4e). In summary, 11 out of 36 pairwise comparisons of simulated fountain darter densities to the densities of fountain darters

captured in drop-net samples collected from the corresponding aquatic vegetation types were statistically significantly different at  $P < 0.05$  (Table 1).

We next compared the distances moved by simulated darters under historical habitat conditions from 2003 to 2013 within in each of the five reaches to movement distances observed in a recent field study. Relocation data on darters tagged in the Upper Spring Run Reach and Blieders Creek of the Comal River indicated mean movements away from their release locations of 20.9m (Bio-West 2014). Mean movements of simulated darters away from the location where they metamorphosed into mobile juveniles (eggs and larvae are immobile) were 19.9m in the Upper Spring Run Reach, and 24.6m, 22.0m, 26.0m, and 15.6m in the Old Channel, Landa Lake, City Park, and I35 reaches, respectively.

Finally, we compared the simulated stock-recruitment relationship to the stock-recruitment relationship that might be expected for fountain darters. Based on their life history, one would expect a Beverton-Holt type spawner-recruit relationship, likely with a weak response (a gradually leveling off curve) characterized by a steepness coefficient of 0.5 to 0.7 (Rose et al. 2001, Kenny Rose, pers. comm.). For these simulations, we used the version of the model representing the Old Channel Reach of the Comal River, with maximum darter densities for the various vegetation types based on drop-net data collected from 2003 to 2010 in the Old Channel Reach of the Comal River. We initialized the model with the distribution of aquatic vegetation types observed in the fall of 2012 and with the mean water discharge (44 cfs), temperature (23.1 C), and DO concentration (7.2 mg/L) associated with the fall period of 2012 (23 October 2012 through 21 April 2013; day-of-year 296 through day-of-year 111). To remove the effect of variable environmental conditions, we maintained these conditions constant throughout each simulation.

The aquatic vegetation during the fall of 2012 yielded the highest estimated maximum darter density ( $\approx 11,000$  juveniles plus adults) for the Old Channel Reach from 2003 through 2013. For these simulations, we initialized the darter population at low densities, ranging from 1 to 20 percent of the estimated maximum density, which allowed observation of annual stock-recruitment relationships at a variety of population sizes as the population grew toward the estimated maximum darter density. We calculated stock size as the mean number of adults alive

during a calendar year (the total number of “adult-days” accumulated during the calendar year divided by 365). We calculated annual recruitment as the number of eggs laid during a calendar year that reached the adult stage within the same calendar year. These simulations yielded a Beverton-Holt type spawner-recruit relationship with a steepness coefficient of 0.3948 ( $r^2 = 0.96$ ) (Fig. 5).

### 2.5 Sensitivity analysis

We first analyzed the sensitivity of model predictions of population dynamics to changes in the manner in which we estimated maximum darter densities for the various vegetation types. In addition to estimating maximum darter densities based on drop-net data collected (1) from 2003 to 2010 in the reach of the river being simulated (as described in Section 1.6), we also estimated the maximum densities based on drop-net data collected (2) from 2003 to 2010 in the entire river. We then compared simulated population dynamics from 2003 to 2013 within each reach based on each of the two manners of estimating maximum darter densities. Mean darter abundances based on data from the entire Comal River averaged  $\approx 7500$  higher than those based on data from the Old Channel Reach, with differences ranging from  $\approx +100$  to  $\approx +10500$ . Maximum abundances based on data from the entire Comal River averaged  $\approx 6400$  higher than those based on data from the Upper Spring Run Reach, with differences ranging from  $\approx 500$  to  $\approx +12000$ . Maximum abundances based on data from the entire Comal River averaged  $\approx 3300$  lower than those based on data from the Landa Lake Reach, with differences ranging from  $\approx -600$  to  $\approx -8400$ . Maximum abundances based on data from the entire San Marcos River averaged  $\approx 8600$  lower than those based on data from the City Park Reach, with differences ranging from  $\approx -2300$  to  $\approx -12000$ . Maximum abundances based on data from the entire San Marcos River averaged  $\approx 1000$  higher than those based on data from the I35 Reach, with differences ranging from  $\approx 0$  to  $\approx 2000$ . The relative sizes of simulated fountain darter populations, of course, reflected these differences in maximum density estimates, but both seasonal and longer-term population trends were qualitatively the same regardless of the manner of estimating maximum darter densities.

We next analyzed the sensitivity of model predictions of population dynamics, as measured by the annual population growth rate ( $\lambda$ ), to changes in 11 demographic/life history parameters and 2 environmental variables that directly affect fountain darter population growth.

Demographic/life history parameters included (1) mean clutch size, (2) proportion of females

laying eggs, base mortality rates of (3) egg, (4) larval, (5) juvenile, (6) young adult, and (7) old adult life stages, duration of (8) egg, (9) larval, (10) juvenile, and (11) young adult life stages, which affect mortality rates. Environmental variables included (1) water temperature and (2) DO level, both of which affect mortality rates of all life stages. For these simulations, we used the version of the model representing the Old Channel Reach of the Comal River, with maximum darter densities for the various vegetation types based on drop-net data collected from 2003 to 2010 in the Old Channel Reach of the Comal River. We initialized the model with the distribution of aquatic vegetation types observed in the fall of 2012 and with the mean water discharge, temperature, and DO concentration associated with the fall period of 2012, as described above for the simulations examining stock-recruitment relationships. To isolate the effect on  $\lambda$  of the parameter being varied, we again maintained these conditions constant throughout each simulation (except, of course, for those simulations specifically examining the effects of adjusting temperature and DO). To allow the simulated population to express its maximum annual growth rate, we again initialized each simulation with the darter population at one percent of the estimated maximum density.

Among the demographic/life history parameters,  $\lambda$  was most sensitive to increases in larval mortality rate, decreases in proportion of females laying eggs and mean clutch size, somewhat less sensitive to increases in duration of larval and egg stages, and was insensitive to changes in egg, juvenile, and adult mortality rates, as well as duration of juvenile and young adult stages (Fig. 6a-j). Over the ranges of values examined,  $\lambda$  always was greater than 3, unless larval mortality rate was increased by >70% relative to its base rate, and remained well above 1 even when larval mortality rate was double its base rate. Among the environmental variables,  $\lambda$  was sensitive to both increases in water temperature and decreases in DO, with  $\lambda$  falling below 1 when water temperatures were held constant at  $\leq 31$  C and when DO levels were held constant at  $\leq 3$  mg/L;  $\lambda$  was  $\approx 1.5$  when water temperatures were held constant at 30 C and  $\approx 2$  when DO levels were held constant at 3.5 mg/L (Fig. 6k-l).

Finally, we analyzed the sensitivity of model predictions of population dynamics to the implementation of several hypothesized forms of density-dependent negative feedback on population growth rate. We hypothesized that as the density of juveniles plus adults increased there would be an increase in the base mortality rates of (1) eggs, (2) larvae, (3) juveniles, and/or (4) adults, and a decrease in (5) the mean number of eggs laid per female and/or (6) the

proportion of females laying eggs. We represented density-dependent increases in the base mortality rates by multiplying them by a density-dependent mortality index ( $DDI_{mort}$ ):

$$DDI_{mort} = \left[ \left( \frac{N}{K} \right)^\theta + 1 \right]^\gamma$$

where  $N$  is the current number of juveniles plus adults in the simulated reach,  $K$  is the estimated maximum number of juveniles plus adults that can be supported by the current aquatic vegetation in the reach ( $\sum MD_i$ ; where  $MD_i$  is the number of juveniles plus adults that can be supported by the vegetation type in habitat cell  $i$ ), and  $\theta$  and  $\gamma$  are parameters that control the slope and the maximum value, respectively, of  $DDI_{mort}$ . We represented density-dependent decreases in the mean number of eggs laid per female and the proportion of females laying eggs multiplying them by a density-dependent reproduction index ( $DDI_{repro}$ ):

$$DDI_{repro} = 1 - \left( \frac{N}{K} \right)^\theta$$

where  $\theta$  controls the slope of  $DDI_{repro}$ . For the present analyses, we assumed that all of these density-dependent relationships were linear ( $\theta = 1$ ) and that the maximum value of  $DDI_{mort}$  was 2 ( $\gamma = 1$ , i.e., double the baseline rate). We simulated the effect of each of these hypothesized relationships operating individually, and also the effect of all operating simultaneously, over a one-year period. For these simulations, we used the version of the model representing the Old Channel Reach of the Comal River, with maximum darter densities for the various vegetation types based on drop-net data collected from 2003 to 2010 in the Old Channel Reach of the Comal River (with the distribution of aquatic vegetation types initialized as observed in the spring of 2003).

Among the hypothesized forms of negative feedback on population growth rate, model predictions of population dynamics were most sensitive to density-dependent increases in larval mortality rate, and were insensitive to density-dependent increases in egg, juvenile, and adult mortality rates, and to density-dependent decreases in proportion of females laying eggs and mean clutch size (Fig. 7). With simultaneous implementation of all six density-dependent effects, model predictions of population dynamics were similar qualitatively to predictions without density-dependent effects, but densities averaged  $\approx 60\%$  of those generated without density-dependent effects (Fig. 7).

Interestingly, implementation of all six density-dependent effects yielded a stock-recruitment relationship more similar to that which might be expected for fountain darters (with a steepness coefficient of 0.5 to 0.7) than when no density-dependent effects were implemented. That is, when we repeated the stock-recruitment simulations described in Section 2.4 with simultaneous implementation of all six density-dependent effects, these simulations yielded a Beverton-Holt type spawner-recruit relationship with a steepness coefficient of 0.4874 ( $r^2 = 0.90$ ) (Fig. 8).

### 3. Model application

#### 3.1 Simulation of HCP long-term average and HCP drought scenarios

To investigate possible responses of fountain darter populations to changes in habitat conditions, we first simulated population dynamics within each of the five reaches under (1) HCP long-term average conditions and (2) HCP drought conditions, and compared the results of these simulations to population dynamics within each of the five reaches simulated under (3) historical (2003 to 2013) aquatic vegetation and hydrological conditions. We ran 3 replicate stochastic (Monte Carlo) simulations of each of these scenarios using versions of the model (1) without any density-dependent effects and (2) with all six density-dependent effects implemented.

General trends in simulated population dynamics were not noticeably different among the three scenarios within any of the five reaches based on either the density-independent or density-dependent versions of the model (Figs. 9-13). Mean darter abundances (number of juveniles + adults in the reach) simulated with the density-dependent version of the model were lower than those simulated with the version of the model without density-dependent negative feedback on population growth, as would be expected. Mean abundances (calculated as the mean of all daily abundances from the 3 replicate stochastic simulations of a given scenario) simulated under HCP long-term average conditions and under HCP drought conditions were all within 12% of abundances simulated under baseline (historical) conditions, regardless of the reach simulated or the version of the model used. The lowest darter abundances (which were produced by the density-dependent version of the model) occurring during simulations of the Old Channel, Upper Spring Run, Landa Lake, City Park, and I35 reaches, were 942, 435, 8387, 10676, and 360 darters in the reach, respectively. These lowest abundances most often occurred during simulations of the HCP drought scenario (Landa Lake, City Park, and I35 reaches), but also

occurred during the HCP long-term average scenario (Old Channel Reach) and the baseline (historical) scenario (Upper Spring Run Reach), again indicating the lack of noticeable differences among the three scenarios within any of the five reaches.

### *3.2 Simulation of “worst case” scenarios*

We next simulated fountain darter population dynamics within each of the five reaches under several “worst case” scenarios in which baseline conditions (historical [2003 to 2013] aquatic vegetation and hydrological conditions) were modified, and again compared the results of these simulations to population dynamics within each of the five reaches simulated under baseline conditions. Modifications included (1) replacing the historical sequence of aquatic vegetation changes with an unchanging aquatic vegetation community that represented the worst fountain darter habitat observed in the reach from 2003 to 2013 (Bad Vegetation), (2) replacing the historical sequence of water temperatures with an annually-repeating sequence of daily water temperatures that represented the year with the highest water temperature observed in the reach from 2003 to 2013 (High Temperature), and (3) implementing both the aquatic vegetation and water temperature modifications (Bad Vegetation + High Temperature). To represent the worst fountain darter habitat in the Old Channel, Upper Spring Run, Landa Lake, City Park, and I35 reaches, we used the historical aquatic vegetation from the spring of 2003, the fall of 2010, the spring of 2013, the fall of 2009, and the fall of 2012, respectively. To represent the year with the highest water temperature for these same reaches, we used the temperature time series for 2010, 2006, 2011, 2012, and 2011 from the drought scenario for the respective reaches. Once again, we ran 3 replicate stochastic (Monte Carlo) simulations of each of these scenarios using versions of the model (1) without any density-dependent effects and (2) with all six density-dependent effects implemented.

General trends in population dynamics simulated under the High Temperature scenario were not noticeably different than those simulated under the baseline (historical) scenario within any of the five reaches based on either the density-independent or density-dependent versions of the model, however, mean darter abundances simulated under the Bad Vegetation scenario and the Bad Vegetation + High Temperature scenario were markedly lower (Figs. 14-18). There were few noticeable differences between mean darter abundances simulated under the Bad Vegetation scenario and those simulated under the Bad Vegetation + High Temperature scenario, although mean abundances decreased to slightly lower levels under the Bad Vegetation + High

Temperature scenario in the Landa Lake and I35 reaches. Mean darter abundances simulated under the High Temperature scenario were within 12% of the mean abundances simulated under baseline (historical) conditions in the Old Channel, Upper Spring Run, and City Park reaches, regardless of the version of the model used. Mean abundances simulated under the High Temperature scenario in Landa Lake were 17% lower than baseline, using either version of the model. Mean abundances simulated under the High Temperature scenario in the I35 Reach were 22% lower than baseline using the density-dependent version of the model, but only 12% lower using the density-independent version. Mean abundances simulated under both the Bad Vegetation and the Bad Vegetation + High Temperature scenarios were more than 50, 80, 20, 40, and 40% lower than baseline in the Old Channel, Upper Spring Run, Landa Lake, City Park, and I35 reaches, respectively, regardless of the version of the model used. The lowest darter abundances (again produced by the density-dependent version of the model) occurring during simulations of the Old Channel, Upper Spring Run, Landa Lake, City Park, and I35 reaches, were 651, 555, 6743, 7829, and 162 darters, respectively. These lowest abundances most often occurred during simulations of the High Temperature scenario (Upper Spring Run, Landa Lake, and I35 reaches), but also occurred during the Bad Vegetation scenario (Old Channel Reach) and the Bad Vegetation + High Temperature scenario (City Park Reach).

The differences among scenarios within reaches with regard to the occurrences of the lowest darter abundances, and, to a lesser extent, the relative levels of the mean darter abundances, are somewhat perplexing at first glance. Nominally, we would expect the lowest abundances and the lowest mean abundances to be associated with simulations of the Bad Vegetation + High Temperature scenario in all of the reaches. But the temporal sequencing of changes in aquatic vegetation conditions and water temperature conditions, superimposed on the demographic momentum of the darter population during any given simulation, complicates the issue. Since one of the years in the High Temperature scenario coincides with the aquatic vegetation community that represented the worst fountain darter habitat (which was used continuously in the Bad Vegetation scenario), and one of the years in the Bad Vegetation scenario coincides with the annually-repeating sequence of daily water temperatures that represented the year with the highest water temperature (which was used repeatedly in the High Temperature scenario), there will be a year during both the High Temperature scenario and the Bad Vegetation scenario with the same aquatic vegetation and water temperature conditions that repeat themselves year after

year in the Bad Vegetation + High Temperature scenario. Differences in the size and stage-structure of the darter population entering the “bad vegetation plus high temperature” year will affect the population response to these conditions, and especially will affect the lowest abundance to which the population might fall. Thus, although mean abundances and lowest abundances resulting from the various scenarios are convenient summary metrics that facilitate comparisons among and within scenarios and reaches, the temporal dynamics of darter populations presented in Figures 9-18 provide a more reliable, albeit perhaps more cumbersome, basis for such comparisons.

**Table 1. Results of t-tests comparing simulated drop-net data to observed drop net data. These statistical tests are associated with the data presented below. Statistically significant differences ( $P < 0.05$ ) are highlighted in yellow.**

**Figure 0-1(a). Fountain darter model (continuous traces) and drop net data (filled circles) in Hygrophila for Old Channel study reach of Comal River, 2003-2010**

**Figure 2-18(b). As Figure 2-18(a) in Ludwigia for Old Channel study reach of Comal River, 2003-2010**

**Figure 2-18(c). As Figure 2-18(a) in filamentous algae for Old Channel study reach of Comal River, 2003-2010 Note change in ordinate axis.**

	Figure 2-18(a)	Figure 2-18(b)	Figure 2-18(c)
t Stat	-1.3934	-1.3598	-1.2981
P(T<=t)	0.1698	0.1821	0.2090

**Figure 0-2(a). Fountain darter model (continuous traces) and drop net data (filled circles) in Hygrophila for Upper Spring Run study reach of Comal River, 2003-2010**

**Figure 2-19(b). As Figure 2-19(a) in Sagittaria for Upper Spring Run study reach of Comal River, 2003-2010**

**Figure 2-19(c). As Figure 2-19(a) in Bryophytes for Upper Spring Run study reach of Comal River, 2003-2010**

	Figure 2-19(a)	Figure 2-19(b)	Figure 2-19(c)
t Stat	-3.9816	-1.7327	-2.6267
P(T<=t)	0.0003	0.0907	0.0125

**Figure 0-3(a). Fountain darter model (continuous traces) and drop net data (filled circles) in Hygrophila for Landa Lake study reach of Comal River, 2003-2010**

**Figure 2-20(b). As Fig. 2-20(a) in Ludwigia for Landa Lake study reach of Comal River, 2003-2010**

**Figure 2-20(c). As Fig. 2-20(a) in Vallisneria for Landa Lake study reach of Comal River, 2003-2010**

**Figure 2-20(d). As Fig. 2-20(a) in Cabomba for Landa Lake study reach of Comal River, 2003-2010**

**Figure 2-20(e). As Fig. 2-20(a) in Bryophytes for Landa Lake study reach of Comal River, 2003-2010**

	Figure 2-20(a)	Figure 2-20(b)	Figure 2-20(c)	Figure 2-20(d)	Figure 2-20(e)
t Stat	-4.1258	-1.6663	-0.5529	-1.6366	-2.6521
P(T<=t)	0.0002	0.1025	0.5835	0.1090	0.0110

**Figure 0-4(a). Fountain darter model (continuous traces) and drop net data (filled circles) in Hygrophila for City Park study reach of San Marcos River, 2003-2010**

**Figure 2-21(b). As Fig. 2-21(a) in Hydrilla for City Park study reach of San Marcos River, 2003-2010**

**Figure 2-21(c). As Fig. 2-21(a) in bare substrate for City Park study reach of San Marcos River, 2003-2010**

**Note change in ordinate axis.**

	Figure 2-21(a)	Figure 2-21(b)	Figure 2-21(c)
t Stat	-0.3835	-0.3922	-1.2303
P(T<=t)	0.7021	0.6968	0.2253

**Figure 0-5(a). Fountain darter model (continuous traces) and drop net data (filled circles) in Hygrophila for IH 35 study reach of San Marcos River, 2003-2010**

**Figure 2-22(b). As Fig. 2-22(a) in Hydrilla for IH 35 study reach of San Marcos River, 2003-2010**

**Figure 2-22(c). As Fig. 2-22(a) in Cabomba for IH 35 study reach of San Marcos River, 2003-2010**

	Figure 2-22(a)	Figure 2-22(b)	Figure 2-22(c)
t Stat	-2.0029	-1.8485	-1.2901
P(T<=t)	0.0512	0.0710	0.2035

**Figure 0-6(a). Fountain darter model (continuous traces) and drop net data (filled circles) in Hygrophila for Old Channel study reach of Comal River, 2011-2013**

**Figure 2-23(b). As Figure 2-23(a) in Ludwigia for Old Channel study reach of Comal River, 2011-2013**

**Figure 2-23(c). As Figure 2-23(a) in Bryophytes for Old Channel study reach of Comal River, 2011-2013**

	Figure 2-23(a)	Figure 2-23(b)	Figure 2-23(c)
t Stat	-2.4682	-0.2512	1.0967
P(T<=t)	0.0199	0.8047	0.3344

**Figure 0-7(a).** Fountain darter model (continuous traces) and drop net data (filled circles) in Hygrophila for Upper Spring Run study reach of Comal River, 2011-2013

**Figure 2-24(b).** As Figure 2-24(a) in Sagittaria for Upper Spring Run study reach of Comal River, 2011-2013

**Figure 2-24(c).** As Figure 2-24(a) in Filamentous Algae for Upper Spring Run study reach of Comal River, 2011-2013

**Figure 2-24(d).** As Figure 2-24(a) in Bryophytes for Upper Spring Run study reach of Comal River, 2011-2013

	Figure 2-24(a)	Figure 2-24(b)	Figure 2-24(c)	Figure 2-24(d)
t Stat	-3.1416	6.9748	-0.6526	-3.5211
P(T<=t)	0.0085	<0.0001	0.5606	0.0042

**Figure 0-8(a).** Fountain darter model (continuous traces) and drop net data (filled circles) in Hygrophila for Landa Lake study reach of Comal River, 2011-2013

**Figure 2-25(b).** As Figure 2-25(a) in Ludwigia for Landa Lake study reach of Comal River, 2011-2013

**Figure 2-25(c).** As Figure 2-25(a) in Vallisneria for Landa Lake study reach of Comal River, 2011-2013

**Figure 2-25(d).** As Figure 2-25(a) in Cabomba for Landa Lake study reach of Comal River, 2011-2013

**Figure 2-25(e).** As Figure 2-25(a) in Bryophytes for Landa Lake study reach of Comal River, 2011-2013

	Figure 2-25(a)	Figure 2-25(b)	Figure 2-25(c)	Figure 2-25(d)	Figure 2-25(e)
t Stat	-6.0135	-2.5298	-0.1847	-0.8867	-6.4573
P(T<=t)	<0.0001	0.0251	0.8564	0.3913	<0.0001

**Figure 0-9(a).** Fountain darter model (continuous traces) and drop net data (filled circles) in Hygrophila for City Park study reach of San Marcos River, 2011-2013

**Figure 2-26(b).** As Figure 2-26(a) in Hydrilla for City Park study reach of San Marcos River, 2011-2013

**Figure 2-26(c).** As Figure 2-26(a) in Sagittaria for City Park study reach of San Marcos River, 2011-2013

**Figure 2-26(d).** As Figure 2-26(a) in Potamogeton for City Park study reach of San Marcos River, 2011-2013

	Figure 2-26(a)	Figure 2-26(b)	Figure 2-26(c)	Figure 2-26(d)
t Stat	-0.4158	-0.7761	-0.4625	0.5239
P(T<=t)	0.6844	0.4506	0.6752	0.6086

**Figure 0-10(a).** Fountain darter model (continuous traces) and drop net data (filled circles) in Hygrophila for IH 35 study reach of San Marcos River, 2011-2013

**Figure 2-27(b).** As Figure 2-27(a) in Hydrilla for IH 35 study reach of San Marcos River, 2011-2013

**Figure 2-27(c).** As Figure 2-27(a) in Sagittaria for IH 35 study reach of San Marcos River, 2011-2013

**Figure 2-27(d).** As Figure 2-27(a) in Cabomba for IH 35 study reach of San Marcos River, 2011-2013

	Figure 2-27(a)	Figure 2-27(b)	Figure 2-27(c)	Figure 2-27(d)
t Stat	0.2862	-1.5415	-0.7901	-0.9709
P(T<=t)	0.7780	0.1455	0.4737	0.3508

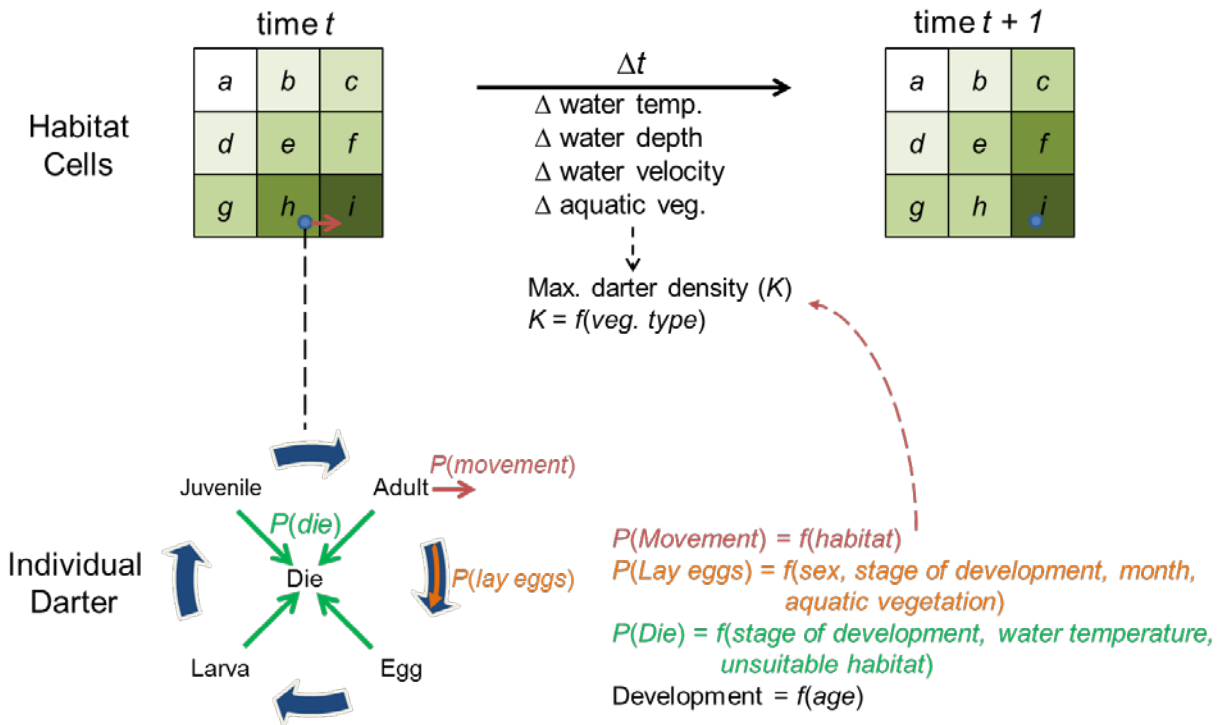


**Figure 1. Conceptual diagram of the spatially-explicit, individual-based, simulation model representing fountain darter population dynamics in response to changes in aquatic vegetation and hydrological conditions.**

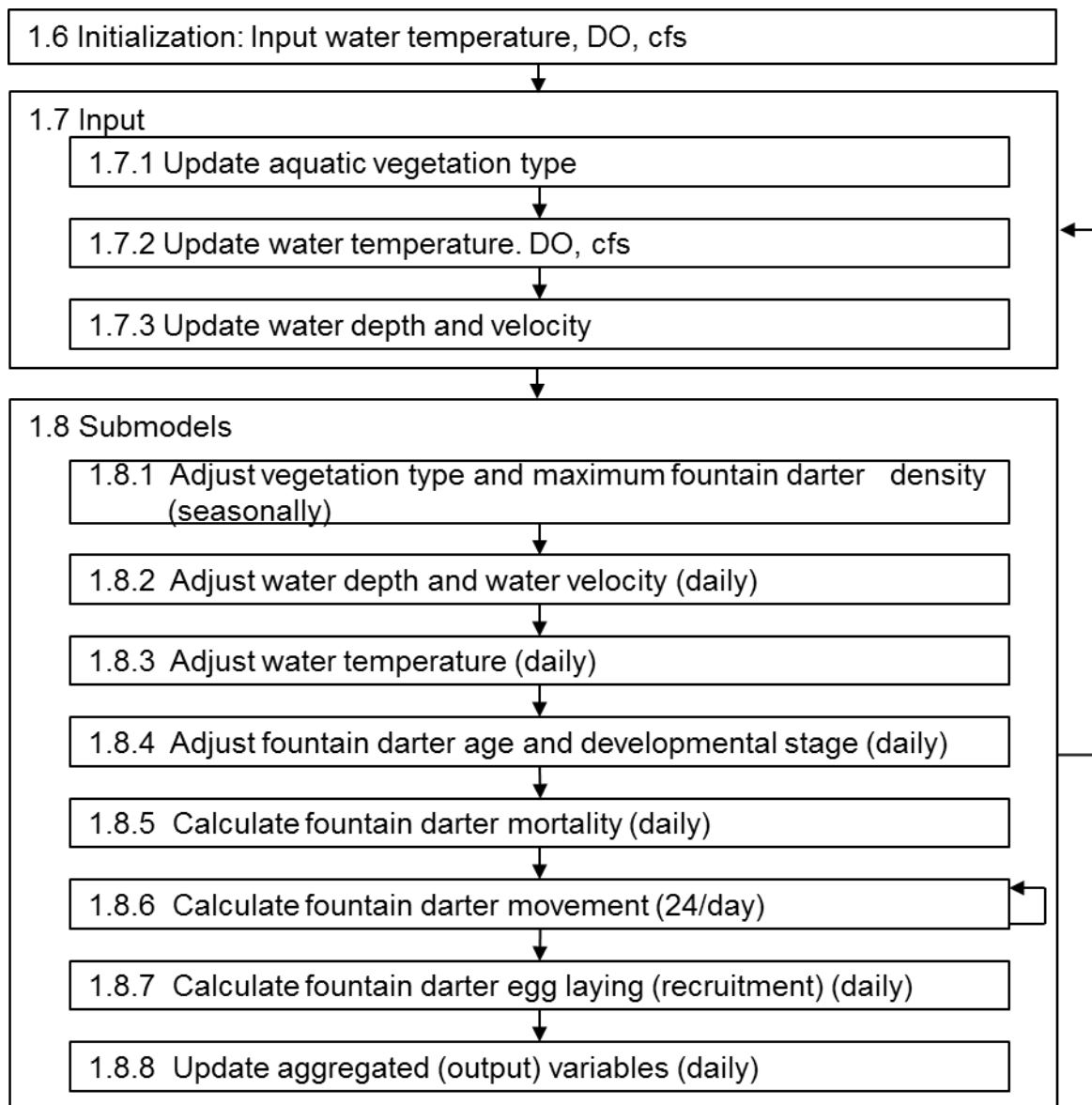
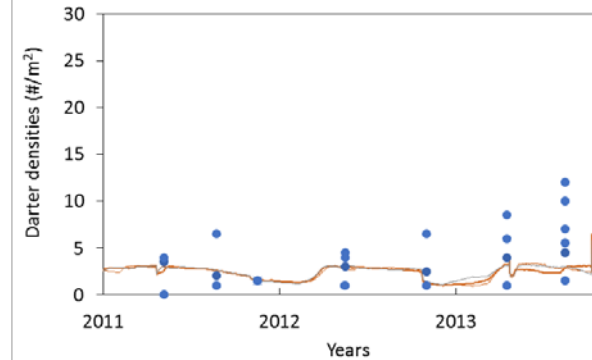


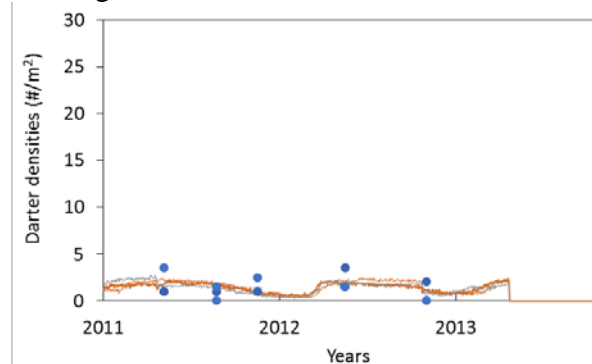
**Figure 2. Overview of the sequence of events and processes involved in the execution of the fountain darter population dynamics model.**



(a) Old Channel Reach  
Hygrophila



Ludwigia



Bryophytes

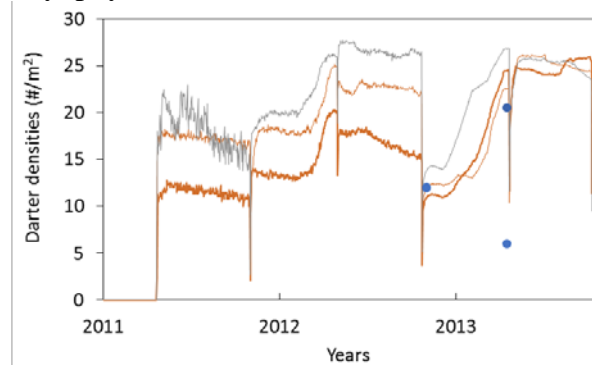
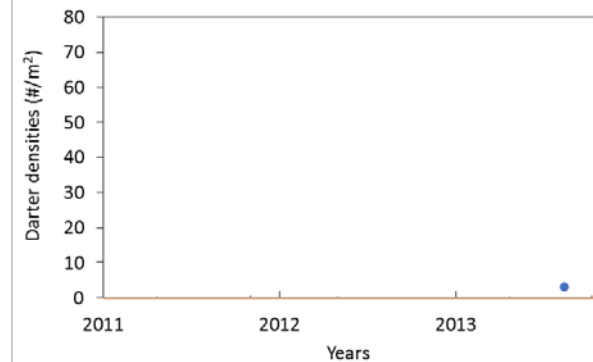
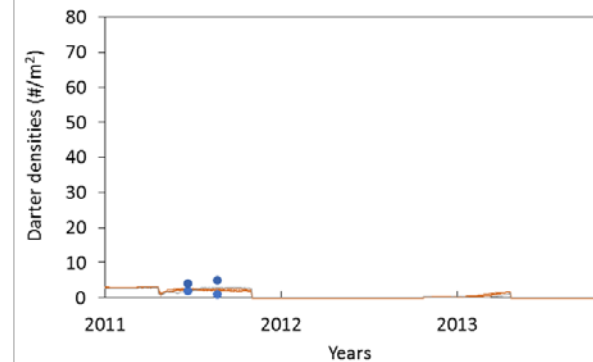


**Figure 4. Comparisons of simulated fountain darter densities within each of the indicated aquatic vegetation types within the (a) Old Channel Reach, (b) Upper Spring Run, and (c) Landa Lake reaches of the Comal River, and the (d) City Park and (e) I35 reaches of the San Marcos River from 2011 through 2013 to the densities of fountain darters captured in drop net samples collected from the corresponding aquatic vegetation types within the corresponding reaches from 2011 through 2013.**

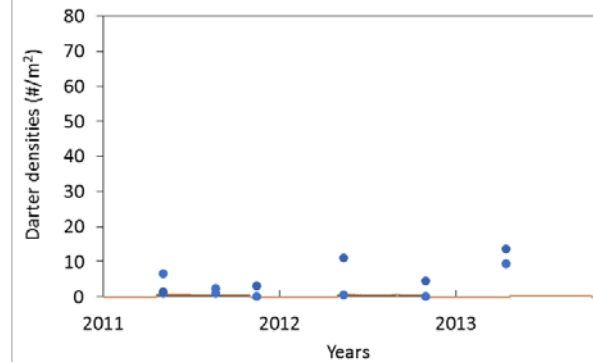
(b) Upper Spring Run  
Bare substrate



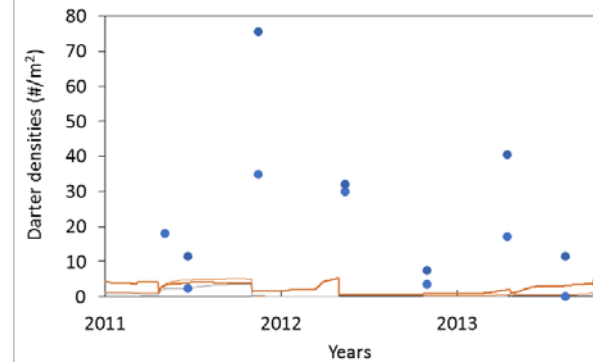
Filamentous algae



Hygrophila



Bryophytes



Sagittaria

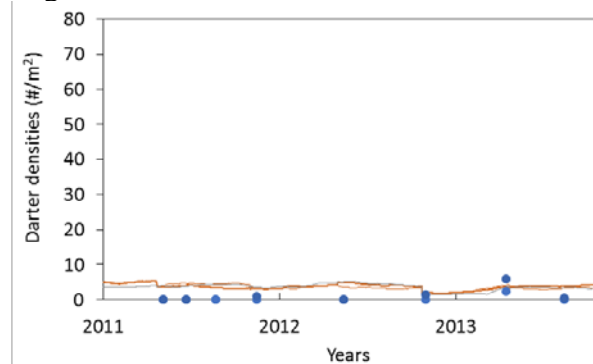
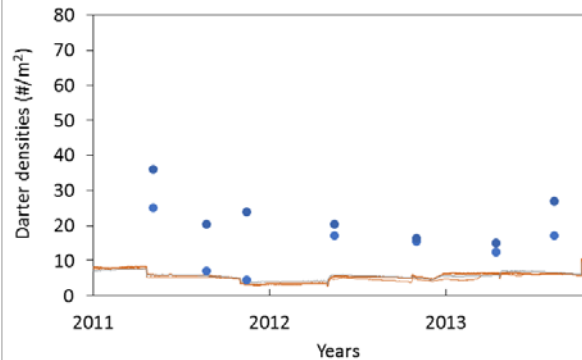
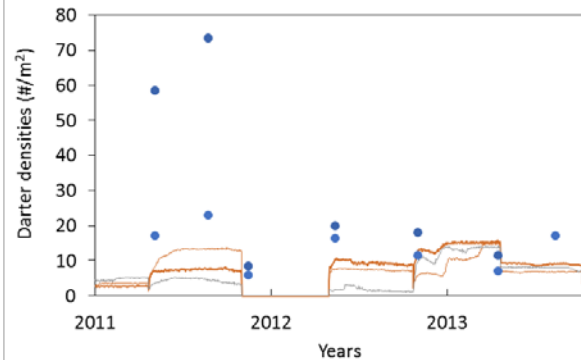


**Figure 4 (continued). Comparisons of simulated fountain darter densities within each of the indicated aquatic vegetation types within the (a) Old Channel Reach, (b) Upper Spring Run, and (c) Landa Lake reaches of the Comal River, and the (d) City Park and (e) I35 reaches of the San Marcos River from 2011 through 2013 to the densities of fountain darters captured in drop net samples collected from the corresponding aquatic vegetation types within the corresponding reaches from 2011 through 2013.**

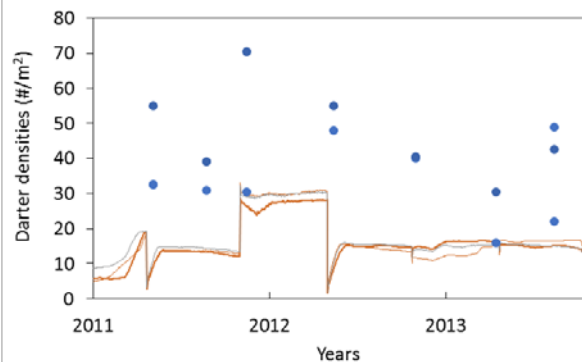
(c) Landa Lake  
Hygrophila



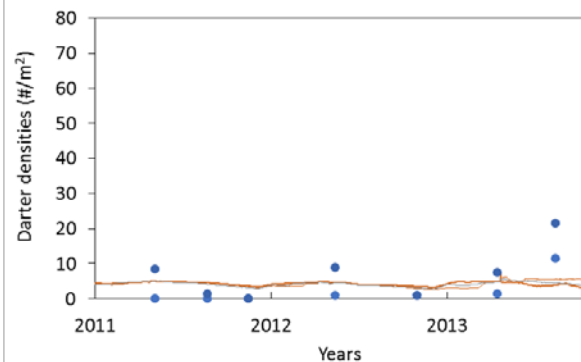
Ludwigia



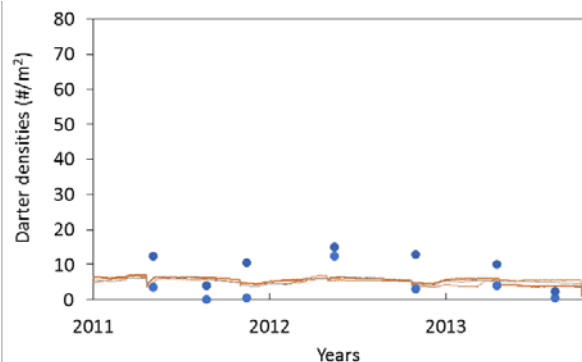
Bryophytes



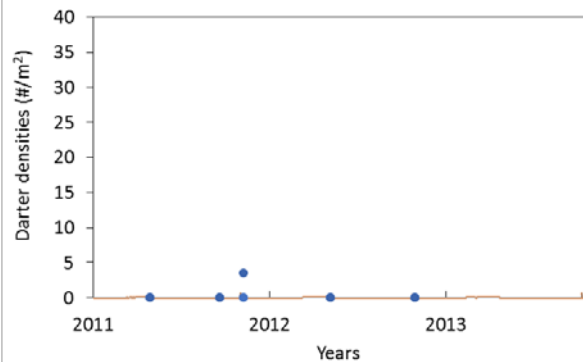
Vallisneria



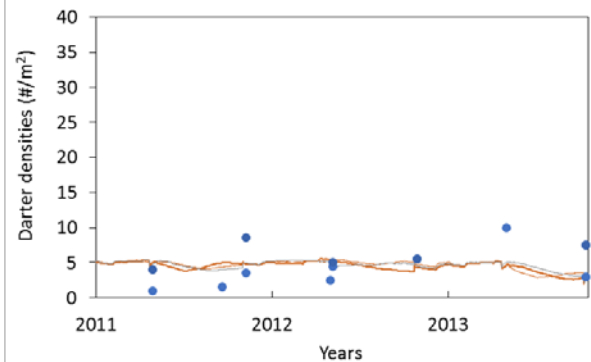
Cabomba



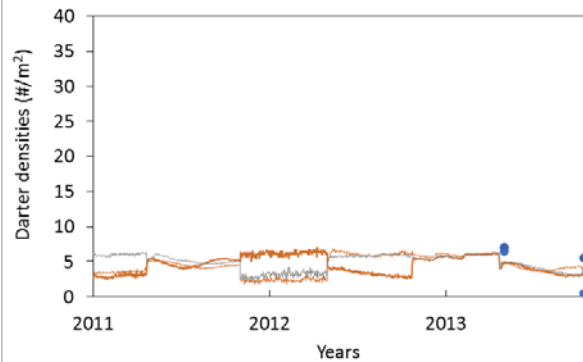
**Figure 4 (continued). Comparisons of simulated fountain darter densities within each of the indicated aquatic vegetation types within the (a) Old Channel Reach, (b) Upper Spring Run, and (c) Landa Lake reaches of the Comal River, and the (d) City Park and (e) I35 reaches of the San Marcos River from 2011 through 2013 to the densities of fountain darters captured in drop net samples collected from the corresponding aquatic vegetation types within the corresponding reaches from 2011 through 2013.**

(d) City Park  
Bare Substrate

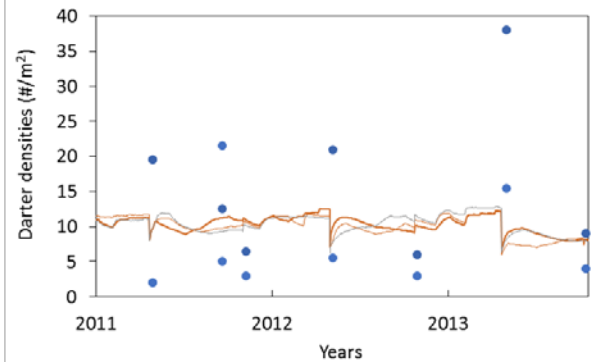
## Hygrophila



## Sagittaria



## Hydrilla



## Potamogeton

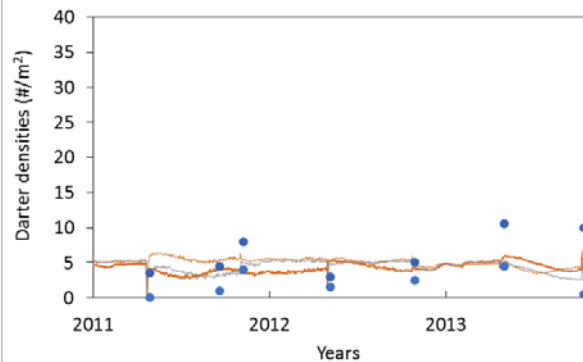
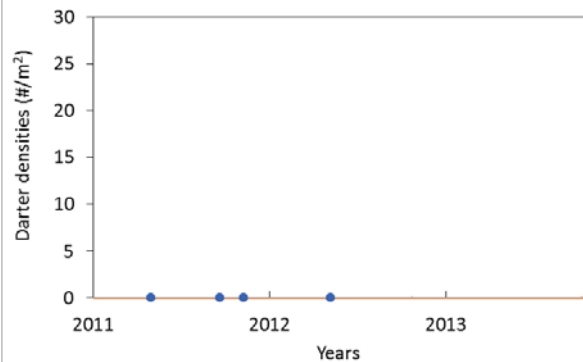
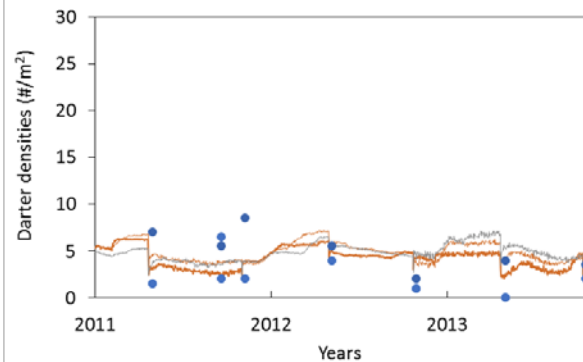


**Figure 4 (continued).** Comparisons of simulated fountain darter densities within each of the indicated aquatic vegetation types within the (a) Old Channel Reach, (b) Upper Spring Run, and (c) Landa Lake reaches of the Comal River, and the (d) City Park and (e) I35 reaches of the San Marcos River from 2011 through 2013 to the densities of fountain darters captured in drop net samples collected from the corresponding aquatic vegetation types within the corresponding reaches from 2011 through 2013.

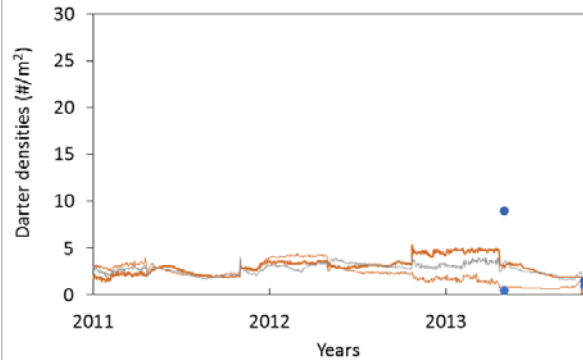
(e) I35 Reach  
Bare Substrate



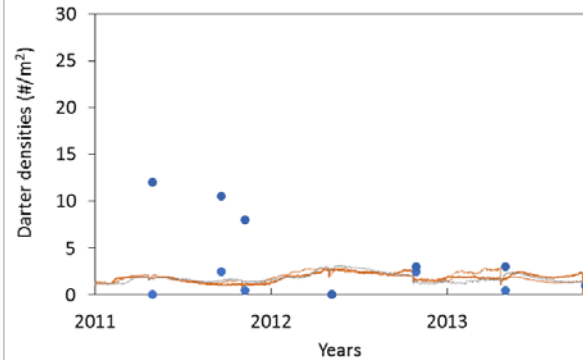
Hygrophila



Sagittaria



Hydrilla



Cabomba

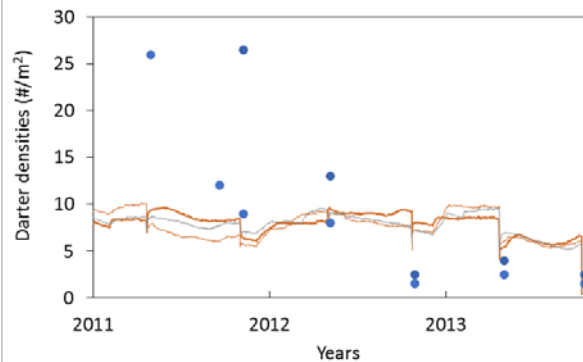


**Figure 4 (continued). Comparisons of simulated fountain darter densities within each of the indicated aquatic vegetation types within the (a) Old Channel Reach, (b) Upper Spring Run, and (c) Landa Lake reaches of the Comal River, and the (d) City Park and (e) I35 reaches of the San Marcos River from 2011 through 2013 to the densities of fountain darters captured in drop net samples collected from the corresponding aquatic vegetation types within the corresponding reaches from 2011 through 2013.**

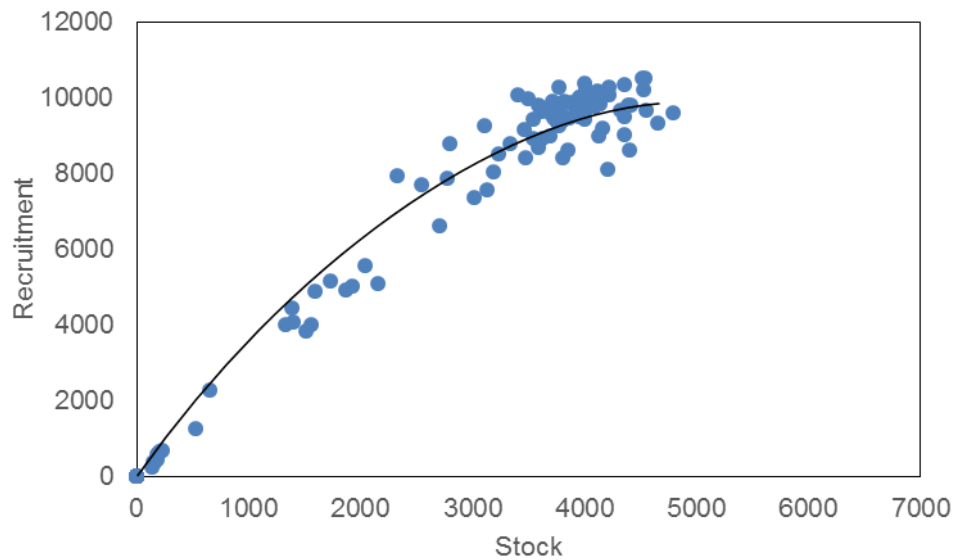
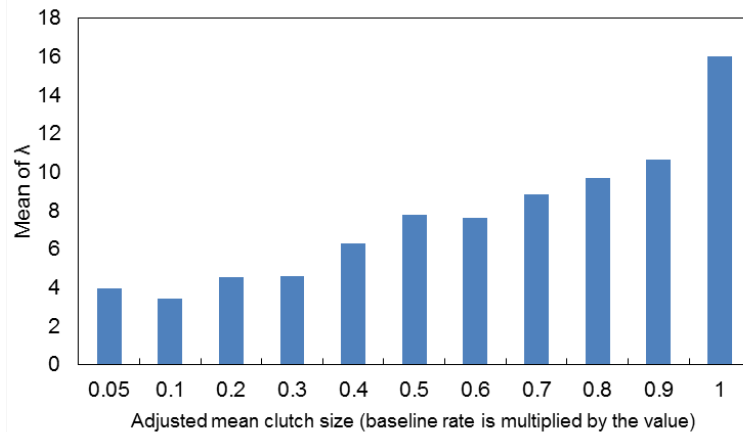
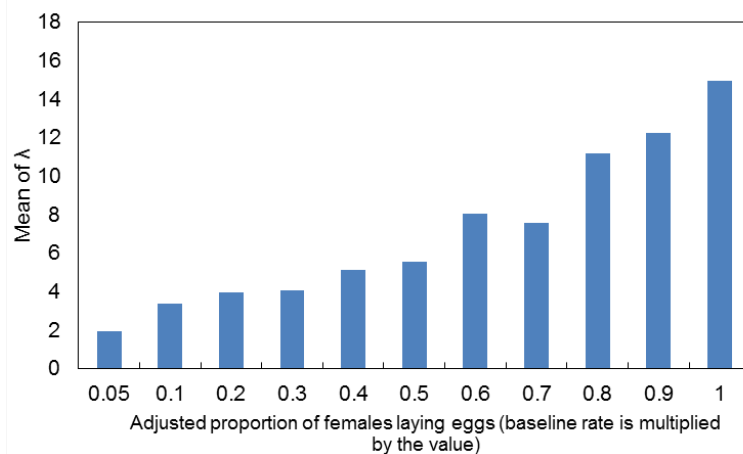


**Figure 5. Comparison of the simulated stock-recruitment relationship to the range of stock-recruitment relationships that might be expected for fountain darters based on their life history. The expected steepness coefficient is between 0.5 and 0.7 (Rose et al. 2001, Kenny Rose, pers. comm.). These simulations yielded a Beverton-Holt type spawner-recruit relationship with a steepness coefficient of 0.3948 ( $r^2 = 0.96$ ). The version of the model representing the Old Channel Reach of the Comal River was used to generate these results.**

(a) Mean clutch size



(b) Proportion of females laying eggs



(c) Base mortality rates of egg stage

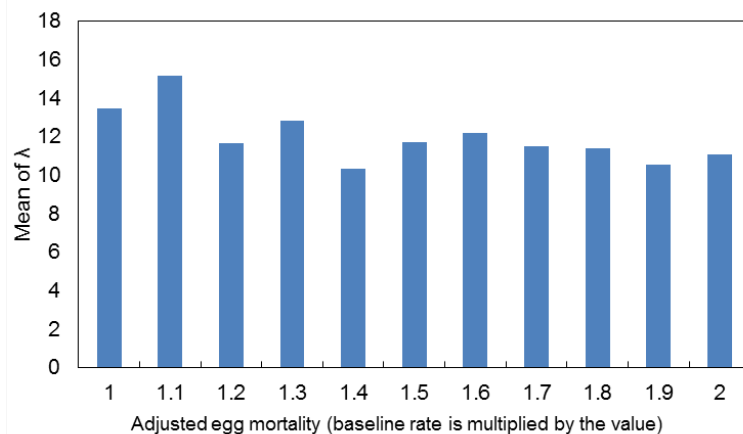
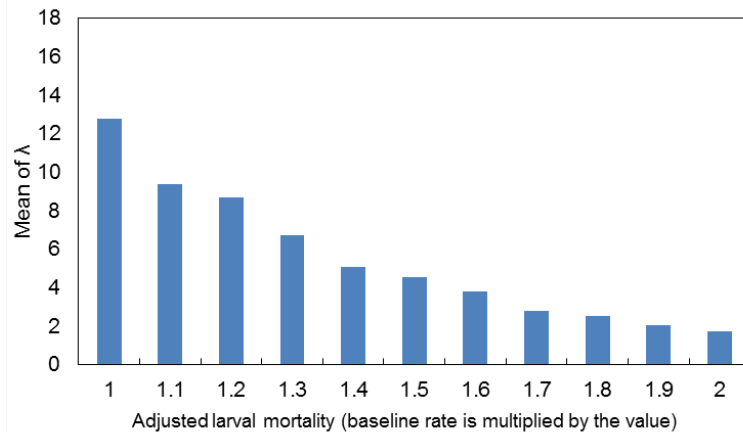
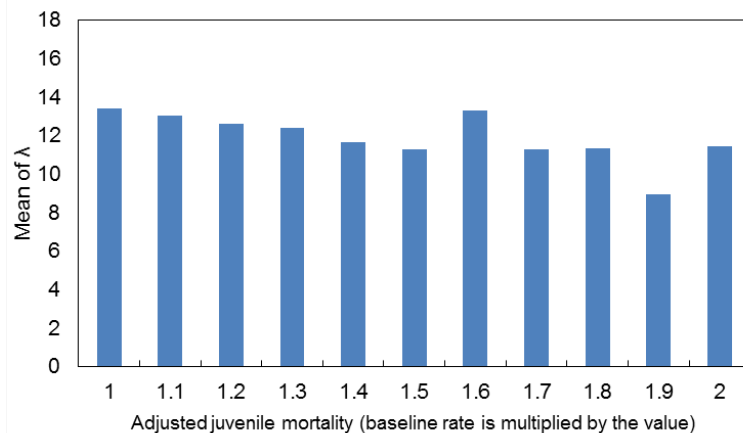


**Figure 6. Sensitivity of model predictions of annual population growth rate ( $\lambda$ ) of fountain darters to changes in 11 demographic/life history parameters and 2 environmental variables: (a) mean clutch size, (b) proportion of females laying eggs, base mortality rates of (c) egg, (d) larval, (e) juvenile, and (f) adult life stages, duration of (g) egg, (h) larval, (i) juvenile, and (j) young adult life stages, (k) water temperature, and (l) DO level. The version of the model representing the Old Channel Reach of the Comal River was used to generate these results.**

(d) Base mortality rates of larval stage



(e) Base mortality rates of juvenile stage



(f) Base mortality rates of adult stage

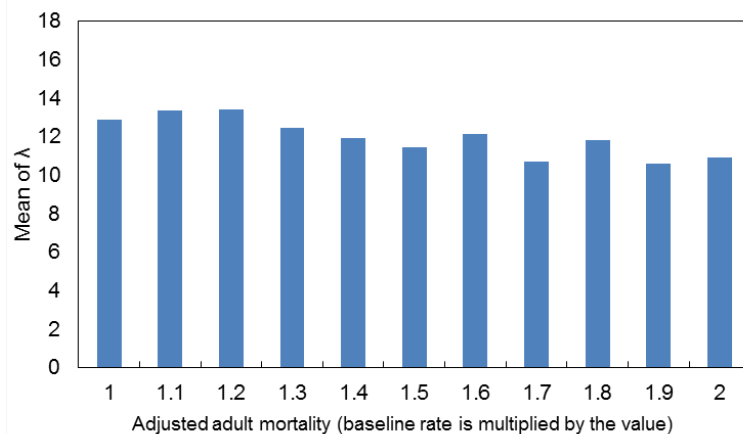
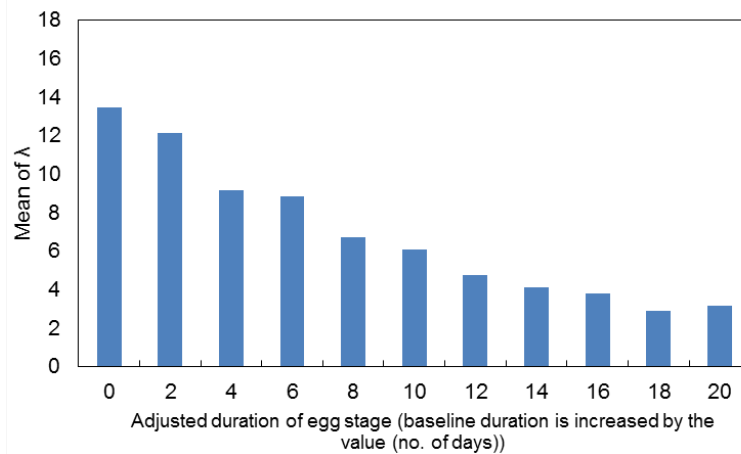
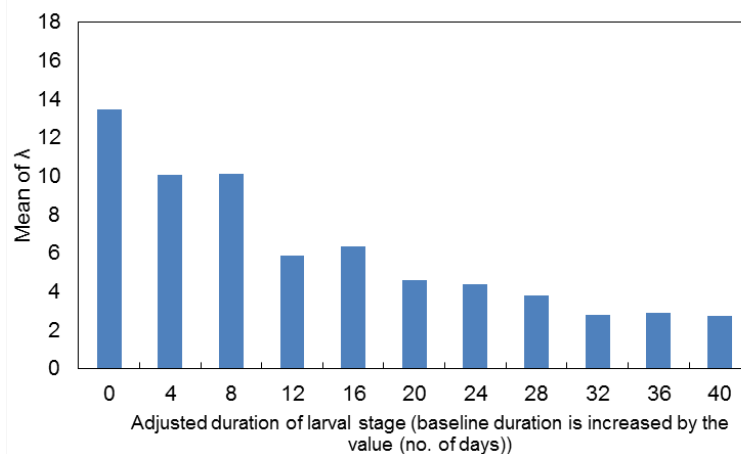


**Figure 6 (continued). Sensitivity of model predictions of annual population growth rate ( $\lambda$ ) of fountain darters to changes in 11 demographic/life history parameters and 2 environmental variables: (a) mean clutch size, (b) proportion of females laying eggs, base mortality rates of (c) egg, (d) larval, (e) juvenile, and (f) adult life stages, duration of (g) egg, (h) larval, (i) juvenile, and (j) young adult life stages, (k) water temperature, and (l) DO level. The version of the model representing the Old Channel Reach of the Comal River was used to generate these results.**

(g) Duration of egg stage



(h) Duration of larval stage



(i) Duration of juvenile stage

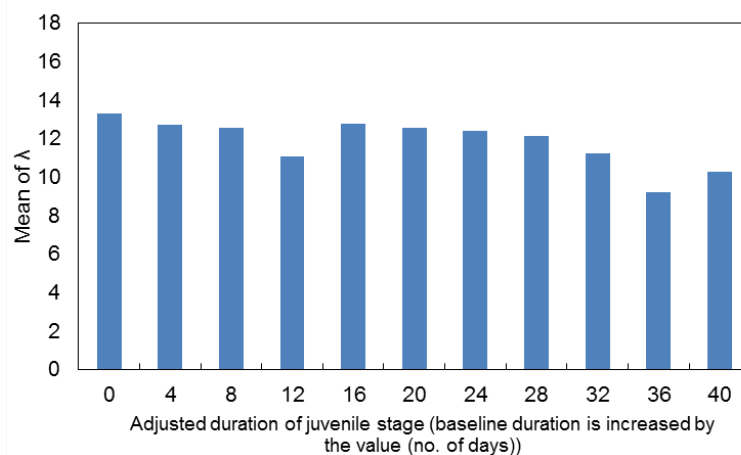
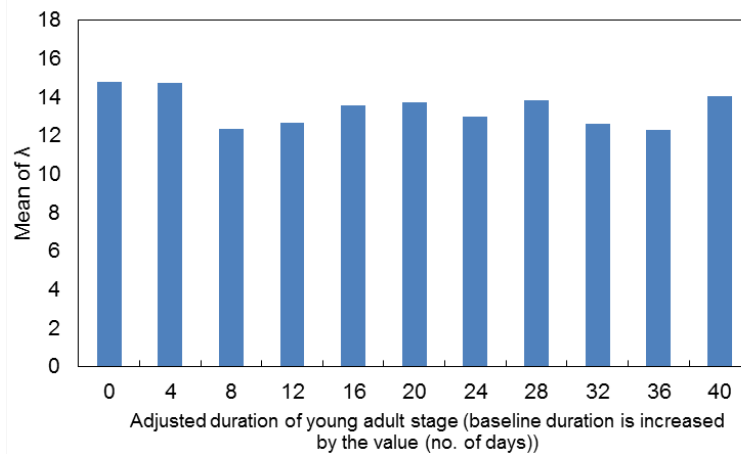
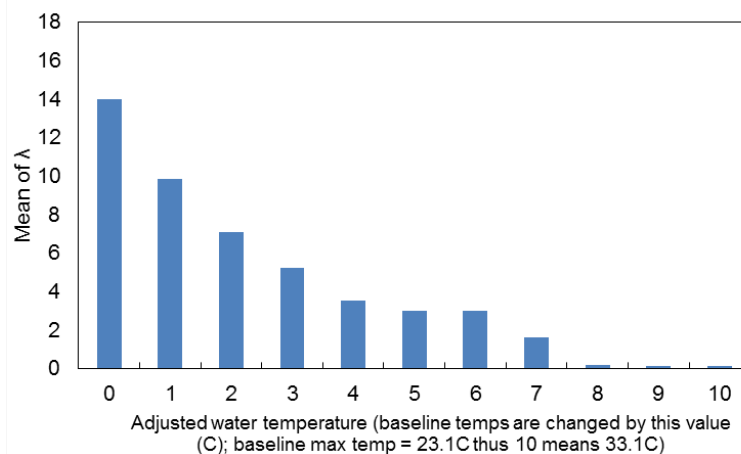


**Figure 6 (continued). Sensitivity of model predictions of annual population growth rate ( $\lambda$ ) of fountain darters to changes in 11 demographic/life history parameters and 2 environmental variables: (a) mean clutch size, (b) proportion of females laying eggs, base mortality rates of (c) egg, (d) larval, (e) juvenile, and (f) adult life stages, duration of (g) egg, (h) larval, (i) juvenile, and (j) young adult life stages, (k) water temperature, and (l) DO level. The version of the model representing the Old Channel Reach of the Comal River was used to generate these results.**

## (j) Duration of young adult life stage



## (k) Water temperature



## (l) DO level

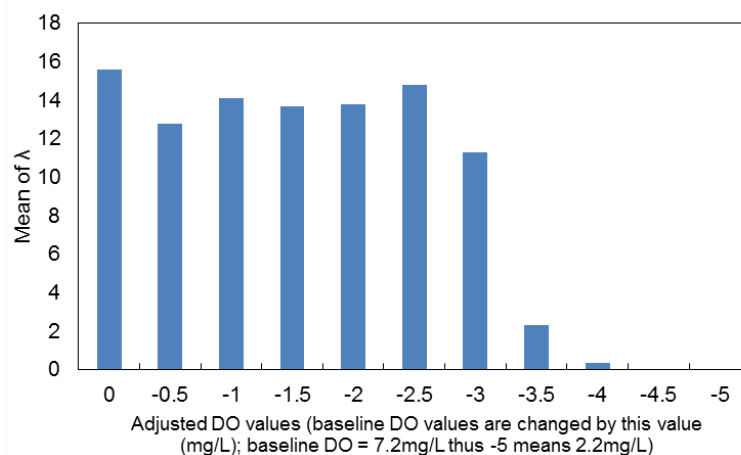


**Figure 6 (continued). Sensitivity of model predictions of annual population growth rate ( $\lambda$ ) of fountain darters to changes in 11 demographic/life history parameters and 2 environmental variables: (a) mean clutch size, (b) proportion of females laying eggs, base mortality rates of (c) egg, (d) larval, (e) juvenile, and (f) adult life stages, duration of (g) egg, (h) larval, (i) juvenile, and (j) young adult life stages, (k) water temperature, and (l) DO level. The version of the model representing the Old Channel Reach of the Comal River was used to generate these results.**

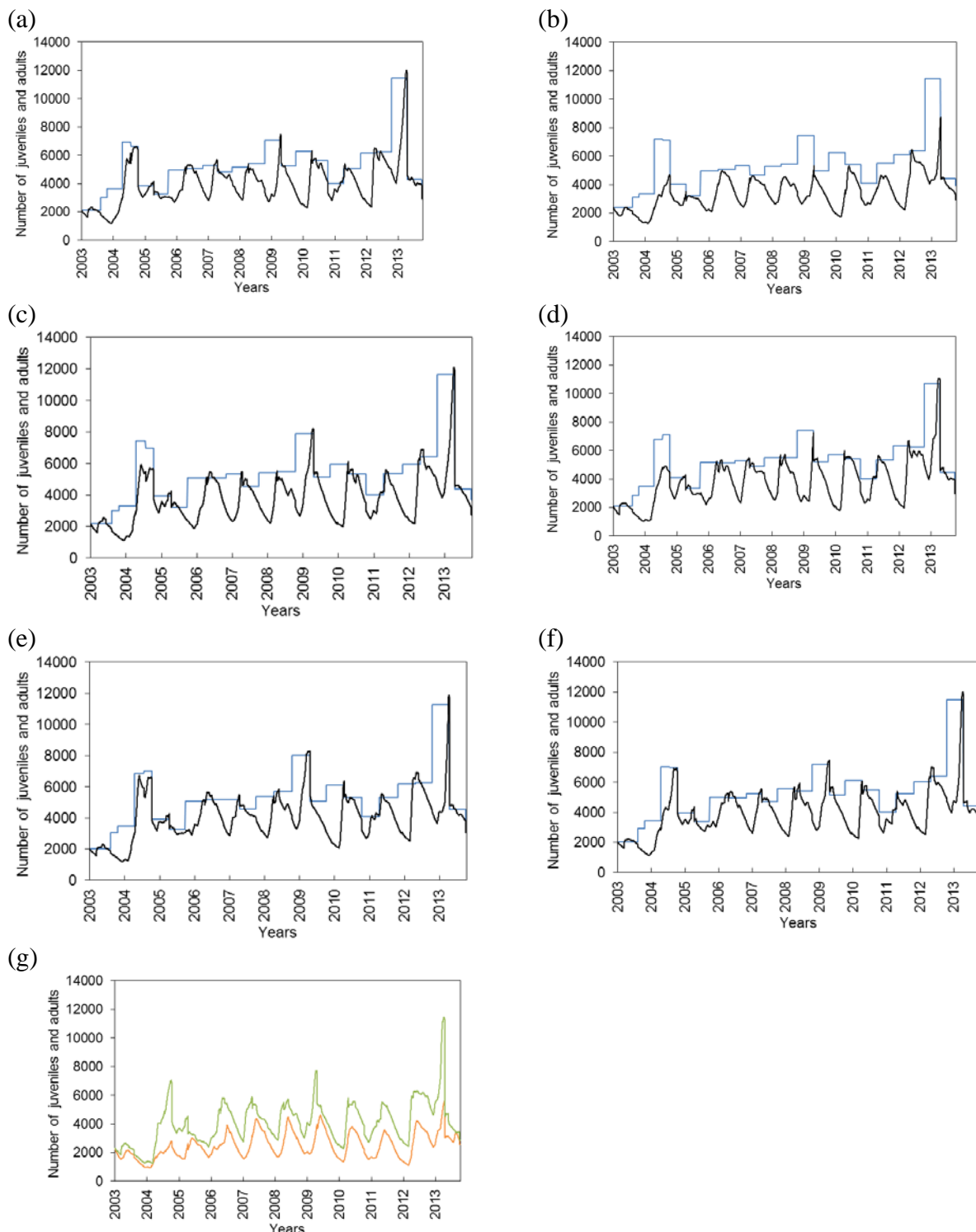


**Figure 7. Sensitivity of model predictions of population dynamics of fountain darters to the implementation of several hypothesized forms of density-dependent negative feedback on population growth rate. As density of juveniles plus adults increased, base mortality rates of (a) eggs, (b) larvae, (c) juveniles, or (d) adults increased, or (e) the mean number of eggs laid per female or (f) the proportion of females laying eggs decreased. In graphs (a) through (f), black lines indicate the number of juvenile plus adult darters and blue lines indicate the maximum number of juvenile plus adult darters that could be supported by the aquatic vegetation present at the time. (g) Comparison of model predictions of population dynamics when all six forms of negative feedback occurred simultaneously (orange line) versus when none of the forms of negative feedback were included (green line). The version of the model representing the Old Channel Reach of the Comal River was used to generate these results. See text for descriptions of the functional forms of negative feedbacks.**

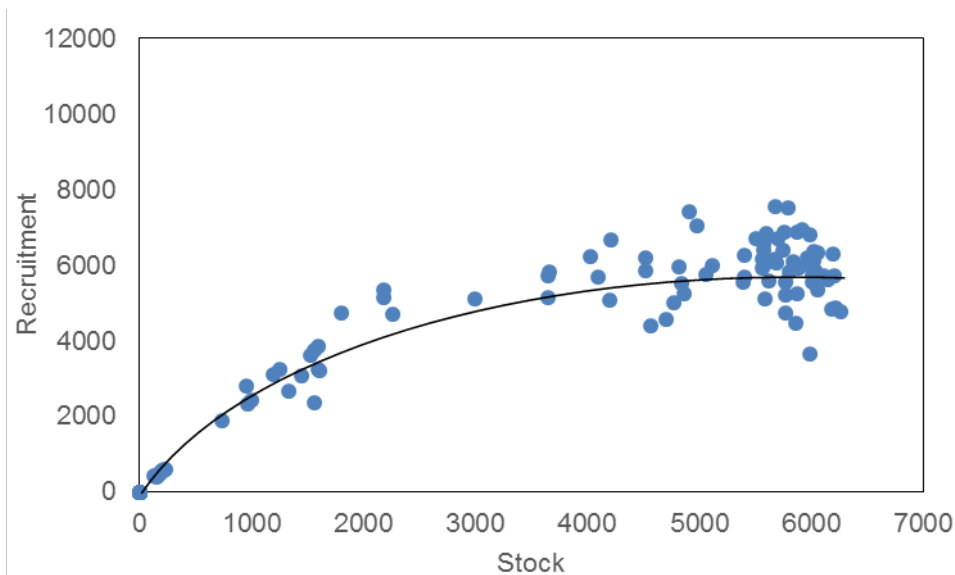
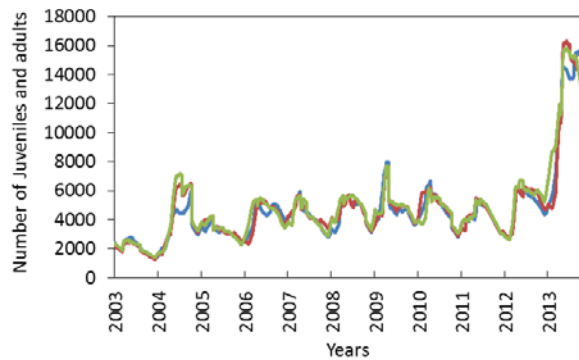


**Figure 8.** Comparison of the simulated stock-recruitment relationship, when all of the six density-dependent effects are implemented in the model, to the range of stock-recruitment relationships that might be expected for fountain darters based on their life history. See text for descriptions of the functional forms of the density-dependent effects. The expected steepness coefficient is between 0.5 and 0.7 (Rose et al. 2001, Kenny Rose, pers. comm.). These simulations yielded a Beverton-Holt type spawner-recruit relationship with a steepness coefficient of 0.4874 ( $r^2 = 0.90$ ). The version of the model representing the Old Channel Reach of the Comal River was used to generate these results.

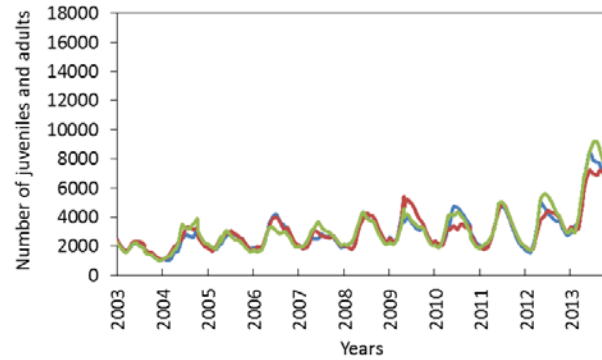
Old Channel Reach, Comal River  
Without DD effect

With DD effect

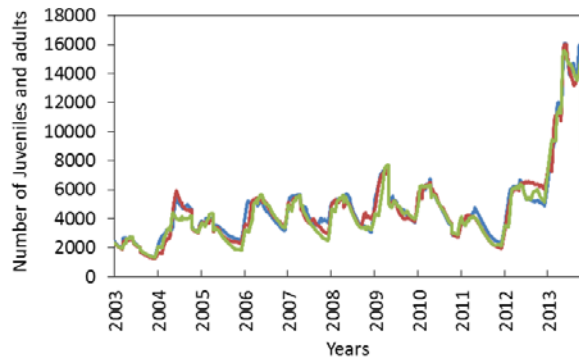
Baseline (historical) conditions



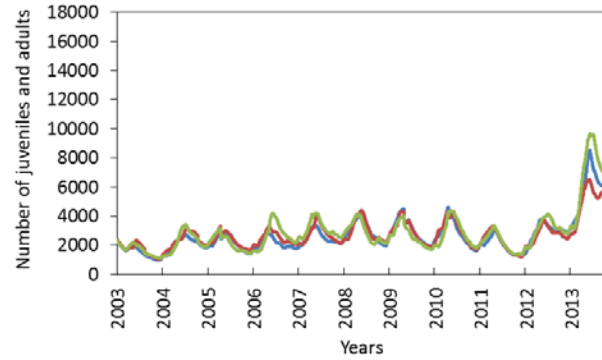
Baseline (historical) conditions



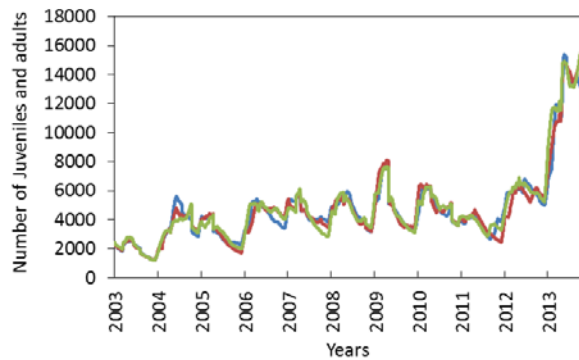
HCP drought conditions



HCP drought conditions



HCP long-term average conditions



HCP long-term average conditions

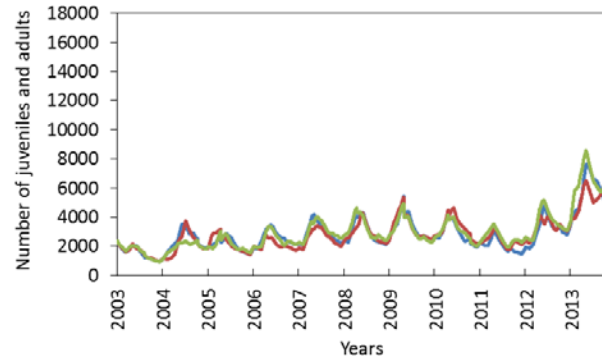
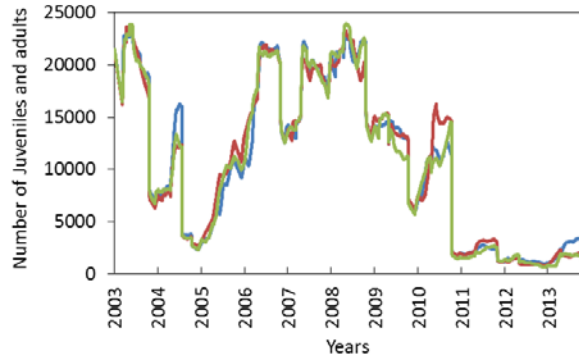


**Figure 9. Comparisons of simulated population dynamics (changes in number of juvenile + adult fountain darters in the reach) within the Old Channel Reach of the Comal River from 2011 through 2013 under HCP long-term average conditions, HCP drought conditions, and baseline conditions (historical [2003 to 2013] aquatic vegetation and hydrological conditions). Graphs show 3 replicate stochastic (Monte Carlo) simulations of each of these scenarios using versions of the model without any density-dependent (DD) effects (left column) and with all six DD effects implemented (right column). (See text for description of DD effects on population growth.)**

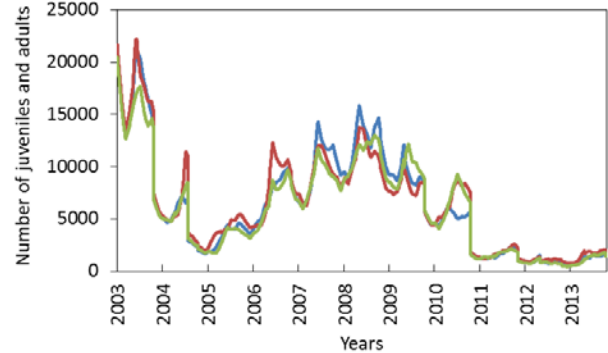
Upper Spring Run Reach, Comal River  
Without DD effect

With DD effect

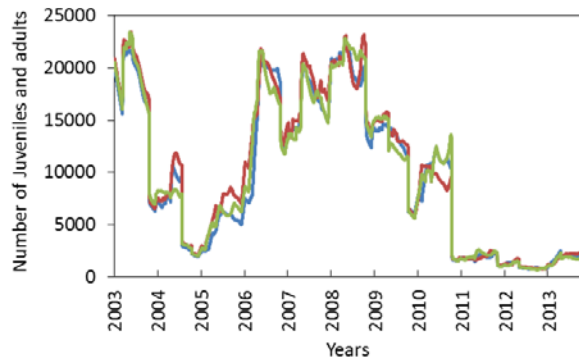
Baseline (historical) conditions



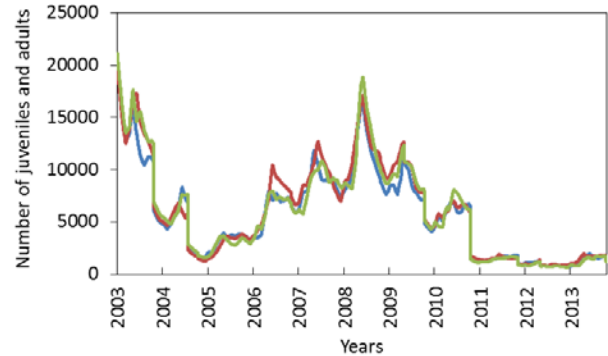
Baseline (historical) conditions



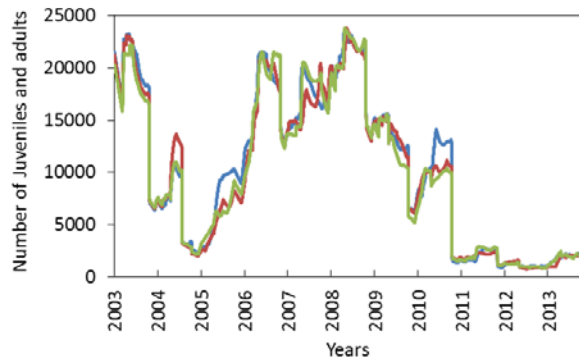
HCP drought conditions



HCP drought conditions



HCP long-term average conditions



HCP long-term average conditions

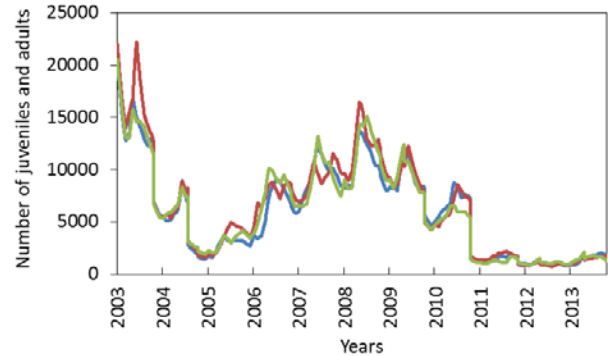
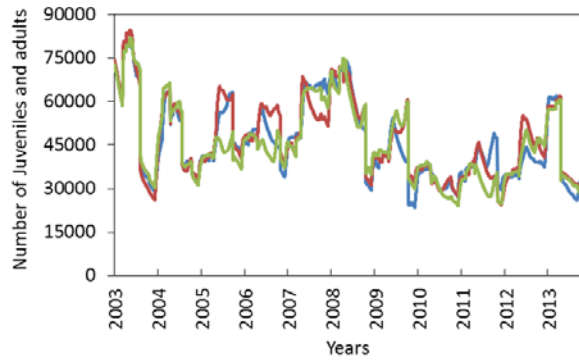


**Figure 10. Comparisons of simulated population dynamics (changes in number of juvenile + adult fountain darters in the reach) within the Upper Spring Run Reach of the Comal River from 2011 through 2013 under HCP long-term average conditions, HCP drought conditions, and baseline conditions (historical [2003 to 2013] aquatic vegetation and hydrological conditions). Graphs show 3 replicate stochastic (Monte Carlo) simulations of each of these scenarios using versions of the model without any density-dependent (DD) effects (left column) and with all six DD effects implemented (right column). (See text for description of DD effects on population growth.)**

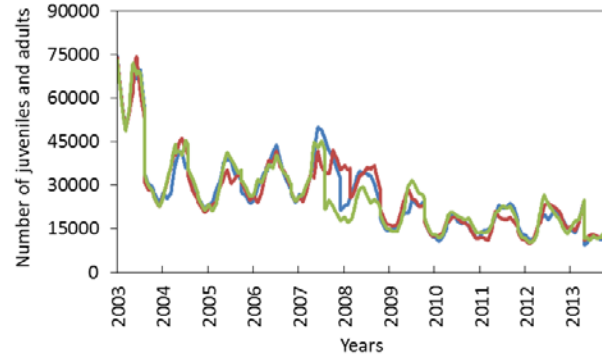
Landa Lake Reach, Comal River  
Without DD effect

With DD effect

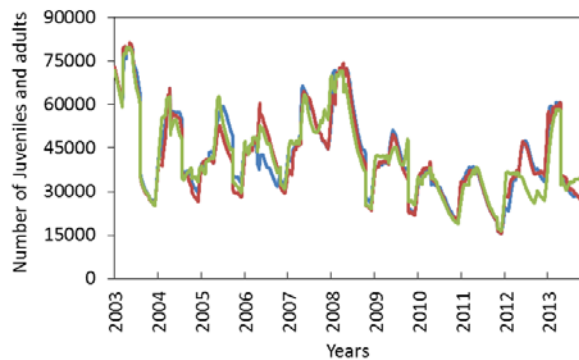
Baseline (historical) conditions



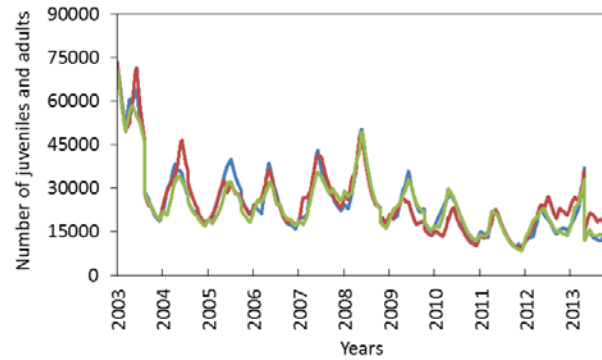
Baseline (historical) conditions



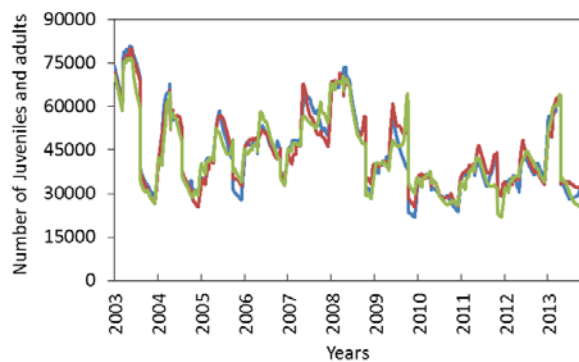
HCP drought conditions



HCP drought conditions



HCP long-term average conditions



HCP long-term average conditions

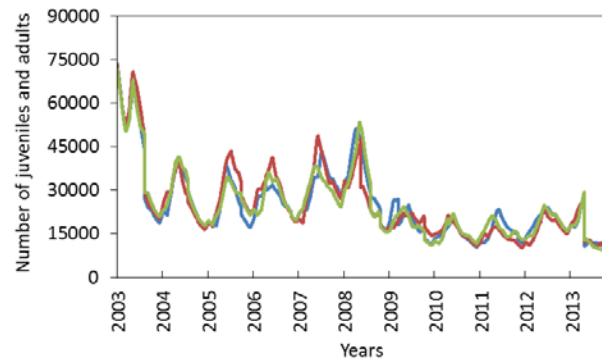
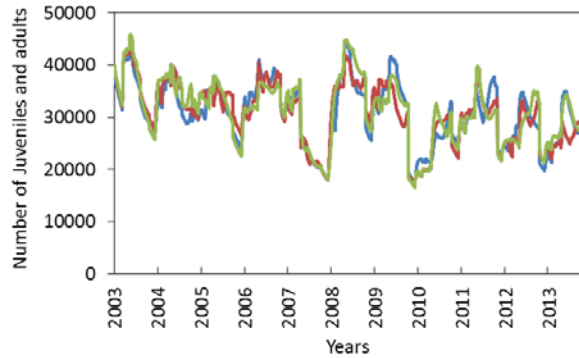


**Figure 11. Comparisons of simulated population dynamics (changes in number of juvenile + adult fountain darters in the reach) within the Landa Lake Reach of the Comal River from 2011 through 2013 under HCP long-term average conditions, HCP drought conditions, and baseline conditions (historical [2003 to 2013] aquatic vegetation and hydrological conditions). Graphs show 3 replicate stochastic (Monte Carlo) simulations of each of these scenarios using versions of the model without any density-dependent (DD) effects (left column) and with all six DD effects implemented (right column). (See text for description of DD effects on population growth.)**

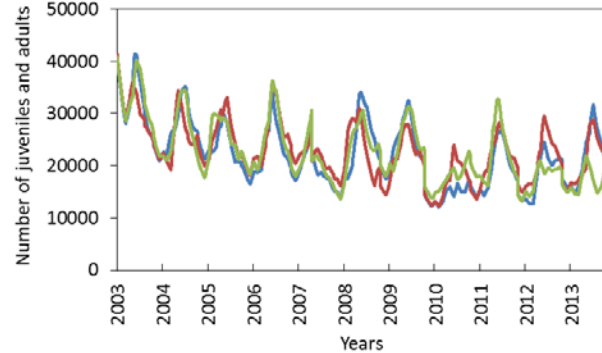
City Park Reach, San Marcos River  
Without DD effect

With DD effect

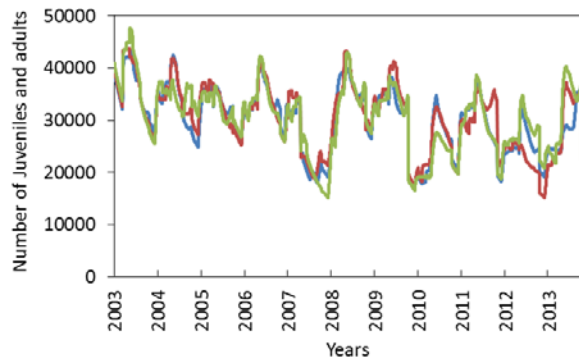
Baseline (historical) conditions



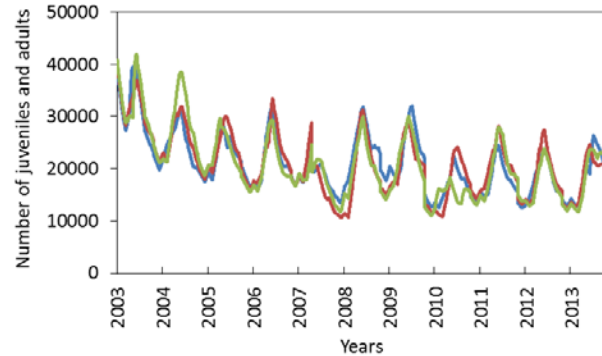
Baseline (historical) conditions



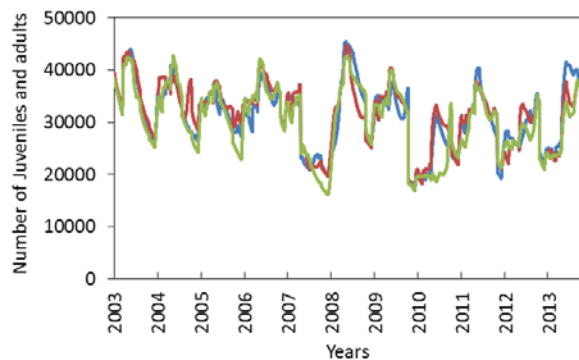
HCP drought conditions



HCP drought conditions



HCP long-term average conditions



HCP long-term average conditions

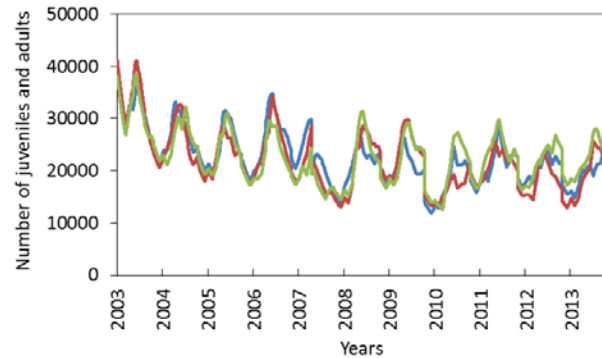
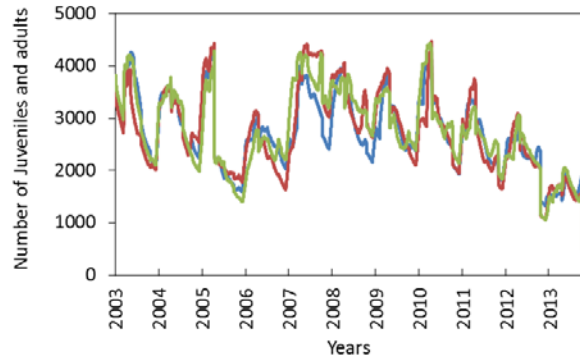


**Figure 12. Comparisons of simulated population dynamics (changes in number of juvenile + adult fountain darters in the reach) within the City Park Reach of the San Marcos River from 2011 through 2013 under HCP long-term average conditions, HCP drought conditions, and baseline conditions (historical [2003 to 2013] aquatic vegetation and hydrological conditions). Graphs show 3 replicate stochastic (Monte Carlo) simulations of each of these scenarios using versions of the model without any density-dependent (DD) effects (left column) and with all six DD effects implemented (right column). (See text for description of DD effects on population growth.)**

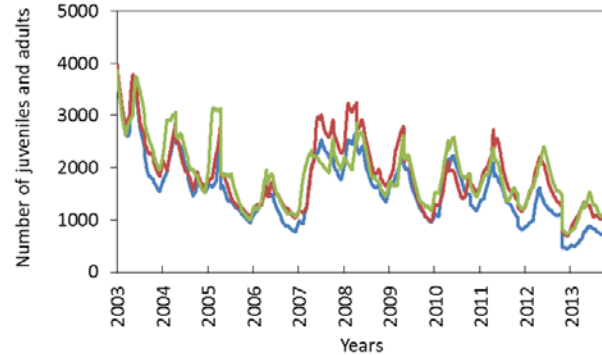
I35 Reach, San Marcos River  
Without DD effect

With DD effect

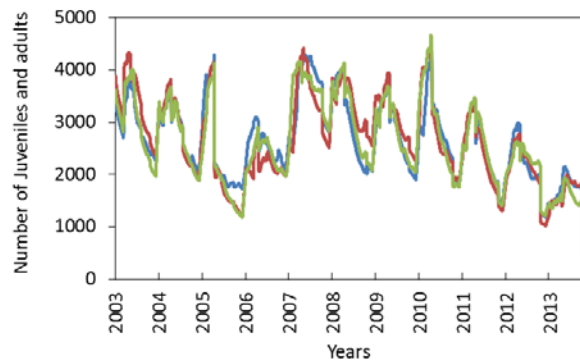
Baseline (historical) conditions



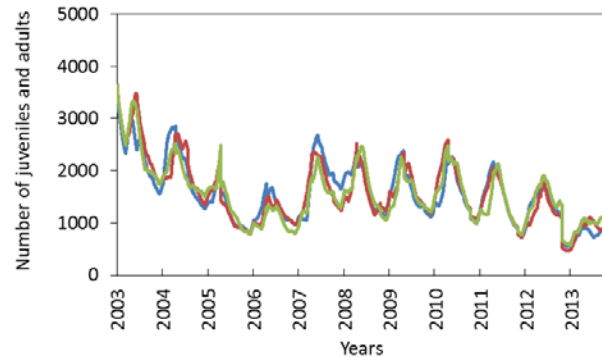
Baseline (historical) conditions



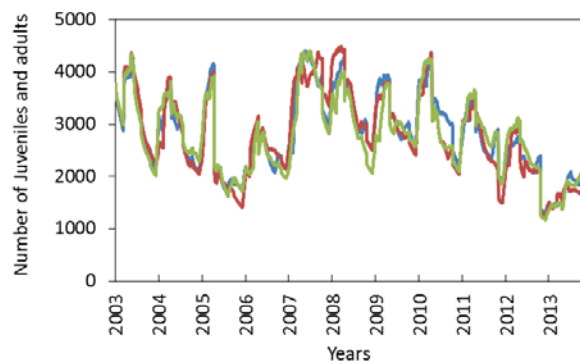
HCP drought conditions



HCP drought conditions



HCP long-term average conditions



HCP long-term average conditions

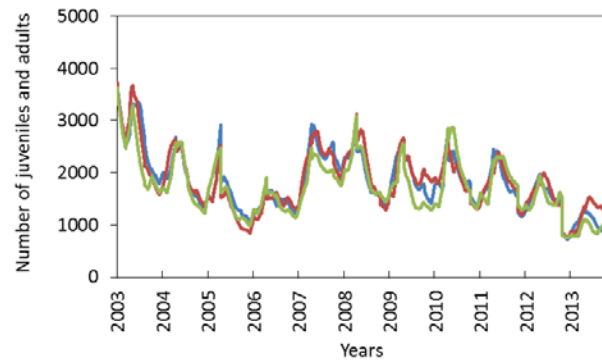
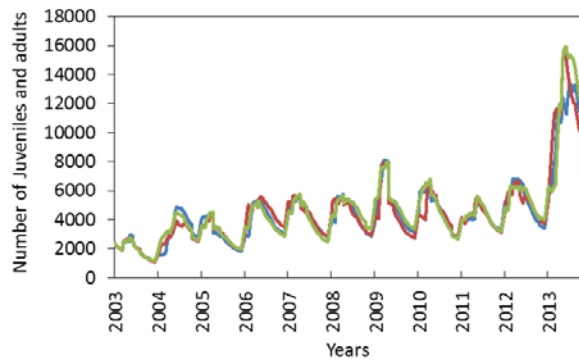


**Figure 13. Comparisons of simulated population dynamics (changes in number of juvenile + adult fountain darters in the reach) within the I35 Reach of the San Marcos River from 2011 through 2013 under HCP long-term average conditions, HCP drought conditions, and baseline conditions (historical [2003 to 2013] aquatic vegetation and hydrological conditions). Graphs show 3 replicate stochastic (Monte Carlo) simulations of each of these scenarios using versions of the model without any density-dependent (DD) effects (left column) and with all six DD effects implemented (right column). (See text for description of DD effects on population growth.)**

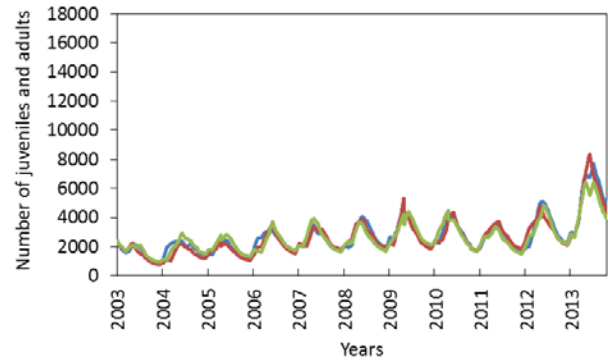
Old Channel Reach, Comal River  
Without DD effect

With DD effect

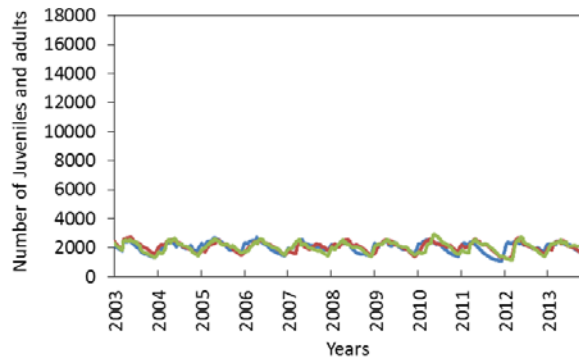
High Temperature



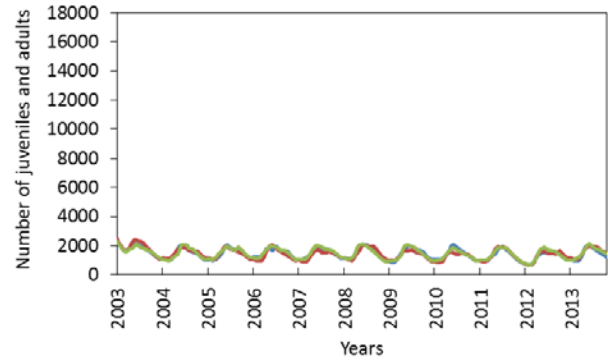
High Temperature



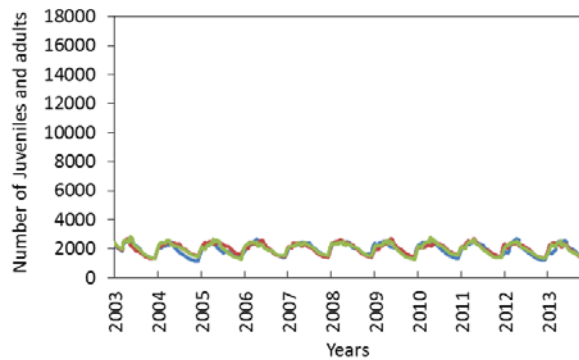
Bad Vegetation



Bad Vegetation



Bad Vegetation + High Temperature



Bad Vegetation + High Temperature

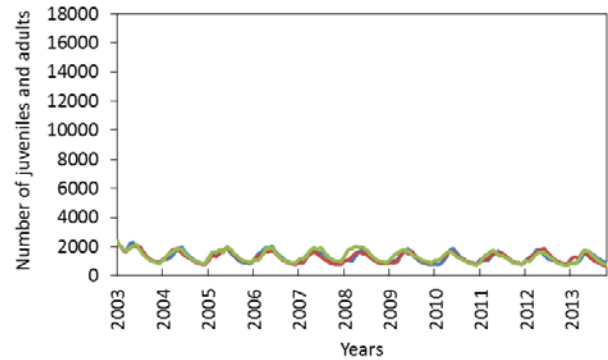
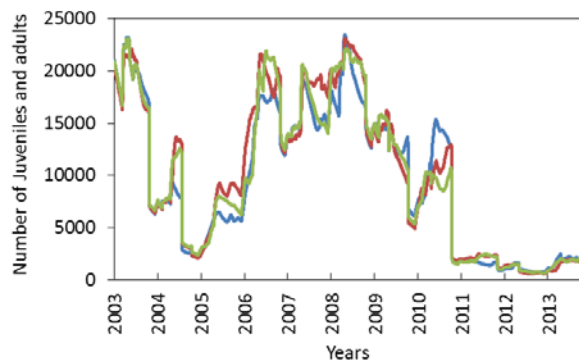


**Figure 14.** Comparisons of simulated population dynamics (changes in number of juvenile + adult fountain darters in the reach) within the Old Channel Reach of the Comal River from 2011 through 2013 under three “worst case” scenarios in which baseline conditions (historical [2003 to 2013] aquatic vegetation and hydrological conditions) were modified. Modifications included replacing the historical sequence of water temperatures with an annually-repeating sequence of daily water temperatures that represented the year with the highest water temperature observed in the reach from 2003 to 2013 (High Temperature), replacing the historical sequence of aquatic vegetation changes with an unchanging aquatic vegetation community that represented the worst fountain darter habitat observed in the reach from 2003 to 2013 (Bad Vegetation), and implementing both the aquatic vegetation and water temperature modifications (Bad Vegetation + High Temperature). Graphs show 3 replicate stochastic (Monte Carlo) simulations of each of these scenarios using versions of the model without any density-dependent (DD) effects (left column) and with all six DD effects implemented (right column). (See text for description of DD effects on population growth.)

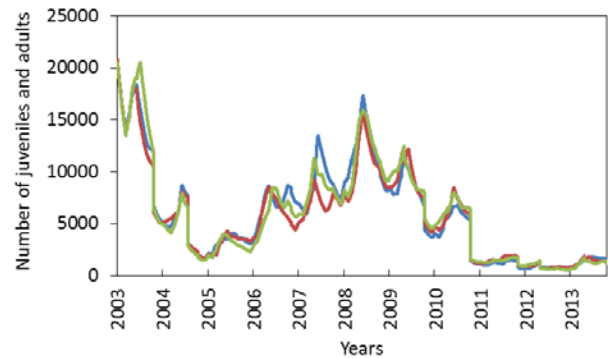
Upper Spring Run Reach, Comal River  
Without DD effect

With DD effect

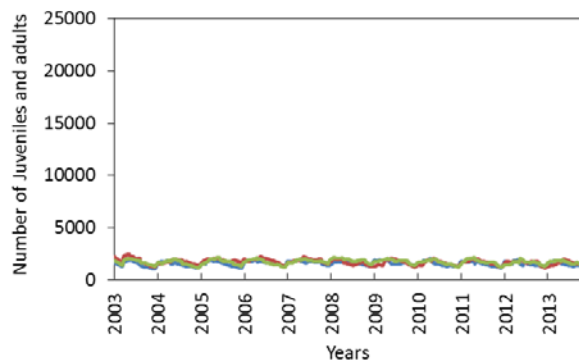
High Temperature



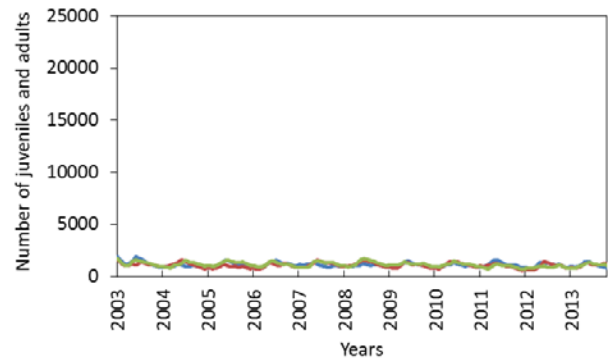
High Temperature



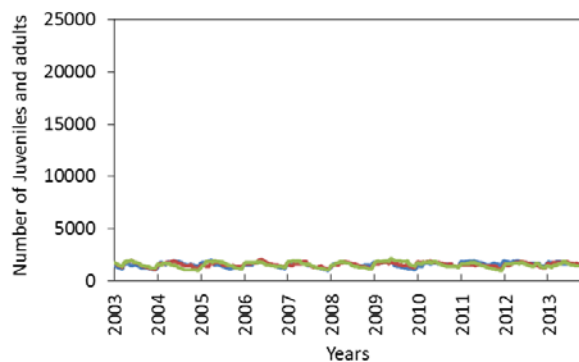
Bad Vegetation



Bad Vegetation



Bad Vegetation + High Temperature



Bad Vegetation + High Temperature

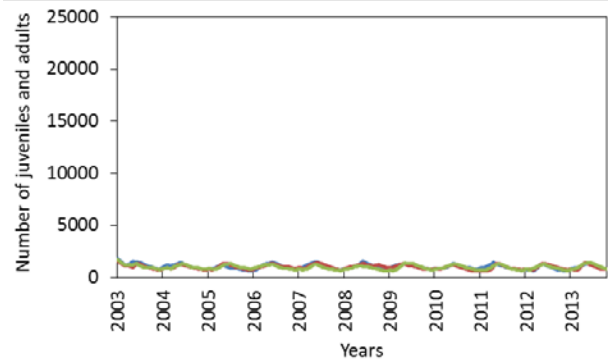
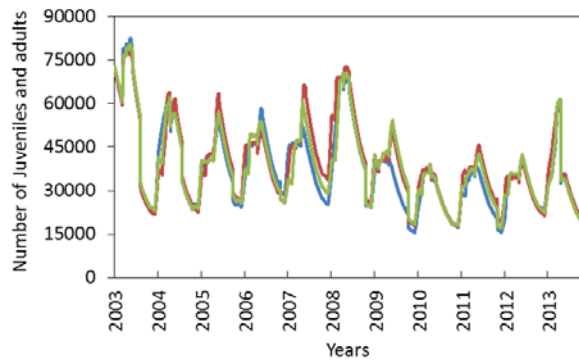


**Figure 15.** Comparisons of simulated population dynamics (changes in number of juvenile + adult fountain darters in the reach) within the Upper Spring Run Reach of the Comal River from 2011 through 2013 under three “worst case” scenarios in which baseline conditions (historical [2003 to 2013] aquatic vegetation and hydrological conditions) were modified. Modifications included replacing the historical sequence of water temperatures with an annually-repeating sequence of daily water temperatures that represented the year with the highest water temperature observed in the reach from 2003 to 2013 (High Temperature), replacing the historical sequence of aquatic vegetation changes with an unchanging aquatic vegetation community that represented the worst fountain darter habitat observed in the reach from 2003 to 2013 (Bad Vegetation), and implementing both the aquatic vegetation and water temperature modifications (Bad Vegetation + High Temperature). Graphs show 3 replicate stochastic (Monte Carlo) simulations of each of these scenarios using versions of the model without any density-dependent (DD) effects (left column) and with all six DD effects implemented (right column). (See text for description of DD effects on population growth.)

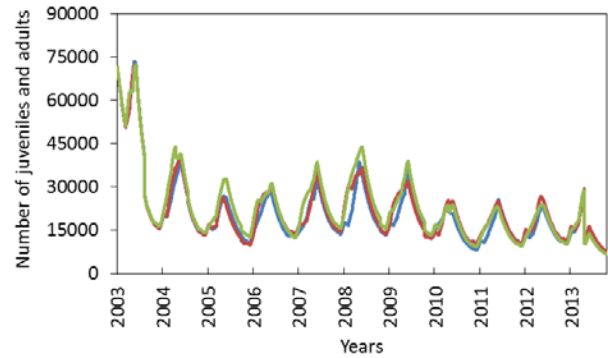
Landa Lake Reach, Comal River  
Without DD effect

With DD effect

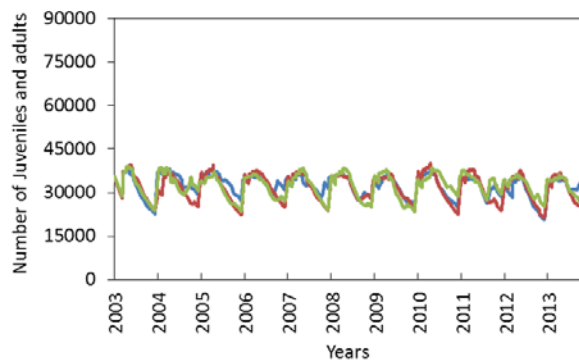
High Temperature



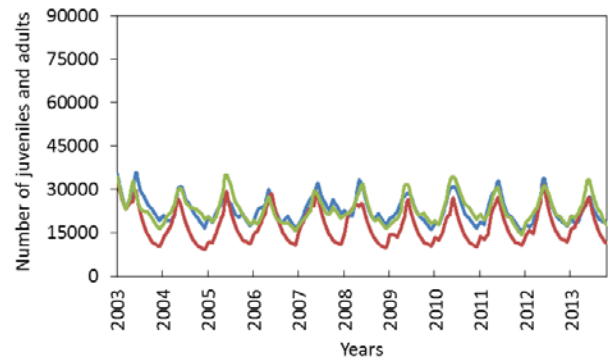
High Temperature



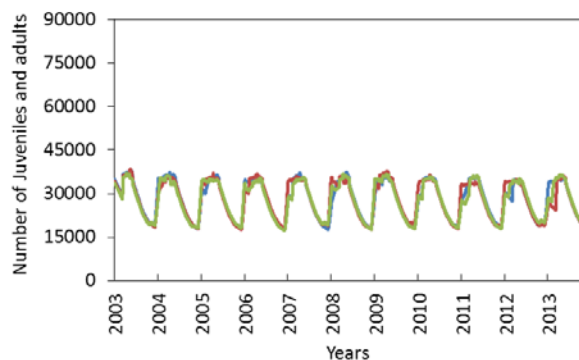
Bad Vegetation



Bad Vegetation



Bad Vegetation + High Temperature



Bad Vegetation + High Temperature

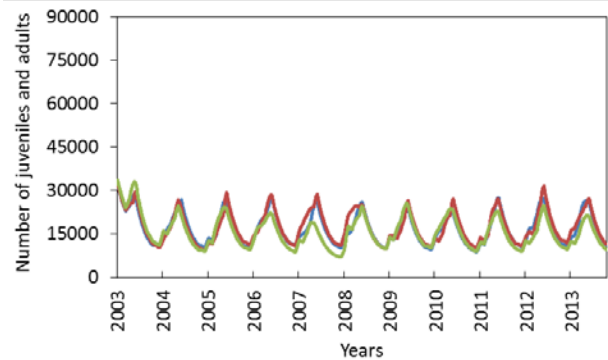


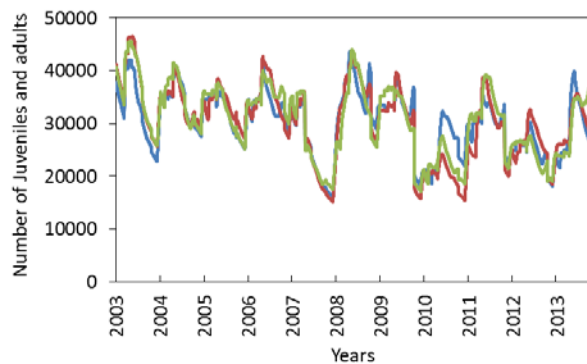
**Figure 16.** Comparisons of simulated population dynamics (changes in number of juvenile + adult fountain darters in the reach) within the Landa Lake Reach of the Comal River from 2011 through 2013 under three “worst case” scenarios in which baseline conditions (historical [2003 to 2013] aquatic vegetation and hydrological conditions) were modified. Modifications included replacing the historical sequence of water temperatures with an annually-repeating sequence of daily water temperatures that represented the year with the highest water temperature observed in the reach from 2003 to 2013 (High Temperature), replacing the historical sequence of aquatic vegetation changes with an unchanging aquatic vegetation community that represented the worst fountain darter habitat observed in the reach from 2003 to 2013 (Bad Vegetation), and implementing both the aquatic vegetation and water temperature modifications (Bad Vegetation + High Temperature). Graphs show 3 replicate stochastic (Monte Carlo) simulations of each of these scenarios using versions of the model without any density-dependent (DD) effects (left column) and with all six DD effects implemented (right column). (See text for description of DD effects on population growth.)

City Park Reach, San Marcos River

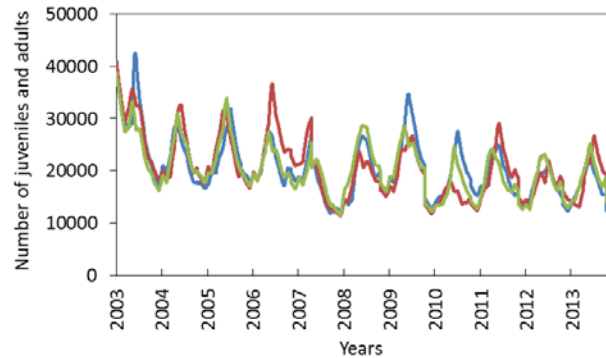
Without DD effect

With DD effect

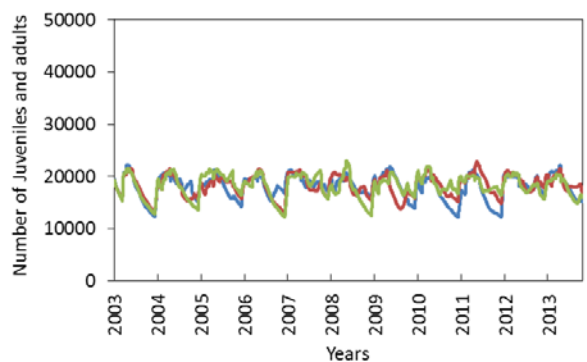
High Temperature



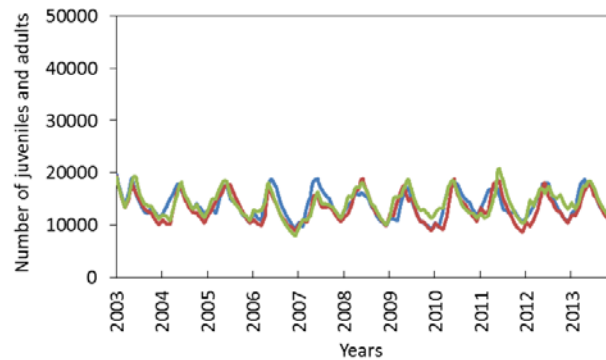
High Temperature



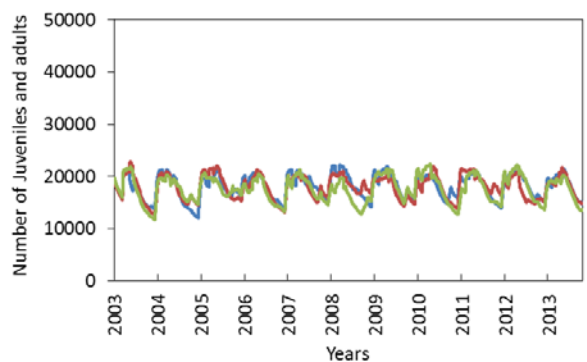
Bad Vegetation



Bad Vegetation



Bad Vegetation + High Temperature



Bad Vegetation + High Temperature

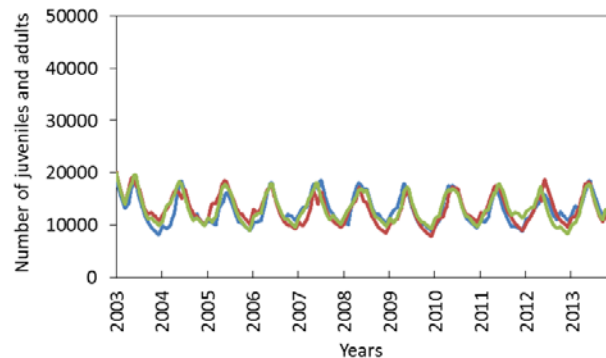


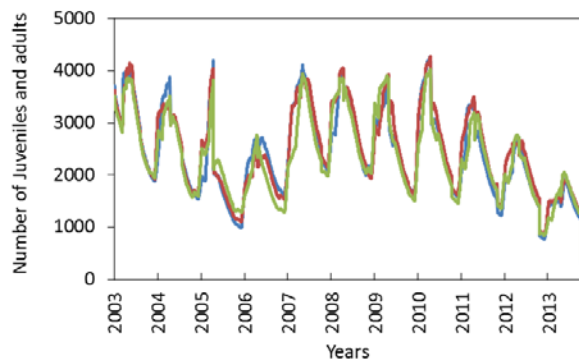
**Figure 17.** Comparisons of simulated population dynamics (changes in number of juvenile + adult fountain darters in the reach) within the City Park Reach of the San Marcos River from 2011 through 2013 under three “worst case” scenarios in which baseline conditions (historical [2003 to 2013] aquatic vegetation and hydrological conditions) were modified.

Modifications included replacing the historical sequence of water temperatures with an annually-repeating sequence of daily water temperatures that represented the year with the highest water temperature observed in the reach from 2003 to 2013 (High Temperature), replacing the historical sequence of aquatic vegetation changes with an unchanging aquatic vegetation community that represented the worst fountain darter habitat observed in the reach from 2003 to 2013 (Bad Vegetation), and implementing both the aquatic vegetation and water temperature modifications (Bad Vegetation + High Temperature). Graphs show 3 replicate stochastic (Monte Carlo) simulations of each of these scenarios using versions of the model without any density-dependent (DD) effects (left column) and with all six DD effects implemented (right column). (See text for description of DD effects on population growth.)

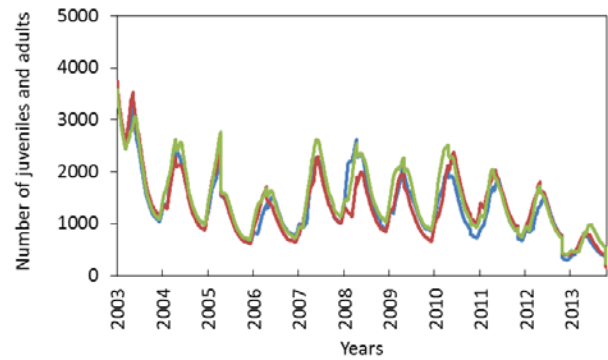
I35 Reach, San Marcos River  
Without DD effect

With DD effect

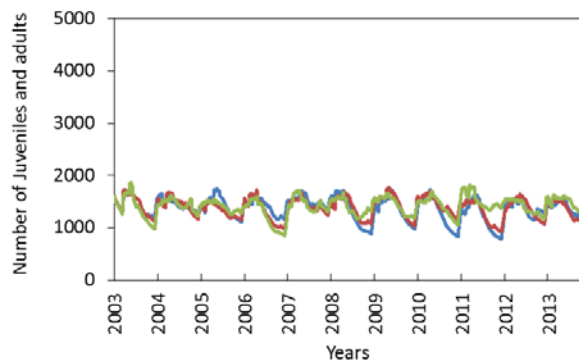
High Temperature



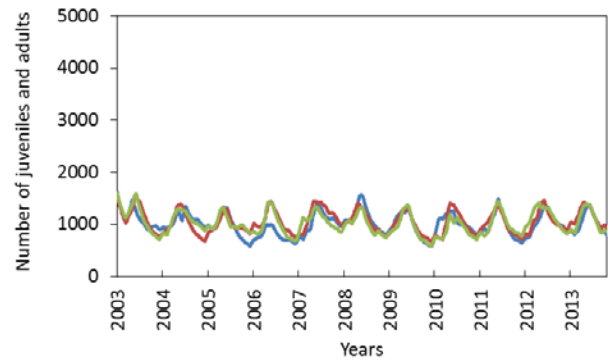
High Temperature



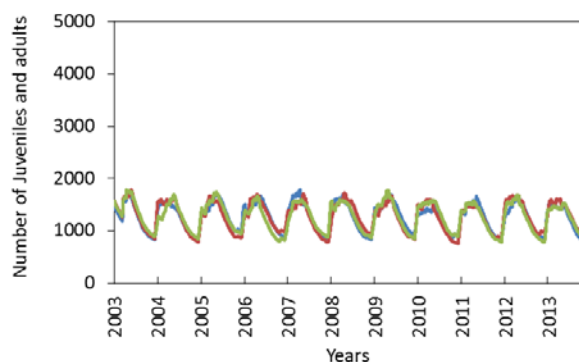
Bad Vegetation



Bad Vegetation



Bad Vegetation + High Temperature



Bad Vegetation + High Temperature

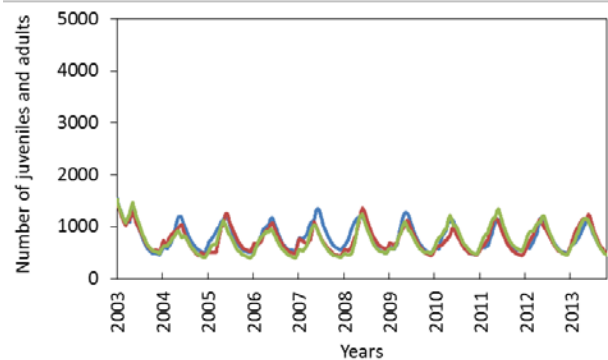


**Figure 18.** Comparisons of simulated population dynamics (changes in number of juvenile + adult fountain darters in the reach) within the I35 Reach of the San Marcos River from 2011 through 2013 under three “worst case” scenarios in which baseline conditions (historical [2003 to 2013] aquatic vegetation and hydrological conditions) were modified. Modifications included replacing the historical sequence of water temperatures with an annually-repeating sequence of daily water temperatures that represented the year with the highest water temperature observed in the reach from 2003 to 2013 (High Temperature), replacing the historical sequence of aquatic vegetation changes with an unchanging aquatic vegetation community that represented the worst fountain darter habitat observed in the reach from 2003 to 2013 (Bad Vegetation), and implementing both the aquatic vegetation and water temperature modifications (Bad Vegetation + High Temperature). Graphs show 3 replicate stochastic (Monte Carlo) simulations of each of these scenarios using versions of the model without any density-dependent (DD) effects (left column) and with all six DD effects implemented (right column). (See text for description of DD effects on population growth.)